A Quantitative Model of the Initiation of DNA Replication in *Saccharomyces cerevisiae*

by

Rohan Dhiraj Gidvani

A thesis

presented to the University of Waterloo

in fulfillment of the

thesis requirement for the degree of

Doctor of Philosophy

in

Biology

Waterloo, Ontario, Canada, 2012

Author's Declaration

I hereby declare that I am the sole author of this thesis. This is a true copy of the thesis, including any required final revisions, as accepted by my examiners. I understand that my thesis may be made electronically available to the public.

Abstract

A crucial step in eukaryotic cell proliferation is the initiation of DNA replication, a tightly regulated process mediated by a multitude of protein factors. In *Saccharomyces cerevisiae*, this occurs as a result of the concerted action of an assembly of proteins acting at origins of replication, known as the pre-replicative complex (pre-RC). While many of the mechanisms pertaining to the functions of these proteins and the associations amongst them have been explored experimentally, mathematical models are needed to effectively explore the network's dynamic behaviour.

An ordinary differential equation (ODE)-based model of the protein-protein interaction network describing DNA replication initiation was constructed. The model was validated against quantified levels of protein factors determined *in vivo* and from the literature over a range of cell cycle timepoints. The model behaviour conforms to perturbation trials previously reported in the literature and accurately predicts the results of knockdown experiments performed herein. Furthermore, the DNA replication model was successfully incorporated into an established model of the entire yeast cell cycle, thus providing a comprehensive description of these processes.

A screen for novel DNA damage response proteins was investigated using a unique proteomics approach that uses chromatin fractionation samples to enrich for factors bound to the DNA. This form of sub-cellular fractionation was combined with differential-in-gel-electrophoresis (DIGE) to detect and quantify low abundance chromatin proteins in the budding yeast proteome. The method was applied to analyze the effect of the DNA damaging agent methyl methanesulfonate (MMS) on levels of chromatin-associated proteins. Up-regulation of several previously characterized DNA

damage checkpoint-regulated proteins, such as Rnr4, Rpa1 and Rpa2, was observed. In addition, several novel DNA damage responsive proteins were identified and assessed for genotoxic sensitivity. A strain in which the expression of the Ran-GTPase binding protein Yrb1 was reduced was found to be hypersensitive to genotoxic stress, pointing to a role for this nuclear import-associated protein in DNA damage response.

The model presented in this thesis provides a tool for exploring the biochemical network of DNA replication. This is germane to the exploration of new cancer therapeutics considering the link between this disease (and others) and errors in proper cell cycle regulation. The high functional conservation between cell cycle mechanisms in humans and yeast allows predictive analyses of the model to be extrapolated towards understanding aberrant human cell proliferation. Importantly, the model is useful in identifying potential targets for cancer treatment and provides insights into developing highly specific anti-cancer drugs. Finally, the characterization of factors in the proteomic screen opens the door to further investigation of the roles of potential DNA damage response proteins.

Acknowledgements

This body of work exists but by the graces of my supervisors and my committee who not only gave me the opportunity to pursue my goals, but also the guidance necessary to achieve them. It was not long ago (then again, it was) that I joined the lab of Dr. Bernie Duncker as a lab neophyte hoping to adapt to my newfound environment and the realities of scientific research. It was not always a smooth ride, but what doesn't kill you, makes you…well, avoid doing the things that almost killed you. At the end of the day, my growth as a scientist has been fueled by his fastidious and meticulous approach to navigating the labyrinth of the cell cycle. Thank you for the years of surely edifying conversations ranging from protein degradation on a blot to the still hotly-contested merits of the Star Wars prequel.

I am thankful to Dr. Brendan McConkey for his role as counterbalance and for his attention to details spanning a vast territory of expertise. Never overbearing, but always to the point, his interest in anything worth being interesting has motivated me to always try to expand my horizons. Thank you for always having an open ear.

The Henry Higgins to my Eliza Doolittle, Dr. Brian Ingalls has patiently mentored me in the ways of mathematics and biological modeling, never revealing a hint of frustration or contempt for my stumbles through a daunting foreign landscape. I am thankful for his unwavering hope that eventually I would be able to derive the proof that the rain in Spain does in fact fall mainly in the X/Y plane.

Thank you to Dr. David Spafford for always ensuring that I be aware of the fact that my best efforts are expected from him and should be from myself. No thank you to

him for exercising his paintball prowess in supposedly friendly battles. Motivation can certainly come in many forms!

To my fellow lab and department mates, past and present, my life over the past six years has been molded by your friendship. Our arduous battles against unwilling experiments, intramurals opponents who highlighted the biological phenomenon of senescence, and the mighty arm of Campus Foods whose merciless regime would exclude the needs of graduate students from the consideration of Tim Hortons' hours of operation, will not go unremembered. We are the 1%!

I distinctly recall my first day in the lab and meeting my future long-time platoon compatriot, Matt Ramer. We certainly will always have Princeton, but I have many more fond memories as well, Batman. One cannot say enough about Lance DaSilva, but I'll try anyway. Generous, caring, perhaps the most inherently humorous individual I know, Lance has been the very image of a good man. That, and he's downright gerbilicious. I tip my hat to you, "Party". A big brother in every sense, I will not soon forget the worldly advice nor the masterful artwork of Ajai Prasad. The eternal question still beckons – How CAN she slap? A modern day Renaissance (or René-ssance more fittingly) man, Julian Wiegelman is proof that wit, humility, brilliance and perseverance are not mutually exclusive. "One of the brightest minds of our time", I have no doubt that our friendship is one for the ages. From foot soup to wrinkled shirts to blades of steel, Robert Aron Broom has been an enigmatic and loyal companion. My sanity or rather the loss of it has been mitigated by the deadpan humour of "Shelly" Liu during her time here. Wallowing in collective despair never seemed so funny. Despite Laura Dindia's general lack of comprehension, concentration or coordination (around me at least), she has managed to

make me smile at the right times purposefully or otherwise. Nataliya, Navdeep and Dinu, your contributions to absolute randomness, absolute cheer and absolut or any other shot-promotion, respectively have been much appreciated. I owe a great debt of grad-itude to my friends Marcel Pinheiro and Andrew Doxey, with whom I also began this journey. Between TMNT and delving into the mysteries of consciousness (or Cracked Canoe…terrible idea), I have enjoyed every moment spent with them and the world will certainly benefit from their talents and flair. The large modeling project that loomed before me would never have gotten off the ground without the help of Peter Sudmant and Grace Li. A man of few words, not one of them uttered by Dr. DongRyoung Kim was ever wasteful. My feeling is that his philosophies will be enjoyed by many. I hope he has found inner peace and the right lens for his camera. Finally, if there were anyone with whom I could communicate telepathically, it would be Darryl Jones. We have always seen eye to eye on matters concerning the merits of sleep and lethargy (read: energy saving). I think I could summarize our relationship with, "I see what you did there!" I wish him all the best in completing his degree and although I know he'll miss me too, I promise that he will find someone else to steal his protein bars.

Finally, my wellbeing and means have continually been supported by my caring parents who, after perusing this thesis hopefully and finally understand the difference between yeast and an amoeba. Although I know you would be proud of me either way, the drive to match your own accomplishments in life has been an integral factor in seeing this objective through to its end. Hopefully I can be like you, incredibly able and humble about it. If there's one person who has always been a role model where the roles should be reversed, it's my sister, Lara. I've always been very proud of you and in your way of

wearing the many hats of moody sister, practical twin (for a month a year at least), substitute mother, cacophonous joke-teller and in your own manner the brother I never had, you keep me grounded and I know I will always have one last line of defense. Thanks DW, #science!

It would be strange if I didn't acknowledge the one thing that permeates my being, that gets me out of bed and that inspires me to believe that I'm part of something bigger than life. Through all the highs and lows (more the former), it has if anything imbued me with true passion, which is the essence of truly living. I'll just say, from Price to Pacioretty, the Rocket to Beliveau, toujours dans mon coeur, Go Habs Go!

Table of Contents

List of Figures

Chapter 1

Chapter 2

Chapter 3

Chapter 4

Appendix A

Appendix B

List of Tables

Chapter 2

Chapter 3

Chapter 4

Appendix A

Appendix B

List of Noteworthy Abbreviations and Acronyms

ACS – ARS consensus sequence
APC – anaphase promoting complex
ARS – autonomously replicating sequence
ATP – adenosine triphosphate
Cdc – cell division cycle
CDK – cyclin-dependent kinase
CKI – CDK inhibitor
Clb or CLB – B-type cyclin (protein or gene)
Cln or CLN – N-type cyclin (protein or gene)
CMG – Cdc45:Mcm2-7:GINS (complex)
DAmP – decreased abundance by mRNA (proteins)
DDK – Dbf4-dependent kinase
DF – differential factor
dH_20 – distilled water
DIGE – differential-in-gel electrophoresis
DNA – deoxyribonucleic acid
Dox – doxycycline
DSB – double strand break
EDTA – ethylenediaminetetraacetic acid
EF – enrichment factor
FACS – fluorescence activated cell sorting
GAL – galactose
GLU – glucose
HU – hydroxyurea
KO – knockout (of a gene)
MCM – mini-chromosome maintenance
MMS – methyl methanesulfonate
ODE—ordinary differential equation
ORC – origin recognition complex
ORF – open reading frame
PAGE – polyacrylamide gel electrophoresis
PCNA – proliferating cell nuclear antigen
PCR – polymerase chain reaction
PEL – pellet (chromatin-bound protein)
pre-RC – pre-replicative complex
pre-IC – pre-initiation complex
RC – replication complex
RFC – replication factor C
RNA – ribonucleic acid
SSB – single strand break
SUP – supernatant (non-chromatin-bound protein)
TEN+T – Tris-HCl, EDTA, NaCl + Tween 20
ts – temperature sensitive
WCE – whole cell extract

Chapter 1: Literature Review and Project Goals

1.1 Yeast as a model organism

1.1.1 Introduction to Budding Yeast

The budding yeast, *Saccharomyces cerevisiae* (also known as baker's yeast) is a unicellular eukaryote belonging to a larger group of yeasts classified under the kingdom Fungi. In total, the 1500 identified yeast species account for 1% of all fungi (Kurtzman and Piškur, 2006). These encompass two distinct phyla: Ascomycota and Basidiomycota. The former includes budding yeast as well as the fission yeast, *Schizosaccharomyces pombe*, also used as a model organism in molecular biology. Perhaps the most commonly known feature of *S. cerevisiae* is its implication in the processes of fermentation. The common names, "baker's" and "brewer's" yeast are derived from its age-old implementation in bread- and winemaking, respectively. Once thought to be non-living, yeast was shown by Louis Pasteur (1860) to indeed be a living catalyst in the process of alcoholic fermentation. In fact, budding yeast is widely believed to be one of the first species to be domesticated for human use, having been found in 4,000-year-old archeological ruins of ancient Egyptian primitive bakeries and featured in even older hieroglyphs. Found ubiquitously in nature, yeast can be found in diverse environments from the skin of grapes to soil and even in the digestive systems of insects (Sláviková and Vadkertiová, 2003). Yeast survive on organic compounds (chemoorganotrophs), not requiring any light source. Multiple carbon sources are used for aerobic growth, such as glucose, maltose and trehalose while galactose and fructose are preferred under anaerobic conditions. Substrate-specific growth preferences are, however strain-specific.

It should be noted that while the designation, *Saccharomyces cerevisiae* is a blanket term for the numerous laboratory stocks of strains of the genus *Saccharomyces*, it generally refers to stocks originating from the interbred stains of Øjvind Winge and Carl Lindegren. These contain genetic elements from numerous species such as *S. bayanus* and *S. carlbergensis* among others, however for the sake of uniformity they are referred to en masse as *S. cerevisiae*, making a distinction between more distantly related *Saccharomyces* species (Lindegren, 1949; Mortimer, 1986). Laboratory strains are, as expected genetically distinct from true wild-type strains occurring in nature. Those used in molecular studies have been interbred to generate desired properties such as auxotrophies and the elimination of extraneous molecular pathways that might only be relevant to survival in the wild. Thus the most common lab strains are those derived from previously mutagenized wild-type stains. These include the haploid strain S288C, which was shown to have as a principle progenitor strain, EM93. This contributes to approximately 88% of the gene pool of S288C, the original strain from which all strains used in this thesis are derived (Mortimer and Johnston, 1986).

The description of *S. cerevisiae* as "budding yeast" is attributed to the visual observation of its vegetative cell division. When environmental conditions are suitable, a mother cell may enter a mitotic cell cycle wherein it produces an ellipsoidal daughter cell that emerges from a point on its surface as a "bud". The daughter cell produced dissociates from the mother and is at this stage smaller in size, requiring an increase in growth in order to serve as a mother cell itself in a subsequent and separate mitotic duplication (Herskowitz, 1988). In contrast, the fission yeast *S. pombe* increases in size

and divides into two equal daughter cells. Budding yeast may enter a quiescent G_0 phase where it may temporarily or permanently exit the division cycle.

Although cell size varies across strains and growth medium, a typical diploid budding yeast cell is ellipsoid in shape with a 5 X 6 μm dimension. Haploid cells are spheroid with a typical dimension of 4 μm in diameter (Mortimer, 1958). A major difference in the budding pattern of haploid cells versus diploid cells is that the former form buds adjacent to the previous bud while the later have subsequent buds emerge at the opposite pole (Friefelder, 1960). Bud scars are formed on the cell wall after each division with each mother cell averaging 20-30 buds over its lifetime (Sherman, 1991). Budding yeast shares the majority of structural and functional cellular components of higher eukaryotes such as a nucleus, cytosol, mitochondrion, endoplasmic reticulum, Golgi apparatus and associated secretory vesicles. Where more complex eukaryotes possess lysosomes, yeast maintains a vacuole as well as a rigid cell wall comprising 15 to 25% of the dry mass of the cell. This envelope, with a width between 100-200 nm provides shape and support to the internal components of the cell. The chitinous cell wall also ensures an optimal osmotic balance with the cell exterior, acts as a barrier against physical stress and serves as a scaffold for various glycoproteins with specialized functions (Klis *et al*., 2006). A 7 nm thick plasma membrane acts as a semi-permeable lipid bilayer to control the osmotic nature and selectivity of the cell. A number of metabolic enzymes reside in the periplasmic space between the cell wall and membrane aiding to rid the cell of unwanted and/or toxic bi-products. The cell wall can be removed via treatment with lytic enzymes such as zymolyase and lyticase (see “chromatin fractionation” under Materials and Methods). This produces a spheroplast, which renders

the cell competent for effective sub-cellular fractionation (discussed in Walker, 1998). Another distinguishing feature of yeast versus higher eukayotes is the retention of the nuclear membrane during mitosis. Rather than dissolving, it pinches off producing a daughter nucleus, which travels to the emerging bud (future daughter cell).

1.1.2 The Genetics of Yeast and its Molecular Engineering

The 2001 Nobel Prize in physiology for medicine was awarded to Leland H. Hartwell, Tim Hunt and Sir Paul M. Nurse for their work in elucidating the regulatory mechanisms of the eukaryotic cell cycle. These meritorious efforts were performed in the yeasts *S. cerevisiae* and *Schizosaccharomyces pombe* in addition to *Xenopus leavis*. Importantly, Hartwell's genetic studies of budding yeast, mutants of genes controlling the cell cycle and its checkpoints were isolated, thus highlighting the roles of their products in cell cycle control (Hartwell *et al*., 1970). The haploid genome of *Saccharomyces cerevisiae* comprises sixteen chromosomes. These have been extensively studied from both a morphological perspective as well as in great genetic detail. In 1996, the entire yeast genome was sequenced (Goffeau *et al*., 2006) and reported as consisting of roughly 12,052 kb of chromosomal DNA including a mitochondrial complement of 78,520 bp. Researchers found 6183 open reading frames (ORFs) exceeding 100 amino acids with just over 5800 expected to specify genes encoding functional proteins. As a comparison, while the total size of the genome is 3.5-fold that of *E. coli*, it only codes for roughly 1.5 times the number of gene products. The majority of *S. cerevisiae* strains possess 2-μm circular plasmids that exist solely for the purpose of self-propagation (such strains are designated cir^{+}). They encode four ORFs and three *cis*-acting sequences, which permit

them to maintain high copy levels (~60) and to segregate into daughter cells during cell division (Falcon *et al*., 2005). Interspersed throughout the genome of budding yeast are viral-like retrotransposons called Ty elements. They are often found to have been inserted at genomic loci known as transpositional "hot spots" where they are most likely to be transcribed, without disrupting the fitness of the host cell. The enzymatic machinery that carries out their integration is postulated to interact with transcription factors and nucleosomes within silent chromatin. This feature is thought to ensure their ability to be maintained and propagated within the genome (Boeke *et al*., 1985). One feature of the yeast genome is its highly compact nature, with 72% of the total sequence corresponding to genes, in contrast to ~2% in humans (International Mouse Genome Sequencing Consortium).

Despite these stark differences in organization, yeast and higher eukaryotes (including humans) share high levels of structural and functional protein homology. The conservation of important genes is high: as an example, budding yeast actin and tubulin have an average of 78% amino acid sequence homology with their human counterparts. Homologous proteins for secretory pathways, heat-shock proteins, transcription factors, G-proteins as well as oncogenes exist between yeast and human, rendering the findings of fundamental yeast research amenable to relevant interpretation in the human context.

Apart from the minor cellular differences between budding yeast and higher eukaryotes, the fundamental processes that drive metabolism, cell proliferation, division and growth are largely conserved. Given the relative size, cost and ease of maintenance of *S. cerevisiae*, it serves as a versatile model organism: Haploid strains typically grow rapidly in rich medium with a doubling time of 90 minutes in log phase. In synthetic

medium, used to select for auxotrophic markers, doubling time is increased to approximately 140 minutes. Other facets of yeast culturing include dispersed cell growth and the ease with which mutants can be isolated via replica plating and large-scale mutant library screening. Commonly referred to as the "*E. coli* of Eukarya", *S. cerevisiae*'s genetic tractability lends itself to facile manipulation of its genome. Technological advances in molecular biology such as PCR and DNA transformation techniques have been particularly useful in the genetic engineering of yeast. Plasmids can be introduced either with the intention of being maintained as extra-chromosomal replicating entities or for the purpose of integrative recombination. Because such integration occurs exclusively via homologous recombination in yeast, its characteristically high rate of gene conversion allows the insertion of exogenous DNA sequences into specified genetic loci. Both synthetic and naturally derived oligonucleotides can be transformed into yeast. This DNA, even partially containing segments homologous to a genomic target can thus be used to direct its recombination into the genome. Thus gene replacement and deletion can be achieved much more simply in yeast compared to most other organisms. Disruption of genes either by complete knockout or by the insertion of a mutant version allows investigations of their impact *in vivo*. These findings can be applied to homologous genes in higher eukaryotes and allow an efficient method of predicting resulting phenotypes (Jelier *et al*., 2011). PCR-based mutagenesis allows for quick and efficient alteration of specific genes to create known or yet uncharacterized alleles enabling the study of the resultant phenotypes. Such molecular techniques are made more appealing given the non-pathogenic nature of *S. cerevisiae*, which in 2001 was granted the status of generally regarded as safe (GRAS) by the U.S. Food and Drug Administration. The low cost and

ready availability of this microorganism makes it an invaluable tool in the fundamental study of eukaryotic systems.

The same techniques that facilitate the study of budding yeast biology allow the extrapolation of such examinations to the level of mammalian biology. Because function is so highly conserved in major pathways between budding yeast and humans, experiments can be carried out in *S. cerevisiae* to circumvent certain obstacles facing efficient genetic manipulation of mammalian cells. While the human genome (but not that of many other eukaryotes) is sequenced, the challenge of deciphering it remains. This involves elucidating the functions of uncharacterized genes, gene networks as well as non-coding sequences. The human genome contains high levels of these non-coding regions including introns (25% compared to 3.8% in *S. cerevisiae*), which complicates the isolation and cloning of genes. Gene replacement is also made more laborious and although transgenic techniques are widely used, they suffer from an inability to be site-specific (Li and Bradley, 2011). The growth time and cost of harvesting mammalian cells are disadvantageous to dissecting their genetic makeup. The ability to study the budding yeast homologs or to introduce mammalian genes directly into yeast for their functional characterization often obviates the need for resource-intensive experiments (Gietz and Wooda, 2002; Wach *et al*., 1994).

Another advantage of the high conservation between humans and yeast is the ability to perform high-throughput examinations of the entire yeast transcriptome under varying environmental conditions (Brown and Botstein, 1999; Cho *et al*., 1998; DeRisi *et al*., 1997; Marc *et al*., 2001). While human cDNA libraries exist for various cell lines including cancerous ones, technical challenges in human transcriptome analyses stem

from a much larger scale of coverage. The design of probes and the isolation of sample DNA from mammalian cells under varying conditions for this purpose is more demanding. Additionally, the presence of non-coding RNAs and the diversity of transcripts between cell types increase the difficulty in creating highly resolved expression data that can detect low abundance transcripts (Mercer *et al*., 2011). The smaller genome of yeast allows a more rarefied environment within which to query target orthologs across Eukarya. Considering the analysis of the yeast genome itself, a library of single gene knockout strains for each of the 6,000 genes has been used to characterize functions of individual coding loci and has shown that at least 5,000 identified genes are non-essential (Giaever *et al*., 2002; Winzeler *et al*., 1999).

The wide availability of tagging modules enables the integration of sequences encoding epitope tags at the C- or N-terminal ends of genes of interest (Longtine *et al*., 1998). The resultant fusion proteins can be used to facilitate detection due to the incorporation of a tag for which high affinity antibodies directed towards it are available. This is particularly useful if the protein of interest is of low abundance in the cell or in the absence of a corresponding commercially available antibody (as was the case in experiments described in chapter 3). Commonly used epitope tags fitting this description are the HA- (human influenza hemagglutinin, Field *et al*., 1988) and Myc- (derived from the c-Myc proto-oncogene, described in Munro and Pelham, 1984) tags. The FLAG-tag is unique in that it is a synthetically-derived epitope, designed and generated before a corresponding monoclonal antibody was raised to it (Einhauer, 2001; Hopp *et al*, 1988). Features of its design such as sequence length and composition (aromatic amino acids flanked by charged residues) optimize its surface exposure to maximize antigenic

properties. In addition, its hydrophilicity reduces interference with the native protein such that it is amenable to use in Western blotting and immunoprecipitation with similar efficiency to the naturally optimal Myc and HA tags. Protein A and polyhistidine (HIS) tags are often used to purify proteins via sepharose or nickel-coated columns, respectively. Tandem affinity purification (TAP) tags allow for multi-step purification in order to isolate protein complexes. The canonical TAP tag consists of a Protein A tag and a calmodulin binding peptide (CBP) separated by a TEV protease cleavage site. Initial binding of the exposed Protein A to an IgG matrix purifies protein complexes loosely associated with the tagged protein of interest. Upon elution, washing and cleavage of the TEV site, a second round of purification ensues as the now-exposed CBP binds to calmodulin-coated beads. This two-step purification enhances the specificity of associated proteins and purity of the complex isolated. The tagging of multiple proteins in a given strain with mutually exclusive peptides permits the investigation of protein-protein interactions via co-immunoprecipitation (reviewed in Knop *et al*., 1999) and the simultaneous observation of their behaviour. Finally, *in situ* visualization of proteins can be carried out via the use of fluorescent tags (e.g., green fluorescent protein, GFP from *Aequorea victoria*). Since their early inception in observing the localization of proteins via microscopy, increasing numbers fluorophores have been developed. These have been optimized for techniques such as fluorescence resonance energy transfer (FRET), which allows the *in vivo* quantification of protein-protein interactions (Sheff and Thorn, 2004).

The expression of a gene of interest can be controlled via the implementation of various promoter systems. By replacing the endogenous promoter with one of the well-characterized regulatory sequences described below, transcript and protein levels can be

regulated as desired. The GAL_1 promoter is activated by a 365-bp UAS that is galactose-inducible and glucose-repressible. A downstream-fused gene can thus be constitutively expressed in the presence of galactose or shut off to observe the resultant phenotype in the presence of glucose. More precise control of gene expression can be exerted with the use of the tetO-regulatable promoter system wherein genes under its control are expressed constitutively unless inhibited by the antibiotic tetracycline or its analog, doxycycline (Belli *et al*., 1998). The concentration of these repressors can be titrated to obtain a precise level of gene transcription. Another method of experimentally controlling gene expression is the use of temperature sensitive (Ts^- or ts) strains which typically possess an allele of a particular gene mutated such that its protein product is destabilized at elevated temperatures. Shifting to such conditions at a desired point in the experiment would effectively inhibit the accumulation of the functional form of the corresponding protein, either by destabilizing it or by inactivating it through aberrant conformation.

The yeast two-hybrid assay is used to determine the degree of interaction between a given pair of proteins using an efficient reporter-based system (Uetz, 2002). This scheme involves the expression of two fusion proteins, one containing a transcriptional activation domain, the other a motif that binds to the regulatory sequence of a genomic reporter. If the proteins of interest interact, activation of the reporter will occur proportionate to the degree of interaction, providing a coarse but useful assay. While this can be implemented for yeast proteins, exogenous genes and their products can also be examined, rendering the yeast cell a veritable living test tube.

The capacity for yeast to express exogenous genes can be exploited on a large scale through the expression of recombinant genes for commercial use. Because yeast can

grow at high densities in controlled medium, it is engineered to produce a variety of heterologous proteins for industrial and biopharmaceutical uses. While budding yeast is capable of these demands, the methanotropic yeast, *Pichia pastoris* is most amenable to such applications (Cregg *et al*., 2009). Prokaryotes lack the post-translational modification machinery necessary for proper eukaryotic protein processing. The eukaryotic post-translational modifications and pathways to secrete mature protein are, however largely conserved in yeast. This provides an optimal background for expressing proteins from more complex organisms on a large scale (reviewed in Cereghino *et al*., 2000 and Guthrie and Fink, 2002).

For the purposes of clarity in specifying the strains and relevant manipulations used, a discussion of genetic nomenclature is appropriate. Given that there have been no alterations to the mitochondrial genome in this body of work, consideration will be limited to chromosomal genes. A gene or locus is specified by three italicized letters followed by a number, e.g., *ARG*2. Dominant alleles are presented in uppercase, while recessive alleles are written in lowercase, e.g., *arg*2. A given allele will be specified by the appropriate locus followed by a number designated to it, e.g., *arg*2-9. Wild-type alleles are simply assigned a superscript "plus" symbol as in $ARG2^{+}$. Deletion of an entire gene is indicated by a delta, e.g., *arg2*Δ, while a partial deletion will specify the amino acids removed from the wild-type sequence starting from the first residue, e.g., *arg2*Δ1-40. In the case of a gene insertion, the code for such gene follows the locus into which the gene has been inserted, separated by the symbol "::". In the case of *arg*2::*LEU*2, the *LEU*2 gene (dominant) has replaced the previously recessive (now non-functional) *ARG*2

locus. Proteins are presented as the product of a given gene, thus usually bearing the same locus name, however in "sentence case", e.g. Arg2 (Sherman, 1991).

1.1.3 The Life Cycle of *S. cerevisiae*

1.1.3.1 Reproduction and Mating Type Switching

Budding yeast has two mating types characterized by one of two alleles (**a** or α) present at the *MAT* locus on chromosome III. Each cell type maintains its identity through the selective transcription of genes. The identity of the *MAT* locus allele governs the regulation of these genes and thus designates the cell as being of either **a**- or α-type in haploids. Each cell type expresses a unique signalling receptor and peptide mating pheromone (e.g., *MAT*α cells secrete α-factor). Cells of opposing mating type respond to each other's pheromone by activating a signalling pathway that causes the cell to assume a pear shaped morphology including a cell membrane projection referred to as a "shmoo". Nuclei from each haploid cell migrate towards one another along the shmoo, finally fusing to create a *MAT*α/*MAT***a** diploid (reviewed in Tkacz and MacKay, 1979). Mating type switching is well-studied phenomenon in epigenetics and its central feature is the interchangeability of genetic elements at the *MAT* locus. Every haploid genome possesses two silent regions on either side of the *MAT* locus. At any given time, this central region will encode and express the genes specifying one of the two cell types, e.g., the *MAT*α locus programs α-specific gene expression. The silent loci, *HML* and *HMR* encode either the α or **a** alleles, respectively of the *MAT* locus. An important concept in understanding the life cycle of budding yeast is the differentiation between two types of fungal life cycles: homothallism and heterothallism. Homothallic strains are

competent for mating type switching and contain a functional copy of the HO endonuclease. This enzyme cuts at a specific site within the mating-type locus creating a double strand break. This is resolved in such a way that the original *MAT* cassette is replaced by the opposite allele. In such a manner, the information encoding the cell type to be converted to is copied into the active *MAT* locus where it will be expressed. The formation of an α/**a** diploid inhibits *HO*. Heterothallic cells possess a defective *HO* gene, *ho* which eliminates the possibility of a mating type switch.

Homothallic haploid cells are capable of producing diploid progeny without the initial requirement of a cell of the opposite mating type. They accomplish this by producing both α and **a** haploids during mitotic divisions. These daughter cells can subsequently mate with each other generating a *MAT*α/*MAT***a** diploid. The ability of a homothallic cell to produce both cell types arises from its aforementioned capacity to change its cell type. A homothallic *MAT***a** cell thus switches to *MAT*α type producing α-type daughters though mitosis. These may then mate with **a**-type daughters produced in previous or subsequent divisions. Heterothallic haploid cells can only produce cells of the same mating type via mitosis. Thus, in order to create an α/**a** diploid, they must mate with cells derived from separate spores of the opposing cell type. When *MAT*α/*MAT***a** diploids generated via either method are exposed to an environment deprived of both nitrogen and carbon, meiotic division occurs. Nutrient supply is provided by a poor quality carbon source (e.g., acetate). Starvation of the cell initiates sporulation by forcing it into G_1 phase. The ensuing meiotic cycle produces four haploid spores encapsulated within a protective sac known as an ascus. When environmental conditions are favourable, the

ascus disintegrates releasing the spores (reviewed in Herskowitz, 1988). The processes described above are illustrated in Figure 1.1.

The majority of laboratory strains are heterothallic and generally *MAT***a** type. This prevents the spontaneous generation of diploids as well as renders them sensitive to α-factor, which arrests these cells in late G_1 phase. This is useful for experiments in which cell synchronization is desired, described below.

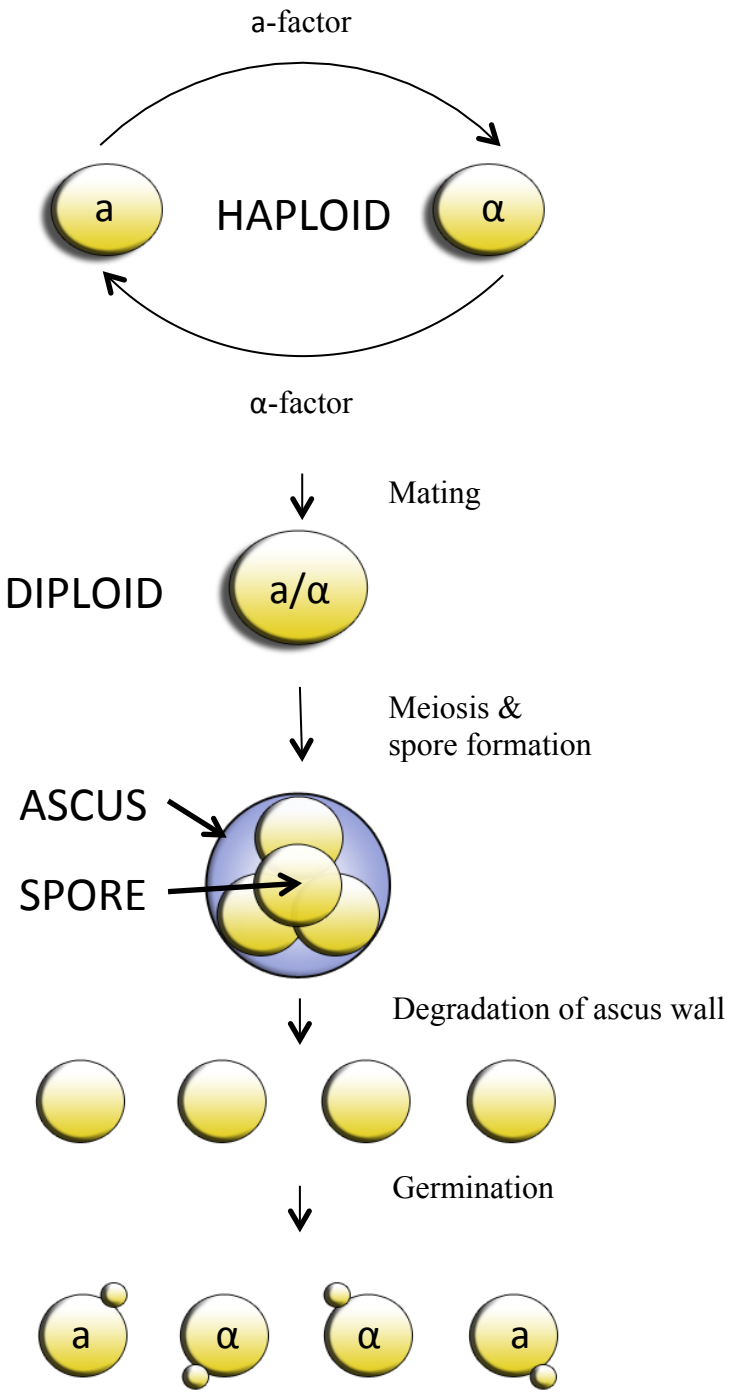
a-factor
a
HAPLOID
α
α-factor
Mating
DIPLOID
a/α
Meiosis &
spore formation
ASCUS
SPORE
Degradation of ascus wall
Germination
a
α
α
a

Figure 1.1. Life cycle of *Saccharomyces cerevisiae*. Haploid cells are able to mate with other haploid cells of the opposite mating type. This is brought about by a pheromone-induced signal transduction cascade specific to each cell type, either **a** or α. Both haploid and diploid cells are capable of mitotic cell division. Mating of haploids produces a diploid zygote while meiotic division of a diploid gives rise to four haploid cells contained within a protective sac, known as an ascus. When environmental conditions are suitable, it degrades, releasing the haploid spores, each entering its own cell cycle and potential mating pathway. Adapted from Herskowitz, 1988.

1.1.3.2 Synchronization of Yeast Cultures

Because the yield of protein or DNA from an individual cell is practically insufficient for gathering meaningful experimental data, large cultures of yeast (at concentrations typically between 5 X 10^6 to 2 X 10^7 cells/ml) are used to analyse a population average. In many cases, to obtain information pertaining to a stage-specific property, the vast majority of cells in these populations must be at the same point in the cell cycle. This enables the study of yeast populations as if they were behaving as a single cell. Various techniques of cell synchronization are used to achieve this goal.

For individual experiments, the question arises concerning the appropriate method of synchronization. Several factors are typically considered: 1) What is the closest arrest point available to the cell cycle range being investigated? Once confirmation of a successful arrest is made, the culture is "released" as needed, resuming its progression through the cell cycle. All cells in the culture will thus be at the same cell cycle stage. 2) The methods by which cells are synchronized can cause significant alterations to physiological conditions in the cell, such as the activation of mating or developmental pathways, stress response or generation of artefacts that may confound the analysis (Cho *et al.*, 1998; Spellman *et al.*, 1998; Wyrick *et al.*, 1999). Depending on the process being examined, it is best to choose the synchronization routine that limits these unwanted products to deduce meaningful conclusions. Additionally, where applicable, more than one synchronization routine can be used. This is useful as some synchronization routines as more effective for a given purpose, thus combining them yields additive benefits. Also, since cells lose synchrony throughout the course of the cell cycle, imposing synchrony

via different regimes at well chosen intervals increases the duration that synchrony will be effectively maintained. Some widely used methods are described below.

α-Factor Arrest and Release

As previously discussed, when *MAT***a** cells are exposed to the mating pheromone α-factor, they initiate a mating pathway that halts cell cycle progression and eventual mitotic division. This is exploited by experimenters wishing to arrest cells at a point in the cell cycle just prior to when the commitment to division has been made. This point is referred to as START and occurs in late in the phase immediately preceding that in which genome duplication occurs. For studying the events leading up to and occurring during this replicative phase, arresting cells just prior to DNA synthesis is ideal. The addition of α-factor to a yeast culture results in such a block by 1) Inducing a mating response preventing DNA synthesis and 2) Inhibiting Cln-Cdc28, which promotes passage past START (Cross, 1995). While all wild-type strains may be used in this protocol, those lacking the *BAR*1 gene (coding for an α-factor-degrading protease) are more easily arrested (Ciejek and Thorner, 1979; MacKay *et al.*, 1988). One advantage, however to using *BAR*1^{+} strains is that they can more readily be released from the pheromone-induced block. In these strains, the α-factor block will be transient due to active degradation of the peptide, thus it must be replenished for a prolonged arrest. Cells are released from the late-G_1 block by thoroughly washing with water to remove α-factor from the medium. Once re-suspended in the appropriate fresh growth medium, cells will resume the cell cycle and soon enter S-phase. Additionally the protease XIV (also known

as Pronase E) derived from *Streptomyces griseus*, when added degrades any remnants of Bar1 protein, thus increasing the efficacy of the release (Breeden, 1997).

Nocodazole & Hydroxyurea

These organic compounds are added to culture medium, bringing about specific cellular responses and are implemented in a block/release fashion. Nocodazole is a microtubule depolymerizer, detrimental to the formation of the mitotic spindle. It thus arrests cells at the G_2/M boundary (Futcher, 1993; Jacobs *et al.*, 1988). Hydroxyurea (HU) is a ribonucleotide reductase inhibitor, effectively depleting the cell's nucleotide pool. This halts DNA synthesis due to an insufficient amount of nucleotides available to be incorporated into nascent strands. Cells treated with HU arrest in mid S-phase (Elledge *et al*., 1993; Futcher, 1999). The effects of these drugs can be removed by comprehensive washing with water after which cells resume progression through the cell cycle.

Centrifugal Elutriation

Because cell size is intimately correlated with cell cycle position, cells can be isolated based on this parameter to obtain those progressing through the same cell cycle stage. G_1 cells can be collected by exposing a culture to centrifugal forces in a chamber, whereby a sedimentation gradient is created based on size (Johnston and Johnson, 1997; Oehlen *et al.*, 1996). Smaller cells, i.e. those in G_1 are forced towards a collection site. A distinction between α-factor arrested G_1 cells and those obtained via elutriation is that the latter will be at an earlier point in G_1 and will thus be smaller. They require more time to reach the critical size required to pass START, but have been minimally altered in their

transcriptional program as in the case with α-factor and nocodazole. Only the physical stresses imposed by this protocol act as potential detriments to maintenance of normal cell shape and function. An advantage of this procedure is that cells need not have specialized genetic requirements such as a *MAT***a** genotype or specific mutations (discussed below). Some strains do not respond well to block and release protocols, while elutriation is uniformly efficient. While the majority of elutriation protocols are designed to isolate G_1 cells, the basis of this isolation is cell size, which corresponds directly with cell cycle stage. Hence elutriation can be used to collect cells from other cell cycle points assuming uniform cell morphology at the specified stage.

Cell Cycle Mutants

Cell cycle progression is dependent on the normal functioning of a vast number of previously identified protein factors. Mutant alleles of the corresponding genes can be used to arrest the cell at the point at which the factor in question plays a critical role. Understanding of the cell cycle was founded in the work that highlighted the Cdc (cell division cycle) proteins as drivers of this process (Hartwell *et al*., 1970). Several mutant alleles have been routinely used to block the cell at well-defined landmarks; the *cdc*28-13 allele arrests cells in G_1 while *cdc*15-2 causes a telophase arrest. These are both ts mutants; hence cells will be arrested when shifted to a **restrictive** temperature at which the protein is destabilized. When cell are shifted back to a **permissive** temperature, *de novo* synthesis of the now stable protein allows a synchronous release. An intermediate temperature (**semi-permissive**) can be used to investigate subtle phenotypes of the mutation (Fitch *et al.*, 1992; Kovacech *et al.*, 1996; Surana *et al.*, 1993). The mutant

alleles of the essential replication kinase Cdc7, *cdc*7-1 and *cdc*7-4 compromise its function, arresting cells just prior to entry into the replicative phase of the cell cycle (S phase, Bousset and Diffley, 1998; Njagi and Kilbey, 1982). In these ts mutants, the structure of Cdc7 is destabilized at an elevated temperature (37°C). Another method of imposing cell cycle arrest is to deplete cells of a critical cell cycle protein. This is accomplished by placing the appropriate gene under the control of either an inducible (e.g., GAL_1) or repressible (e.g., MET_3) promoter. In the case of the former, the gene will only be expressed in galactose medium. Gene shutoff in glucose medium is remarkably tight. It should be noted, however that genes are generally overexpressed under control of the GAL_1 promoter and if the protein being employed is detrimental to the cell in excess, it cannot be used in such a regimen. In this case, the more temperate expression levels generated by the MET_3 promoter would be more suitable. It is so-named for its ability to be repressed by methionine (Guthrie and Fink, 2002).

To monitor synchrony, simple phase contrast microscopy distinguishes cell morphologies pertinent to a given cell cycle stage. Cells that have recently progressed from G_1 to S phase will exhibit a small bud, while cells emerging from mitosis will take on a dumbbell shape due to the similar, but not equal size of the mother and daughter cells immediately prior to cytokinesis. If cells in a culture maintain similar size ratios of mother to bud/daughter, one can assume they remain synchronized. With the complementary use of fluorescence activated cell sorting (FACS) analysis to determine DNA content, cell synchrony can more precisely be confirmed (Futcher, 1993; Haase and Lew, 1997). The use of *in situ* immunofluorescence can aid in the observation of mitotic spindles and structures related to passage through M phase (Kilmartin and Adams, 1984).

1.2 The Cell Cycle

1.2.1 Overview

The evolution of a coordinated and ordered molecular system underlies cell propagation. Its function is to duplicate the genome and subsequently segregate the copies precisely into two genetically identical cells. The first observation of this phenomenon was made early in the nineteenth century by Tomas Schleiden and Theodor Schwann, distilled to "cells arise from pre-existing cells" (Schwann, 1839). For any cell to produce identical progeny it must enter into a life cycle whereby a facsimile of its complement of DNA, mostly arranged into one or more chromosomes is made through the process of DNA replication. The pair of genetic blueprints produced is equally divided between two resultant cells, representing the mitotic life cycle. Bacterial genomes typically consist of one circular chromosome, which is replicated and segregated into two identical cells by binary fission. In prokaryotes, chromosome duplication and cell division must occur in that order, but there is no clear division of the cell cycle into discrete functional stages. Eukaryotes have a more complex cell cycle divided into four distinct phases. The eukaryotic nucleus encapsulates the genome, which is only duplicated during one of these cell cycle stages (S phase).

The discrete phases of the cell cycle are delineated by their roles and ultimately by the underlying molecular mechanisms being carried during them, each fulfilling a particular function culminating in cell division. The four phases of the eukaryotic cell cycle are: G_1, S, G_2 and M, in that order, discussed in detail below (Figure 1.2). The bulk of the cell cycle is spent growing and synthesizing new DNA in anticipation of cell

division. This preparatory stage is known as interphase and comprises G_1, S and G_2 phases. Mitosis (M phase) involves the careful coordination of molecular scaffolds to separate the newly duplicated DNA into two cells, which eventually divide via cytokinesis. The entire four-phase cell cycle is crucial as each one sets the stage for the next consistent with a "dependent pathway model" (Hartwell, 1974). Yeast cells undergo a virtually identical cell cycle to more complex or higher eukaryotes save for some key differences. Yeast chromosomes are divided in a closed mitosis wherein the nucleus remains intact rather than disintegrating until the following G_1 phase (reviewed in Heath, 1980). The yeast genome contains numerous well-defined and highly conserved sequences that specify potential start sites of DNA replication. This is in contrast to metazoans and even fission yeast where such sites, known as origins of replication are determined stochastically (reviewed in Méchali, 2010). Nevertheless, the major features are conserved and using yeast as a model for cell cycle studies has yielded great advances in understanding the process at a molecular level.

In order to maintain the fidelity of the replicative cycle, multiple ordered regulatory switch-like mechanisms have evolved. These link distinct cellular events ensuring that the cell progresses through each phase only after having performed critical functions in proper sequence (e.g., mitosis must come after replication of the chromosomes). External factors influence the control of the cell cycle, allowing it to respond appropriately by increasing the rate of certain processes or by halting the cell cycle until the proper conditions arise. A brief discussion of the four main phases of the yeast cell cycle follows.

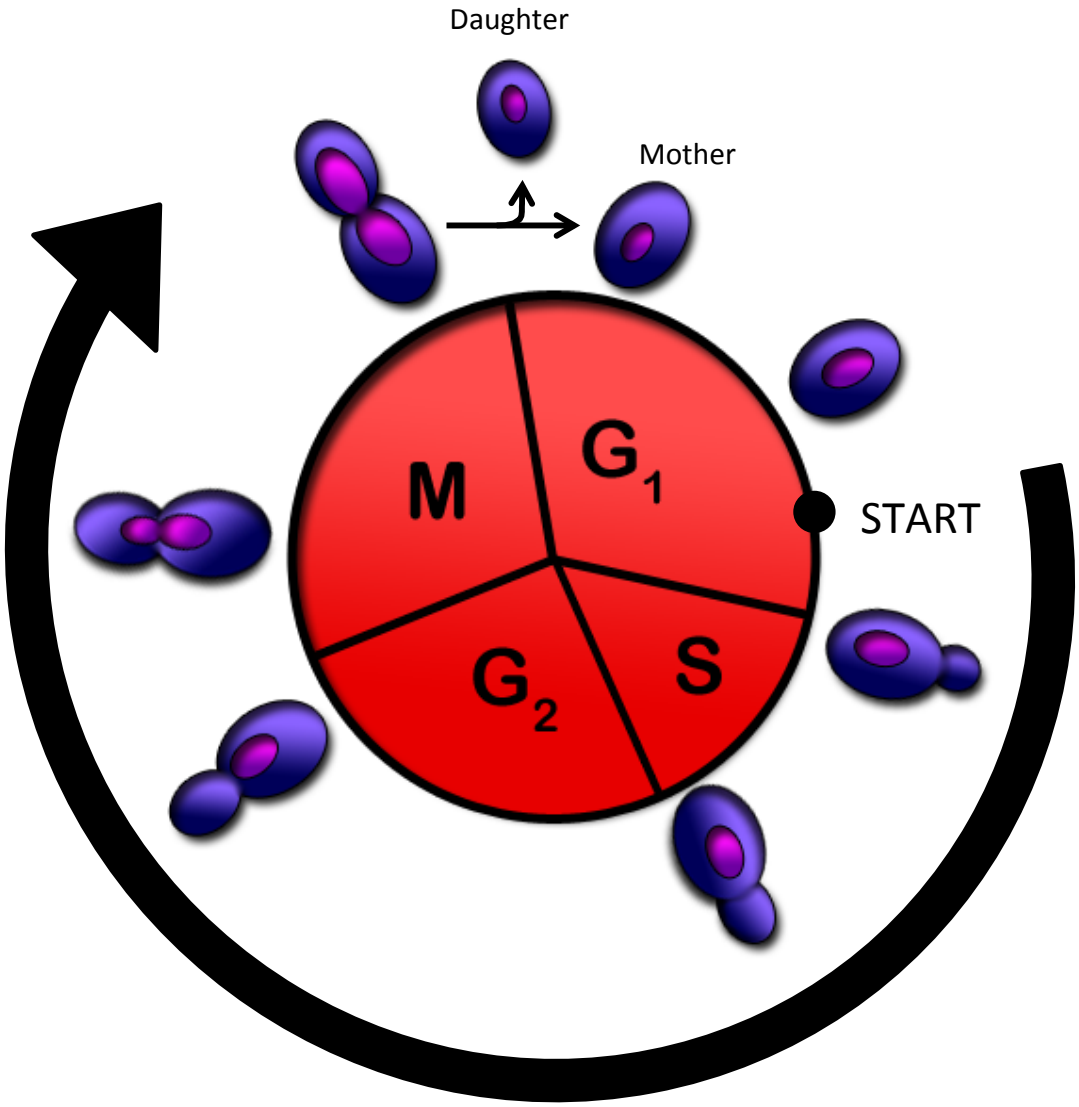

Figure 1.2. Cell cycle of *Saccharomyces cerevisiae*. Representation of the four cell cycle stages of a mitotic cycle. Once a G_1 cell passes START, it is irrevocably committed to DNA synthesis and cell division. Included in this schematic are the various stages of nuclear duplication and segregation, shown in magenta. Adapted from Herskowitz, 1988.

1.2.2 The Four Cell Cycle Stages

G_1 phase

Because the two most notable features of the cell cycle are DNA synthesis and mitosis, the periods of growth between them are known as "gap" phases. The first such phase is hence known as Gap1 or G_1. Yeast cells engaged in the mitotic cell cycle, i.e. those that are not in a quiescent G_0 state are primarily found to exist in G_1 phase. This division of time spent between phases, however varies amongst eukaryotes as well as between cell types (e.g., early embryonic cell cycles lack gap phases altogether). New daughter cells, once separated from mother cells begin in G_1 during which they increase in size and prepare for entry into S-phase.

Cells starved for a particular nutrient will arrest at a point after mitosis, but before bud emergence and DNA synthesis (Williamson and Scopes, 1960). Mutant analysis of a group of cell division cycle (Cdc) genes by Hartwell (1974) suggested that cells remain in G_1 until the sufficient accumulation of nutrients and factors necessary for duplication of the genome occurs. This actually represents exit from the division cycle into the non-proliferating G_0 state. Once conditions favouring DNA replication and cell division arise, cells re-enter the cell cycle at G_1, thus it can be thought to represent the beginning of the cell cycle. An extended generation or doubling time of cells in a population is intimately correlated with the preponderance of unbudded cells (Beck and von Meyenburg, 1968). This suggests that such unbudded cells (in G_1) have not yet reached a threshold amount of energy or molecular entities crucial for commencing the budding program and DNA synthesis (Kuenzi and Fiechter, 1969). While this may appear similar to exit from the cycle and entry into a G_0 state, it actually represents a prolonged G_1 as the cells continue

to grow. The ability of budding yeast cells to respond to extracellular stimuli such as the quality of their growth medium has been widely documented (reviewed in Johnston *et al*., 1979). Thus important molecular mechanisms exist linking cell growth, size and duration of G_1 phase. As previously mentioned, the crucial point at which the cell commits to entering a replicative cycle is known as START. Beyond this point, the mating response is inhibited and a cell treated with the appropriate mating pheromone (MAT**a** with α-factor) will undergo the steps of DNA synthesis and cell division before re-entering a new G_1 and arresting prior to START.

Cells synchronize growth and division such that the replicative cycle commences only after a threshold size has been reached (Mitchison, 1971). Molecular switches thus exist to impose this coordinated function (reviewed in Wells, 2002). One example is the mutual antagonism between the cyclin, Cln3 and the cyclin dependent inhibitor (CKI), Far1. Cln3 in association with the kinase Cdc28 activates transcription factors (MBF and SBF) that promote entry into the replicative stage of the cell cycle (De Bruin *et al*, 2004). Far1 inhibition of Cln3-Cdc28 is initially dominant such that cells are held in G_1. Cln3 accumulates linearly with cells growth, resulting in a shift in the balance between the reciprocal inactivation. At an appropriate size, Cln3 overcomes its inhibitor and "flips the switch" towards entry into S-phase (Fu *et al*., 2003; reviewed in Alberghina *et al*., 2004). Other similar switches exist in G_1 (as well at other cell cycle junctures) acting to maximize the coherence between cell size, entry into S phase and division. These are, of course, subject to external factors. Thus in nutrient-rich environments, cells assume larger G_1 sizes before budding to maintain cell size homeostasis and vice-versa (Fantes and Nurse, 1977).

Many of the Cdc mutants from budding and fission yeast observed by Hartwell (1974) and Nurse (Nasmyth and Nurse, 1981; Nurse *et al*., 1976), respectively, elucidated a series of switches that determined the transition from G_1 to S-phase. In large part, these consisted of kinase-dependent reactions acting on a complex of proteins assembled in early G_1, creating a trigger for the initiation of DNA replication. It is with this emphasis that we consider the events occurring in G_1 phase, namely the establishment of a pre-replicative complex (pre-RC). Discussed in detail in the following section, pre-RC assembly involves the equipping of origins of replication for eventual "firing" once the essential signals present themselves. Firing of the first origin marks the transition from G_1 to S phase of the cell cycle.

S phase

Once the switches maintaining a G_1 state are flipped by the activity of multiple Cdc28-dependent steps, the cell enters a stage in which its genome is duplicated. The synthesis of new strands of DNA is what gives this cell cycle stage its name. Beginning at origins of replication, the DNA double helix is unwound by a protein complex known as the helicase. The nucleotide sequence of the unwound single-stranded DNA is copied by a group of enzymes known as polymerases, each one performing a specific and crucial function. In order to prevent unwound DNA from re-annealing to its complementary strand, it is coated with the single strand DNA-binding protein, RPA (Wold, 1997).

Because initiation almost always starts between the two ends of a chromosome and because it is initiated bidirectionally, a structure known as a replication bubble is produced. This bubble increases in size as the two replication forks travel in opposing

directions. Considering one half of this bubble, a single replication fork travels towards one end of the chromosome. Although sites specifying replication origins are scattered throughout the genome, some remain dormant or are not fired before an already established fork passes though them, thus passively replicating them. DNA synthesis in yeast is semiconservative and semidiscontinuous. The former refers to the annealing of one nascent strand to one of the parental strands, creating two nascent-parental strand combinations for each section of the double helix being replicated. The semidiscontinuous nature of replication describes the manner in which replication occurs in only one direction, i.e. 5' to 3', referring to the polarity of DNA (Figure 1.3). A nucleotide is added to the 3' hydroxyl group at the end of a growing chain, creating a phosphodiester bond with its complementary base pair on the template. Before a nucleotide can be added to a nascent DNA strand, an initial primer sequence must be created and annealed to the region of the parental DNA at which replication will commence. The DNA polymerase α-primase complex synthesizes a short RNA-based primer complementary to a sequence on the parental strand. Polymerase pol-α extends this primer into a short stretch of DNA, which is then recognized by polymerase δ or ε, displacing pol-α. In order for either pol-δ or pol-ε to scan the template strand, actively replicating it, there is a requirement for a sliding clamp known as the proliferating cell nuclear antigen (PCNA) to tether it to the DNA. As is the case with many DNA clamps including the helicase, they require a loading mechanism. The eukaryotic PCNA clamp loader is RF-C. The double helix conformation of DNA is such that two complementary strands are anti-parallel, i.e. the 5' end of one is the 3' end of the other. Thus, as shown in Figure 1.3, when a replication fork is created, the two parental strands generated at a fork

will have opposing polarity. This is an important consideration, since as previously mentioned, polymerases will only replicate processively in a 5' → 3' direction. Thus, only one of the exposed template strands can be replicated continuously, in the same direction as the moving replication fork. The newly synthesized DNA copied off this strand grows uninterrupted as the parental strand is unwound and is known as the leading strand. Once the primer synthesized at the 3' end of the parental strand is recognized by pol-ε, the leading strand is replicated by processively by it. Because the other template strand has a 5' → 3' polarity as it is unwound, the polymerase (pol-δ in this case) cannot replicate it processively towards the start of the fork. Instead, as this parental strand is unwound, synthesis of the nascent strand must wait until a substantial length of the template is exposed. For this reason, the newly synthesized strand is known as the lagging strand. Primers are synthesized as new template DNA becomes available and as in the case of the leading strand, are recognized by the appropriate polymerase. Along with PCNA, the pol-δ slides along the short stretch of template DNA, away from the replication fork, replicating it in the correct 5' → 3' manner until it reaches the start of the adjacent primer. The short semidiscontinuous stretches of lagging strand DNA are known as Okazaki fragments. Pol-δ's exonuclease activity removes the multiple primers on the lagging strand and the Okazaki fragments are joined by DNA ligase.

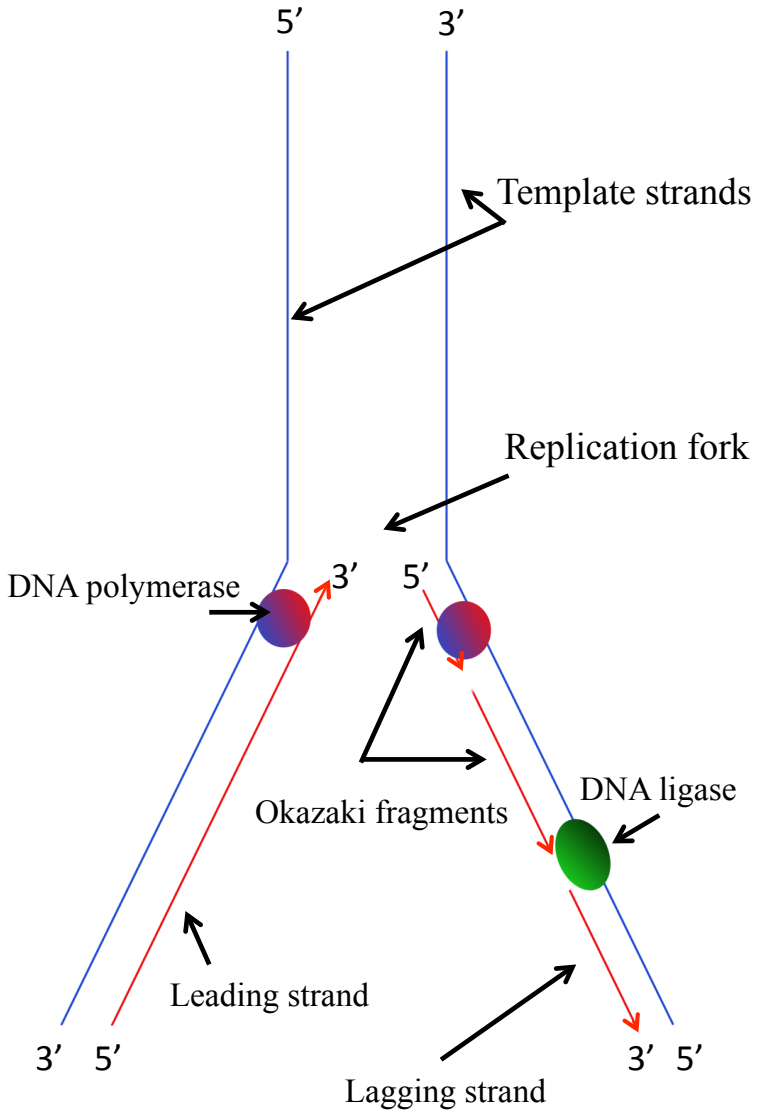

Figure 1.3. Activities at a DNA replication fork. When DNA is unwound at a replication fork, it creates two parental template strands. Due to the anti-parallel nature of the double helix, each of these strands will be in opposing orientations. Because DNA polymerase can only synthesize DNA in a 5' to 3' direction, only one of the nascent strands can be replicated processively as a continuous stretch (leading strand). The other parental strand will be replicated discontinuously as short stretches called Okazaki fragments. These fragments are later ligated to form a continuous strand of DNA. Adapted from ch. 20 of Weaver, 1999.

As each fork traverses the chromosome, the unwinding activity of DNA helicase builds up torsional strain in the double helix as a result of its rotation. Topoisomerases relieve the strain in supercoiled DNA by creating temporary nicks. In addition to allowing replication to proceed undeterred, this helps to avoid the entanglement of double stranded DNA ahead of the helicase and the newly synthesized double helix (Dickerson, 1983; Garg and Burgers, 2005; Weaver, 1999).

In order for a cell to duplicate its genome with high fidelity and create a flawless genetic copy, it must reduce the potential errors in base pair matching during replication. This is apart from the threat of spontaneous mutation and must be highly surveyed to avoid lasting errors in the DNA sequence. Deleterious mutations in the genome would ostensibly be passed down to future generations and might encode lethal alleles or proteins of compromised function. The maintenance of replication fidelity in multicellular organisms is paramount to avoiding cancerous mutations or those associated with developmental or neurodegenerative disorders. Yeast polymerases are believed to pair the wrong nucleotide once every 10^4-10^6 base pairs. To correct for this error, they possess proofreading mechanisms to limit misincorporated base pairs. Pol-δ and pol-ε both have 3' exonuclease activity that removes 90% – 99.99% of erroneous base pair mismatches (Kunkel, 2004). Over and above this, the cell possesses post-replication repair pathways such as mismatch repair (MMR) and base-excision repair (BER) which when combined greatly reduce the potential for deleterious mutations during replication (Nickoloff, 1998; Scheuerman and Echols, 1984). MMR has been estimated to correct between 97% – 99.8% of mismatches (McElhinny *et al*., 2010), while BER improves the fidelity of replication by 2-3 fold resulting in an overall error frequency of approximately

10^{-9} (Kunkel, 2004). At the replication fork, the polymerases acting on either strand form a coordinated unit with each other and with accessory proteins. Collectively this is known as the replisome.

G_2 phase

Once chromosomes are replicated and cells, by this definition exit S-phase, the cell continues to grow in size. It must, however be sure to prevent chromosomal segregation (in the following M-phase) as long as unreplicated chromosomes or DNA damage artefacts remain. If these are found to be lacking, the cell passes quickly through G_2. Thus this stage serves as a gap (as in Gap 2 phase) between S and M phases. The two nuclei generated in S-phase part within the mother during G_2, with one of them migrating to the bud (Kormanec *et al*., 1991). Because spindle formation occurs in S-phase, there is significant overlap between the period of DNA synthesis and chromosomal segregation arguing for a practically insignificant G_2 phase is budding yeast (Nurse, 1985).

M phase (Mitosis)

The chromosomes having being duplicated in S-phase are ready for equal segregation between mother and daughter cell. As a result of replication two identical copies of each chromosome (sister chromatids) are generated and are initially connected via a structure known as the centromere. Before progressing, cellular surveillance mechanisms verify that replication has been correctly executed, or that errors have been dealt with. Once these checkpoint conditions are satisfied, the mitotic phase is devoted to the separation of sister chromatids and their localization to opposite poles. At the centromere, each

chromatid possesses a point of attachment for microtubules called a kinetochore. In yeast, the microtubule-organizing centre is known as the spindle pole body (SPB). Because the nuclear membrane remains intact in the mitotic cell cycle of yeast (a "closed mitosis"), the SPB remains embedded within the nucleus. Since the commitment to cell division occurs at START, the SPB duplicates as early as this point in G_1 in anticipation of its role in mitosis. Thus, two SPBs migrate to opposing poles of the nucleus as early as S-phase and establish a network of interdigitating microtubules. The bipolar spindle created as a result assumes an active role in mitosis, acting as a scaffold whose function is to align and separate sister chromatids equally between mother and daughter cells (Nasmyth, 1995). This is essential to ensuring that each cell has exactly one copy of the genome. The events of mitosis are divided themselves, into four stages: prophase, metaphase, anaphase and telophase.

In prophase, chromatin becomes more organized and condenses into chromosomes, visible under a light microscope. Kinetochores of each sister chromatid are bound by opposing microtubules during the early stages of metaphase. Some microtubules of the spindle do not bind to the chromatids; rather they associate with their polar counterpart from the opposing SPB. At this point the spindle becomes distinct and ATP-dependent molecular motors associated with the microtubules direct the pulling apart of sister chromatid kinetochores by the two polar SPBs. Tension is created along the mitotic spindle causing the chromosomes to become aligned along the metaphase plane, equidistant from either pole. During this stage, any unattached kinetochores signal that proper alignment has not occurred. This invokes a molecular cascade known as the mitotic spindle checkpoint, which blocks progression into anaphase.

Chromatids are held together at their kinetochores by ring-like structures known as cohesins (Nasmyth and Haering, 2005). Given the proper signal (see "anaphase-promoting complex" in section 1.2.3) cohesins are cleaved by the protease separase, triggering sister chromatid disjunction (Uhlmann *et al*., 2000). Marking the start of anaphase, the non-kinetochore bound microtubules extend creating a force that pushes each SPB to the opposite end of the now-elongated and budded cell (Segal and Bloom, 2001). The now freed sister chromatids, attached to microtubules of opposing SPBs are pulled apart and towards different poles. The mother and the daughter cell/bud thus receive an exact complement of the genome. At the end of M phase (telophase) the spindle disintegrates and the nucleus splits into two nuclei, one remaining in the mother cell and the other migrating to the daughter (Winey *et al*., 2001). Finally, chromosomes relax into uncondensed chromatin.

The final step in cell division is the actual separation of the common plasma membrane between mother and daughter cell, called cytokinesis. It is essential that chromosomes are correctly segregated between the two cells to avoid aneuploidy or polyploidy. Early in G_1, a group of GTP-binding proteins known as septins form a cytoskeletal framework for establishing the asymmetric division (daughter cells are smaller than their mothers; Chang and Peter, 2003). At the onset of bud emergence, the septins form a ring around the bud neck to provide structure and to establish a diffusion barrier between the two cells. This imparts a polarity to the growing budded cell demarcating two separate cellular compartments (reviewed in Caudron and Barral, 2009). Another feature of the bud neck is a contractile actomyosin ring, which through

ingression creates a cleavage furrow, separating the membranes of mother and daughter (reviewed in Glotzer, 2005).

1.2.3 Regulatory Mechanisms and Cell Cycle Control

Fundamental to the proper chronological execution of these phases is a family of proteins called cyclins, so named for their cyclical fluctuations in expression, which ultimately dictate the activation of key cellular modifiers. They work in conjunction with specific kinases forming active complexes that stimulate crucial events. In *S. cerevisiae*, the N-type cyclins (Clns) are the first to act with Cln3 being expressed early in G_1, as mentioned earlier. Like all other budding yeast cyclins, Cln3 is a regulatory subunit of a major kinase that regulates the cell cycle, Cdc28 (Lew and Kornbluth, 1996; Nasmyth, 1993 and 1996). Cdc28 is thus known as a cyclin-dependent kinase (CDK) although this abbreviation generally refers to its active form (a cyclin-Cdc28 complex). In order to transition from G_1 to S phase, the attainment of various protein concentration thresholds must be met. This represents one of the molecular switches that coordinate cell growth and division, previously discussed. Early in G_1, Cln3 concentration increases with cell mass. Cln3 and the protein Far1 are mutually antagonistic, however as cell growth proceeds, Cln3 levels eventually surpass a threshold (Henchoz *et al*., 1997). The resulting level of active Cln3-Cdc28 promotes the expression of G_1 transcription factors. This leads to the accumulation of cyclins Cln1 and Cln2 and sets the stage for S phase entry (Alberghina *et al*., 2004; Cosma *et al*., 2001; Dirick and Nasymth, 1991; Tyers *et al*., 1993). A second molecular switch involves the transcription and expression of the B-type cyclins (Clbs), Clb5 and Clb6, which also form individual complexes with Cdc28.

Transcriptional activation of *CLB*5, *CLB*6 as well as of *CLN*1 and *CLN*2 is mediated by transcription factors MBF (Mbp1-Swi6) and SBF (Swi4-Swi6), they themselves being expressed through Cln3-Cdc28 activity (Hadwiger *et al*., 1989; reviewed by Koch and Nasmyth, 1994).

Clns are essential for promoting exit from G_1 by activating Cdc28 and by inhibiting the CDK inhibitor (CKI), Sic1 (Calzada *et al*., 2001). The accumulation of Cln1 and Cln2 to threshold concentrations defines the exact point at which the cell makes the irreversible decision to divide, i.e., START (Dirick *et al*., 1995). The activated Clb5-Cdc28 complex is tasked with triggering the initiation of DNA replication (reviewed in Nasmyth, 1996). Clb6-Cdc28 has an overlapping role and while Clb6 shares functional homology with Clb5, cells lacking Clb5 cannot initiate replication as efficiently as Clb6Δ cells (Schwob and Nasmyth, 1993; Schwob *et al*., 1994). *CLB*3 and *CLB*4 transcripts appear near the start of S-phase and are present until late anaphase (Fitch *et al.*, 1992). While their protein products are able to partially replace the roles of Clb5 and Clb6 in initiation, they are mainly associated with triggering the formation of the mitotic spindle (Richardson *et al*., 1992). Clb1 and Clb2 are required for entry into mitosis, however Clb2 alone is sufficient (Surana *et al*., 1991). Its activity is necessary throughout M phase as it orchestrates the transition from metaphase to anaphase via the degradation of Pds1 and phosphorylation of components of the anaphase promoting complex or APC (Rahal and Amon, 2008). One outcome of these activities is the promotion of sister chromatid disjunction as cohesin is cleaved in the absence of Pds1. The fluctuating levels of cyclins over the course of the cell cycle are depicted in Figure 1.4.

The APC is an E3 ubiquitin ligase charged with targeting numerous cell cycle proteins for degradation, Clb2 being among them (Irniger *et al*., 1995). Its two cofactors, Cdh1 and Cdc20 regulate its target specificity. APC^{Cdc20} is activated by Clb2 (Shirayama, 1998), while APC^{Cdh1} formation is inhibited by it (Zachariae, 1998). Cdc14 phosphatase reverses inhibition of APC^{Cdh1}, which plays an important role in establishing the G_1 state (Azzam *et al*., 2004; Jaspersen, 1999; Zachariae, 1998; Zachariae and Nasmyth, 1999). Pds1 binds Esp1, a protein that binds to and cleaves cohesin. The destruction of Pds1 by APC^{Cdc20} removes the former's inhibition of Esp1, which is then able to perform its role in cleaving cohesin (Ciosk *et al.*, 1998; Schwab *et al*., 1997; Visintin *et al*, 1997). As discussed before, this results in the separation of sister chromatids and an exit from mitosis (Uhlmann *et al*., 1999). A main characteristic of the regulatory coordination of cell cycle activities by CDK is its mutual antagonism with CKIs and APC isoforms.

Whereas APC destroys the regulatory cyclins, CDK inactivates the APC via phosphorylation. Clb2-Cdc28 and Clb5-Cdc28 phosphorylate and inactivate Cdh1 (Zachariae *et al*., 1998). APC^{Cdh1} reciprocally contributes to Clb2 degradation amongst other mitotic cyclins (Burton *et al*., 2001; Hendrickson *et al*., 2001; Pfleger and Kirschner, 2000; Schwab *et al*., 2001). Inactivation of Cdh1 allows the accumulation of Clb2, which turns off MBF- and SBF-dependent transcription and creates an active APC^{Cdc20} complex. Representing a feedback loop, APC^{Cdc20} ubiquitinates both Clb2 and Clb5, targeting them for destruction (Glotzer *et al*., 1991; Irniger & Nasmyth 1997; Shirayama *et al*., 1999). This is significant as the levels of cyclins that promote mitosis (Clb2) and that inhibit G_1 proteins (Clb5) are reduced towards the end of M phase, promoting a G_1-stable state for the ensuing cell cycle.

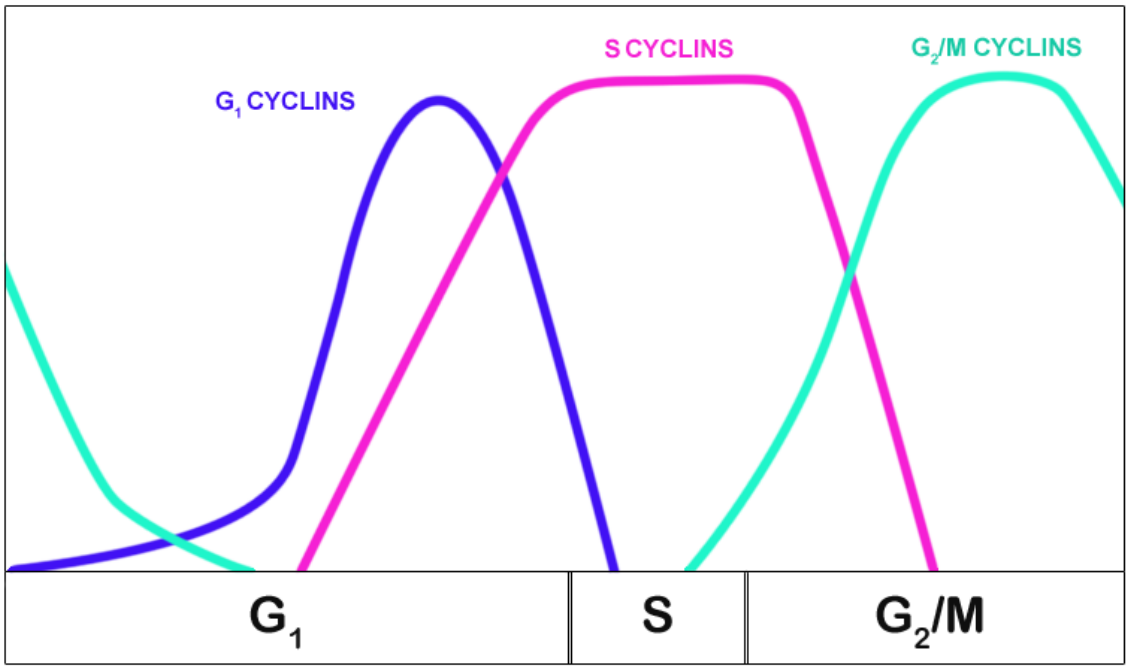

Figure 1.4. Fluctuations in cyclin levels mediate ordered passage through the cell cycle. Cln3 levels increase in early G_1 leading to the transcription of Cln1 and Cln2 (G_1 cyclins). This overcomes a threshold that allows the accumulation of Clb5 and Clb6, which are responsible for entry into S phase (S cyclins). Clb3 and Clb4 promote spindle assembly while Clb1 and Clb2 contribute to passage into and through mitosis (G_2/M cyclins). Adapted from Nasmyth, 1996.

1.2.4 Cell Cycle Checkpoints

The timely and thorough replication of the genome as well the separation of mother and daughter cells with identical genetic information, are processes careful overseen by the cell's regulatory machinery. Checkpoints represent a network of surveillance mechanisms present at various junctures throughout the cell cycle. If damage to the DNA is detected at these points in the cell cycle, repair mechanisms are brought into action to restore genomic integrity and to ensure that mutations are not propagated to the next generation (reviewed in Elledge, 1996 and Hartwell and Weinert, 1989). DNA damage can occur by naturally occurring errors in replication or by exogenous insults. Robust checkpoint mechanisms halt cell cycle progression until adequate repair can take place. Multiple protein factors have been well characterized to be chiefly responsible for ensuring the repair of DNA and the stabilization of stalled replication forks, depending on the nature of the checkpoint arrest (Nyberg *et al*., 2002). Although the checkpoint programs are functionally conserved in budding yeast, fission yeast as well as higher eukaryotes, this section will focus on the checkpoint functions of *Saccharomyces cerevisiae*.

The two main types of DNA damage are double-strand breaks (DSBs) and the more common single-strand breaks (SSBs). Left untreated, they lead to genomic instability and errors in completing replication and/or mitosis (reviewed in Cann and Hicks, 2007 and Ismail *et al*., 2005). This includes the segregation of damaged chromosomes with a faulty genetic blueprint. Checkpoints are invoked when DNA damage is sensed. Their function is to halt the cell cycle, promote repair and aid in recovery once the damage has been successfully dealt with (reviewed in Harrison and Haber, 2006). A host of protein factors mediate checkpoint responses, categorized as

sensors, transducers and effectors. Sensors, aptly named, detect damage, relay the signal via transducer-mediated signal cascades to effectors, which are usually kinases that activate or inactivate downstream targets (reviewed in Kolodner *et al*., 2002).

Endogenous cellular processes such as oxidation (in the form of reactive oxygen species), alkylation of base pairs and hydrolysis can themselves cause damage to the DNA. Extrinsic insults in the form of ultraviolet (UV) light, ionizing radiation (IR) and alkylating agents are potent genotoxic threats (reviewed in Hakem, 2008). Exposure to these as well as chemical agents such as bleomycin can cause single-stranded as well as double-stranded breaks in the DNA. SSBs often result in replication fork collapse and generation of a double-strand break. Genotoxic agents such as methyl methanesulfonate (MMS), phleomycin and campothecin exclusively produce DSBs, which are processed by several mechanisms including non-homologous end joining (NHEJ) and homologous recombination (Chu, 1997; reviewed in Borde and Cobb, 2009). Because each successive event in the cell cycle in dependent on the completion of a previous step, a system to monitor the successful execution of these steps, ensuring fidelity of the genome at various points exists. Three temporally separated checkpoints are invoked at disparate points during the cell cycle, giving rise to the G_1/S, intra-S and G_2/M DNA damage checkpoints.

Due to the G_1/S checkpoint response, cell cycle arrest occurs before entry into S phase if damage is detected in G_1, even past START. An elaborate coordination of checkpoint factors occurs as a result, with many of the same proteins charged with repairing damaged DNA during S phase in response to unreplicated DNA and production of lesions, representing the intra-S phase checkpoint (Longhese *et al*., 1998, Zegerman and Diffley, 2010). Finally, before segregation of the chromosomes, genomic integrity is

once again verified at the G_2/M checkpoint. A second S-phase specific checkpoint is activated when the process of DNA replication is impeded by lesions, stalled forks or other physical perturbations to the normal structure of the DNA or to the replication machinery. This is called the DNA replication checkpoint (Lopes *et al*., 2001). Lastly, before cell division, the spindle assembly checkpoint arrests the cells if chromosomes have not been properly segregated (Visintin *et al*., 1999).

In order to study these checkpoints, various genotoxic agents are used to precipitate DNA damage for experimental purposes. Amongst the most well known and employed for studying these processes are hydroxyurea (HU), a ribonucleotide reductase inhibitor and MMS, mentioned above. The former reduces the pool of nucleotides causing fork stalling (discussed in Koç and Wheeler, 2004), while MMS induces DNA lesions, which may be further exacerbated when left unrepaired (Lundin *et al*., 2005). These threats are corrected by the repair mechanisms described below.

DNA Damage Checkpoints

The two main sensors at the apex of the G_1 and intra-S DNA damage checkpoints are Mec1 and Tel1 (ATM and ATR in higher eukaryotes). Mec1 has a predominant role in sensing damage and relaying the checkpoint signal downstream (Friedel *et al.*, 2009; Navadgi-Patil and Burgers, 2009). In the event of DNA damage, single-stranded (ss) DNA is generated as a result of an SSBs or DSBs. The recruitment of the ssDNA-binding protein RPA to coat these lesions follows, a process mediated by its interaction with Ddc2. Mec1 is regulated by Ddc2, and recruited to sites of DNA damage through the Ddc2-RPA association (Rouse and Jackson, 2002; Zou and Elledge, 2003).

The 9-1-1 checkpoint clamp (Ddc1-Mec3-Rad17, so named after the mammalian homologues Rad9-Rad1-Hus1) is loaded onto sites of DNA damage where it recruits additional repair factors. This is promoted by the phosphorylation of Ddc1 by Mec1, which also phosphorylates RPA and histone H2A. Although a target of Mec1, the 9-1-1 clamp is an activator of Mec1, as is the adaptor protein Dpb11 (Majka *et al.*, 2006; Mordes *et al.*, 2009; Navadgi-Patil and Burgers 2008, 2009 and 2011). DNA damage induces phosphorylation of Ddc1, which only then associates with Dpb11 (Furuya *et al.*, 2004; Puddu *et al.*, 2008). Mec1 is auto-activating in that the Ddc1-Dpb11 interaction it stimulates strengthens its own recruitment to the chromatin. H2A phosphorylation occurring as a result then promotes recruitment of the mediator protein Rad9 (Giannattasio *et al.*, 2005; Huyen *et al.*, 2004; Nakamura *et al.*, 2004).

Rad9 has been shown to be alternatively recruited by a complex formed by 9-1-1 and Dbp11, an interaction dependent on phosphorylation of Rad9 by CDK (Furuya *et al.*, 2004; Pfander and Diffley, 2011; Puddu *et al*., 2008). In either case, activation of Rad9 by Mec1 ensues, attracting the Rad53 kinase, which binds to Rad9 phosphorylated residues through its characteristic FHA domains (Schwartz *et al*., 2002). Through its Rad9 association, Mec1 phosphorylates Rad53, activating it (Gilbert *et al*, 2001; Sweeney *et al*., 2005; Usui *et al*., 2009). As a key checkpoint effector, active Rad53 is then localized to its multiple downstream substrates. These interactions are depicted in Figure 1.5.

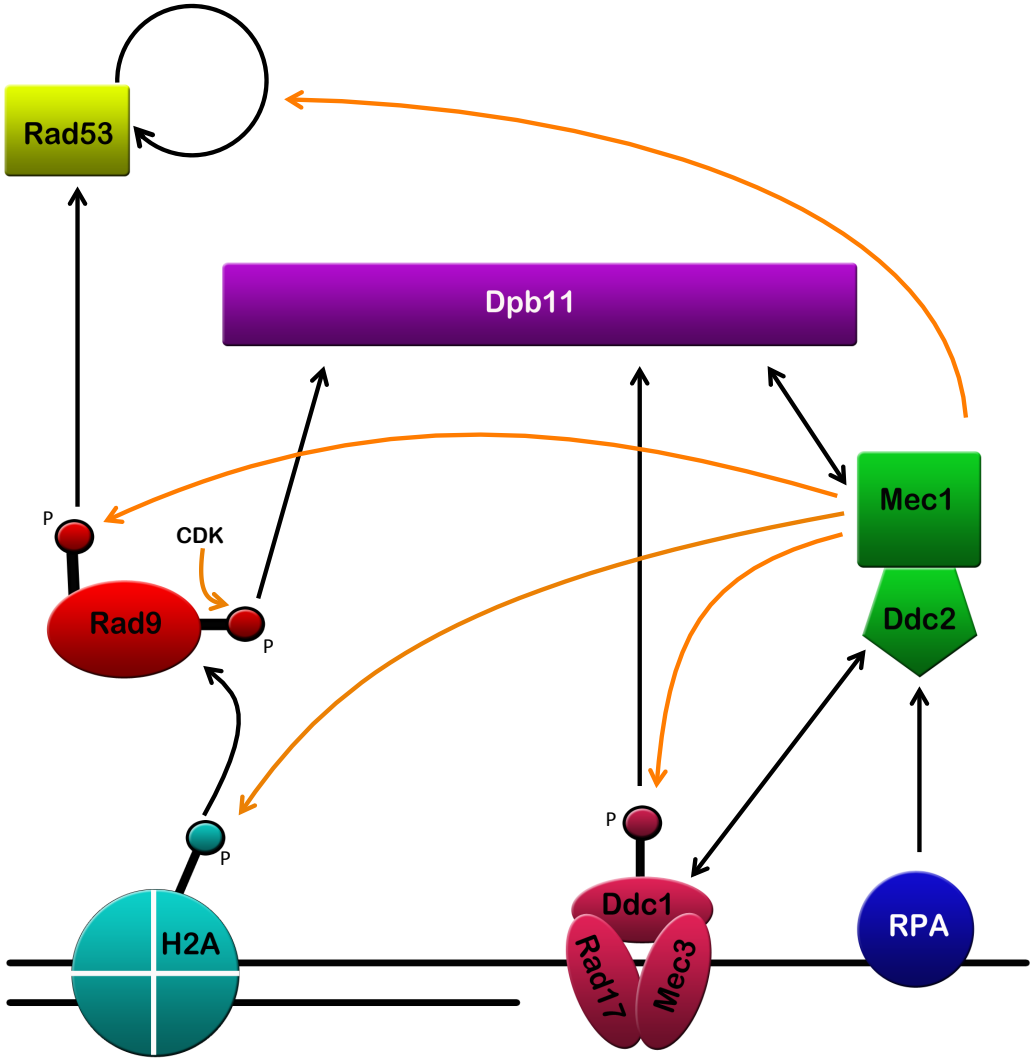

Figure 1.5. Schematic of the factors involved in the checkpoint response. Ddc2 and Dpb11 activate the sensor kinase Mec1. This results in Mec1 phosphorylation of Ddc1 of the 9-1-1 complex, histone H2A and Rad9. Mec1 is localized to damaged chromatin via the interaction between Ddc2 and RPA, which binds to single stranded DNA created as a result of damage. Dbp11 and the active 9-1-1 complex interact to strengthen the activity of Mec1 at sites of DNA damage as well as to recruit Rad9 via a CDK-dependent mechanism. Rad9 then recruits the Rad53 kinase, subsequently phosphorylated by Mec1. Rad53 when activated is capable of auto-activation, enhancing the checkpoint response. Downstream targets in this pathway such as Rad9 and Rad53 are also activated by another sensor kinase, Tel1, however the intermediary steps involved in activating these targets is not shown. Interactions are shown in solid black arrows (mutual recruitment by double-ended arrows), while orange arrows indicate phosphorylation. Circles marker by "P"s represent phosphorylation of the corresponding protein. Adapted from Pfander and Diffley (2011).

*MEC*1 mutants show defects in cell cycle arrest and response to DNA damage. Initial studies demonstrated that the *tel*1Δ mutant does not confer sensitivity to DNA damage or inhibition of DNA replication, however *mec1tel1* double mutants showed a more dire phenotype than *mec*1 mutants alone (Morrow *et al*., 1995; Sanchez *et al*., 1996; Weinert *et al*., 1994). Later investigations implicated Tel1 as having a more prominent role in regulating damage at telomeres, however like Mec1, its deletion resulted in gross chromosomal rearrangements suggesting that the two kinases are in fact functionally redundant for at least some forms of DNA damage (Craven *et al*., 2002; Myung *et al*., 2001). Although Tel1 acts in a parallel pathway to Mec1, activating similar effectors such as Rad9 and Rad53, it does not require activation by Ddc1 or Dpb11. Rather, its activation and ability to orchestrate DNA damage repair is contingent upon its association with a complex comprised of the factors Mre11, Rad50 and Xrs2 (Giannattasio *et al*., 2002; Nakada *et al*., 2003).

At the G_2/M checkpoint, similar mechanisms are invoked although additional proteins have been implicated. A general model posits that Rad9 and Rad24 detect DNA damage with the signal being transduced to Mec1 and consequently the effector kinases Rad53 and Dun1. Pds1, an anaphase-metaphase regulator implicated in the mitotic spindle checkpoint is similarly activated by Mec1. Cells are prevented from entering mitosis until DNA damage is repaired. The repair mechanisms at this checkpoint are similar to those of the G_1/S and intra-S checkpoints, however involve two parallel pathways – a Rad53/Dun1 pathway where each kinase has an equal contribution towards the G_2/M arrest and a pathway solely involving Pds1 (reviewed in Gardner *et al*., 1999).

DNA Replication Checkpoint

The DNA replication checkpoint is similar to the DNA damage checkpoint in the commonality of factors comprising the pathway. Nevertheless some differences exist such as the identity of the Mec1-activating factor. Whereas Rad9 performs this function in the DNA damage pathway, Mrc1, a replication fork member activates Mec1 at stalled replication forks (Alcasabas *et al*., 2001). This highlights another key difference between the two mechanisms – repair during replication takes place at initiated forks that have stalled. The fact that Mrc1 moves with the fork precludes the requirement for its localization to sites of damage (Katou *et al*., 2003; Osborn and Elledge, 2003). While the Mec1 activators Ddc1 and Dpb11 can perform the same function as they do in DNA damage repair, it has been suggested that they are not essential for Mec1 activation at stalled forks (Navadgi-Patil and Burgers, 2009; Puddu *et al*., 2011). Berens and Toczyski (2012) demonstrated that Mec1 is able to phosphorylate Rad53 in the absence of the activating factors Ddc1 and Dpb11. Mrc1, in high concentrations at stalled forks is also phosphorylated by Mec1 (independent of Dpb11 and Ddc1), further promoting Rad53 association. This represents positive feedback as Rad53 accumulation promotes additional activation of Mrc1 by Mec1.

Active Rad53 exerts its checkpoint function in a number of ways. Genes encoding DNA repair proteins are transcribed at a greater rate. This occurs primarily through the inhibition of the gene suppressor Crt1 by Rad53, Mec1 and Dun1 (Huang *et al*., 1998). The firing pattern of the numerous origins of replication is temporally divided into three categories – early-, middle- and late-firing. The inhibition of late-origin firing in cells exposed to DNA-damaging agents has been well documented (Santocanale and Diffley,

1998; Shirahige *et al*., 1998; Tercero and Diffley, 2001). The rate of fork progression is reduced in response to DNA damage (Paulovich and Hartwell, 1995), however this may be an indirect result of structural damage impeding the fork as opposed to a direct checkpoint-induced slowdown. A rationale for late-origin inhibition by the checkpoint is the potential repository of intact, unfired and competent origins, should stalled forks collapse (Santocanale and Diffley, 1998). The mechanism for origin-firing inhibition has been elucidated by Zegerman and Diffley (2010) who showed that Rad53 targets the replication proteins Dbf4 and Sld3. Hypersensitivty to genotoxic stress is observed in Dbf4 mutants and those of the kinase it regulates, Cdc7 (Pasero *et al*. 1999 and 2003; reviewed in Sclafani 2000). Sld3 phosphorylation renders it unable to interact with its replisome partners, Cdc45 and Dpb11.

The DNA replication checkpoint thus performs its role by slowing late origin firing, reducing the rate of fork progression and mediating repair gene transcription. Its most critical function, however is postulated to be the stabilization of replication forks through Mec1 and Rad53 activity (Branzei and Foiani, 2009; Lopes *et al*., 2001; Paulovich and Hartwell, 1995) and their subsequent restart upon damage repair, mediated by Rad53 and the Dbf4-dependent kinase complex, DDK (Jones *et al*., 2010; Szyjka *et al*., 2008; Varrin *et al*., 2005). A recent study by de Piccoli *et al*. (2012) challenges the inference that the checkpoint kinases Rad53 and Mec1 stabilize forks by maintaining integrity of the replisome (the assembly of proteins that unwinds and replicates DNA at replication forks). Their roles in fork stability remain to be elucidated.

An *S. pombe* model suggests that upon fork arrest, the helicase activity of the Mcm2-7 complex is uncoupled from its role in further DNA replication such that it creates a small

amount of ssDNA. RPA binds this, triggering the localization of Rad53 via the mechanisms previously described. Phosphorylation of Mcm2-7 occurs contributing to one of several fork stabilization mechanisms (Forsburg, 2008).

Resumption of replication occurs after the DNA damage has been repaired. This fork recovery is essential for genomic stability and successful completion of S phase (reviewed in Tourrière and Pasero, 2007). Replication fork stalling also occurs in an unperturbed S phase (Deshpande and Newlon, 1996) and a role for Dbf4 in replication fork restart may aid cells in overcoming intrinsic as well as extrinsic damage (Varrin *et al*., 2005). As discussed, during an S phase checkpoint, Rad53 phosphorylates Dbf4, removing it from chromatin (Pasero *et al*., 2003; Weinreich and Stillman, 1999; Zegerman and Diffley, 2010). This is dependent on a physical interaction between Rad53 and the N-motif of Dbf4 (Duncker *et al*., 2002). A Dbf4 C-terminus mutant showed sensitivity to long-term exposure to MMS and HU concomitant with a weakened interaction with Mcm2 (Jones *et al*., 2010). No effect on viability was observed, however when exposed to short term doses of the genotoxic agents raising the possibility that Dbf4 plays a role in fork restart via its interaction with Rad53 and Mcm2. This might occur by resumption of its role in initiation, via DDK phosphorylation of Mcm2-7 or other targets, identified *in vitro* such as Cdc45 and pol α (Nougarède, Della Sera *et al*., 2000; Weinreich and Stillman, 1999). Other hallmarks of the checkpoint, such as the phosphorylation of histone H2A may increase accessibility of factors to chromatin to aid in fork restart (Cobb *et al*., 2005).

Spindle Assembly Checkpoint

The mitotic spindle assembly checkpoint is invoked by improper or lack of attachment of chromosomes to the spindle. The checkpoint protein Mad2 inactivates APC^{Cdc20} preventing the cell from premature mitotic exit (Hwang *et al*., 1998; reviewed in Amon, 1999). Correct chromosome alignment ensures proper spindle attachment, which triggers the exit from the nucleolus of the phosphatase Cdc14, normally sequestered by a competitive inhibitor and regulator of anaphase, Net1. This release is promoted by active APC^{Cdc20}, representing its function in the exit from mitosis (Jaspersen *et al*., 1999; Shou *et al*., 1999; Visintin *et al*., 1999). APC^{Cdc20} stimulates the Tem1 GTPase-dependent activation of Cdc15 kinase, which in turn precipitates the release of Cdc14 via Net1 phosphorylation (Rock and Amon, 2011; Visintin *et al*., 2003). Cdc14 acts on targets such as Esp1 (discussed earlier), marking the end of the mitotic exit network (MEN). The G_1-specific transcription factor Swi5 is kept inactivated by Clb2-dependent phosphorylation (Nasmyth *et al*., 1990). Once Clb2 levels have been reduced and Cdc14 levels rise via the mechanisms described above, Swi5 and Cdh1 are active, CDKs are inhibited and CKIs are allowed to accumulate creating conditions ripe for a new G_1-phase (Visintin *et al*., 1998).

1.3 DNA Replication

1.3.1 Overview

A highly complex regulatory system controls passage from START through S phase, cell division and eventually sets the stage for a new G_1 phase. Once cells commit to division, passing the "point of no return", i.e. START, an ordered set of molecular events is initiated to accomplish the following:

1) Identification of genomic loci from which replication forks will arise, known as origins of replication

2) Establishment of a multi-protein molecular machine tasked with loading the DNA helicase at origins

3) Activating the helicase, thus promoting unwinding of the DNA

4) Facilitating the action of DNA polymerases, which travel with replication forks with associated factors to faithfully replicate the entire genome

5) Preventing these steps from recurring until the next G_1 phase in order to avoid copying the DNA more than once (thus maintaining one copy of the genome per cell)

The details of this cellular program are described below.

1.3.2 Origins and the pre-Replicative Complex

In eukaryotes, a functionally-conserved heterohexameric protein complex, ORC (Origin Recognition Complex), acts as a selector for origins of DNA replication (Dutta and Bell, 1997; Bell and Stillman, 1992; Li and Herskowitz, 1993; Aparicio *et al*., 1997 and Tanaka *et al*., 1997). While this selection process is poorly understood in higher eukaryotes, budding yeast ORC acts in a highly DNA-sequence-specific manner. Regions known as autonomously replicating sequences (ARSs) are target sites for the binding of this complex. Each contains a highly conserved 11 bp ARS consensus sequence (ACS or A-element) distinguishing budding yeast from other eukaryotes in that its origins are highly sequence-specific. The ARS acts as the binding site for ORC**,** which associates with chromatin throughout the cell cycle (Aparicio *et al*., 1997; Liang and Stillman, 1997). ORC bound to origins serves as a scaffold for the association of a number of additional replication factors, culminating in the formation of the pre-replicative complex or pre-RC (Figure 1.6). Although only Orc1-5 are essential for DNA binding (Lee and Bell, 1997), Orc6 is essential for cell viability (Li and Herskowitz, 1993) and plays a role in maintaining the pre-RC in late G_1 (Chen *et al*., 2007; Semple *et al*., 2006). The protein encoded by the CDC6 gene is also essential and is required for initiation via its crucial role in loading the heterohexameric MCM (minichromosome maintenance) complex onto origin DNA (Aparicio *et al*., 1997; Bowers *et al*., 2004 and Speck *et al*., 2005).

The six subunits, Mcm2-7 form an active complex that acts as the replicative helicase (Labib and Diffley, 2001; Tye and Sawyer, 2000). Formed in the cytoplasm, the complex is co-transported to the nucleus with Cdt1 and is recruited to the pre-RC (Nishitani *et al*., 2000; Tanaka and Diffley, 2002; Wu *et al*., 2012). This is promoted by a

direct interaction between Orc6 and Cdt1, representing the essential function of Orc6 (Chen *et al*., 2007).

In relatively high abundance, only a fraction of Mcm2-7 complexes are recruited to origins (Donovan *et al*., 1997; Liang and Stillman 1997; Mendez and Stillman, 2000) and an even more restricted subset participate in replication forks (Edwards *et al*., 2002; Gambus *et al*. 2006; Ge *et al*., 2007). While approximately twenty MCM complexes are recruited per origin, between two to four are tightly "loaded" to subsequently unwind the DNA bidirectionally and provide access to the DNA polymerases. The establishment of a pre-RC with loaded Mcm2-7 complexes at an origin designates it as being "licensed" for initiation (Bell and Dutta, 2002).

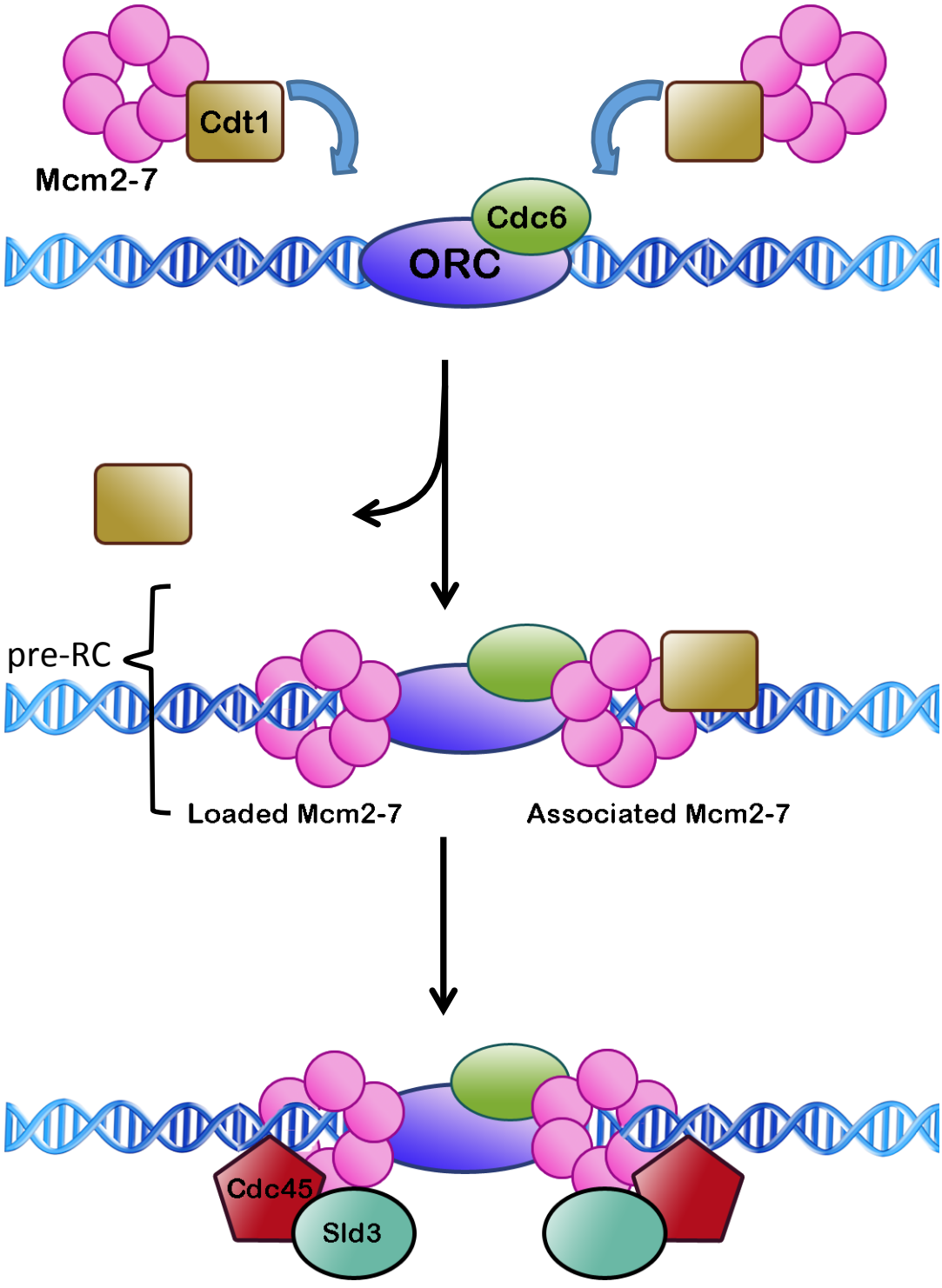
Cdt1
Mcm2-7
Cdc6
ORC
pre-RC
Loaded Mcm2-7
Associated Mcm2-7
Cdc45
Sld3

Figure 1.6. Assembly of the pre-replicative complex in G_1 phase. ORC binds to origin sequences and promotes the association of Cdc6. Heptamers of Cdt1·Mcm2-7 bind via the interaction between Cdt1 and Orc6. Mcm2-7 complexes are reiteratively loaded through multiple ATP hydrolysis driven steps leading to the displacement of Cdt1. The association versus tight loading of the Mcm2-7 complex is depicted. Once a head to head loading of two MCM complexes occurs, the origin is said to be licensed. The factors comprising this structure, i.e., ORC, Cdc6 and Mcm2-7 constitute the pre-replicative complex (pre-RC). Sld3 and Cdc45 associate with early but not late licensed origins. Adapted from Sclafani and Holzen, 2007.

Early examinations of helicase and DNA stoichiometry suggested that four MCM complexes are loaded at each origin (Bowers *et al*., 2004). Further studies, however established the commonly accepted view that two hexamers are loaded onto origins in opposing orientations and this constituted the necessary and sufficient quantity of helicase to initiate replication at an origin (Ervin *et al*., 2009; Remus *et al*., 2009). Loading implies encirclement of DNA and a robust association resistant to salt washing, which removes loosely bound proteins, including Cdc6 and ORC (Donovan *et al*., 1997; Edwards *et al*., 2002; Rowles *et al*., 1999). The loading step itself requires a stepwise ATP-hydrolysis dependent mechanism involving Cdc6 and ORC. Randell *et al.* (2006) showed that ATP hydrolysis by Cdc6 directs tight association of the first MCM complex to origins, presumably by displacing Cdt1 and stabilizing the helicase on the DNA. A second ATP hydrolysis-driven step is mediated by ORC and is required for the tight loading of the second MCM hexamer. This has been described as a dynamic process as Cdt1 tethered to origins cannot load multiple MCM complexes. Its displacement from and ostensibly its re-association with the pre-RC machinery at multiple origins are requisite for continued reiterative MCM loading in late G_1 (Chen *et al*., 2007). This dynamic requirement for pre-RC factors after initial MCM loading extends to other pre-RC factors (Semple *et al*, 2006; Aparicio *et al*., 1997, Gibson *et al*., 2006).

Cdc6 and Orc1 exhibit extremely high amino acid sequence similarity and are both members of the AAA^+ family of proteins, as are Orc4, Orc5 and all of the Mcm2-7 subunits. Comparable groups of interacting proteins, such as those involved in the association of the PCNA ring or the bacterial DNA helicase C with DNA (the RFC and γ complexes, respectively) are likened to a clamp-loading mechanism (Davey *et al*., 2002;

Neuwald *et al*., 1999). Common possession of highly conserved ATP-binding (Walker A) and ATP-hydrolysis (Walker B) domains bestow clamp loaders with the ability to act as molecular architects, altering the conformations and structures of larger molecules. Activation of one or more AAA^+ proteins in such a complex often leads to ATP-hydrolysis in an adjacent member, e.g., Orc1 acts through an Orc4 arginine finger (Bowers *et al*., 2004). The ORC-Cdc6 dynamo is thought to act in this sense, as a clamp loader. Its primary role is the opening of MCM rings and their positioning such that they may subsequently close, encircling origin DNA (reviewed in Sclafani and Holzen, 2007 and Stillman, 2005).

1.3.3 Initiation of DNA Replication

As previously described, at the core of the switch-like regulation of the cell are cyclins. G_1 cyclins modulate cell sizing and promote expression of S phase cyclins. The S phase B-cyclins, Clb5 and Clb6 activate the Cdc28 kinase for a role in replication initiation (Figure 1.7). While both of these Clbs are implicated in the steps that trigger origin firing and its control, they have functionally overlapping roles. While Clb6-Cdc28 is able to initiate replication in the absence of Clb5, it requires all Clns and results in a prolonged S-phase due to inefficient firing of late origins. Conversely, a *cln*1Δ*cln*2Δ*cln*3Δ mutant overexpressing Clb5 is capable of proper and timely replication initiation (Nasmyth, 1996; Schwob and Nasmyth, 1993). As discussed, because Cdc28 must be associated with one of many cyclins to form an active complex, it is commonly referred to as Cdk1 or simply CDK (cyclin-dependent kinase) in its active form. When this notation is used, it

generally (and exclusively in this thesis) refers to the kinase bound to its regulatory cyclin subunit.

While there exist roughly 12,000 potential ORC-binding sites in the budding yeast genome, only about 332 of these act consistently as active origins (Nieduszynski *et al*., 2006; Pessoa-Brandao and Sclafani, 2004; Raghuraman *et al*., 2001; Yakubi *et al*., 2002). Origins are classified as being early-, middle- and late-firing according to their temporal pattern of activation. One interesting characteristic of the replication process is that pre-RCs are set up at all of the 300-500 predicted origins (by sequence) by the end of late G_1 (Raghuraman *et al*., 2001; Yakubi *et al*., 2002). The firing of a particular origin, however is dependent upon the association of another group of proteins consisting of Cdc45, Sld2, Sld3, Dpb11 and the GINS complex. This is engendered by the phosphorylation of Sld2 and Sld3 by Clb5-Cdc28, which promotes their interaction with the tandem BRCT repeat protein, Dpb11 (Tak *et al*., 2006; Tanaka *et al*., 2007; Zegerman and Diffley, 2007). This represents the essential role of CDK in DNA replication initiation. Phosphorylated Sld2 and Sld3 along with Dpb11 associate with the GINS (Go Ichi Ni San) complex as well as Cdc45 (Labib and Gambus, 2007; Takayama *et al*., 2003). As a result, a trimeric complex formed by Cdc45, Mcm2-7 and GINS, known as CMG is stabilized at pre-RCs, which are now referred to as pre-initiation complexes (pre-ICs). Upon origin firing, CMG travels with the replication fork, unwinding the double helix ahead of it and activating DNA polymerase, pol ε (Pacek *et al*., 2006; Ilves *et al*., 2010; Gambus *et al*., 2006). This is illustrated in Figure 1.7.

The formation and activation of primed origins also depends on the Dbf4-dependent kinase complex, Dbf4-Cdc7. DDK phosphorylates members of the MCM

complex, triggering DNA unwinding. While levels of Cdc7 remain constant throughout the cell cycle, its regulatory subunit, Dbf4 fluctuates such that it peaks at the G_1/S boundary, creating an active DDK (Cheng *et al*., 1999; Nougarède *et al*., 2000). While both Mcm4 and Mcm6 phosphorylation is DDK-dependent, Mcm4 is thought to be the essential target of DDK. Mcm4 possesses a domain that inhibits helicase activation. (Cho *et al*., 2006; Francis *et al*., 2009; Hardy *et al*., 1997; Lei *et al*., 1997; Masai and Arai, 2002; Masai *et al*., 2006; Sheu and Stillman 2006 and 2010). Thus the essential role of DDK is to phosphorylate residues in this domain, alleviating inhibition of the helicase.

Figure 1.7. Initiation of DNA replication. The activation of the Dbf4-dependent kinase (DDK) and the cyclin-dependent kinase (CDK) result in the phosphorylation of their essential susbstrates (depicted by circles marked with "P"s). This leads to the association of a complex comprising Sld2, Sld3, Dpb11 and GINS. Phosphorylation of MCM subunits causes a conformation change leading to the stable formation of a Cdc45-Mcm2-7-GINS complex. This stabilizes DNA polymerase ε at the origin. Two replication forks are established which move outward, away from one another, the GINS complex migrating with each one as polymerase synthesizes nascent strands of DNA. Sld2, Sld3 and Dbp11 do not migrate with the replication fork and are displaced from the fired origin. Adapted from Labib, 2010.

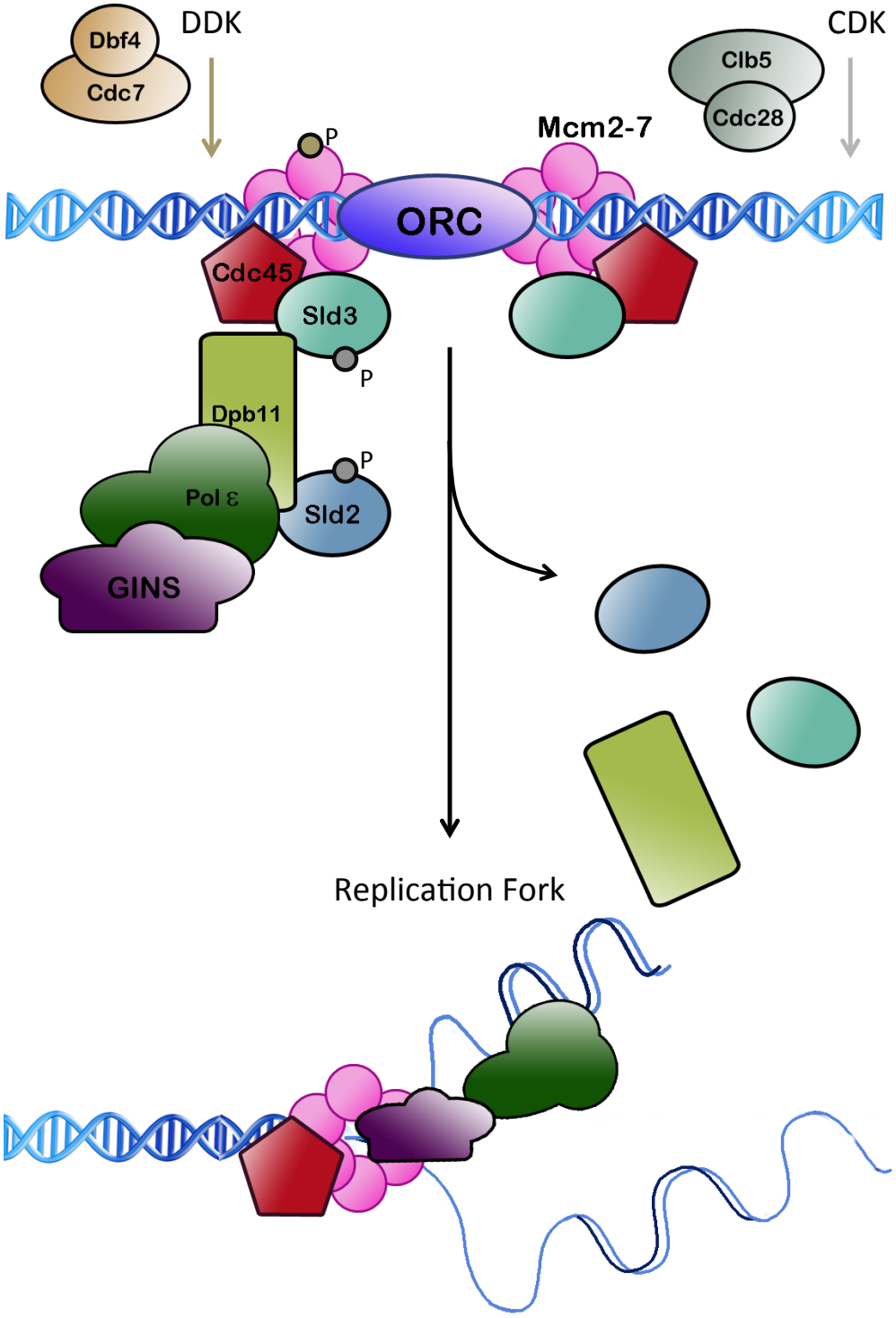
DDK
Dbf4
Cdc7
CDK
Clb5
Cdc28
Mcm2-7
P
ORC
Cdc45
Sld3
P
Dpb11
P
Pol ε
Sld2
GINS
Replication Fork

Of the 300-500 origins that fire per cell per cell cycle, only a subset fire at the G_1/S transition, with some remaining dormant. The mechanisms that regulate the temporal activation pattern are of great interest and a positive correlation between trancriptionally-active regions and those containing early-firing origins has been observed (Diller and Raghuraman, 2004). The opposite is true for late origins. Additionally, the accessibility of the chromatin at a given origin has been suggested to be a major determinant of its timing profile (Friedman *et al*., 1996; Mechali, 2010). An example of this is the modification of chromatin structure by inhibiting deactylation and thus rendering the DNA accessible to the replication machinery. This induces typically late origins to fire prematurely (Aparicio *et al*., 2004; Vogelauer *et al*., 2002). The pattern of origin firing appears to be established in late M or early G_1 phase (Dimitrova and Gilbert, 1999; Raghuraman *et al*., 1997; Wu and Gilbert, 1996).

Sld3, Sld7 and Cdc45 associate with early origins in G_1 (Figure 1.6), before CDK levels rise (Heller *et al*., 2011; Kamimura *et al*., 2001; Nougarède, 2000; Muramatsu *et al*., 2010; Tanaka *et al*., 2011). Once cells enter S-phase, the recruitment of limiting DDK to origins and the CDK-dependent association of CMG promote sequential origin firing. This is thought to specify their temporal firing pattern (Bousset and Diffley, 1998; Donaldson *et al*., 1998; Patel *et al*., 2008; Labib, 2010). Unlike CMG, Sld2, Sld3, Sld7 and Dpb11 no not travel with the replication fork as shown in Figure 1.7 (Kanemaki and Labib, 2006; Masumoto *et al*., 2000; Tanaka *et al*., 2011).

1.3.4 Inhibition of Rereplication

In order to maintain genomic stability and prevent over- or under-replication of the genome, the cell has evolved mechanisms to ensure that DNA replication occurs exactly once per cell cycle. This is paramount to avoid loss of cell viability and/or genome integrity (Green and Li, 2005). Once an origin fires, a new pre-RC cannot be established until the next cell cycle due to the inhibitory effects of S-CDKs, which peak during S phase and remain high until the middle of mitosis. It is in this respect that CDKs possess a somewhat dichotomous role in regulating cell cycle dynamics. As described above, they are essential for activation of origins, but are equally implicated in the block to re-replication. The mechanisms that block re-replication act by preventing helicase loading outside of G_1 (Arias and Walter, 2007). This amounts to antagonizing pre-RC assembly once CDK levels are sufficiently high, i.e. just after passage into S phase. Dutta and Bell (1997) showed Cdc6 to be a substrate for CDK phosphorylation. This leads to targeting of the protein by the SCF^{cdc4} complex to the proteasome, by which it is degraded (Drury *et al*., 1997; Elsasser *et al*., 1999). Interestingly, Cdc6 is, in turn, able to inhibit certain CDKs, thus providing a mechanism by which overexpression of the former can lead to defects in other processes in which CDKs are implicated such as exit from mitosis (Bueno and Russell, 1992 and reviewed in Honey and Futcher, 2007).

Orc2 and Orc6 are phosphorylated *in vivo* by CDKs (Green *et al*., 2006; Nguyen *et al*., 2001; Tanny *et al*., 2006; Vas *et al*., 2001). Orc6 is directly bound by Clb5-Cdc28 at an "RXL" motif near its N-terminus (Wilmes *et al*., 2004). Chen and Bell (2011) showed the phosphorylation of ORC by CDK inhibited helicase loading *in vitro*. Because Orc6 is required to recruit Cdt1 (and hence Mcm2-7) to origins (Chen *et al*., 2007),

abrogating this interaction results in the replication defect. Two Cdt1 binding sites were found on Orc6, one N-terminal and the other C-terminal (Chen *et al*., 2007). A model proposed by the work presented in Chen and Bell (2011) and Takara and Bell (2011) posits that the MCM double hexamer loaded at origins is a product of recruiting two Cdt1•Mcm2-7 heptamers by single Orc6. Because Orc2 mutants only show rereplication defects when combined with one or both Orc6 mutations, it is believed that Orc6 is the primary target of CDK inhibition.

Mcm2-7 localization to the nucleus during G_1 is fundamentally important for constructing the replisome. An integral component of replication forks, the helicase moves with a given fork, allowing processive DNA replication by the polymerases. Once it has completed its role and is released from the DNA, it is exported from the nucleus via a CDK-dependent mechanism (Labib *et al*., 1999; Nguyen *et al*., 2000 and Tanaka and Diffley, 2002). This was shown to be brought about through the phosphorylation of the nuclear export signal of Mcm3 (Wu *et al*., 2012). The cell thus possesses several redundant mechanisms to ensure the prevention of rereplication since each of these CDK-inhibited factors is required for initiation (Green and Li, 2005; Nguyen *et al*., 2001).

1.4 Biological Systems Modeling

1.4.1 Overview

"Any darn fool can make something complex; it takes a genius to make something simple."

— Pete Seeger

The study of biological systems strives to present a coherent and intuitive picture of a given element, be it the digestive pathway in humans or the neural networks of the sea urchin. A major tactic, as practiced through textbook learning is the simplification of the given biological process into its central constituent parts and its overall function. The metabolites in a pathway, the flux of macromolecules through a cascade and the relationship between the components produce a "cartoon" version which suffices in conveying the necessary information to objectively understand the system. As proposed by Tyson *et al.* (2002), such models provide a relatively qualitative comprehension without testing the rigor and fidelity of the observations claimed. Molecular biology provides us with experimentally-derived theories defining the mechanistic involvement of system components. The representative diagrams produced as a result of this process do not quantitatively examine the process in question from a holistic perspective. Discrete information about a system is systematically collected and used to construct a testable working model that investigates the claims made by pre-existing biological data. Thus, we can look to modeling of a biological entity for two reasons: 1) For a more comprehensive understanding of the fundamental pathways, circuitry and molecular

activities that govern its function and 2) To exploit this information with the aim of re-engineering it and/or utilizing its discrete mechanisms as components in a synthetic system.

With the advent of high-throughput techniques for analysing protein-protein interactions (e.g. Yeast-two hybrid assay; Ito *et al*., 2001; Uetz, 2002) and genome-scale "interactomes" (Tyers and Mann 2003), the modeling concept of *networks* has emerged. *S. cerevisiae*, through its ease of molecular manipulation has produced a plethora of studies establishing such protein interaction networks. The combination of deletion mutant (Winzeler *et al*., 1999) and protein overexpression (Sopko *et al*., 2006) strain collections with sensitivity profiling (Parsons *et al*., 2006) and synthetic lethality screens (Tong *et al*., 2001) has led to great efforts in defining protein networks of apparent functional relevance (Uetz *et al*., 2000; reviewed in Kuroda *et al*., 2006). Techniques such as 2D gel electrophoresis and its unique manipulation, 2D-Differential In Gel Electrophoresis (2D-DIGE, Tong *et al*, 2001) allow the high throughput analysis of protein data. This has led to significant advances in exploring the proteomic space of multiple organisms (e.g. ch. 4 of Alzate, 2009; Cheng *et al*., 2010; Duncan and McConkey, 1982) and specifically in yeast systems biology (e.g., Hu *et al*., 2003; Perrot *et al*., 1999; Wildgruber *et al*., 2002). Sub-cellular fractionation and purified sample analysis using 2D-DIGE allows the identification of key network players through their response to varied cellular environments (El-Bayoumy *et al*., 2012; Scaife *et al*., 2010). Chapter 4 addresses novel findings contributing to the understanding of the *S. cerevisiae* response to genotoxic stress utilizing a unique combination of cellular fractionation and 2D-DIGE.

The systematic cataloguing of cellular and subcellular molecules typically results in the production of a "graph", representing groups of proteins or genes, which cluster together, presumably signifying functional modules. The results from multiple organisms often produce interacting clusters each representing disparate functional units of hierarchical nature (Ravasz *et al*., 2002). For the identification of cellular functional groups, which might represent a metabolic or signalling pathway, an interaction graph is by nature static. In contrast, most processes within a cell that we wish to investigate are dynamic, in that their functions are not limited in time and space, thus interaction graphs fail to grasp the system's function in a realistic manner. The regulatory mechanisms that dynamically alter binding partners, affinities and spatial distributions render the modeling of static graphs inadequate. Instead, mathematical modeling applied to systems which have described their components in terms of dynamic function, better convey the underlying behaviour. Much like in an electronic circuit that has individual elements performing specific but inter-related roles, so too does a "biological circuit". Feedback and regulation, key aspects to both platforms are crucially integrated into this view of modeling a cell or groups of cells (Sauro and Kholodenko, 2004). Amalgamating the concepts of network graphing and dynamic biological "circuits" produces a more useful model for investigating the properties of a biological system (discussed in Palumbo *et al*. 2010).

While understanding the significance of connectivity amongst interacting factors is crucial, identifying yet unknown cellular mechanisms, completing the picture is of equal importance.

1.4.2 Modeling the Cell

The cell is an incredibly complex machine equipped with elaborate tools and a regulatory framework that promotes its viability and propagation. A vast influx of external stimuli arrives at the cell membrane, being processed and transduced to the inner nuclear control centre. Also numerous are the internal signals relaying information pertaining to protein levels, energy allocation, the monitoring of genomic fidelity, and a virtually endless checklist of cellular functions to regulate. Primarily, the cell enacts its program by carefully modulating the level of gene expression, protein degradation, macromolecule localization, catalytic activations and signal transduction cascades among the many processes that are carried out. As articulated by Bray (1995), the requirement of a cell to process such vast amounts of information falls under the purview of intricate gene and protein networks. Tyson *et al.* (2002) point to seminal statements regarding the perspective of theoretical molecular cell biology (Hartwell *et al.*, 1999), stating that the study of this field must reflect two objectives: 1) that complex biochemical pathways be accurately described and simulated with highly predictive capabilities and 2) that this exploration be based on the determination of how protein-mediated regulatory networks control cell function. This is cogent to discussion of the cell cycle given the high degree of regulation required and the processes by which protein-based switch-like mechanisms permit this.

1.4.3 ODE-based modeling

This topic has been thoroughly discussed in works by Tyson *et al*. (1996, 2000 and 2001). Essentially, a rudimentary circuit describing a set of molecular reactions is converted into a series of rate equations. This is interchangeably called a network and is not to be confused with an interaction graph. These may be written using Mass Action equations or in cases where the interaction involves non-linear kinetics, Michealis-Menten laws, Goldbeter-Koshland switches or Hill functions may be used. The choice of equation structure depends on understanding the nature and details of the reaction. It is usually best to choose the most parsimonious description that doesn't exclude essential details. The changing state, generally over time, of a given variable in the network is described by a differential equation. It is classified as an ordinary differential equation (ODE) as the dependent variable and its derivatives are written as a function of the single independent variable, in this example, time. The set of ODEs thus represent the dynamic network and the behaviour of the system is observed by solving them. Of equal importance are the structure of the reaction network and the parameters governing the rates of these reactions. Specification of parameters may be through direct assignment in cases where some *a priori* knowledge about a particular kinetic reaction is known (e.g. half-life of a protein). In other cases parameters are estimated through algorithms that fit the ODE solutions to experimental data (exemplified by Sugimoto *et al*., 2005). Often referred to as *in silico* modeling, the set of ODEs are solved computationally by non-linear integrators using assigned parameter values and specified starting conditions. The result is a depiction of how each variable (or species) changes over time.

Assuming time to be the independent variable, for any given instant, the differential equations dictate the state of the system (for our purposes, the concentration of a protein species). Each species occupies one dimension in an n-dimensional space, where n = total number of species. Considering a single species that navigates through this multi-dimensional space, its state is determined by the rate reactions. For each incremental advancement in time, the differential equations inform the velocity with which the state of the species will change. If the concentrations of a set of proteins over a given amount of time cause their rate of change to be zero, the system has achieved a stable state. If a change in direction of a given species state (change in concentration) causes disruption of global behaviour, the state is unstable. Oscillatory mechanisms in a dynamic system often exist, as is the case with the cell cycle, whose regulation is based on oscillating concentrations of cyclins. ODE-based models evolve where necessary: they serve as an initial analytical tool to survey the mechanistic description of a biological process. Provided it fits the experimental constraints, the model can be provisionally accepted. Otherwise, further analysis of the mathematical model construction and parameter value determination ensues. In some cases, the model may depict an accepted understanding of a process accurately, but there remain inconsistencies with experimental observations. The model then sheds light on a potentially misconstrued aspect of the "cartoon" model.

Systems involving well-characterized mechanisms consisting of a complex biochemical network have largely been studied using an ODE-based approach. This reflects the adaptability and robustness of the models produced as modifications to parameters and network structure are accomplished with ease. Refinement of the system

is produced through adjustment of the reaction network and/or parameter values (de, Jong, 2002; Kitano, 2002). While the field of cell cycle modeling has benefitted greatly from ODE-based systems, metabolic pathways (Ideker *et al*., 2001), genetic regulatory pathways (Cao *et al*., 2012; Elowitz and Leibler, 2000; Wang *et al*., 2011), MAP kinase signalling (Orton *et al*., 2005) and apoptotic pathways (Ryu *et al*., 2008) are among the many other systems that have been explored using this method.

For the purposes of the model described in this dissertation, the modified form of the balance equation for representing the complete set of ODEs in this thesis is given by:

$$\frac{dX_i}{dt} = F_i(X_1, X_2, ..., X_N) = \sum_{r=1}^{M} (v_{ir}^{+} - v_{ir}^{-}) R_r(X_1, X_2, ..., X_N; k_r), i = 1, ..., N. \quad (1)$$

, where the non-linear functions $F_i(X_1, X_2, ..., X_N)$ describe the *i*-th state variable's change in concentration in terms of the differential between its coefficients of production (v_{ir}^{+}) and consumption (v_{ir}^{-}). The rate reactions (*R*) are dependent on the substrate concentrations and on any kinetic constant natively associated with the reaction (k_r).

1.4.4 Existing Cell Cycle Models

Although ODE-based approaches to modeling cellular processes have existed for more than four decades (Kauffman and Wille, 1975, reviewed in ch. 10 of Goldbeter, 1996), the dearth of molecular data on which to base such models limited their ability to inform us about the system. Nevertheless some of the later-to-be-discovered hallmarks of cell cycle biology, namely the cyclical nature of its regulatory pathways and proteins were represented. A series of studies exploring the oscillatory mechanisms controlling early embryonic development in *Xenopus laevis* incorporated knowledge of biochemical and mechanistic features (Hyver and Le Guyader, 1990; Goldbeter, 1991; Norel and Agur, 1991; Tyson, 1991). It was discovered that the maturation-promoting factor (MPF) guides cells towards mitosis, but is inhibited by a CDK. MPF is activated by cyclin and its accumulation leads to the degradation of the same cyclin. MPF levels then decrease in a CDK-dependent manner, allowing cyclin levels to rise. This produces the oscillatory program underlying the characteristic feedback function of the cell cycle. In these studies, the concepts of thresholds and time delays in cell cycle control were elucidated. These models were improved by introducing a greater number of variables and feedback loops (Srividhya and Gopinathan, 2006). The demonstration of a time delay-dependent checkpoint arising through an APC-MPF relationship was made, foreshadowing later, more complex examinations of this phenomenon. More recently, the switches and oscillators that act in modular motifs have been described in a model by Francis and Fertig (2012).

Another discrete feature of the cell cycle is the coupling of cell size and division. This was found to be dependent on the shuttling of proteins between the nucleus and

cytoplasm that formed a threshold-dependent switch mechanism (Yang *et al*., 2006). An internal clock controls the critical size of the cell at the time of division, regulating the G_1/S transition. The modulation of this critical size in response to external conditions has been modelled (Alarcón and Tindall, 2007; Barberis and Klipp, 2007). Experimental data was used to calibrate a model of osmotic shock response in yeast and was able to predict the outcomes of different types of perturbations to this system (Klipp *et al*., 2005). While this is not strictly an example of cell cycle modeling, it serves as an example of where experimental data informs the model. This is an important strategy in developing a model that accurately depicts real-cell conditions and that can predict network behaviour with more confidence.

Chen *et al*., (2000) provided the initial framework for a comprehensive cell cycle model of *S. cerevisiae*. In this description, the oscillatory character of the cell cycle is again highlighted; the cell exists in two stable states – G_1 and S/M, each self-enforcing. This is postulated to be a function of the dichotomous role of CDKs. While S-cyclins activate DNA replication, they inhibit rereplication. Similarly, Clb-dependant activation of the APC (leading to passage through Mitosis) results in an active complex that destroys Clbs (and thus CDK activity). To construct this model, experimental data from the literature was used to specify biochemical constants such as the rates of proteolysis, gene expression as well as to determine stoichiometric ratios between interacting partners. Ultimately, this data was limited and could not uniformly describe the relationships between different modules of the cell cycle. Gene deletion and expression level mutants were used to refine the model. The concentrations of nine species representing CDKs, CKIs, cell mass and factors involved in budding and spindle

formation were followed over the course of the cell cycle. While this model is predictive and can account for the biochemically-determined behaviour of the system, a quantitative description of its components is missing.

The seminal work of Chen *et al.* (2000) is used as the backdrop for a model that explores two distinct oscillatory mechanisms driving the cell cycle: replication and morphogenesis (Cross, 2003). While it treats them as abstract units, the processes are described as being dependent on the cyclical nature of cyclins and consequently the active form of Cdc28. Replication is promoted by CDK activity while morphogenesis is inhibited by it. Thus a single oscillation of CDK concentration moves cells from replication to division and back again though the use of a feedback oscillator and a relaxation oscillator, independent of one another. The differential equations used to create the model describe discrete modules of the cell cycle. Cross, as in Klipp *et al.* (2005) uses experimental observations to set some parameter values, an exercise that minimizes the hypothetical nature of its conclusions about the cell cycle.

The Chen *et al.* (2000) model was subsequently appended with an extensive description of the M to G_1 transition, i.e., the exit from mitosis (Chen *et al.*, 2004). Like the original model, a great deal of experimental data was used to infer interaction details of key cell cycle contributors. The result was the construction of a robust description of the various discontinuous modules that together represent the entire cell cycle. A great number of cell cycle mutants (>100) described in the literature were simulated by their model and in the majority of cases, good agreement was found. Additionally, by revealing instances where disagreement occurred or where there was missing information in the literature, Chen *et al.* (2004) shed light on aspects of the budding yeast cell cycle

that must be further addressed, both experimentally and *in silico*. Again, the quantitation of cell cycle factors was lacking, an issue addressed in a further improvement (Barik *et al*., 2010). The levels of key regulatory proteins such as cyclins were integrated, producing a dynamic picture of the cell cycle in more concrete terms. Nevertheless the module of DNA replication was not explored beyond its consideration as a "black box", without much detail about the process so fundamental to cell proliferation.

Quantitative models of replication presented by Spiesser *et al*. (2009), de Moura *et al*. (2010) and Yang *et al.* (2010) investigate the temporal regulation of genome replication. These models investigate how chromosomes are duplicated with only a subset of potential origins firing and with the literature-suggested differences in origin efficiencies. All three models take into consideration (but incorporate to varying degrees) certain characteristics of origins as described by the experiments of Raghuraman *et al.* (2001) and Yakubi *et al.*, (2001): a) origin spacing along the chromosome, b) length of the chromosome to be replicated, c) the probability of an origin firing in a given cell cycle (efficiency), d) observed firing times for various origins from population averages and e) the rate of fork progression. The model of Spiesser *et al.* uses a Boolean approach to reconstitute the temporal firing pattern observed in Raghuraman *et al.* by assuming that the firing program is fixed and deterministic. It was highlighted that only certain combinations of fired origins were able to match the experimental data.

De Moura *et al.* (2010) and Yang *et al.* (2010) propose that origin firing most likely has a stochastic component. While origin sequences in yeast are highly conserved, in higher eukaryotes such as humans and Xenopus and even in fission yeast, replication origins are determined by largely random factors. This being the case, the temporal firing

program would be expected to be more heterogeneous on a single cell level than population averaged experiments imply. The authors give evidence to suggest that origin firing may be stochastic in budding yeast as well, as evidenced by the highly variable pattern of origin firing on chromosome VI. Both models propose that there is a mix of deterministic origin firing with a certain level of stochasticity such that some origins have a high probability of firing early (irrespective of the effects of being passively replicated) and some have a high probability of firing late, but that the probability distributions of firing can overlap. Because population averaged studies cannot distinguish between an inefficient early origin and an efficient late origin, it is possible that experimental data does not provide a good indication of the levels of stochastic firing. Ultimately if origins fire completely stochastically, there lies the risk of having large stretches of unreplicated DNA between fired origins (e.g., if they cluster together), referred to as the "random gap" problem. Alternatively if the temporal pattern is completely deterministic, cells to not have a buffer against perturbations, where one or more high-efficiency origins might not fire, leading to incomplete or delayed replication. Yang *et al.* propose a mechanism to reconcile the deterministic and stochastic models of origin firing – origins have an intrinsic probability of firing in a given cell cycle. This probability, however increases as S phase progresses such that an origin that has not yet fired late in S phase has an increased probability of firing compared to earlier on in S phase.

In order to justify an increasing probability of origin firing through S phase, Yang *et al.* (2010) suggest that the abundance of a limiting factor of DNA replication might increase relative to the proportion of unreplicated DNA. They also propose that a mechanism for imparting efficiency to origins might be the differential accumulation of

MCM complexes at an origin prior to firing. Hence, origins that attract more MCMs during early to late G_1 would have a greater probability of firing upon entry into S phase.

The models of Chen *et al*. (2000, 2004) provided a strong foundation for building on the representation of the budding yeast cell cycle. The description of DNA replication and its regulation throughout the cell cycle however, remained abstract. The model of Brümmer *et al*. (2010) specifically explores the network of DNA replication initiation. While many replication factors are quantitatively modeled, their approach involves fitting to chromosomal duplication data, an indirect and less faithful measurement of the factors being modeled. Additionally, parameter values were tightly restricted to satisfy constraints loosely hypothesized to generate an artificially optimal outcome. Modeling DNA replication by directly using data for the key factors involved has not been previously attempted.

1.5 Project Goals

The proteins that interact in order to initiate DNA replication in *S. cerevisiae* have been well studied in terms of their molecular functions. Mathematical modeling of the biochemical details of this network allows a dynamic understanding of its behavior. This is useful in being able to predict the inherent characteristics of the model such as kinetic rates and relative sensitivities to individual factors. It is also useful for making predictions about perturbations to the native state of the system. Existing cell cycle models have either abstracted the network of DNA replication initiation in their description of the global process or have focused on the temporal dynamics of origin firing. The replication initiation model of Brümmer *et al.* (2010) does include the protein factors that comprise the initiation of DNA replication, however the results from this study are based on indirect measurements of these proteins factors. Additionally, the estimation of model parameters is idealized to fit a set of requirements that are too stringent to accurately describe the origin firing program. One of the major goals of this thesis was to gather experimental data from live cells for the levels of replication initiation proteins through the cell cycle.

The next goal was to build a quantitative ODE-based framework for the analysis of system behaviour. Using the experimental data gathered, parameters associated with the network's rate reactions would be derived using various global and local search techniques. Through model refinement based on matching *in vivo* observations to model simulations, construction of the network was to be revised until a reliable depiction of the protein network is obtained. To ensure model robustness, predictions were to be made

about the state of the system upon perturbation. These were to be compared to experimental observations in the literature as well as to experiments performed in this study that mimic the model perturbations.

As previously mentioned, a quantitative description of DNA replication was lacking in an established model of the entire yeast cell cycle. The next goal was to integrate the present model into the established cell cycle model.

In building a comprehensive model of replication, new elements should continually be incorporated. If new mechanisms controlling the regulation of replication are discovered or if old ones are called into question, these details should be reflected in a revised model. High-throughput proteomic screening is a useful approach to provide insight into yet uncharacterized roles for replication proteins or for the identification of novel ones. As a proof of principle, a goal of this project was to analyze chromatin fractions with 2D-DIGE to identify proteins that are enriched on the DNA. The cellular response to DNA damaging agents involves the functional enrichment of proteins on the chromatin. To highlight proteins potentially involved in DNA damage response, another objective was to use 2D-DIGE to identify differential chromatin association of budding yeast proteins in response to genotoxic stress. Once potential candidates were highlighted, a final goal was to examine their contribution to genotoxic sensitivity or resistance.

Chapter 2: Materials and Methods

2.1 Yeast Strains

Strains DY-82, DY-123, DY-128, DY-139, DY-140, DY-142, DY-143, DY-255 and DY-256 are isogenic to the DY-26 wild-type strain (*MATa, his3Δ200, leu2Δ, met15Δ0, trp1Δ63, ura3Δ0*), which is itself derived from the ATCC strain BY4473 (see Table 2.1 for details). Chromatin fractionation for cell cycle timecourses used to gather data for the model in chapter 3 was performed using DY-26, DY-82 and DY-128. Tagged strains were created by genomic tagging of the corresponding ORF by homologous recombination with linear PCR fragments amplified using plasmid templates, as described by Longtine *et al*., (1998). Epitope tagging cassettes were amplified from Longtine plasmid vectors which also contained selectable marker genes to allow for the selection of integrants. Specifically, the Longtine plasmid pFA6a-TRP1-PGAL1-3HA was used to create DY-139 (*MATa, his3Δ200, leu2Δ0, met15Δ0, trp1Δ63, ura3Δ0, cdc6::Pgal-3HA-CDC6 [TRP1]*), DY-140 (*MATa, his3Δ200, leu2Δ0, met15Δ0, trp1Δ63, ura3Δ0, cdt1::Pgal-3HA-CDT1 [TRP1]*) and DY-255 (*MATa, his3Δ200, leu2Δ0, met15Δ0, trp1Δ63, ura3Δ0, dbf4 ::Pgal-3HA-DBF4 [TRP1]*). pFA6a-3HA-TRP1 was used to create DY-142 (*MATa, his3Δ200, leu2Δ0, met15Δ0, trp1Δ63, ura3Δ0, cdc6::CDC6-3HA [TRP1]*), DY-143 (*MATa, his3Δ200, leu2Δ0, met15Δ0, trp1Δ63, ura3Δ0, cdt1::CDT1-3HA [TRP1]*), and DY-256 (*MATa, his3Δ200, leu2Δ0, met15Δ0, trp1Δ63, ura3Δ0, dbf4::DBF4-3HA [TRP1]*). These six strains were used in the GAL_1 shutoff/knock-down experiments. Amplification of plasmid-based cassettes was accomplished using primers that possessed complementary sequences to target regions in the genome, thus allowing for homologous recombination upon transformation. In the case of DY-142, DY-143 and DY-256, which possess C-terminal 3HA-tags, the forward

PCR primer used for amplification contained a sequence that allowed for recombination immediately upstream of the stop codon, while the reverse primer contained a sequence that allowed for recombination downstream of the ORF. Thus the tag was incorporated in-frame immediately after the last coding codon, resulting in a C-terminal fusion protein. In strains DY-139, DY-140 and DY-255, the corresponding gene was placed under control of the GAL_1 promoter and expressed an N-terminal 3HA-tag. For PCR amplification of the cassette used in homologous recombination-based integration, the forward primer contained a sequence that allowed for recombination 50 bp upstream of the start codon, while the reverse primer contained a sequence that allowed for recombination in the first 13 codons of the gene. DY-82 and DY-128 were created similarly to the 3HA-tagged strains, however the pFA6a-13Myc-TRP plasmid was used as a PCR template to create C-terminal 13Myc-tagged fusion proteins for ease of detection in the cell cycle timecourse experiments. Proper integration in these strains was confirmed by PCR using primers that flanked the region of recombination and proper expression was confirmed by Western blot. BY-4733 (Open Biosystems) was used in large-scale chromatin fractionation for the 2D-DIGE-based proteomic screen. For the genotoxic sensitivity assays, either haploid knockout (KO) or DAmP strains were used (both from Open Biosystems in a BY-4741 background). In the former, a KanMX cassette (Wach *et al*., 1994) possessing a forward primer homologous to the 5' end and reverse primer homologous to the 3' end of the corresponding gene was used to replace it with a sequence conferring kanamycin resistance. DAmP strains (Decreased Abundance by mRNA Proteins) were created by insertion of the same KanMX cassette into the 3' UTR of the corresponding gene, destabilizing its mRNA transcript. In the TH-5854 strain

(BY-4174 background, Open Biosystems) a one-step integration of the tTA transactivator, under the control of the CMV promoter was performed at the *URA*3 locus. Following this, a plasmid carrying a kanR-tetO7-TATA cassette with sequences homologous to the promoter of CDC45 was then integrated into the genome replacing the endogenous promoter. Thus, the expression of the gene can be switched off or titrated down by the addition of doxycycline to the growth medium. This was used in the Cdc45 knock-down perturbation experiment.

Table 2.1. Yeast strains used in this study.

Strain	Genotype
DY-26	*MATa, his3Δ200, leu2Δ, met15Δ0, trp1Δ63, ura3Δ0*
DY-82	*MATa, his3Δ200, leu2Δ0, met15Δ0, trp1Δ63, ura3Δ0, cdc45::CDC45-13Myc (HIS3)*
DY-123	*MATa, ade2-1, can1-100, his3-11,-15, leu2-3, -112, trp1-1, rad53::rad53-11 (URA3)*
DY-128	*MATa, his3Δ200, leu2Δ0, met15Δ0, trp1Δ63, ura3Δ0, CDC6::CDC6-13Myc (HIS3)*
DY-139	*MATa, his3Δ200, leu2Δ0, met15Δ0, trp1Δ63, ura3Δ0, cdc6::Pgal-3HA-CDC6 (TRP1)*
DY-140	*MATa, his3Δ200, leu2Δ0, met15Δ0, trp1Δ63, ura3Δ0, cdt1::Pgal-3HA-CDT1 (TRP1)*
DY-142	*MATa, his3Δ200, leu2Δ0, met15Δ0, trp1Δ63, ura3Δ0, cdc6::CDC6-3HA (TRP1)*
DY-143	*MATa, his3Δ200, leu2Δ0, met15Δ0, trp1Δ63, ura3Δ0, cdt1::CDT1-3HA (TRP1)*
DY-255	*MATa, his3Δ200, leu2Δ0, met15Δ0, trp1Δ63, ura3Δ0, dbf4::Pgal-3HA-DBF4 (TRP1)*
DY-256	*MATa, his3Δ200, leu2Δ0, met15Δ0, trp1Δ63, ura3Δ0, dbf4::DBF4-3HA (TRP1)*
TH-5854	*MATa, his3-1, leu2-0, met15-0, cdc45::kanR-teto7-TATA-CDC45 URA3::CMV-tTA*
BY4733	*MATa, his3Δ200, leu2Δ0, met15Δ0, trpΔ63, ura3Δ0*
BY4741	*MATa, his3Δ1, leu2Δ0, met15Δ0, ura3Δ0*
YAR007C DAmP	*MATa, his3Δ1, leu2Δ0, met15Δ0, ura3Δ0, rpa1::DAmP*
YNL312W DAmP	*MATa, his3Δ1, leu2Δ0, met15Δ0, ura3Δ0, rpa2::DAmP*
YDR002W DAmP	*MATa, his3Δ1, leu2Δ0, met15Δ0, ura3Δ0, yrb1::DAmP*
YJR065C DAmP	*MATa, his3Δ1, leu2Δ0, met15Δ0, ura3Δ0, arp3::DAmP*
YCR004C KO	*MATa, his3Δ1, leu2Δ0, met15Δ0, ura3Δ0, ycp4::KanMX/YCP4*
YPL004C KO	*MATa, his3Δ1, leu2Δ0, met15Δ0, ura3Δ0, lsp1::KanMX/LSP1*
YDR032C KO	*MATa, his3Δ1, leu2Δ0, met15Δ0, ura3Δ0, pst2::KanMX/PST2*
YER177W KO	*MATa, his3Δ1, leu2Δ0, met15Δ0, ura3Δ0, bmh1::KanMX/BMH1*
YDR533C KO	*MATa, his3Δ1, leu2Δ0, met15Δ0, ura3Δ0, hsp31::KanMX/HSP31*
YLR144C KO	*MATa, his3Δ1, leu2Δ0, met15Δ0, ura3Δ0, acf2::KanMX/ACF2*
YOR212W KO	*MATa, his3Δ1, leu2Δ0, met15Δ0, ura3Δ0, ste4::KanMX/STE4*
YGR180C KO	*MATa, his3Δ1, leu2Δ0, met15Δ0, ura3Δ0, rnr4::KanMX/RNR4*
YPL061W KO	*MATa, his3Δ1, leu2Δ0, met15Δ0, ura3Δ0, ald6::KanMX/ALD6*
YGR282C KO	*MATa, his3Δ1, leu2Δ0, met15Δ0, ura3Δ0, bgl2::KanMX/BGL2*
YDR099W KO	*MATa, his3Δ1, leu2Δ0, met15Δ0, ura3Δ0, bmh2::KanMX/BMH2*
YLR044C KO	*MATa, his3Δ1, leu2Δ0, met15Δ0, ura3Δ0, pdc1::KanMX/PDC1*
YDL229W KO	*MATa, his3Δ1, leu2Δ0, met15Δ0, ura3Δ0, ssb1::KanMX/SSB1*
YNL209W KO	*MATa, his3Δ1, leu2Δ0, met15Δ0, ura3Δ0, ssb2::KanMX/SSB2*
YKL056C KO	*MATa, his3Δ1, leu2Δ0, met15Δ0, ura3Δ0, tma19::KanMX/TMA19*
YBL039C KO	*MATa, his3Δ1, leu2Δ0, met15Δ0, ura3Δ0, ura7::KanMX/URA7*

2.2 Cell cycle Timecourse

DY-26 cells were grown in YPD medium (1% Bacto-yeast extract, 2% Bacto-peptone, 2% dextrose) to exponential phase at 30°C, washed with dH_20 and resuspended in fresh YPD at a concentration of 1 x 10^7 cells/ml. Cultures were subsequently arrested in late G_1 phase with the addition of 5µg/ml α-factor peptide (Sigma-Aldrich) for 3 h. Cells were monitored for late G_1 arrest through microscope observation of the percentage of unbudded cells. Approximately 1.5 x 10^7 cells were collected and treated with 0.1% sodium azide then kept on ice at 4°C. The remainder of the arrested culture was then centrifuged at 200*g* and the pellet was washed twice with dH_20. All cells were *BAR*1^+ and thus secrete the Bar1 protein, which degrades the α-factor pheromone used. Medium was collected and saved during centrifugation of the original logarithmic culture containing this protein and was subsequently used to resuspend the cells for the release from G_1 phase. Additionally, Pronase E (Sigma-Aldrich), an enzyme that also hydrolyzes alpha-factor, was added at a concentration of 10µg/ml to facilitate a synchronous release. Roughly the same number of cells collected in the G_1-arrested samples were collected at the other time points following release and similarly treated with sodium azide and kept on ice until the completion of the time course. A scheme for this procedure as well as the ensuing chromatin fractionation of samples collected here is depicted in Figure 2.1.

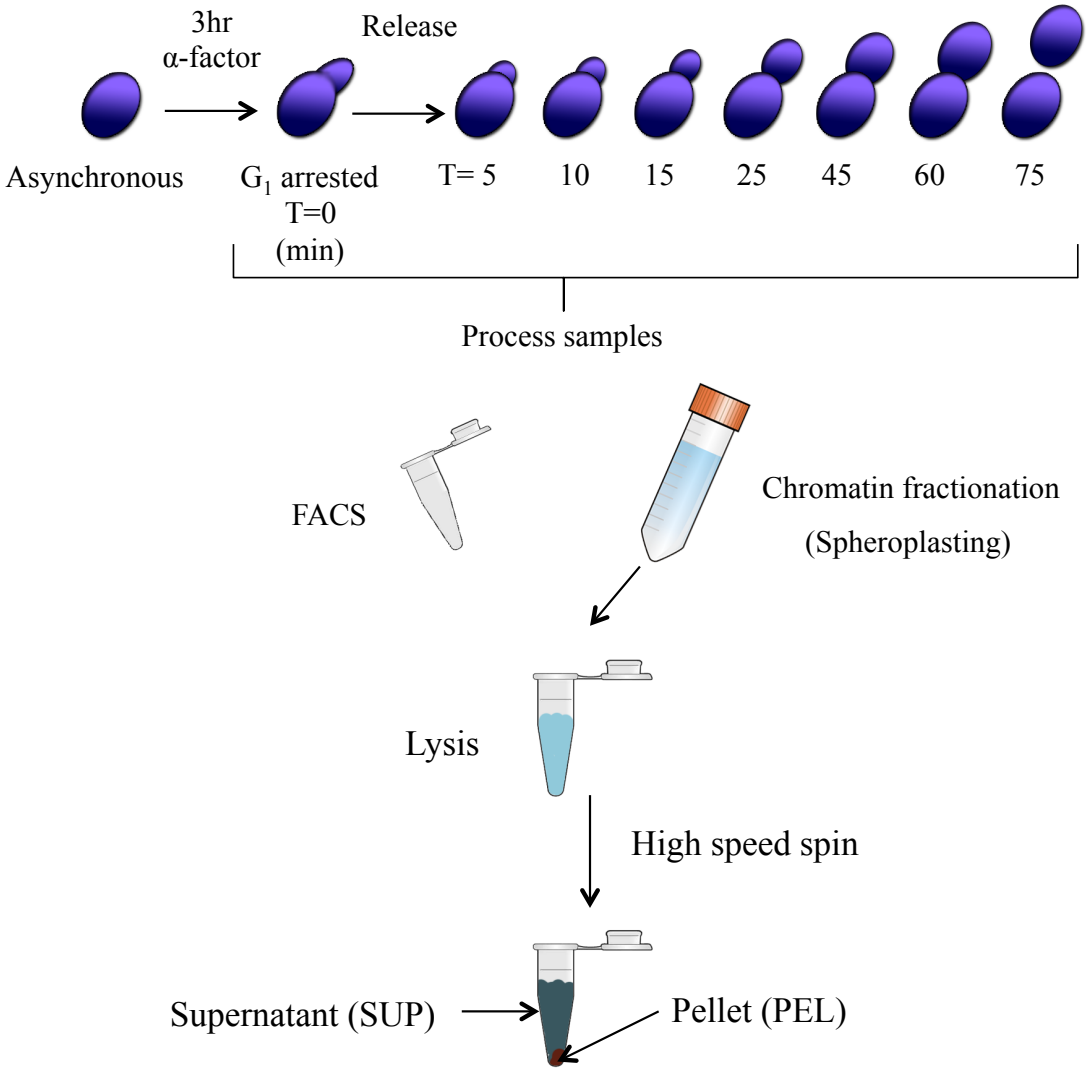

Figure 2.1. Schematic for cell cycle timecourse experiments and chromatin fractionation. Logarithmically growing yeast cultures were spun down, washed and resuspended in fresh medium containing α-factor. After three hours, samples were taken for FACS analysis and for fractionation. Cells were spun down, washed and resuspended in fresh media lacking α-factor, thus allowing them to resume the cell synchronously. Samples were taken at the indicated timepoints (minutes after release from the G1 arrest). Aliquots of these samples were collected for FACS analysis to verify cell culture synchrony. The remainder of each sample was subjected to chromatin fractionation. This permitted the separation of chromatin bound and unbound proteins, which were subsequently analyzed via Western blotting.

2.3 Cell Culture for Chromatin Fractionation Samples used in 2D-DIGE Experiments

For large-scale cultures, 10-20 μl of saturated seed culture (BY4733) was transferred to 300 ml YPD medium in a 2 L flask and incubated with shaking at 30°C until a cell density of 2-3 × 10^7/ml was achieved. For MMS treatment experiments, the 300 ml sample was centrifuged, the cell pellet was resuspended in 600 ml fresh YPD medium, and then divided equally into two 2 L flasks, and then further cultured at 30°C for 2 hrs. MMS was added to 0.03% for one of the flasks, and both were cultured at 30°C for another 90 min. The final cell density was not more than 3 × 10^7/ml.

2.4 Whole Cell Extract Preparation

Cells were pelleted at 4000 rpm for 3.5 min and resuspended in 400 µl of ice-cold lysis buffer (10 mM Tris-HCl, pH 8; 140 mM NaCl; 1% Triton X-100; 1 mM EDTA; PMSF and protease inhibitor tablet from Roche, Germany). The suspension was transferred to a 2 ml screw- cap tube containing 0.3 g of 0.5 mm glass beads, on ice. Samples were lysed by 6 cycles of bead beating (Biospec) with 30 sec on/30 sec on ice. The slurry was then spun at 13,000 rpm for 30 sec and the supernatant transferred to a fresh tube. This was processed for Western blotting as described below (section 2.7).

2.5 Fluorescence Activated Cell Sorting (FACS)

To assess cell synchrony, 1.5 x 10^6 cells were removed from each time point sample. They were immediately centrifuged, re-suspended in 1ml of ice-cold 70% ethanol and stored overnight at 4°C. Cells were then re-suspended in 500 µl of 50 mM Tris-HCl pH 8

containing 10 mg/ml of RNase A and incubated for 2 hours at 37°C. This was followed by centrifugation and re-suspension in 500 µl 50 mM Tris-HCl 7.5 with 2 mg/ml Proteinase K. Incubation at 50°C for an hour was performed prior to final resuspension in 100 µl FACS buffer (200 mM Tris-HCl 7.5, 200 mM NaCl and 78 mM $MgCl_2$). Cells were stained with SYTOX Green dye (5 µM; Molecular Probes) for at least one hour and then analyzed using a Becton-Dickinson FACScan. This analysis was performed with a BD FACSVantage SE cell sorting system in the Molecular Core Facility of the Department of Biology at the University of Waterloo.

2.6 Cdc45 *in vivo* Knock-down

Logarithmically growing yeast cells in YPD and expressing Cdc45 endogenously from the tetracycline-repressible tetO7 promoter in a BY4741 background (*BAR*1$^+$) were split into two cultures. Each was arrested for 90 min in YPD medium containing 5µg/ml α-factor. 50µg/ml of doxycycline, a tetracycline analog, was added to one culture and both were maintained in the late G_1 block for 6 h. Following this, cultures were washed in dH_2O as described in 2.1 and were released into fresh YPD medium, lacking α-factor and containing 100µg/ml Pronase E (Sigma-Aldrich). Timepoints were taken and analysed by FACS.

2.7 Western Blotting

2.7.1 Of Cell Cycle Timcourse Chromatin Fractionation Samples and of Whole Cell Extracts from Knock-down Experiments (Chapter 3)

Chromatin fractionation samples (supernatant and chromatin pellet) were assayed for protein concentration using the Bradford assay (Biorad) to calculate volumes for equal loading. Proteins were denatured by the addition of a half-volume of sample buffer (60% 4x buffer [15% SDS; 40% glycerol, 166 mM tris-base]; 0.26 M DTT; 7% bromophenol blue) to each sample followed by boiling for 10 min. The sample was then stored at -20°C until it was run on a 7.5% SDS polyacrylamide gel. The proteins in the polyacrylamide gel were transferred to a nitrocellulose membrane by sandwiching the gel and the membrane between two pieces of Watman paper and sponges in a cassette that was then transferred using an OWL transfer apparatus containing transfer buffer (200 mM glycine; 25 mM tris-base; 20% MeOH; 0.05% SDS). The transfer was carried out at 30-50 volts at 4°C for 2-16 h. The membranes were stained with 0.1% Ponceau S dye (Sigma), and imaged. The membranes were then destained with TEN+T (20 mM Tris-HCl; 1mM EDTA; 0.14 M NaCl; 0.05% Tween 20). Detections were carried out by first blocking the membrane in TEN+T with 5% skim milk powder for 45 min at room temperature or overnight at 4°C. The membrane was then incubated with primary antibody in TEN+T with 5% skim milk powder for 1-2 h at room temperature with gentle rocking. Following 2-3 five min washes in TEN+T, the membrane was incubated in secondary antibody in TEN+T for 45 min-1 h at RT with gentle rocking; for Alexa Fluor antibodies this incubation was carried out in the dark. The membrane was then washed twice in TEN+T and once in dH_2O.

Mouse monoclonal α-Myc (Sigma, 1:5000) and Alexa Fluor 488 goat α-mouse IgG (Invitrogen, 1:5000) antibodies were used to detect Myc-tagged Cdc45 and Cdc6. α-Mcm2 antibody (yN-19 goat polyclonal, Santa Cruz, 1:500) along with Alexa Fluor 488 donkey α-goat IgG (Invitrogen, 1:3000) antibodies were used to detect Mcm2. Blots were incubated in primary and secondary antibodies for 2 h each, proceeding 4 h of blocking in 5% skim milk. Between blocking and each antibody treatment, blots were washed for 2 x 10 min with 1 x TEN+0.05% Tween-20. The Typhoon 9400™ Variable Mode Imager (GE Healthcare) was used to analyze the blots via the fluorophores conjugated to the secondary antibodies. Densitometry readings were performed using Image Quant TL software (BD) and were normalized to total protein concentration as judged by the Ponceau S stain and/or tubulin band intensity detected using the mouse monoclonal α-TAT1 antibody (1:500, Sherwin and Gull, 1989) along with Alexa Fluor 488 donkey α-goat IgG (Invitrogen, 1:3000). The same protocol for Western blotting was used in perturbation (knock-down) experiments involving HA-tagged strains. In this case, mouse monoclonal α-HA (Sigma, 1:5000) and Alexa Fluor 488 goat α-mouse IgG (Invitrogen, 1:3000) antibodies were used to determine levels of Cdc6, Cdt1 and Dbf4.

2.7.2 For Detecting Levels of DAmP Strain Proteins and Chromatin Fractionation Efficiency (Chapter 4)

Western blotting was performed as described above. RpaI was detected with rabbit polyclonal α-RFA antibody (1:2000 dilution, Agrisera) and a 1:3000 dilution of the Alexa Fluor 647 goat anti-rabbit IgG secondary antibody. Arp3 was detected with the goat

polyclonal α-Arp3 antibody (1:1000 dilution, Santa Cruz) and a 1:3000 dilution of the Alexa Fluor 488 donkey anti-goat IgG secondary antibody.

Initial whole cell extract (WCE), as well as supernatant (SUP) and chromatin (PEL) fractions were subjected to SDS-PAGE and transferred to a nitrocellulose membrane as described above. Detection was carried out with rabbit polyclonal α-Orc2 (1:1000 dilution, Duncker *et al*., 2002), mouse monoclonal α-TAT1 (1:500 dilution, Sherwin and Gull, 1989), and rabbit polyclonal α-histone H2B (1:1000 dilution, Cedarlane), using 1:3000 dilutions of either Alexa Fluor 647 goat anti-rabbit IgG or Alexa Fluor 488 goat anti-mouse IgG secondary antibodies. With efficient fractionation, PEL fractions in this version of the assay (considering resuspension volumes) are concentrated tenfold relative to WCE and SUP. In each case, equal volumes of WCE and SUP fractions were loaded, with double (histone H2B, α-tubulin detection) or triple (Orc2 detection) the volume of the PEL fraction loaded. Refer to Appendix B, Figure B1. A summary of the antibodies used is shown below in Table 2.2.

Table 2.2. Antibodies used in this project for use in Western blotting.

Antibody	Source	Dilution
α-Myc (mouse monoclonal)	Sigma	1:5000
α-HA (mouse monoclonal)	Sigma	1:5000
α-Mcm2 (goat polyclonal)	Santa Cruz	1:500
α-RFA (rabbit polyclonal)	Agrisera	1:2000
α-TAT1 (mouse monoclonal)	Gift from Gull lab	1:500
α-Arp3 (goat polyclonal)	Santa Cruz	1:1000
α-histone H2B (rabbit polyclonal)	Cedarlane	1:1000
α-Orc2 (rabbit polyclonal)	Gift from Gasser lab	1:1000
Alexa Fluor donkey α-goat	Invitrogen	1:3000
Alexa Fluor goat α-mouse	Invitrogen	1:3000
Alexa Fluor goat α-rabbit	Invitrogen	1:3000

2.8 Densitometric Analysis of Cell Cycle Timecourse Samples

Determination of *in vivo* cellular concentrations for each factor was performed for each time point. Normalization of densitometry readings was carried out by averaging the means of all SUP values from each set of experiments for a given protein. This average was divided by the means of the SUPs for each trial to give a scaling factor (S1) for each trial. Each SUP value for a given trial was then multiplied by its scaling factor. The same procedure was applied to all PEL sample values. In general, when a protein is in the chromatin fraction it is DNA-bound. To correct for non-specific DNA-binding, for each protein, a background level of non-specific binding was determined corresponding to the observed abundance from a time-point at which the factor is known to be absent from origins. To obtain densitometric values, the program Imgage Quant™ was used to analyze blots scanned by a Typhoon™ 9400 imager (both GE Healthcare). To convert the densitometry measures to molecules/cell concentrations, a scaling factor (S2) for each protein was determined from the molecule counts reported in Huh *et al*. (2003). For each experiment, the total densitometry measure (SUP plus PEL) was averaged across the time-points to arrive at an averaged asynchronous densitometry reading (weighted according to the time contribution of each sample to a 90 minute cycle), which was then compared to the database to arrive at a scaling factor. This procedure could not be followed for Cdc6 or Dbf4, since they are not included in the database presented in Huh *et al*. (2003). A scaling factor was determined for these proteins by comparing asynchronous whole cell extract levels of Cdc6-Myc and Cdc45-Myc and Cdc6-HA and Dbf4-HA. A sample conversion is shown in Appendix A, Table A1. Western blotting and densitometric analysis provided an asynchronous value of 576 molecules/cell for Cdc6

($Cdc6_{Total}$ = 576). This was one third of the value reported for the concentration of Cdc45, i.e. 1730 copies/cell according to Huh *et al*. (2003) ($Cdc45_{Total}$=1730). Similarly, the concentration of Dbf4 in an asynchronous population was 170 molecules/cell ($Dbf4_{Total}$ = 170). The copy/cell number used for Mcm2 was 40,000 (Lei *et al*., 1996) while that for Cdt1 was 2190 (Huh *et al*., 2003) ($Cdt1_{Total}$ = 2190).

2.9 Chromatin Fractionation

Chromatin fractionation was performed as described in Semple *et al*. (2006) with some modifications. Approximately 1 x 10^7 cells collected from each time point were incubated in 7.5 ml pre- spheroplasting buffer (100 mM EDTA-KOH pH 8, 10 mM DTT), after washing once with dH_2O. They were then incubated at 30°C for 10 min with gentle shaking. Cells were centrifuged and re-suspended in 7.5 ml spheroplasting buffer (1 X YPD, 1.1 M sorbitol) containing 0.5 mg/ml Zymolyase 20T (Seikagaku Corp., Japan) and 0.1 mg/ml Oxalyticase (Sigma), followed by shaking at 30°C for 30-45 min with gentle mixing. Cells were then washed once with 20 ml spheroplasting buffer containing 0.5 mM PMSF followed by resuspension in 1 ml ice-cold wash buffer (5 mM Tris–HCl pH 7.4, 20 mM KCl, 2 mM EDTA-KOH pH 7.4, 1 M sorbitol, 1% thiodiglycol, 125 mM spermidine, 50 mM spermine). Wash, Breakage and Lysis buffers all contained 1 tablet/10ml of EDTA-free protease inhibitors (Roche) and were supplemented with 0.5 mM PMSF. Cells were centrifuged at 400*g* for 1 min at 4°C, washed twice with 1 ml of Wash buffer and then re-suspended in 800 µl of Breakage buffer (5 mM Tris–HCl pH 7.4, 20 mM KCl, 2 mM EDTA-KOH pH 7.4, 0.4 M sorbitol, 1% thiodiglycol, 125 mM spermidine, 50 mM spermine). To these cells, 1ml of Lysis buffer (Breakage buffer

supplemented with 1% Triton X-100) was added and after repeated inversion (until the solution turned clear), cells were pelleted at 16,000*g* for 10 min. This separated the proteins bound to the chromatin (residing in the pellet, referred to as PEL) from those solubilized in the non-chromatin fraction (supernatant or SUP). After removal of the supernatant, an additional 1 min spin at 16,000*g* was performed to isolate any residual supernatant and the pellet was re-suspended in 100 µl Breakage buffer. $MgCl_2$ (5 mM) and DNaseI (2 µg/ml) were added to the PEL fractions to solubilize the chromatin and associated proteins. After 10 min, the reaction was quenched with the addition of 2 µl 0.5 M EDTA. 10 µl of each SUP and PEL sample were collected for protein quantification via the Bradford assay. To the remaining of each sample, a half volume of sample loading buffer was added and processed for Western blotting, as described in section 2.7. For an equal volume, PEL samples were 20-fold more concentrated than SUP samples due to the fact that approximately 5% of proteins are chromatin-bound.

2.10 Perturbation experiments

DY-139 (*GAL1-CDC6-HA*), DY-140 (*GAL1-CDT1-HA*) and DY-255 (*GAL1-DBF4-HA*) strains were grown to 1 x 10^7 cells/ml in 2% galactose/1% raffinose medium (GAL) at 30°C, centrifuged at 6000*g* for 5min and washed with dH_20. Cells were then resuspended in 2% glucose medium, maintaining the same cell concentration. Culture aliquots were removed for FACS analysis and preparation of whole cell extracts (as described in Varrin *et al*., 2005), both before, and at various intervals after the switch to glucose. As references for normal endogenous protein levels, whole cell extracts were also prepared from strains expressing Cdc6 (*CDC6-HA*, DY-142), Cdt1 (*CDT1-HA,* DY-143) and Dbf4

(*DBF4-HA,* DY-256) from their endogenous promoters. All strains produced fusion proteins with a 3HA epitope tag to facilitate visualization via Western blotting.

2.11 Time-Varying Model Inputs

Protein data was collected from yeast strains, which were observed to have a generation time of ~ 90 min in log phase. In order to fit the data to the timescale of the Chen *et al*. (2004) model, which has a period of 101.2 min, the experimental time-course was scaled to reflect this change in timing. This value, as described in the Chen model, is chosen to reflect the longer cycle of daughter cells (which are smaller than mother cells in asymmetric cell division). Time-point samples were collected from an α-factor arrest in late G_1 phase, corresponding to experimental timepoint T=0. Additional samples were collected at 5, 10, 15, 30, 45, 60 and 75 min after synchronous release from the alpha factor block. The experimental timepoint T=0 corresponds to 19 min after the beginning of G_1 phase in the 101.2 min model. This number was determined by comparing the point at which cells entered S phase *in vivo* (~15 min after α-factor release as determined by FACS analysis) and the corresponding start of S phase in the model.

One of the two inputs used from the Chen model was the APC co-factor Cdc20. Its role in the present is to activate the APC, which rapidly degrades Dbf4. In the Chen model, Cdc20 serves exclusively as a signal to exit mitosis. The Cdc20 degradation rate is a function of the parameter k_{mad2}, which describes the activity level of the protein Mad2, a key factor in the spindle assembly checkpoint. In order to prevent the occurrence of mitosis before replicated chromosomes have been properly attached to the mitotic spindle (representing the spindle assembly checkpoint), the value of k_{mad2} jumps

discontinuously from 0.01 to 8 once DNA replication has commenced. This is signified by the lumped Chen model variable ORI reaching a threshold value of 1. This sequence of events ensures that Cdc20 levels are low, thus preventing premature activation of the MEN pathway. Later, when correct spindle assembly is specified by other factors, the value of k_{mad2} falls back to 0.01, allowing Cdc20 to accumulate. The signal for this event is a second lumped parameter, SPN, hitting its threshold value of 1. As a result of these discontinuous transitions in k_{mad2}, the Cdc20 profile shows rather sharp shifts in behaviour. When this profile was applied as an input to the DNA replication model, the Dbf4 profile showed a precautious and abrupt spike compared to laboratory observations; this discrepancy was not observed in the Chen model since that model does not address the influence of Cdc20 on Dbf4. To address this inconsistency, the k_{mad2} profile was smoothed to allow for a gradual decline in Mad2 activity. The timing of this activity was chosen to match these *in vivo* Dbf4 observations. The original formulation for k_{mad2} specifies a value of 0.01 when ORI is less than 1 or SPN is greater than 1, and otherwise is equal to 8. This condition was replaced with:

$$K_{mad2} = (7.99\times(ORI/15)^{(1/2)}\times(1/1 + SPN^{300})) + 0.01 \quad (2)$$

The difference between the original Cdc20 profile and the modified version is shown in Figure 3.8.

2.12 Implementation of a combined model

In order to implement a combined model, the loop between the DNA replication model and the cell cycle model of Chen *et al*. (2004) was closed by eliminating the lumped species ORI and replacing it with an indication of the progress of replication, represented

by the FORK species. In this combined model the formula for k_{mad2} shown above was modified by replacing the ratio (ORI/15) with $(\int FORK / 500)$, where the integration begins at the start of the cell cycle. Since each model incorporates a description of Cdc6 dynamics, they were merged by including the dynamics of origin binding from the DNA replication model with the Cdc6 dynamics of the Chen model. This resulted in good accordance between the behaviour of the replication initiation network within the combined model. The only noticeable differences (Figure 3.9) are caused by the merged description of Cdc6 dynamics. Firstly, due to the fact that the internal model uses a Clb5 profile generated by scaling from arbitrary units, it is nearly, but not exactly identical to the Chen model Clb5 profile. The Chen Clb5 profile extends farther past the 101.2 min mark than in the internal model resulting in a more rapid dephosphorylation of RC7 in the internal model. Thus, RC7 persists for ~5 min longer in the combined model. Secondly, because the merged Cdc6 decreases in concentration earlier than in the DNA replication model in isolation, RC1 levels stay high until fork firing occurs. Despite these differences, the essential dynamics of the system are preserved: replication fork firing follows the same pattern, with the RC7→RC1 delay having no effect on timing of firing. The behaviours of the Chen model species are not perceptibly altered by the removal of ORI and the combination of the two models (Figure 3.9).

The effects of combining the models are shown to be minimal in the wildtype case (Figure 3.9). Comparing mutations used to fit the Chen model in the combined model, the same phenotypes are observed (Appendix A, Figure A4). This exemplifies the efficacy with which the DNA replication initiation module replaces the corresponding black box in Chen *et al*.'s whole cell cycle model.

2.13 Parameter Estimation and Error Analysis

For parameter estimation, an initial global parameter search was performed using a variation of the commonly used simulated annealing technique – "adaptive simulated annealing" (ASA; Ingber, 1996). This was used to statistically find the best global fit to the nonlinear constrained non-convex cost-function over a D-dimensional space. In the case of the DNA replication model, the cost function corresponds to the sum of squared error (SSE), which is defined as the cumulative difference between measured data points and the corresponding simulated values. The search was performed in a 24-dimensional space. A crucial difference with ASA compared to other forms of simulated annealing is that it permits adaptation to changing sensitivities over the multi-dimensional space, such that individual parameters are afforded an individualized cooling schedule. This schedule refers to the speed at which convergence occurs (a higher cooling rate will arrive at a solution more quickly, but with the tradeoff of an increasing likelihood of not finding the global minimum).

Additionally, a local search was performed using the Nelder-Mead simplex algorithm to optimize the parameter estimate at the previously determined global minimum (Nelder and Mead, 1965).

Parameter error was estimated as a way of identifying or testing the invalidity of the model. In other words, a global optimum can never be confirmed, only inferred based on evaluation of statistics representing the congruence between observed data and model-derived estimation of parameters. While in some cases, global optimization routines use a parameter error calculation to decide whether to continue searching, a *post-hoc* error analysis of the parameter set was performed in Chapter 3. This was after

qualitatively determining that the SSE was sufficiently low so as to represent good accordance between data and model simulation derived by the ASA regimen.

The goal of parameter estimation is to statistically minimize the difference between the derived parameter values and their true value. This is a function of the data, the estimated parameters and the variance within the data. If the vector of the parameter set describing the observed data, *x* is represented by θ, it gives rise to a probability distribution $P(x|\theta)$, where θ is an unknown fixed constant within the distribution. An unbiased estimator, $\hat{\theta}$ maps observed data to values that are hopefully close to θ. To obtain the lower bound on the variance (Var) of the unbiased estimator, the variance of $\hat{\theta}$ must satisfy the conditions:

$$\mathrm{Var}\left\{\hat{\theta}\right\} \geq \frac{1}{\left\langle\left[\frac{\partial}{\partial\theta}\ln P(x|\theta)\right]^2\right\rangle_{P|\theta}} \tag{3}$$

, where the denominator is known as the Fisher information matrix (FIM; Emery and Nenarokomov, 1998). This gives the lower bound of the inverse of the FIM and is known as the Cramer-Rao bound. It is reported in this thesis as a percentage by scaling each error estimate to the maximum error estimate over the entire time course of the simulated vector (reviewed in Gadkar *et al*., 2005). Scaling to a maximum value eliminates spurious interpretation of the error estimate where the parameter values are very low. The Cramer-Rao bound effectively allows for the maximization of the expected accuracy in the nominal parameter set such that the estimated parameters have minimum variance. An assumption made is that the errors in measurement between estimated and true parameter values follow a Gaussian or normal distribution.

2.14 Protein Extraction for Use in DIGE

Chromatin pellets from the chromatin preparation were resuspended in two volumes of extraction buffer (50 mM Tris-HCl, pH 8.5, 2% (w/v) SDS, 50 mM DTT), and incubated in a boiling water bath for 10 min. Protein extracts were separated by centrifugation at 14,000*g* for 10 min. The supernatants were collected then desalted using a 2-D Clean-Up kit (Amersham Biosciences). Protein pellets from the 2-D Clean-Up treatment were dissolved in IEF rehydration buffer (7 M urea, 2 M thiourea, 4% (w/v) CHAPS). Protein concentration was measured using the Bradford assay (Bio-Rad). Protein yield of the chromatin fraction was calculated based on the amount in the pellet compared to the total amount in the WCE. A typical 300 ml culture at ~3×10^7cells/ml yielded approximately 200 +/- 100 µg of protein in the chromatin fraction.

2.15 Differential-in-gel-electrophoresis (DIGE)

DIGE was performed based on recommended protocols of the manufacturer (GE Healthcare) using minimal labeling CyDye™ DIGE Fluors of Cy2, Cy3 and Cy5. For the CyDye™ labeling reaction, 40 µg of protein sample in 50 µl of rehydration buffer containing 25 mM Tris-HCl, pH 8.5 was used for each dye. 1 µl CyDye™ solution (200 pmol/µl in 100% dimethylformamide) was added to samples on ice. The reaction was incubated for 40 min on ice, after which 1 µl of 10 mM lysine was added to stop the reaction. After incubation for 10 min, three sets of 50 µl samples (labeled with Cy2, Cy3 and Cy5) were combined and mixed with 45 µl of 1 M DTT, 4.5 µl of 1% (v/v) IEF buffer 4-7, 1 µl of 1% (w/v) bromophenol blue (BPB) and 250 µl of the rehydration buffer.

Immobiline™ DryStrip gels (IPG pH4-7/24 cm, GE Healthcare) were used for isoelectric focusing as the first dimensional separation. The strips were passively rehydrated with 450 µl of labeled protein sample in the rehydration buffer overnight at room temperature. Isoelectric focusing (IEF) was performed using an Ettan™ IPGphor II system (GE Healthcare) with oil immersion and paper wicks at electrode contacts. The voltage profile used for IEF was as follows: hold at 500 V for 1 h, gradient to 1,000 V for 3 h, gradient to 3,000 V for 3 h, hold at 3,000 V for 2 h, gradient to 8,000 V for 3 h, at 8,000 V for 10.5 h, and step to a final voltage of 500 V.

After the 1st dimension separation, IEF strips were incubated in equilibration buffer (6 M urea, 2% (w/v) SDS, 50 mM Tris-HCl (pH 8.8), 30% (v/v) glycerol, 0.002% (w/v) BPB) containing DTT (10 mg/ml) for 20 min and then a further 20 min with the same buffer containing iodoacetamide (25 mg/ml). The strips were loaded onto 10% Tris-glycine SDS-polyacrylamide gels and run at 15 W per gel by using an Ettan™ DALTsix electrophoresis unit (GE Healthcare). Scanning of the DIGE gels was done using Typhoon 9400™ Variable Mode Imager (GE Healthcare).

A three-dye system was employed with four biologically independent replicates using an independent Cy2 dye channel as internal standard for each gel. The internal standard was composed of an equal mixture of control and test samples. The control and test samples used either Cy3 or Cy5 with dye swapping. Gel image analysis was performed using DeCyder™ 2-D differential analysis software version 6.0 (GE Healthcare), with the peak detection threshold set to an expected value of 2500 spots. Protein spots were quantified using peak volumes calculated by the DeCyder™ software. Each gel was normalized based on the independent Cy2 channel using the differential in-

gel analysis (DIA) module. Biological variation analysis (BVA) was done for four replicates, including 4 internal standards, 4 controls and 4 test samples. Statistical analysis of spots was performed by the Student's t-test with FDR (false discovery rate) correction as previously described (Karp *et al*., 2007; Molloy *et al*., 2003). Average spot ratios for treated to control samples were calculated based on spot volumes for each matched spot, along with *p*-values. For the chromatin enrichment analysis, the enrichment factor (EF) was defined as the average ratio of normalized spot volumes in the chromatin fraction vs. WCE. EF values were calculated by the DeCyder software as fold change (EF = chromatin abundance/WCE), when chromatin abundance exceeded WCE abundance for the target protein, and as a negative fold change (EF = -WCE/chromatin abundance) otherwise. For experiments comparing the MMS-treated vs. non-treated chromatin fraction, differential factors (DF) were similarly calculated, where DF = (MMS treated/control) when treated ≥ control, and as a negative fold change (DF = -control/MMS treated) otherwise. As with the chromatin abundance experiment, the average ratio of spot volumes of the two DIGE channels being compared is reported. Calculated enrichment factors (EF) provide a measure of chromatin association (protein localization) independent of total protein abundance, whereas the differential factors (DF) measure changes in abundance in the chromatin fraction, including both changes in total abundance in the cell and changes in protein localization.

For graphical presentation, a log scale is used and values are presented as $\log_2$ (treated/control). To determine the magnitude of change that is likely to be detected, a *post-hoc* power analysis was conducted using the statistical analysis package R (Team RDC). Standard deviations were calculated for all spots appearing on 10 or more gel

image channels (i.e. 10 from 12 total on 4 gels), and used to estimate the expected detectable fold change with a power of 0.80 ($\beta = 0.20$).

2.16 Preparative 2D-PAGE

For preparative 2D-PAGE, 0.7 to 1.0 mg of protein was separated on large-format gels using a 24 cm IPG 4-7 strip for 1st dimension separation and an SDS-PAGE gel for the second dimension as described above. Preparative gels were visualized by the colloidal Coomassie-staining method (Candiano *et al*., 2004) and scanned using a Typhoon 9400™ Variable Mode Imager (GE Healthcare). Spots of interest were matched between DIGE images and the preparative gel, and spots manually excised for protein identification. Spots were prioritized for identification using an FDR corrected *p*-value cut-off of 0.05 and a change in expression of 1.4 or greater.

2.17 Mass spectrometry

Protein spots excised from the preparative gel were cut into approximately 1 mm^3 pieces, then reduced and alkylated by treatment with 10 mM DTT and 55 mM iodoacetamide in 50 mM ammonium bicarbonate buffer (Granvogl *et al*., 2007). Gel pieces were washed with 50 mM ammonium bicarbonate buffer and dehydrated in a SpeedVac® concentrator (Savant) for 1 h, soaked with 3-10 µl of 20 ng/µl trypsin solution (sequencing grade modified trypsin, Promega) in 50 mM acetic acid on ice for 20 min, then washed again with buffer. Protein digestion was performed in the same buffer (50 µl) overnight at 35°C. Reaction supernatant was recovered and gel pieces were further extracted by 2× sonication in 50 µl 50% acetonitrile/1% trifluroacetic acid, and then dried using a

SpeedVac® concentrator (Savant). Mass spectrometry for higher abundance spots was performed using a Waters micromass quadrupole time of flight (Q-TOF) Ultima mass spectrometer with a nanospray ESI injection at the mass spectrometry facility at University of Waterloo. Samples analyzed using the Q-Tof were desalted prior to analysis using C_{18} ZipTip® pipette tips (Millipore) and eluted using 50% acetonitrile in water with 0.2% formic acid. For lower abundance spots, trypsin-digested peptides were analyzed (without ZipTip desalting) using an Applied Biosystems Q-Trap mass spectrometry system at the Proteomics Core Facility of Dalhousie University (Halifax, Nova Scotia).

2.18 Protein identification

Protein identification was performed using Peaks Studio (version 2.4, Bioinformatics Solutions, Waterloo), which combines auto *de novo* sequencing and homology-based database searching, with the non-redundant MSDB database (Dr. D.N Perkins, Imperial College London, Release 20063108, 3239079 sequences). Mass error tolerances of parental and fragment ions were set at 0.1 for Q-TOF spectra and 0.3 or 0.4 for Q-Trap spectra, with 0.3 used if a more restrictive search was required. Confidence of protein identifications were based on the Peaks database search score (%) according to the algorithm of Ma *et al*. (2005). Protein identifications were accepted if the homology search score was higher than 80% (i.e. extremely high confidence) and identified a single yeast protein. For Peaks scores less than 80%, protein identity was additionally confirmed using the web-based Mascot search engine (version 4) in the MS/MS ion search module (Matrix Science, http://www.matrixscience.com) with MSDB by restricted to *Saccharomyces cerevisiae* (10742 sequences) as the target organism. Protein matches

were retained if the Mascot search had a significance threshold of $p < 0.05$, with default mass error tolerances of 1.2 and 0.6 Da for parental and fragment ions, respectively. Finally, the false discovery rate (threshold set to 0.01) was confirmed by performing the Mascot decoy database search. For both the Peaks and Mascot database searches, trypsin was set as the digestive protease allowing one missed cleavage, and carbamidomethylation of cysteine and oxidation of methionine were set as the fixed and variable modifications, respectively. For counting number of unique peptides matching to hit proteins, only peptide ions that are doubly or triply charged were included. Peptide sequence coverage (%) was obtained based on the matching peptide sequences from Peaks.

2.19 Genotoxic sensitivity assays

To identify potential genotoxic effects of targeted proteins, spotting growth assays were performed to assess MMS or hydroxyurea (HU) resistance (Hanway *et al*., 2002; Varrin *et al*., 2005) in gene knockout cell lines or cells with lowered mRNA expression. Haploid knockout and DAmP cell lines in a BY4741 background were purchased from Open Biosystems (Thermo Fisher Scientific Inc.). BY4741 wild type and DNA damage checkpoint-compromised *rad53-11* (DY-123, Santocanale and Diffley, 1998) strains were used as controls. Cultures of cells were grown to saturation (~2×10^8 cells/ml) and serial 10-fold dilutions, ranging from 10^7 cells/ml to 10^4 cells/ml, were prepared for each strain. 5 µl of each dilution was spotted onto a series of YPD plates with varying concentrations of MMS (up to 0.04%) or HU (up to 100 mM). The plates were incubated at 30°C for 2 days.

Chapter 3: A Quantitative Model of the Initiation of DNA Replication in *Saccharomyces cerevisiae* Predicts the Effects of System Perturbations

3.1 Introduction

The machinery of the eukaryotic cell cycle has been extensively dissected and described, in both simple and complex organisms. Proliferation hinges on the cell's ability to replicate the genome with high fidelity, segregate the chromosomes equally, and ultimately divide into two genetically identical cells. A fundamental process in the regulation of DNA replication is the step-wise assembly of the pre-replicative complex (pre-RC) at origins of replication facilitated by the six-subunit origin recognition complex (ORC), which, in the budding yeast *Saccharomyces cerevisiae,* binds an 11 bp consensus sequence (Bell and Sillman, 1992; Rao and Stillman, 1995; Rowley *et al*., 1995; Speck *et al*., 2005 and 2007; Tanaka *et al*., 2007). The co-import of Cdt1 and the Mcm2-7 complex (MCM) into the nucleus follows (Tanaka and Diffley, 2002), and the MCM•Cdt1 heptamer is then targeted to origins by an interaction between Cdt1 and Orc6 (Semple *et al*., 2006; Chen and Bell, 2007). Reiterative loading of multiple MCM molecules occurs via Cdc6 and ORC ATP-hydrolysis (Randell *et al*., 2006), resulting in two rings at each origin (Bowers *et al*., 2004; Ervin *et al*. 2004; Remus *et al*., 2009). At this point origins are said to be licensed. In late G_1 phase, a burst of Dbf4 synthesis activates the Dbf4-dependent kinase Cdc7 (DDK), which then phosphorylates multiple MCM subunits, stimulating the complex (Francis *et al*., 2009; Lei *et al*., 1997, Randell *et al*., 2010; Sheu and Stillman, 2010). Dbf4 levels decrease over the course of S-phase and, starting at the metaphase/anaphase transition, Dbf4 is actively degraded by the anaphase promoting complex (APC) and its activating co-factor, Cdc20 (Cheng *et al*., 1999; Eytan *et al*. 2006; Ferreira *et al*., 2000; Oshiro *et al*., 1999; Zachariae and Nasmyth, 1999). In this way, Dbf4 levels are prevented from rising until the next G_1/S transition.

The phosphorylation of MCM by DDK is coincident with the phosphorylation of the protein factors Sld2 and Sld3 by Clb5-Cdc28, a cyclin-dependent kinase (CDK) complex, the activity of which rises just prior to S-phase entry. The Sld proteins, once phosphorylated, are stabilized as a complex with the adaptor protein Dpb11 and the tetrameric GINS complex, forming a module that interacts with Cdc45 (Gambus *et al*., 2006; Kanemaki and Labib, 2006; Zegerman and Diffley, 2007). The end result is the tight association of Cdc45, MCM and GINS (collectively known as CMG) with origins, allowing the unwinding of DNA and processive replication by DNA polymerase (Bruck and Kaplan, 2011). This represents the essential role of CDK in stabilizing polymerase at the moving replication fork and switching the system from a pre-replicative state to a replicative one. From this point until mitosis, CDK levels remain high. This continued CDK activity prevents re-establishment of pre-RCs at origins that have already fired through a number of mechanisms. Firstly, CDK phosphorylates Cdc6, thus causing the SCF^{Cdc4} complex to target Cdc6 to the proteasome for degradation (Drury *et al*., 1997 and 2000; Dutta and Bell, 1997; Elsasser *et al*., 1999). Secondly, Orc2 and Orc6 are phosphorylated by CDK (Nguyen *et al*., 2001; Vas *et al*., 2001; Wilmes *et al*., 2004), with the phosphorylation of Orc6 rendering it refractory to interaction with Cdt1 (Chen and Bell, 2011), thereby preventing further MCM loading. Finally, CDK facilitates the nuclear export of both MCM and Cdt1, at different time points. Just prior to initiation, Cdt1 exits via a CDK-dependent mechanism, while MCM complexes fall off the DNA upon fork termination and are then exported in a CDK-dependent manner (Labib *et al*., 1999; Liku *et al*. 2005; Nguyen *et al*., 2000; Tanaka and Diffley 2002). Thus, while CDK initiates replication, it subsequently prevents pre-RC reassembly.

Mathematical modeling has been successfully used in the past to address various aspects of the cell cycle. Early models (e.g. Kauffman and Wille, 1975) did not incorporate specific biochemical mechanisms; they were hypothetical representations of periodic cellular activity. As the molecular mechanisms driving the cell cycle were revealed, models appeared that incorporated these findings (e.g. Hyver and Le Guyader, 1990; Goldbeter, 1991; Norel and Agur, 1991; Tyson, 1991). For *S. cerevisiae* in particular, multiple modeling approaches have been applied, based both on network descriptions (Li *et al*., 2004) and on specific molecular details such as gene expression and biochemical kinetics (Chen *et al*., 2000 and 2004; Klipp *et al*. 2005 and reviewed in Ingalls *et al*., 2007). Some modeling efforts have been comprehensive, such as the Tyson group's ordinary differential equation (ODE)-based models (Chen *et al*., 2000 and 2004), while others address specific cell-cycle phenomena, such as the links between cell size and cycle progression (Alcarón and Tindall, 2007; Barberis *et al*., 2007). Spiesser *et al*. (2009), de Moura *et al*., (2010), Yang *et al*. (2010) and Retkute *et al*., (2011) present deterministic as well as stochastic aspects of the temporal pattern of origin firing.

A recent report (Brümmer *et al*., 2010) presented an ODE-based model describing the initiation of DNA replication, incorporating origin licensing, firing and the network of regulatory phosphorylation events. The model parameters were partly calibrated against experimental data, but largely selected through an optimization routine designed to attain an idealized function, resulting in a model that is particularly suited to exploring events specifically at the G_1/S transition.

Here, a new model of the initiation of DNA replication is presented. In contrast to the work of Brümmer *et al*. (2010), a 'bottom-up' approach was taken through the

gathering of *in vivo* data for the precise protein levels at time-points throughout the cell cycle, then calibrated the model against these values. Rather than limiting the model to the observation of firing near the G_1/S transition and fitting to DNA-specific replication profiles, it was validated against the behaviour of the constituent protein complexes throughout the replication cycle. To facilitate the use of the model in a comprehensive description of the cell cycle, it was designed to integrate easily with the model of Chen *et al*. (2004). Finally, the model was validated by comparing *in silico* predictions to experimental observations, using both knockdown experiments performed in this study and by results from the literature.

3.2 Results

Construction of the model was initiated by identifying the important players in replication initiation and establishing an interaction network, as shown in Figure 3.1. After selecting appropriate descriptions of reaction kinetics, an ODE-based model was generated and the model parameters were calibrated to *in vivo* data.

3.2.1 Description of Model Components

The model describes sixteen molecular species (twelve of which are dynamically independent) and depends on twenty-four parameters, which characterize the rates of seventeen biochemical processes (protein expression and degradation, complex association/dissociation, and transport across the nuclear membrane). The model describes the following molecular species (Figure 3.1).

RC1 (Replication complex, state 1): origin-bound ORC

RC2: origin-bound ORC associated with CDC6

RC3: origin-bound ORC associated with CDC6, with MCM loaded

RC4: origin-bound ORC, with MCM loaded

RC5: origin-bound ORC, with MCM loaded and DBF4 associated

RC6: origin-bound ORC, with MCM loaded and DBF4 and CDC45 associated

RC7: origin-bound phosphorylated ORC

FORK: the elongation fork, with MCM and CDC45 associated

$CDC6_N$: non-chromatin associated nuclear Cdc6

$DBF4_N$: non-chromatin associated nuclear Dbf4

$CDC45_N$: non-chromatin associated nuclear Cdc45

MCM_C: cytosolic MCM

$CDT1_C$: cytosolic CDT1

MCM•$CDT1_N$: non-chromatin associated nuclear MCM bound to Cdt1

$CDT1_N$: non-chromatin associated nuclear Cdt1

MCM_N: non-chromatin associated nuclear MCM

The MCM species corresponds to dimers of Mcm2-7 heterohexamers, as two complexes are loaded at each origin. Similarly, the CDC45 species corresponds to a dimer, as described by (Bowers *et al*., 2004). Concentrations are described in units of molecules per cell.

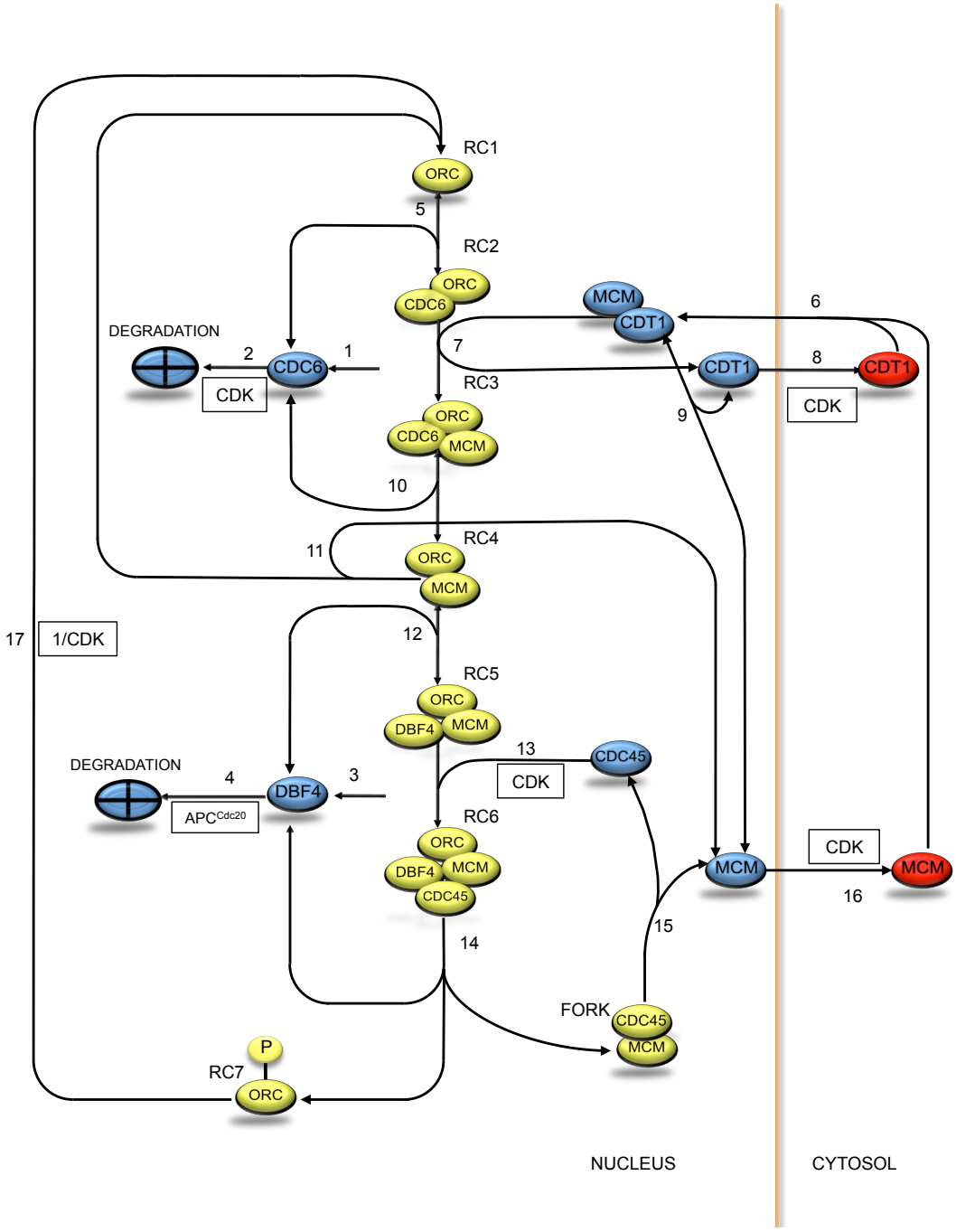
RC1
ORC
5
RC2
ORC
CDC6
MCM
CDT1
6
DEGRADATION
2
CDC6
1
7
CDT1
8
CDT1
CDK
RC3
CDK
ORC
CDC6
MCM
9
10
RC4
11
ORC
MCM
17
1/CDK
12
RC5
ORC
DBF4
MCM
13
CDC45
DEGRADATION
4
DBF4
3
CDK
APC Cdc20
RC6
ORC
DBF4
MCM
CDC45
CDK
MCM
MCM
16
15
14
FORK
CDC45
MCM
P
RC7
ORC
NUCLEUS
CYTOSOL

Figure 3.1. Network diagram for the initiation of DNA replication. Chromatin-bound species are shown in yellow. Reactions have considered reversible are shown with an arrowhead at each end. ORC-bound DNA (RC1) specifies a complex that has bound origin sequences following DNA replication of the previous cycle. Cdc6 reversibly binds ORC-bound DNA starting in late M-phase to form RC2. The Mcm2-7 hexamers, chaperoned by Cdt1 are localized to origins where they are loaded onto the double helix (RC3). Cdt1 is later exported from the nucleus by a CDK-dependent mechanism (i.e. by Clb5-Cdc28). Free Cdc6 is targeted for proteolysis in a CDK-dependent manner. Upon Cdc6 dissociation, the complex of MCM and ORC (RC4) is also subject to dissociation. RC4 awaits association of and activation by a complex of Dbf4 and Cdc7 (DDK), which phosphorylates various MCM subunits (RC5). Required ultimately for the stabilization of DNA polymerase, Cdc45 binds in response to specific CDK phosphorylation events (RC6, also called the Pre-IC). DNA replication begins as forks are established (FORK). Dbf4 dissociates soon after initiation and is constitutively degraded throughout S-phase. Its levels cannot rise until late G1 since it is actively targeted for degradation by APC^{Cdc20}, whose low in G1 are sufficient for this inhibition. Once a replication fork terminates, both Cdc45 and the MCM fall off the chromatin. Free MCM complexes are exported to the cytoplasm via a CDK-dependent mechanism. ORC is phosphorylated by CDK (RC7) and cannot interact with pre-RC components until it is dephosphorylated, returning it to the RC1 state.

3.2.2 Reaction events

The seventeen reactions that make up the model are shown in Table 3.1. Their rates depend on the species concentrations, the model parameters, and on two fixed, time-varying input functions describing the abundance of Clb5 (representing activated CDK) and of Cdc20.

In choosing reaction kinetics, the complexity of the model was balanced against its ability to adequately describe the behaviour of the overall system. The description of initiation was limited to the interactions between the pre-RC and replisome proteins that were thought to be the essential core of the network (e.g. Dbf4 representing the Dbf4-Cdc7 complex, discussed below). As a result, certain processes were combined into single events, some reactions were presumed irreversible, and only some reaction rates were presumed to have non-linear kinetics.

Except for RC7, phosphorylation states are not explicitly described, as no data for the individual phosphorylation events is available. This is acceptable for the purposes of the model as the lumped function of CDK in each case is consistent with a scenario where the effect of CDK is proportional to its concentration (i.e. [Clb5]). Additionally, processes that involve multi-protein complexes are represented by a single member – one CMG (Cdc45•Mcm2-7•GINS) complex stabilizes DNA polymerase at each replication fork. Of the three protein factors it is comprised of, Cdc45 is limiting. Although MCM is also included in the GINS complex, both MCM and Cdc45 are modeled as separate species. Dbf4 represents the Dbf4-Cdc7 kinase complex and Mcm2 represents the Mcm2-7 helicase. Although the protein factors Cdc45, Dbp11, Sld2, Sld3 and GINS interact to facilitate formation of the pre-initiation complex at origins, only Cdc45 is modeled,

which is the limiting factor in the CMG complex (Tanaka *et al.*, 2011); ultimately the number of forks fired (described by **the** model) is dependent on the Cdc45 concentration. Dbf4, which is the limiting regulatory subunit of Cdc7, is taken as representative of active DDK, which is one of the limiting factors in replication initiation (Mantiero *et al.*, 2011). Mcm2 is used to represent MCM complexes; the Mcm2 concentration has been reported to approximate the number of total complexes per cell in an asynchronous population (Donovan *et al.*, 1997; Lei *et al.*, 1996). The replication complexes in the models exist only on chromatin and therefore represent the activity of these proteins at the DNA as opposed to soluble complexes.

The network shown in Figure 3.1 includes both reversible and irreversible reactions as indicated. Association/dissociation reactions are considered reversible, in accordance with a dynamic pre-RC/pre-IC loading mechanism as described above. In most cases, phosphorylation events are modeled as irreversible, in the absence of identified countervailing enzymes. Most reaction rates were found to be sufficiently described by mass action kinetics. In cases where saturation occurs (the nuclear import of MCM•Cdt1, v_6, and the association of Cdc45 with ORC, v_{13}), Michaelis-Menten kinetics were employed. To simplify the description of the phosphorylation of ORC by CDK (RC7), phosporylation and dephosphorylation are not described explicitly, but are combined into a single dephosphorylation event whose rate is inversely proportional to the level of CDK (v_{17}). Cooperativity in this mechanism is introduced to account for multiple phosphorylation events (Nguyen *et al*., 2001) or an additional inhibitory CDK-Orc6 binding mechanism (Chen and Bell, 2011; Wilmes *et al.*, 2004).

The establishment of replication complexes in the model reflects the sequential binding of proteins that constitute the pre-replicative complex. In some cases the association and dissociation of pre-RC components is reversible. The loading and maintenance of Mcm2-7 helicase complexes is treated as a dynamic process, which is dependent on the concentrations of the factors ORC, Cdc6, Cdt1 and Mcm2-7 itself. A mechanistic model for the dynamic assembly of pre-RCs was first described by the Bell lab (Aparicio *et al.*, 1997). The requirement of pre-RC factors for maintenance of helicase-loaded origins in late G_1 has been further demonstrated by work from these researchers as well by published and unpublished data from the Duncker lab (Chen and Bell, 2007; Gibson *et al.* 2006; Semple *et al.*, 2006).

3.2.3 Network and Differential Equations

Referring to Figure 3.1 and Table 3.1, the dynamics of the system are described as:

$$\frac{dRC2}{dt} = v_5 - v_7 \qquad \frac{dFORK}{dt} = v_{14} - v_{15}$$

$$\frac{dRC3}{dt} = v_7 - v_{10} \qquad \frac{dCDC6_N}{dt} = v_1 + v_{10} - v_5 - v_2$$

$$\frac{dRC4}{dt} = v_{10} - v_{12} - v_{11} \qquad \frac{dDBF4_N}{dt} = v_3 + v_{14} - v_{12} - v_4$$

$$\frac{dRC5}{dt} = v_{12} - v_{13} \qquad \frac{dCDT1_N}{dt} = v_7 - v_8 + v_9$$

$$\frac{dRC6}{dt} = v_{13} - v_{14} \qquad \frac{dMCM_N}{dt} = v_{15} + v_{11} + v_9 - v_{16}$$

$$\frac{dRC7}{dt} = v_{14} - v_{17} \qquad \frac{dMCM \bullet Cdt1_N}{dt} = v_6 - v_9 - v_7$$

The remaining state variables are constrained by the following conservations:

$RC1 = RC_{Total} - RC2 - RC3 - RC4 - RC5 - RC6 - RC7$

$CDT1_C = CDT1_{Total} - CDT1_N$

$MCM_C = MCM_{Total} - MCM_N - RC3 - RC4 - RC5 - RC6 - FORK - MCM\bullet CDT1$

$CDC45_N = CDC45_{Total} - RC6 - FORK,$

where RC_{Total}, $CDT1_{Total}$, MCM_{Total}, and $CDC45_{Total}$ are the fixed total number of origins, Cdt1 molecules, Mcm2-7 complexes, and Cdc45 dimers, respectively. These four factors have been shown to be present at constant levels throughout the cell cycle (Forsburg, 2004; Hopwood and Dalton, 1996; Liang and Stillman, 1997; Owens and Detweiler, 1997; Tanaka and Diffley, 2002). The value for RC_{Total} used in the model is 332, as described in (Raghuraman *et al*., 2001).

3.2.4 System Inputs

The biological network responsible for the initiation of DNA replication does not oscillate autonomously; it displays periodic behaviour when driven by periodic signals from the cell cycle. Likewise, the model displays oscillations only when driven by periodic forcing input. In order to facilitate the combination of the model with the cell cycle model of Chen *et al*. (2004), the simulated profiles of Clb5 and Cdc20 from their model were used as periodic inputs to the present model. Cdc20 mediates the degradation of Dbf4 (reaction v_4). Clb5 is responsible for Cdc6 degradation (v_2), loading of Cdc45 (v_{13}), nuclear export of free MCM (v_{16}) and Cdt1 (v_8), and phosphorylation of Orc2 and Orc6 (v_{17}). The time-varying profiles of Clb5 from the Chen *et al*. (2004) model were converted to molecules-per-cell units using the genome-wide GFP tagging experiments described in Huh *et al*. (2003) and Ghaemmaghami *et al*. (2003). The profile of Cdc20 was similarly obtained by scaling to cellular abundance levels reported in another study – while Cdc20 has been determined to peak at 2200 copies in a haploid cell, the functional APC^{Cdc20} level can be estimated by considering the APC cyclosome subunit Cdc27 (Poddar *et al*., 2005, Schreiber *et al*., 2011). This was reported in different studies to be 593 mol/cell in an asynchronous population (Huh *et al*., 2003) and at its maximal value of 750 mol/cell in metaphase (Poddar *et al*. 2005).

Table 3.1. Kinetic Reaction Rates Describing the Network.

Rate	Description	Rate Equation
	Expression & Degradation	
v_1	Expression of CDC6	k_1
v_2	Degradation of CDC6	k_2CLB5·CDC6
v_3	Expression of DBF4	k_3
v_4	Degradation of DBF4	k_4DBF4·CDC20
	Formation of the Pre-Replicative Complex	
v_5	Association of ORC and CDC6	k_5RC1·CDC6 – k_{5r}RC2
v_6	Association and nuclear import of MCM and CDT1	$k_6MCM_C \cdot CDT1_C/(KM_1 + MCM_C)$
v_7	Loading of MCM by CDT1	k_7RC2·MCM•CDT1
v_8	Nuclear export of CDT1	k_8CLB5·CDT1
v_9	Dissociation of nuclear MCM-CDT1 complex	k_9MCM•CDT1 – k_{9r}MCM·CDT1
v_{10}	Dissociation of CDC6 from the Pre-RC	k_{10}RC3 – k_{10r}CDC6·RC4
	Formation of the Pre-Initiation Complex	
v_{11}	Dissociation of ORC and MCM from Pre-RC	k_{11}RC4
v_{12}	Association of DBF4 and the Pre-RC	k_{12}RC4·DBF4 – k_{12r}RC5
v_{13}	Association of CDC45 and the Pre-RC	$k_{13}RC5 \cdot CDC45 \cdot CLB5/(KM_2 + CDC45)$
	Post-Replicative Complex and Ensuing Events	
v_{14}	Origin firing	k_{14}RC6
v_{15}	Breakup of the elongation fork	k_{15}FORK
v_{16}	Nuclear export of the MCM	k_{16}MCM·CLB5
v_{17}	Phosphorylation of ORC	$k_{17}RC7/(1+(CLB5/k_{18})^5)$

3.2.5 Data Acquisition

Data for Cdc45 and Cdc6 levels were obtained from individual isogenic strains in which the open reading frame of the corresponding gene was fused to a sequence encoding a 13Myc epitope tag (Longtine *et al*., 1996). In Figure 3.2, a representative western blot for Cdc45-Myc is shown (panel A), with the corresponding FACS analysis (panel B). The levels of Mcm2 were determined using an anti-Mcm2 antibody. In each time course experiment, cells were first arrested in late G1 phase with the mating pheromone α-factor and then released synchronously into the cell cycle, as described in Materials and

Methods. From the literature, time course data for chromatin-bound and soluble Dbf4 and Mcm2 (to supplement *in vivo* data collected in this thesis) from (Pasero *et al*., 1999) and quantitation of the nuclear fraction of Cdt1 (Tanaka and Diffley, 2002) was used. In order to convert relative measures of protein abundance to molecule-per-cell numbers, scaling factors obtained from the database provided by Ghaemmagham *et al*. (2003) were used. The data is shown along with a best-fit simulation in Figure 3.3. Raw timecourse data can be found in Appendix A, Figures A1-A3 with an example of molecule/cell derivation in Table A1. The fits in Figure 3 represent the best solution to a trade-off between quality of fit and model complexity. The effect of adding additional species and parameters were explored. These additional features could, in some cases, provide minor improvements to the fit, but confidence in the parameter estimates suffered as the complexity of the model grew.

While the model is quantitative in that it reports proteins and complex concentrations in absolute units of molecules/cell, accuracy regarding these values is restricted by the literature-reported cellular abundances for the various protein factors. Discretion has been used when inconsistencies arise, choosing the reported values that are closest to what is observed across multiple cell cycle studies. It should be noted that, while a strength of this model is its quantitative aspect, changing the global protein level for a particular factor does not abolish its network dynamics. While the relative abundances of protein factors would change, scaling of the appropriate rate constant(s) (a relatively simple feat) would return the system to its nominal behaviour. This is an important consideration regarding the conversion of densitometry readings to absolute values as the overall levels are ultimately determined by a literature-derived scaling

factor. Densitometry readings and quantitative data acquisition are, however, crucial to developing protein level profiles through the cell cycle. In the event that new data arises confirming different estimates of protein abundances, these changes can be easily incorporated into the model without having to alter system dynamics.

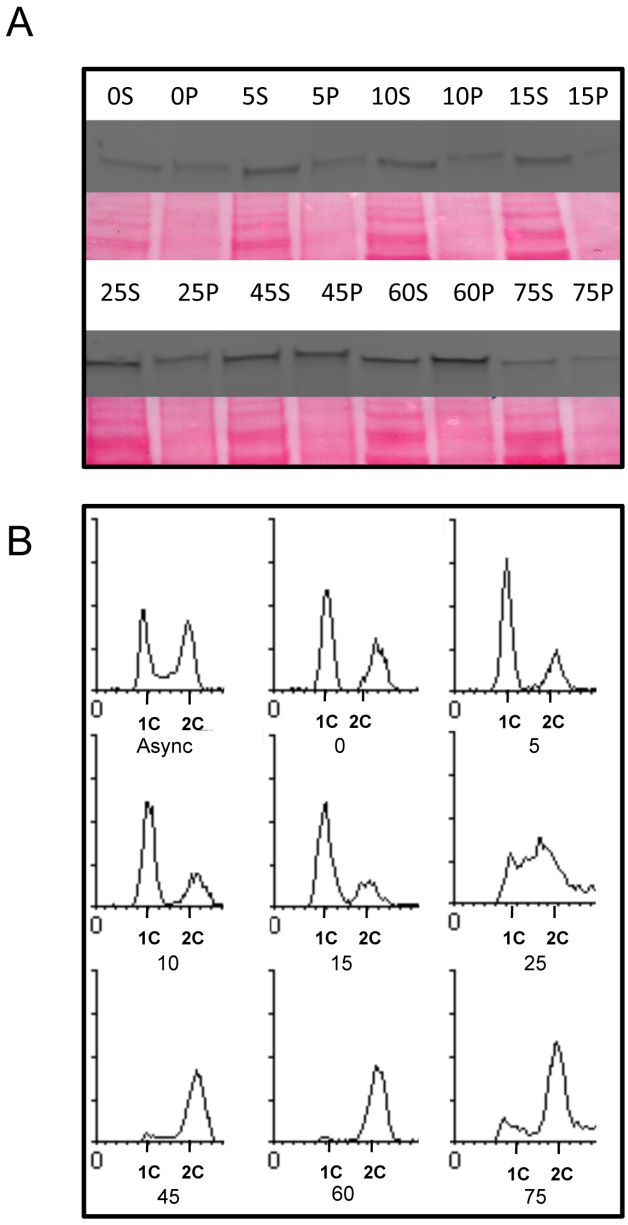

Figure 3.2. Example of *in vivo* timecourse experiment. (A) Western blot probed with α-Myc antibody to detect the Cdc45-Myc fusion protein. The corresponding Ponceau-S membrane stains are shown; these serve as loading controls to which densitometric readings were normalized. The labels indicate the time (min) elapsed since release from α-factor; S and P denote the supernatant (soluble protein) and pellet (DNA-bound) fractions, respectively. **(B)** FACS analysis of the samples described in A, along with an asynchronous culture sample (Async) prior to α-factor arrest.

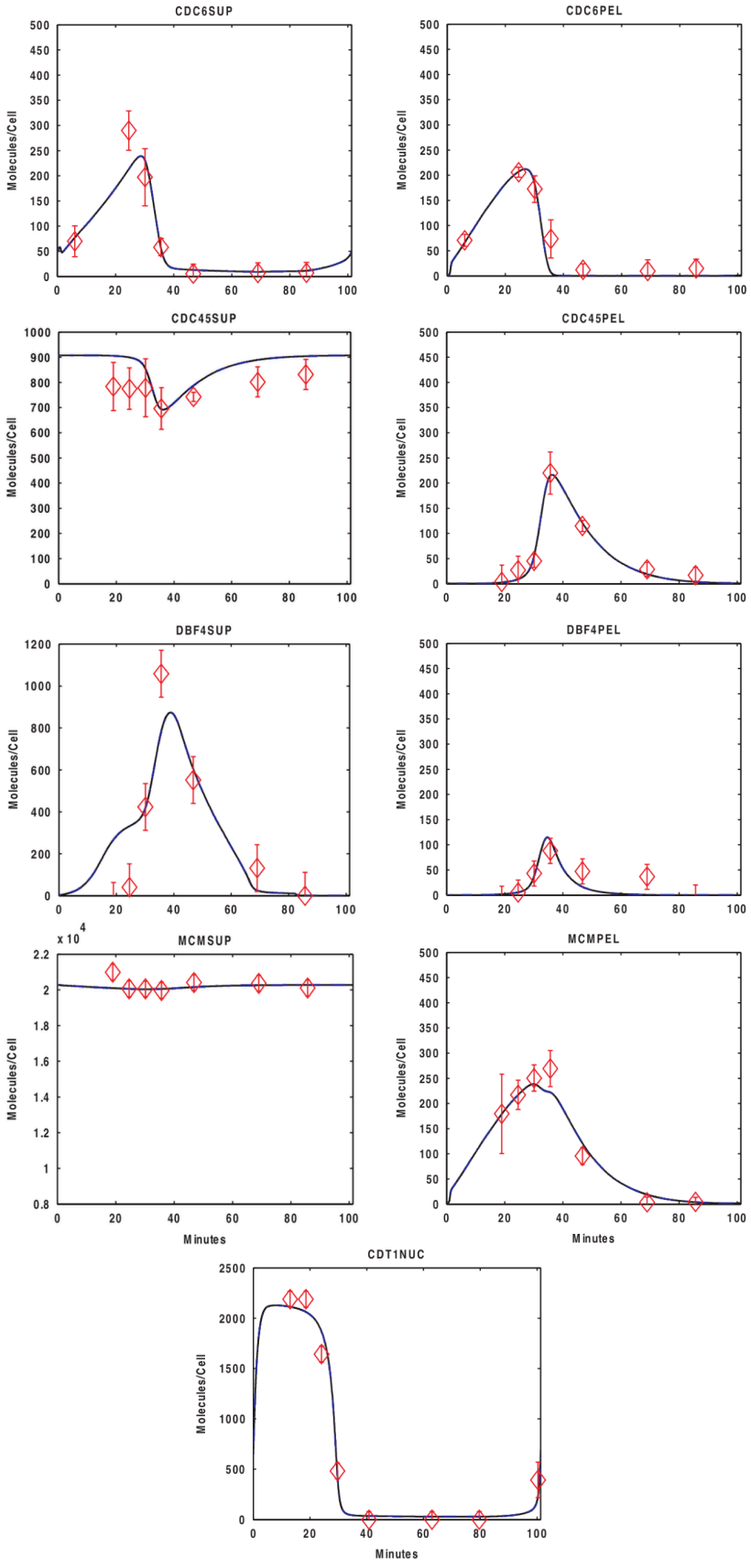
CDC6SUP
CDC6PEL
CDC45SUP
CDC45PEL
DBF4SUP
DBF4PEL
MCMSUP
MCMPEL
CDT1NUC
Molecules/Cell
Minutes
x 10^4

Figure 3.3. Model-generated best fits. Blue lines represent model simulation; red diamonds represent in vivo data points. PEL indicates a chromatin-bound species (pellet); SUP indicates non-chromatin bound (supernatant); NUC indicates nuclear fraction. The error bars indicate the variance calculated from triplicate experiments. Since the Cdt1 and Dbf4 data (Tanaka and Diffley, 2002 and Pasero *et al*., 1999, respectively) was not reported with variance values, values were assigned to these factors equal to the variance from the corresponding time-point for Cdc45, as these have similar abundances compared to other proteins in the model. The observed quantities correspond to the model state variables as follows: CDC6PEL = RC2+RC3, CDC6SUP = $CDC6_N$, CDC45PEL = RC6 + FORK, CDC45SUP = $CDC45_N$, DBF4PEL = RC5 + RC6, DBF4SUP = $DBF4_N$, MCMPEL = RC3 + RC4 + RC5 + RC6 + FORK, MCMSUP = MCM_N + MCM•$CDT1_N$ + MCM_C, and CDT1NUC = $CDT1_N$ + MCM•$CDT1_N$. One MCM molecule represents two MCM hexamers. Similarly one molecule of Cdc45 represents two individual such proteins.

3.2.6 Parameter Calibration

The model parameters were calibrated using a weighted least-squares comparison with the data described above. A combination of global optimization (adaptive simulated annealing) and local search (Nelder-Mead simplex method) was used to find the best-fit parameter set shown in Table 3.2. The table also shows the percent error associated with each parameter estimate. The percent error is the relative size of a 95% confidence interval for the estimate, calculated via the Fisher information matrix and the Cramer-Rao bound (Gadkar *et al*., 2005). The percentage errors show that some parameters are estimated with high confidence while others are represented with less accuracy. Parameter values that were well constrained by the data include the rates of production, degradation and association of Cdc6 (k_1, k_2, k_5) and Dbf4 (k_3, k_4, k_{12}) as well as the rate of origin firing (k_{14}). This reflects the strong reliability of the data for these two protein factors as well as for the proteins that form the replication complex (RC6) that gives rise to active forks.

Parameters values in which there is low confidence include those that govern the loading of MCM by Cdt1 (v_7), Cdc6 dissociation from RC3 (k_{5r}), and the phosphorylation of ORC (k_{17}). The reversible dissociation of Cdc6 is needed to accurately fit the data and there is no evidence suggesting that ORC-Cdc6 binding is irreversible. Nevertheless, it is clear that experimental observations specific to this process are required to more precisely estimate this parameter value. The reaction whereby the Cdt1•MCM species loads the MCM complex (v_7) is extremely transient (Randell *et al*., 2006). Provided parameter k_7 is sufficiently large, the kinetics of this reaction will be rapid enough to fit the data. Consequently, the data cannot support a

precise estimate of the parameter value. This observation suggests that MCM loading is an extremely rapid biochemical step in pre-RC assembly. It may point to a role for Cdt1 in repeatedly targeting MCM complexes to origins throughout G_1. Such a phenomenon is consistent with the requirement for a dynamic loading mechanism that ensures pre-RC fidelity up until the G_1/S transition. Finally, the phosphorylation of ORC (characterized by k_{17}) contributes to the prevention of repeated origin firing. However, this mechanism has not been well characterized, and the data is unable to accurately constrain the specifics of this process.

The kinetic rates in this network have not been the subject of prior experiments, but previous reports of protein half-lives are consistent with the model-predicted parameter values. Drury *et al*., (1997) estimated that Cdc6 is reduced below the point of detection within 5 minutes of S-phase entry, corresponding to a half-life no longer than 1.5 min. Similarly, (Cheng *et al*., 1999) reported that Dbf4 is reduced below visible levels within 10 minutes by the APC-dependent pathway, indicating a half-life no longer than 3 min. Model-based predictions of degradation rates correspond to half-lives of 1 min. and 2.5 min. for Cdc6 and Dbf4 respectively, in good agreement with these earlier findings.

Figure 3.4 shows the simulated model behaviour for the best-fit parameter set. Some replication complex species – RC2, RC4 and RC5 – are extremely transient. Their low levels of abundance are shown separately from other RCs, on an appropriate scale. Simulations were carried out in Matlab.

Table 3.2. Optimal Values of Parameters Used to Describe the Network. These values were used to solve the ODEs in the consensus model. The percentage error for each parameter is indicated.

Description	Parameter	Value	Units	% Error
Cdc6 production	k_1	15.982	(Mol./cell) x min^{-1}	8.86
Cdc6 degradation	k_2	0.001	$(Mol./cell)^{-1}$ x min^{-1}	22.76
Dbf4 production	k_3	1368.220	(Mol./cell) x min^{-1}	17.18
Dbf4 degradation	k_4	2.440	$(Mol./cell)^{-1}$ x min^{-1}	17.82
Cdc6 association with ORC	k_5	0.016	$(Mol./cell)^{-1}$ x min^{-1}	30.86
Cdc6 dissociation from ORC	k_{5r}	675.422	min^{-1}	861.23
MCM-Cdt1 import	k_6	1.015	$(Mol./cell)^{-1}$ x min^{-1}	24.88
MCM loading	k_7	275.675	$(Mol./cell)^{-1}$ x min^{-1}	827.56
Cdt1 export	k_8	1.732	$(Mol./cell)^{-1}$ x min^{-1}	41.81
Dissociation of MCM-Cdt1	k_9	100.881	min^{-1}	39.84
Re-assocation of MCM-Cdt1	k_{9r}	1042.739	$(Mol./cell)^{-1}$ x min^{-1}	41.98
Dissociation of Cdc6 from RC3	k_{10}	936.745	min^{-1}	32.07
Re-assocation of Cdc6 with RC3	k_{10r}	352.504	$(Mol./cell)^{-1}$ x min^{-1}	29.39
Unloading of MCM from RC4	k_{11}	885.147	min^{-1}	29.61
Dbf4 association with RC4	k_{12}	0.568	$(Mol./cell)^{-1}$ x min^{-1}	38.91
Dbf4 dissociation with RC4	k_{12r}	192.628	min^{-1}	54.52
Association of Cdc45 with RC5	k_{13}	0.528	$(Mol./cell)^{-1}$ x min^{-1}	54.16
Fork Firing	k_{14}	0.237	min^{-1}	30.08
Fork disassembly	k_{15}	0.097	min^{-1}	16.52
MCM export	k_{16}	3.196	min^{-1}	41.82
Phosphorylation of ORC	k_{17}	13.313	min^{-1}	239.26
Dephosphorylation of ORC	k_{18}	2.497	Mol./cell	43.63
Michealis constant for import of MCM	KM_1	195.302	Mol./cell	2123.53
Michealis constant for association of Cdc45	KM_2	8.248	Mol./cell	2094.64

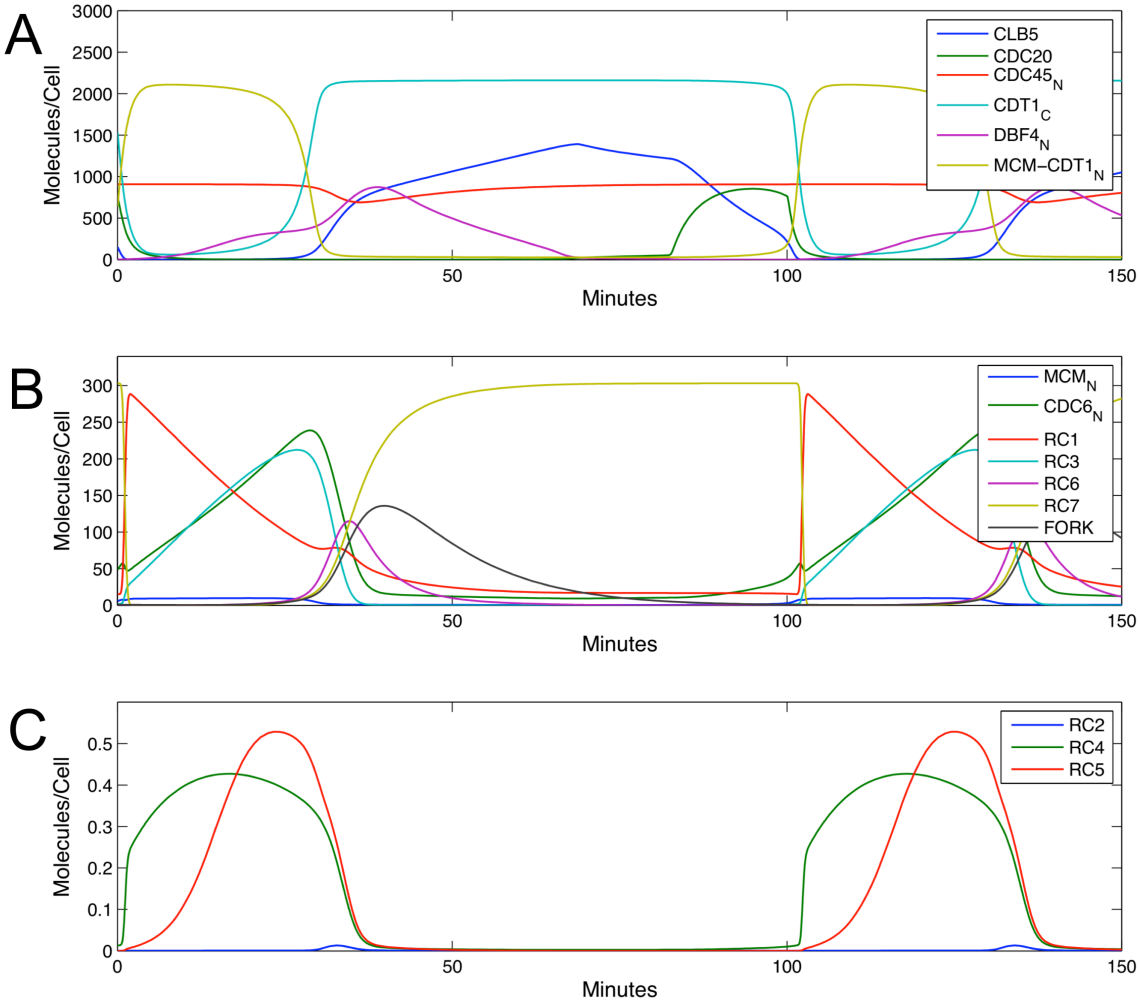

Figure 3.4. Protein concentration profiles simulated by the model. Panel **(A)** includes the inputs from the Chen *et al*., model used to drive the network (Clb5 and Cdc20), scaled from arbitrary units to molecules/cell. Included are the behaviours of various protein factors within the model. Additional factors, replication complexes (RCs) as well as the FORK species are shown in panel **(B)**. The transient RC species (RC2, RC4 and RC5) are shown in panel **(C)**.

3.2.7 Perturbations

Initial explorations of the model revealed that the network's behaviour is particularly sensitive to the abundance of Dbf4 and Cdc6 and relatively insensitive to the level of Cdt1. The effects of perturbations by simulating reductions in Dbf4, Cdt1 and Cdc6 (Figure 3.5) in the model were investigated. When the Cdc6 production rate (v_1) was reduced to 10% of its nominal (wild-type) value, persistence of the RC1 complex was observed. Similarly, when the Dbf4 production rate (v_3) is reduced by the same relative amount, an accumulation of RC3 occurs. In both cases, the perturbation interferes with pre-initiation complex assembly and blocks the system at the nearest previous persistent RC state (RC4 is not persistent since the unloading of MCM causes a rapid transition back to RC1). It is worth noting that because MCM can dissociate from ORC (v_{22}), RC4 represents a complex containing MCMs that will be functionally incorporated into replication forks as opposed to those that loosely associate with origins. Because the timing of the model is fixed, the various state concentrations (RC levels) indicate the progression from licensing to firing. A reduction in the FORK species compared to the wild-type case suggests a slow-down in S-phase because fewer origins are firing within the prescribed time. Using the peak abundance of the FORK species as a measure of replicative efficiency, significant reductions in both simulated knock-downs were observed (by 68% for Dbf4 and 73% for Cdc6, Figure 3.5 panels B and C, respectively). Conversely when the reduction of Cdt1 abundance to 10% of nominal values was simulated, origin firing was only reduced by 23%, suggesting that the network is relatively refractory to depletion of Cdt1 (Figure 3.5 panel D).

To investigate the accuracy of these mathematical predictions, corresponding wet lab depletion experiments were carried out. Reducing Dbf4 or Cdc6 concentrations in yeast cells to roughly 90% below normal endogenous levels resulted in a rapid G1 phase arrest, evident after 2 h of depletion, as judged by FACS analysis indicating the accumulation of cells with 1C (unreplicated) DNA content (Figure 3.6). In contrast, a corresponding depletion of Cdt1 had no appreciable effect, and DNA replication defects were only evident after 6 h of further reduction. Thus, simulations using the nominal parameter set were predictive of *in vivo* perturbations. These experiments were used to validate the model; they were not used for calibration.

The insensitivity to perturbations in Cdt1 levels is consistent with its apparent excess relative to origins (Ghaemmaghami *et al*., 2003), although the number of Cdt1 molecules that act at each origin has not yet been characterized. Moreover, the mechanism by which Cdt1 aids in recruiting the helicase molecules to pre-RCs is extremely transient (Randell *et al*., 2006).

While many factors are limiting, the system appears to be highly sensitive to the levels of Cdc6. Due to its low abundance relative to MCM and Cdt1, even a moderate depletion of Cdc6 significantly alters the dynamics of pre-RC loading. The same is true for Dbf4, although in this case its role in activation of the Cdc7 kinase renders the system highly sensitive to its concentration; firing cannot occur without the Dbf4-Cdc7 complex. Since Dbf4 is, like Cdc6, limiting, flow through the network is blocked when the kinase does not reach a threshold level. Additionally at limiting levels, the number of replication forks produced by the model is significantly reduced, consistent with *in vivo* reports from the literature showing a lengthening of S-phase (Sheu and Stillman, 2006).

Further model validation comes from comparison with additional *in vivo* experiments reported in the literature. Jones *et al*. (2010) showed that the interaction between the MCM complex and Dbf4 was reduced to half its wild-type level when a Dbf4 domain that binds Mcm2 was mutated, impairing S-phase progression. This effect was mimicked by reducing the rate of association of Dbf4 with RC4 (k_{12}) by 50%, leading to a similar result (compare Figure 3.7 panels A and B). Similarly, it was reported (Zou *et al*., 1997) that the *cdc45-1* mutant shows an aberrant growth phenotype at the non-permissive temperature. This is thought to be due to a disruption of Cdc45's ability to interact with MCM and ORC (RC6). As shown in Figure 3.7, panel C, by reducing the rate of Cdc45 interaction with RC6 (k_{13}) by 50%, a marked reduction in the peak abundance of the FORK species results, indicative of a slower S-phase, as observed when the mutant was grown at the non-permissive temperature. The actual reduction in Cdc45's association with the pre-RC due to conformational changes in the mutant might be even more pronounced than a 2-fold reduction. In any case, the model's simulation is consistent with Cdc45's origin-initiation role being compromised by impairing its ability to interact with its ligands to leading to its incorporation into the CMG complex.

To further demonstrate the sensitivity of the system to the levels of Cdc45, cell cycle progression following release from an α-factor block was investigated in cells having wild-type or reduced levels of the protein (Figure 3.8). Cells expressing Cdc45 endogenously from the tetracycline- repressible tetO7 promoter were split into two cultures, each arrested for 90 min in medium containing α-factor. Doxycycline or "Dox" (an analog of tetracycline) was added to one culture and both were maintained in a late G_1 block for 6 h. Following this, both cultures were released into fresh medium, lacking

α-factor to initiate release from the block. Cells that were treated with Dox, in which Cdc45 expression was presumably reduced below endogenous wild-type levels, progressed more slowly through S-phase compared to those not treated with Dox (see timepoint T= 40 min). As shown in Figure 3.7, panel C, Cdc45 is a limiting factor in the assembly of the pre-initiation complex. Its reduction below a threshold level would ostensibly result in less origins firing per cell cycle, thus extending the time taken to completely replicate the chromosomes.

While simulations of protein knock-downs validate the model in light of experimental observations, overexpression of network factors also provide useful insight. Simulating the results of Tanaka *et al*. (2011), overexpression and increase in RC association (v_{13}) of a complex containing Cdc45 leads to a greater number of origins fired (134% increase compared to wild-type). This is in good accordance with the experimental observation. Similarly, either overexpressing (v_2) or increasing the chromatin association (v_{11}) of another limiting factor, Dbf4 results in an increase in origin firing. While these predictions might seem like an obvious result of network construction, comparing these results to a similar degree of Cdt1 overexpression (note that the cellular levels of Cdt1 and Cdc45 are similar) shows that the system is more sensitive to particular nodes and factors. An interesting observation is that increasing Cdt1 and Cdc45 levels and chromatin association by the same amount causes very little increase in origin firing in the case of Cdt1 and a linear increase in origin firing for Cdc45 (as well as for Dbf4) together with an increase in the amount of re-replication.

A number of literature-described hypomorphic mutants were simulated by the model. A summary of these and other mutants as well as a comparison of *in silico* results versus experimental observations is given in Table 3.3.

Table 3.3. Cell cycle mutants simulated by the model of DNA replication initiation. Results of *in silico* perturbations were matched against phenotypes observed in the literature, where available.

Mutant/Perturbation	Observations from Model Simulation	Experimental Phenotype	Origins fired/cell cycle (% WT)	Reference
Wild-type	–	–	100	This study
Cdc6 knockdown (to 10%)	73% peak [FORK] height reduction	G1 arrest within 2 h	24.6	This study
Dbf4 knockdown (to 10%)	68% peak [FORK] height reduction	G1 arrest within 2 h	29.6	This study
Cdt1 knockdown (to 10%)	23% peak [FORK] height reduction	G1 arrest within 8 h	84.2	This study
Dbf4-Mcm2 interaction halved	11% longer S phase	Slower S-phase, reduced initiation at origins	62.59	Jones *et al.* (2010)
cdc45-1 (pre-RC association halved*)	17% longer S phase	Slower S-phase, reduced initiation at origins	48.55	Zou *et al.* (1997)
cdc6Δ	No replication fork firing	Inviable	0	SGDP***
dbf4Δ	No replication fork firing	Inviable	0	SGDP***
cdt1Δ	No replication fork firing	Inviable	0	SGDP***
mcm2Δ	No replication fork firing	Inviable	0	SGDP***
cdc45Δ	No replication fork firing	Inviable	0	SGDP***
Cdc45/Sld3/Sld7 overexpression**	Increase in origins fired	Increase in fired origins to 134% of wild-type	139	Tanaka *et al.* (2011)
Cdt1 M-G1 deplete	Mcm2-7 excluded from nucleus	Mcm2-7 excluded from nucleus	0	Tanaka *et al.* (2002)
mcm2-1	v14 reduced to zero: S phase 49% longer	Delayed passage through S phase/initiation defect	87.21	Yan *et al.* (1991)
mcm3-1	v14 reduced to zero: no FORK produced	Inviable at restrictive temperature	0	Yan *et al.* (1993)
orc2-1	v24 reduced by 20%: reduced origin firing	ORC-DNA binding defect	11.14	Gibson *et al.* (2006)
cdc6-1	Arrest in RC2 state (G1)	G1 arrest	0	Detweiler and Li (1997)
cdc7-1	Arrest in RC5 state (G1)	G1 arrest (failure to enter S-phase)	0	Bousset and Diffley (1998)
DDK activity increased 10-fold	(re-fired origins increased by 12.42/cell cycle)	–	105	_
Cdc45 activity increased 10-fold	(re-fired origins increased by 12.66/cell cycle)	–	108	_
Cdt1 activity increased 10-fold	No extra origins re-fire****	–	100.7	_

*** This is an estimate of the defect of *cdc45-1* in initiating replication. It is likely that the phenotype is more severe *in vivo*.**
**** This is simulated using Cdc45 as a proxy for the complex that stabilizes CMG at origins. A three-fold increase in levels and association was simulated by the model based on Western blotting results from Tanaka *et al*. (2011).**
***** Saccharomyces Genome Deletion Project**
****** Although 100.7% of origins fire compared to wild-type, this represents a small decrease in unused RC species amongst the 332 potential origins, not re-replication.**

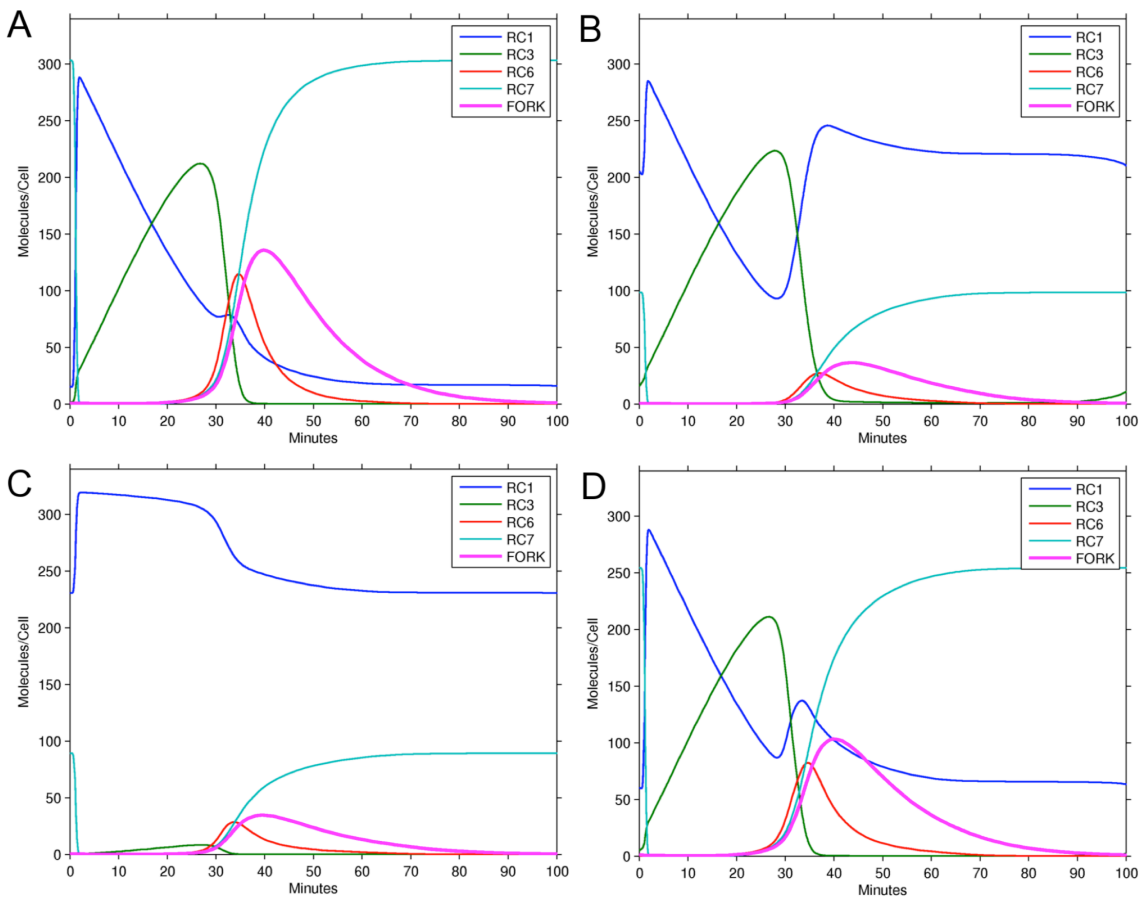

Figure 3.5. *In silico* simulations of perturbations. **(A)** Wild-type behaviour. **(B)** Expression of Dbf4 reduced to 10% of nominal. **(C)** Expression of Cdc6 reduced to 10% of nominal. **(D)** Total abundance of Cdt1 reduced to 10% of nominal. Perturbations of Cdc6 and Dbf4 had a significant impact on replicative efficiency, as evidence by a reduced abundance of activated replication forks (FORK). In contrast, a similar reduction in Cdt1 levels had much less impact.

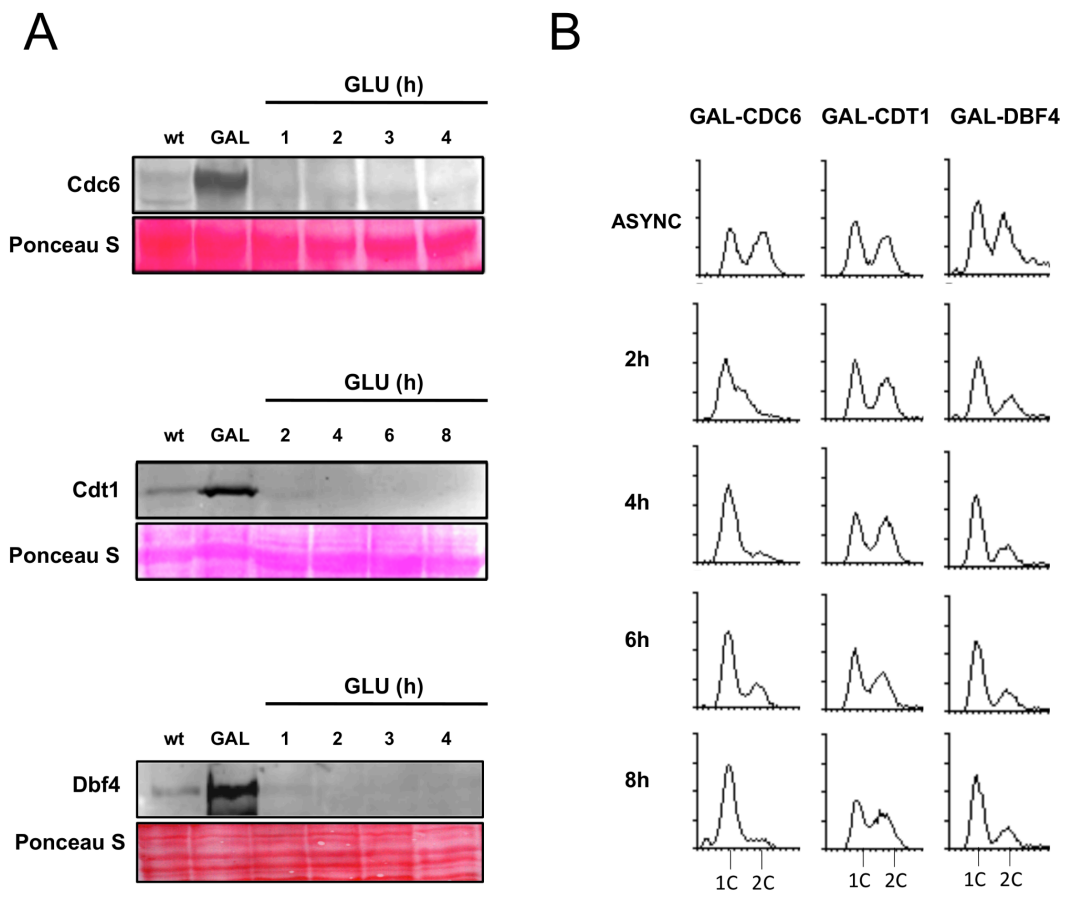

Figure 3.6. Experimental investigation of protein depletion below normal endogenous levels for Dbf4, Cdc6 and Cdt1. (A) Asynchronous cultures of *GAL1-CDC6* (DY-139), *GAL1-CDT1* (DY-140), *GAL1-DBF4* (DY-255) and their wild-type counterparts DY-142, DY-143 and DY-256, respectively, were grown to 10^6 cells/ml in galactose (GAL) medium, washed and resuspended in glucose (GLU) medium. Whole-cell extracts were prepared from culture aliquots taken prior and post shift from galactose to glucose with indicated time points corresponding to time in glucose medium. HA-tagged Cdc6 and HA-tagged Cdt1 were detected using an anti-HA antibody (Sigma) and a fluorescent secondary antibody (Invitrogen). Ponceau S staining of the region detected by the blot to judge loading of whole-cell extracts is also shown. **(B)** FACS analysis of culture aliquots from either asynchronous (Async) cultures, or at the indicated times after cell resuspension in glucose medium. The 1C and 2C markers refer to the amount of DNA present (C = Complement of the genome) in cells within the population – 1C corresponds to G_1 phase, while 2C corresponds to cells that have replicated their DNA, but not undergone cell division.

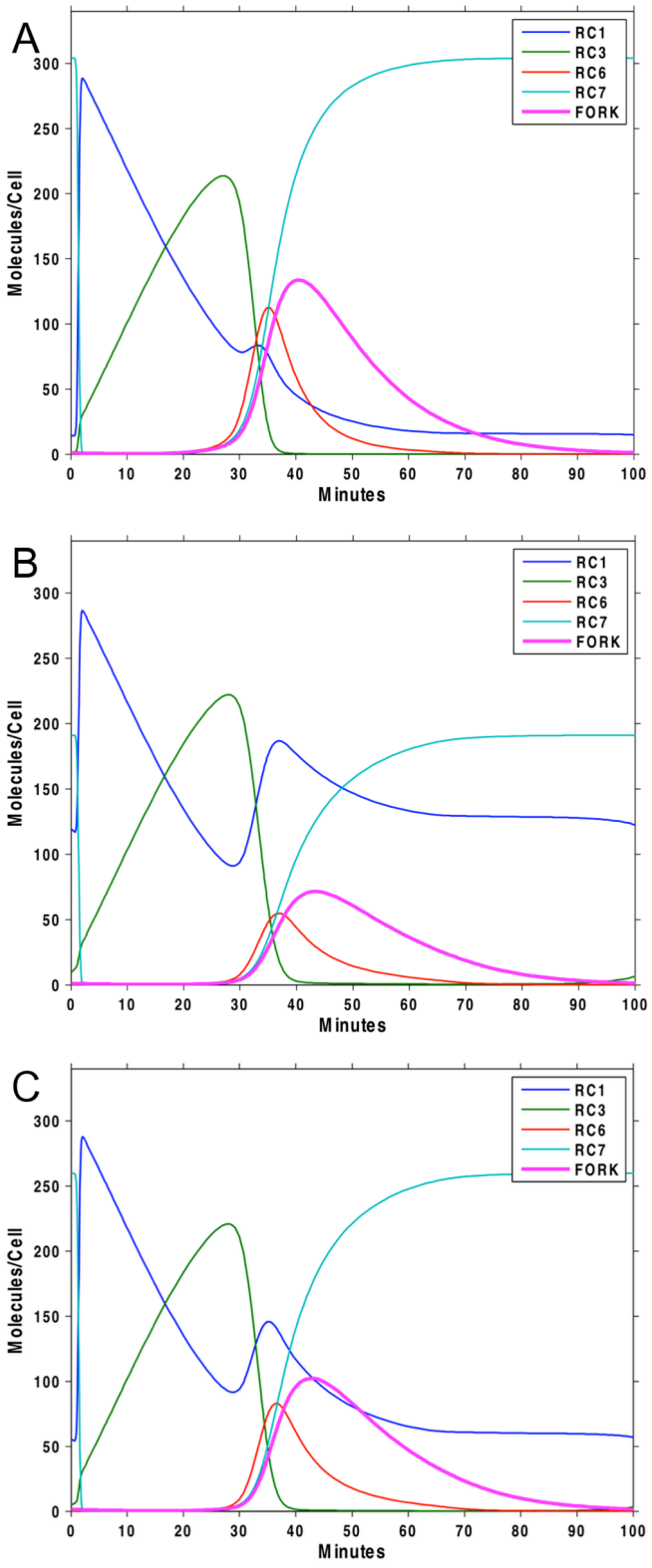
A
B
C
RC1
RC3
RC6
RC7
FORK
Molecules/Cell
Minutes
0
50
100
150
200
250
300
0
10
20
30
40
50
60
70
80
90
100

Figure 3.7. ***In silico*** **perturbations to the consensus model agree with reported** ***in vivo*** **cell cycle defects. (A)** Wild-type behaviour. **(B)** Reduction of the rate of Dbf4-MCM association (k_{12}) to 50% of the nominal value. **(C)** Reduction of the rate of Cdc45 interaction with the pre-RC (k_{13}) to 50% of the nominal value. In both cases, a decrease in the abundance of the FORK species indicates a defect in DNA replication.

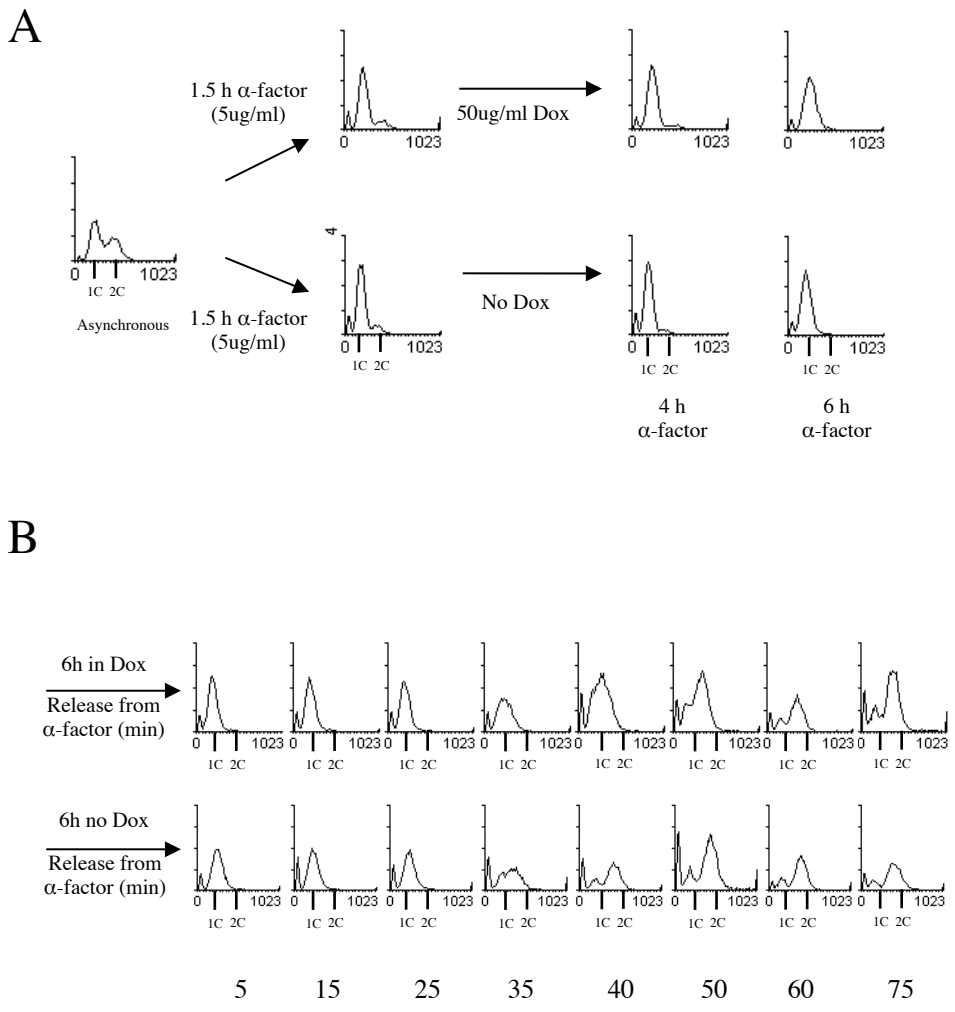

Figure 3.8. Cells depleted of Cdc45 in late G_1 progress more slowly through S phase. Cells expressing Cdc45 under the control of a doxycycline (Dox)-repressible promoter were split into two cultures, each treated with α-factor to arrest them in late G_1. Cells were held in this block for 6 h **(A)**, after which each culture was transferred to fresh medium lacking α-factor to release them into the cell cycle **(B)**. FACS profiles are shown demonstrating tight G_1 arrest through the 6h. DNA content is shown for samples collected at the indicated timepoints (minutes) following α-factor release.

3.2.8. Linking the DNA replication initiation model to a previously established cell cycle model

The model of the replication initiation presented here only displays oscillatory behaviour when forced with periodic signals from the cell cycle. By choosing to incorporate signals that correspond to species in the cell cycle model of Chen *et al*. (2004), the two models could be merged in a straightforward manner. In the Chen model, the initiation of DNA replication is represented by a single lumped state variable, called ORI. At the beginning of the cell cycle, ORI has value zero. Its rate of growth depends linearly on Clb5. When it reaches a threshold value, DNA synthesis is presumed to have begun, and triggers an increase in the value of the parameter k_{mad2} (activity level of the Mad2 protein) leading to an inactivation of Cdc20, which is required for mitotic exit. This Mad2-dependent inhibition of Cdc20 represents the spindle assembly checkpoint (Yu, 2002), ensuring that cells with replicated DNA do not complete mitosis without properly aligning the chromosomes. When chromosomes have properly aligned on the metaphase plane k_{mad2} drops and Cdc20 promotes exit from mitosis. The Chen *et al*. (2004) Cdc20 profile in scaled mol/cell units is depicted in Figure 3.9. In the replication model, the level of DNA synthesis is represented by the FORK species. To merge the two models, the ORI state was removed from the Chen model, and the FORK species was used instead to trigger the change in k_{mad2}, as detailed in Materials and Methods.

Besides "closing the loop" between the two models by incorporating two-way inter-model signalling (involving Clb5, Cdc20, and FORK), both models include a single shared species, describing the dynamics of Cdc6. A merged description of Cdc6 behaviour was produced by incorporating the dynamics of replication complex

association and dissociation into the Chen model's formulation of Cdc6 behaviour. Details are described in Materials and Methods. The resulting combined model behaves only marginally differently from either model in isolation, as shown in Figure 3.10.

A

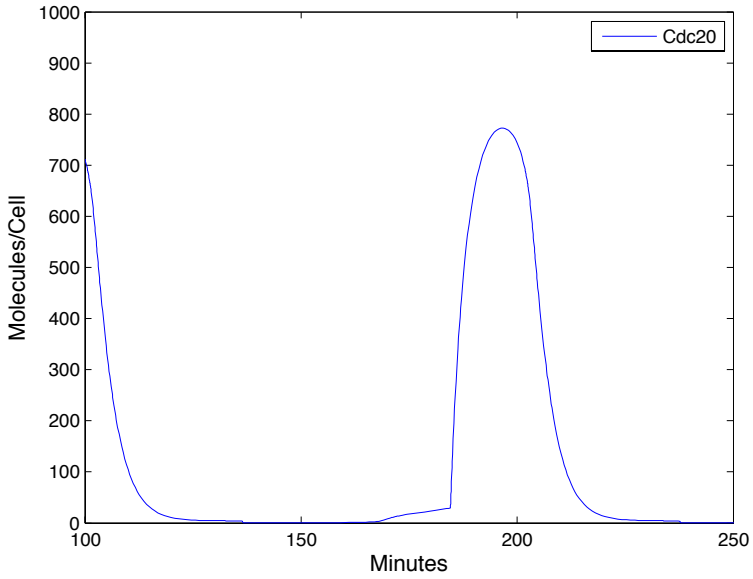
Cdc20
Molecules/Cell
Minutes
0
100
200
300
400
500
600
700
800
900
1000
100
150
200
250

B

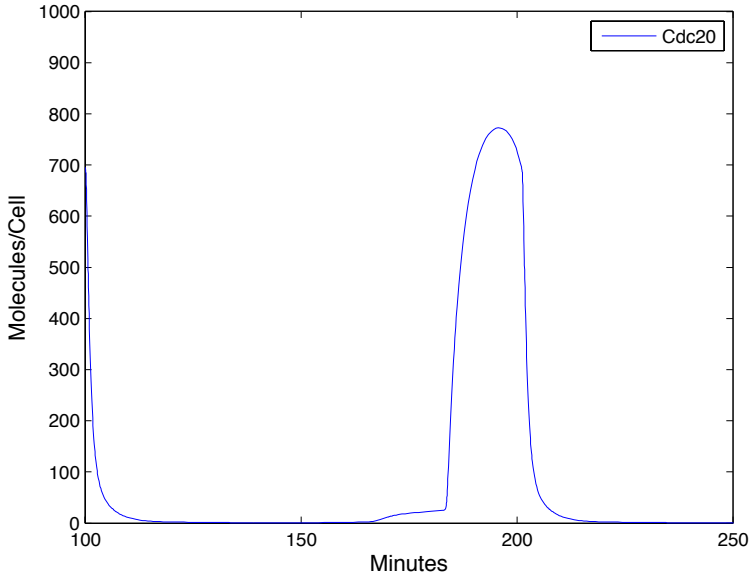
Cdc20
Molecules/Cell
Minutes
0
100
200
300
400
500
600
700
800
900
1000
100
150
200
250

Figure 3.9. Comparison of Cdc20 profiles cycling over the course of a 101.2 minute cell cycle. (A) Time-varying Cdc20 concentration (scaled from arbitrary units to molecules/cell) from the original Chen *et al*., (2004) model. **(B)** Modification for use in the present model of Cdc20 where the control of the levels of its inhibitor, Mad2 replaces a step function with a smoother function. This results in lower Cdc20 levels in mid and late G_1 phase, thus allowing Dbf4 to gradually accumulate, peaking at the start of S phase.

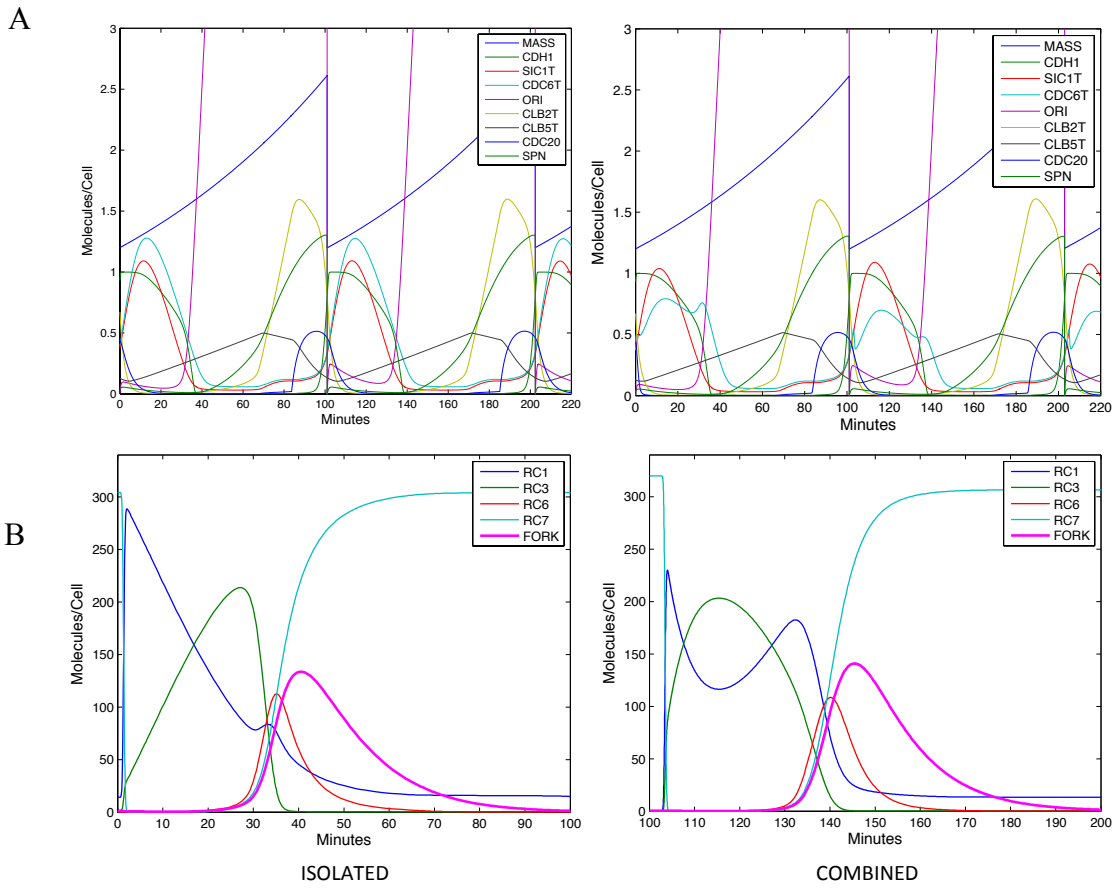

Figure 3.10. Combining models does not alter either's behaviour in isolation. **(A)** Chen *et al*. (2004) model species in the combined model are only marginally altered temporally. Several species are shown including Cdc20 (enlarged in Figure 3.9). **(B)** DNA replication model species within the combined do not deviate significantly from the model simulated in isolation. Shown are the four stable replication complex species (RCs) as well as the FORK species. In both cases, the minor deviations in species profiles can be attributed to the sharing of a common species, Cdc6 (teal in panel A).

3.3 Discussion

While the model provides a sound description of the initiation of DNA replication, a number of aspects of the network remain unresolved: for example, the kinetics of MCM loading, the mechanism by which CDK phosphorylates ORC, and the details of the association of the GINS complex, Sld2, and Sld3. While modeling Cdc45 captures the events regarding CMG formation at origins, being its limiting factor, a future version of the model could better distinguish the initial Cdc45 association at origins from subsequent CMG formation. While this has minimal effect on network dynamics and no effect on the blocking of re-replication, it would provide a better resolution of events at origins just prior to the G_1/S transition. Incorporating timecourse experiment data for levels of a GINS complex member would aid in this analysis. Nevertheless, the assumptions made allow the approximation of the aforementioned processes, simplifying the network without losing information about system behaviour at the level intended to model. With the nominal parameter set, the system is observed to behave as the ordered accumulation of proteins forming a loading complex at origins throughout the genome. Activation by increasing S-CDK levels and the concentration of Dbf4 (regulating kinase activity of Cdc7) increase linearly the number of replication forks set up at the various loading complexes. It should be noted that as is found *in vivo*, not all origins fire, while they are all furnished with MCM-containing pre-RCs. Replication is maximal at the G_1/S transition, but continues into S-phase as origin firing is temporally spaced. This is thought to ensure sufficient time to address any defects in replication and is mediated by the limiting nature of one of the initiation activators, DDK (reviewed in Mantiero *et al*., 2011 and Tanaka *et al*., 2011). The *in vivo* perturbation of Dbf4 levels reproduces this

consequence and points to other system observations: Cdc6 levels are intimately controlled by CDK levels to avoid re-replication, however this mechanism is tightly regulated such that Clb5 levels rising too soon would prevent the assembly of the pre-RC in G1, a feature of the system well documented. Additionally, Cdt1 appears to act catalytically rather than stoichiometrically given the system is relatively impervious to reductions in this factor to 10% of its widtype level. This might play into its role in chaperoning Mcm2-7 hexamers to origins, where they are loaded subsequently leading to the release of Cdt1, which may be then recycled to aid the loading of other MCMs. This aspect of the system has not yet been investigated experimentally and would be of future interest.

As an example of the agreement of the simulated values with literature-observed origin stoichiometry, Mcm2 (representing the MCM complex) was present at levels that were consistent with having two MCM complexes bound to each origin. This reflects the head to head placement of the heterododecamer at the origin. Once firing occurs, two forks are produced, illustrated in the model as one Mcm2-7•Cdc45 species molecule being generated (each FORK in the model represents a pair of these complexes). The levels of chromatin-associated MCM protein that were obtained corresponds to roughly 300 origins being bound in this manner, which is the range of the number of origins that are reported to *potentially* fire according to various global origin characterization studies (Feng *et al*., 2006; Nieduszynski *et al*., 2006; Raghuraman *et al*., 2001; Wyrick *et al*., 2001).

The recently published model of Brümmer *et al*. (2010) also describes the network responsible for the initiation of DNA replication. The 51 free parameters of that

model were chosen by a combination of fitting and optimization. The authors used literature-derived data to fix 28 of the kinetic parameters. The remaining 23 free parameters were not fit to data, but were selected through a procedure that optimized the coherence of origin firing and minimized re-replication (selected as hypothetical goals of evolutionary 'design'). While it is impossible to assess the accuracy of the parameter values obtained from this procedure, the resulting idealized model provides a useful starting point for examining how the network structure constrains the system behaviour.

The model of Brümmer *et al*. (2010) focuses on early origin firing and so represents the mechanics of firing at the start of S-phase. In contrast, the model presented here describes firing dynamics throughout S-phase in order to fit into the broader context of the cell cycle (Goldar *et al*., 2009; Hyrien *et al*., 2003; McCune *et al*. 2008). The parameter set driving the system is not filtered to retain only those that produce replication dynamics consistent with coherent firing just at the G_1/S boundary. Rather, they are specified by the actual cellular concentrations of the active protein factors generating replication forks. While both models incorporate the important role of CDK, Brümmer *et al*. emphasize the multi-site phosphorylations of several factors involved in mechanisms that minimize potential re-replication. To this end, they employed a metric to assess re-replication. Their idealized model exhibits 0.0028 re-replication events per cycle. Applying the same measure to the bottom-up model presented in this thesis yields 0.36 re-replication events per cycle (although that can readily be reduced by modifying parameters from their best-fit values). The near-zero value obtained by Brümmer *et al*. is close to their idealized target of zero. Both estimates are consistent with the belief that re-replication occurs in wildtype cells, but at an

extremely low rate (Green *et al*., 2006). Because the nature of the dephosphylation of ORC (RC7→RC1 transition) remains uncharacterized, a conservative estimate of the number of ORC phosphorylation sites is used. Increasing this number by twofold, consistent with the number of CDK target residues on ORC (Nguyen *et al*., 2001) reduces re-replication to a value on the same order of magnitude as Brümmer's value. Thus, both models effectively deal with representing control and prevention of rereplication.

Many human orthologs of the yeast proteins described in the model's network have been associated with cellular pathologies. The model presented here is specific to the replication machinery in budding yeast, but the mechanisms driving this process are highly conserved throughout Eukarya. Efforts to develop an analogous model in mammalian cells would be useful in understanding and dissecting cell proliferation in humans. A number of models of the mammalian cell cycle have been proposed (Chassagnole *et al*., 2006; Gerard and Goldbeter, 2010; Novak and Tyson, 2004; Qu *et al*., 2003; Swat *et al*., 2004). For example, incorrect pre-RC formation has been linked to impaired DNA damage repair pathways in humans (Lau and Jiang, 2006), while both Orc6 (Gavin *et al*., 2008) and members of the Mcm2-7 (reviewed in Gonzalez *et al*., 2005) have been shown to be reliable cancer biomarkers. Recent work by Bicknell *et al*. (2011a, 2011b) has shown that point mutations in the human ORC1, ORC4, ORC6, CDT1 and CDC6 genes are associated with Meier-Gorlin syndrome, a form of primordial dwarfism, and several of these mutations were determined to interfere with proper pre-RC formation. These findings highlight the potential utility of *in silico* mammalian models in further exploring the molecular basis of such disorders. Given that the model shows good predictive capability, it serves not only as an informational tool for yeast

biology, but also as a proof of principle for higher order system models. Despite the requirement for a mammalian model to comprehensively verify specific mechanisms, the system of DNA replication initiation is conserved well enough that perturbations to proteins such as those described above can, in fact be preliminarily examined.

Although previously established replication models (de Moura *et al*., 2010; Retkute *et al*., 2011; Spiesser *et al*. 2009) consider the ordered timing of origin firing based on genomic replication profiles, the goal of this model was to represent the temporal organization of origin firing as a function of the concentration of active replication species. A focus on using real protein levels as a determinant of replication dynamics is a novel approach. When used in concert with models describing genome-level origin characteristics and/or combining the findings with models exploring other cell-cycle modules, a well-rounded picture of DNA replication initiation can be generated.

Chapter 4: Differential chromatin proteomics of the MMS-induced DNA damage response in *Saccharomyces cerevisiae*

Contributions to this chapter were made by Dr. DongRyoung Kim as follows:

All 2D-DIGE experiments and statistical analysis post chromatin fractionation
Figures 4.1, 4.2, 4.3, 4.4, 4.5, and 4.7
Tables 4.1, 4.2, B1 and B2

Chromatin fractionation optimization procedures and controls, genotoxic sensitivity assays as well as controls for DAmP strain expression were performed by the author of this thesis.

This chapter is published as a manuscript in the journal Proteome Science. Permission from the journal for use of this material herein has been granted.

Kim *et al*. (2011)

4.1 Introduction

Within many proteomic studies, protein abundance and complexity can affect practical detection sensitivity, even with advances in differential in-gel electrophoresis (DIGE) (Tonge *et al*., 2001) and MS-based approaches (Aerbersold *et al*., 2003). For example, certain functional classes of proteins such as transcription factors and cell cycle proteins are present at low abundance in whole cell extracts compared to other structural and metabolic proteins (Ghaemmaghami *et al*., 2003). In response to the issues of low abundance and dynamic range limitations of quantitative proteomics methods (e.g., LC-MS or DIGE), one strategy is to minimize sample complexity through enrichment approaches, such as affinity capture of protein complexes (e.g. tandem affinity purification) (Gavin *et al*., 2002) selection of phosphopeptides (Smolka *et al*., 2007), and sub-cellular fractionation (Anderson and Mann, 2006; Forner *et al*., 2006; Yates *et al*., 2005). Although targeted affinity-based methods can lead to high levels of enrichment, they have a high probability of excluding relevant proteins. An attractive alternative approach is a sub-cellular fractionation, where overall protein complexity and stoichiometry can be largely retained during the fractionation. Based on this rationale, cellular organelles have been subjected to proteomic analysis, including mitochondria and chloroplasts, demonstrating that the combination of sub-cellular fractionation and proteomics techniques provides a practical means for the analysis of low-abundance proteins localized in discrete regions of the cell.

Though it is not a separate organelle per se, chromatin is physically organized in the cell and, due to the importance of chromatin in molecular analyses of DNA replication and epigenetics, procedures to separate chromatin from other cellular

components have become well established in budding yeast (Liang and Stillman, 1997; Rattner *et al*., 1982; Szent-Gyorgyi and Isenberg, 1983). By using fractionated chromatin samples, MS-based approaches have been employed to identify a wide range of chromatin-associated proteins, including those from developing *Xenopus* embryos (Khoudoli *et al*., 2008) and *C. elegans* sperm (Chu *et al*., 2006). As demonstrated in such studies based on chromatography and/or mass spectrometry-based analysis of digested peptides, initial fractionation coupled with downstream proteomics methods is extremely valuable for addressing the relatively low abundance of many chromatin-associated proteins, especially in the context of large-scale protein identification. However, it can still be challenging to address differential expression using fractionated chromatin, as technical variability during its preparation can interfere with multiplex sampling and stringent statistical evaluation is needed to minimize false discovery rates. In addressing this aspect, gel-based proteomics is a promising approach to accommodate multiplex experimentation effectively while minimizing systemic experimental variation. In addition, the DIGE method is extremely useful for identifying various protein forms resulting from posttranslational modifications such as phosphorylation (Tang *et al*., 2008) and evaluating their relative abundance.

Chromatin-associated proteins mediate a multitude of biological processes such as DNA replication, repair, and transcription (Bernstein and Schreiber, 2002; Morgan and Loog, 2005; Sclafani and Holzen, 2007)), through complex regulatory mechanisms. The structure of chromatin changes as a function of the cell cycle, adopting a more condensed conformation during mitotic phase relative to interphase, when DNA is duplicated. When chromatin integrity is compromised as a result of exposure to genotoxic agents, the

cellular repair machinery is recruited to sites of DNA damage (Harrison and Haber, 2006; Koundrioukoff *et al*., 2004). The appropriate regulation of each process requires a multitude of mechanisms such as histone modification (Jiang *et al*., 2004), chromatin remodeling (Pollard and Peterson, 1998), and formation of diverse protein complexes. In studies of biological mechanisms, the qualitative and quantitative analyses of interactions and/or binding with chromatin are crucial in order to investigate protein function, signaling pathways, and modular networks (Rodriguez and Huang, 2005). Therefore, global proteomic profiling of chromatin provides an effective means to gain valuable information about these central biological processes (Rodriguez and Huang, 2005), and has widespread applications such as acceleration of pharmaceutical development (Jiang *et al*., 2004).

In this study, an analysis of differential protein expression using 2D-DIGE was conducted in combination with chromatin fractionation of budding yeast. Initially the effectiveness of the approach consisting of isolating and detecting chromatin-associated proteins using DIGE was assessed. The combination of DIGE with fractionation allows both identification of differential abundance due to an applied treatment, and additionally provides a means to estimate changes in protein localization, or in this case, chromatin affinity. The potential utility of this novel approach was then confirmed by applying the method to screen for differentially expressed proteins following treatment with the DNA damaging methyl methanesulfonate (MMS), resulting in the detection of both known and novel DNA damage response proteins.

4.2 Results

4.2.1 Initial DIGE Based Identification of Chromatin Fraction Proteins

Yeast protein extracts from whole cells and from chromatin enrichment were compared using DIGE. Candidate proteins were selected for identification on the basis of chromatin enrichment factor (EF), defined for a given spot as the average ratio of spot volume in the chromatin fraction vs. the whole cell extract in DIGE images (Figure 4.1). Enrichment factors were calculated for paired chromatin and WCE samples in the four DIGE gels using the BVA analysis module within the DeCyder™ software package. *P*-values were also calculated for protein spots, but as two different sample types are being compared these provide only a relative measure of variability and enrichment. As the initial fractionation procedure retained approximately 5% of the total cellular protein on average, the theoretical upper limit of the enrichment factor is approximately 20-fold. To verify that the fractionation was successful at targeting chromatin-associated proteins, a subset of enriched protein spots was analyzed by mass spectrometry. A Coomassie-stained gel was prepared from a chromatin-enriched yeast fraction for protein identification (Figure 4.2). Spots with an experimental enrichment factor greater than 1.4 fold were selected for MS analysis, and 33 of these were identified (Figure 4.1, Table 4.1). Based on annotations from the Saccharomyces Genome Database (http://www.yeastgenome.org), the organelle database (http://organelledb.lsi.umich.edu), and literature sources, the majority have been previously identified as localizing to the nucleus and include many functionally important chromatin proteins. Estimated protein copy number per cell (Ghaemmaghami *et al*., 2003) is shown in Table 4.1 for known chromatin-associated proteins identified in the chromatin fraction (Figure 4.1). Overall,

the fractionation procedure was effective at enriching low-abundance chromatin associated proteins. Interestingly, a number of the identified proteins had very low expected cellular levels (e.g. 1070 copies/cell for Arp4 and 1360 for Arp7) based on previous GFP fusion experiments (Ghaemmaghami *et al*., 2003). The quality of the chromatin fractionation was verified by performing western blots for aliquots of the initial WCE, as well as chromatin and supernatant fractions, with antibodies for Orc2 and histone H2B which should both be chromatin-bound, as well as α-tubulin, which should be in the supernatant (Liang and Stillman, 1997). The results are shown in Appendix B, Figure B1.

Among the identified proteins, some belong to well-known complexes involved in chromatin remodeling, such as SWI/SNF and INO80 (Saha *et al*., 2006). These include Swi3, Taf14, Arp4, Arp7, Arp9, and Rvb2. Members of RNA polymerase complexes (Jourdain *et al*., 2003, Lalo *et al*., 1993) were also identified, including the proteins Rpc40, Rpb3, and Tfc7. In addition, some proteins important for telomere capping and remodeling were found, such as Stm1 (Nelson *et al*., 2000) and Cgi121 (Downey *et al*., 2006). In many cases, proteins were identified along with other factors they normally interact with, implying good retention and co-enrichment of complex subunits. This result strongly suggests that chromatin fractionation was effective at enriching for functional chromatin proteins.

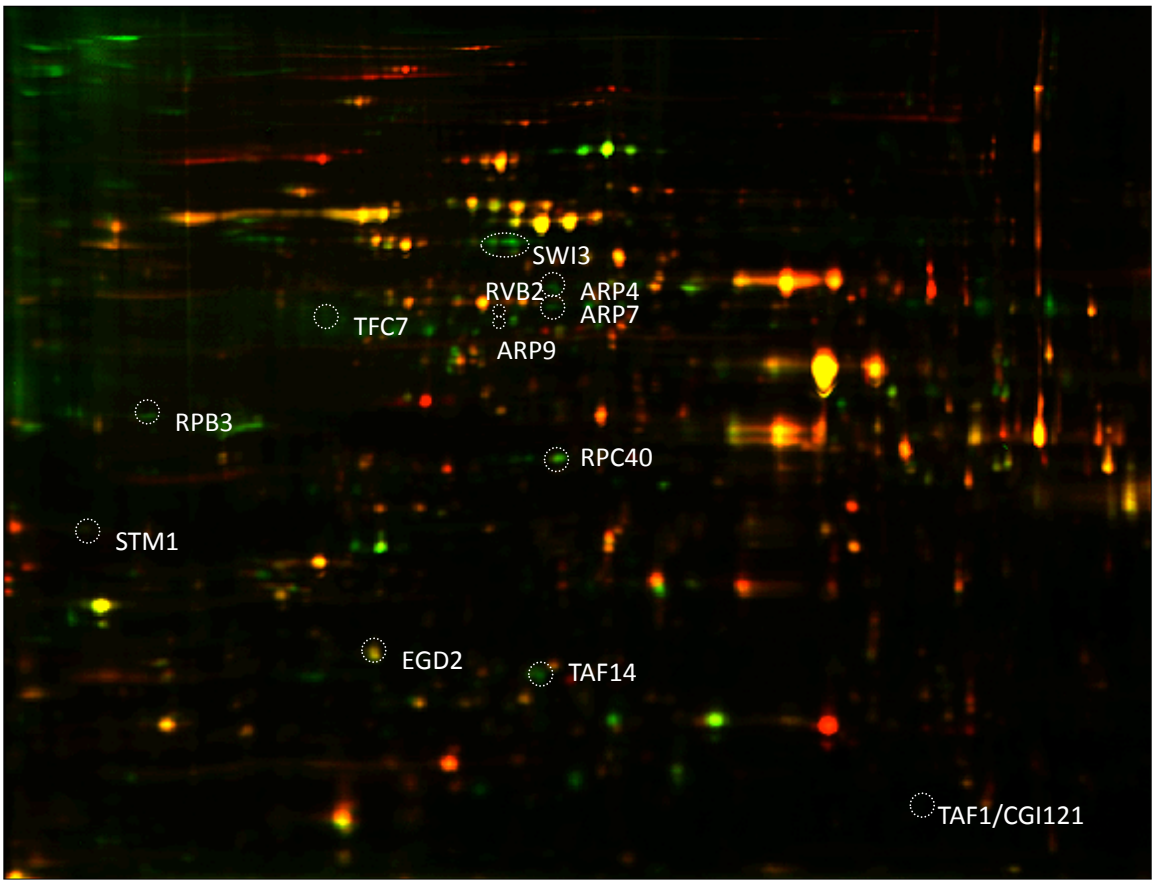

Figure 4.1. DIGE gel image comparing a chromatin fraction (green, Cy3) and whole cell extract (red, Cy5). The Cy2 channel used for the internal control is not shown. Four replicates of biologically independent samples were tested in four different gels with two by two dye swapping. The chromatin-enriched spots appear predominantly green in this representative image. Selected identified proteins with known chromatin-association are indicated.

Table 4.1 Proteins identified within the chromatin enriched fraction. DIGE was used to compare the chromatin fraction vs. whole cell yeast extract, and protein spots with an enrichment factor greater than +1.40 were selected for identification. The source for copy/cell numbers are denoted by the following: a - Protein copy numbers per cell are from Ghaemmaghami *et al*. (2003), b - unless otherwise noted, localizations were obtained from Huh *et al* (2003), c - localization was obtained from the organelle database. Functional descriptions were obtained from the Saccharomyces Genome Database.

Protein name	Enrichment factor	Estimated copies/cell[a]	Cellular Localization[b]	Description
Arp3	1.74	6650	Cytoskeleton, Nucleus (Yoo *et al*., 2006)	Actin-related protein 3, actin filament organization
Arp4	4.2	1070	Nucleus	Actin-related protein 4, chromatin remodeling
Arp7	2.53	1360	Nucleus	Actin-related protein 7, chromatin remodeling
Arp9	3.35	1790	Nucleus[c]	Actin-related protein 9, chromatin remodeling
Asc1	2.88	333000	Cytoplasm	G protein beta subunit, small subunit ribosomal protein
Atp2	1.43	164000	Mitochondrion	F1-ATPase beta chain, mitochondrial ATP synthesis
Cdc10	3.09	14100	Septin ring, cytosketelon, nucleusd	Septin ring protein, cell division
Cgi121	3.37	N.D.	Nucleus (Downey *et al*., 2006)	Component of KEOPS, telomere uncapping and elongation
Crn1	4.06	2900	Contractile ring, Cytoskeleton[c]	Coronin, actin filament organization
Cys3	1.65	38300	Cytoplasm	Gamma-cystathionase, Cysteine biosynthesis
Egd2	1.55	38000	Cytoplasm, Nucleus (Franke *et al*., 2001)	Component of NAC, ribosome associated
End3	10.4	2600	Cytoskeleton	EH domain protein, actin cytoskeletal organization
Gdi1	1.58	7280	Cytoplasm	GDP dissociation inhibitor, vesicle mediated transport
Ilv2	13.4	31900	Mitochondrion	Acetolactate synthase, amino acid synthesis
Ilv5	1.95	883000	Nucleus, Mitochondrion[c]	Acetohydroxy-acid isomerase, amino acid synthesis
Lat1	2.42	5440	Mitochondrion	Dihydrolipoamide acetyl-transferase, pyruvate metabolism
Lsp1	5.54	104000	Cytoplasm (punctate composite)	Component of eisosome, endocytosis
Pdb1	3.93	9970	Mitochrondrion, Nucleus[c]	Pyruvate dehydrogenase, pyruvate metabolism
Pil1	+1.65, Pil1(a) +2.31, Pil1(b)	115000	Cytoplasm (punctate composite)	Component of eisosome, endocytosis
Pst2	3.37	2330	Mitochondrion, Nucleus (Valencia-Burton *et al*., 2006)	Flavodoxin-like protein
Qcr2	1.73	35700	Mitochondrion	Ubiquinol cytochrome C reductase, respiration
Raf1	3.37	N.D.	Nucleus (Murray *et al*., 1987)	FLP1recombinase activating factor, plasmid maintenance
Rpb3	3.38	10000	Nucleus	DNA directed RNA polymerase II
Rpc40	3.98	13000	Nucleus	Component of RNA polymerases I
Rpt1	1.92	105	Nucleus	ATPase subunit of proteosome
Rvb2	4.03	3030	Nucleus[d]	Transcription, chromatin remodeling
Stm1	2.21	46800	Cytoplasm, Nucleus[c]	TOR signaling, telomere structure
Swi3	6.85	3150	Nucleus	Chromatin remodeling complex, SWI/SNF
Taf14	4.32	3120	Nucleus	Subunit of TFIID, TFIIF, INO80, SWI/SNF, NUA3 complexes, chromatin remodeling
Tfc7	3.89	2660	Cytoplasm, Nucleus	RNA polymerase IIIc
Tub2	3.73	N.D.	Nucleus, Cytoskeleton[c]	Tublin 2, microtubule component
Ume1	2.22	3040	Cytoplasm, Nucleus	Negative regulator of meosis, binding to histone deacetylase RPD3.
Ura7	3.73	57600	Cytoplasm	CTP synthase, phospholipid biosynthesis

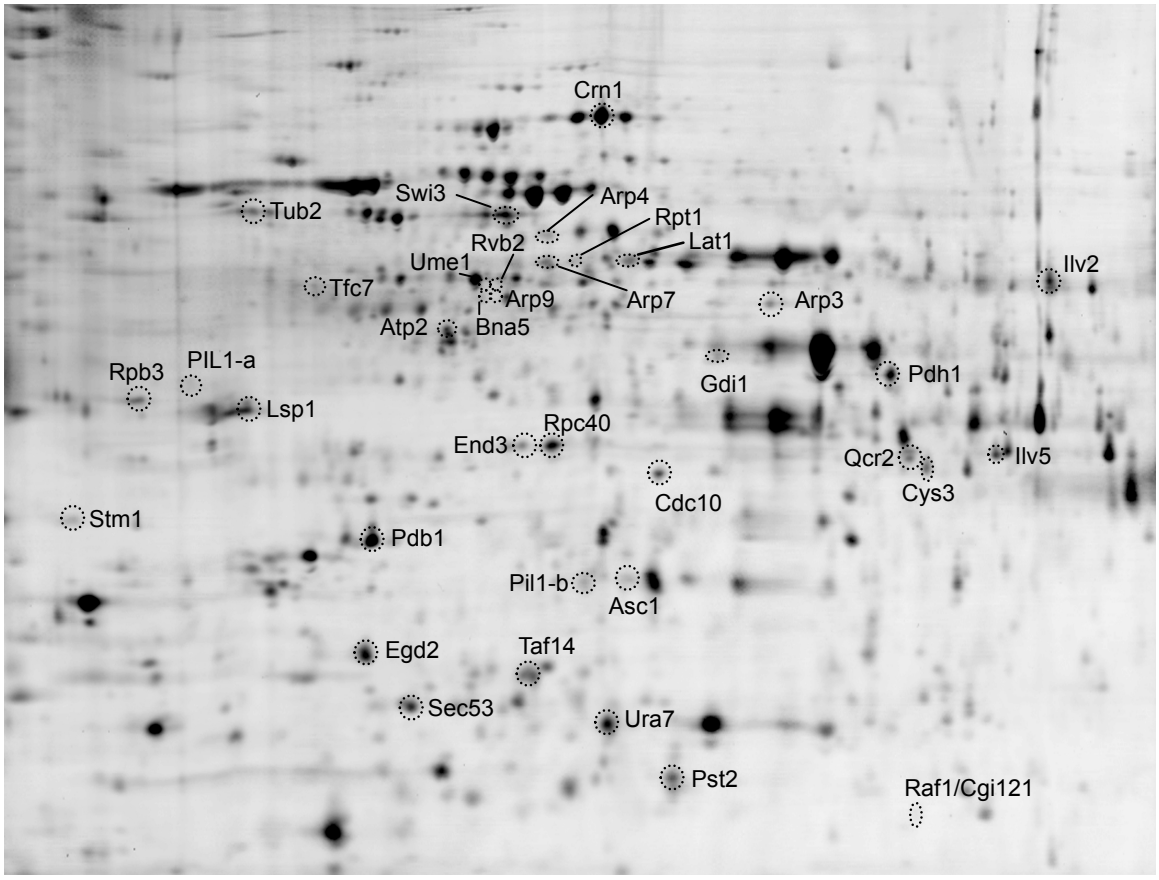

Figure 4.2. 2D-protein spot map of the yeast chromatin fraction. Representative proteins enriched in the chromatin fraction were identified by mass spectrometry and are marked with corresponding protein names. Protein identification data are summarized in Appendix B, Table B1, with respective chromatin enrichment factors and p-values.

4.2.2 Changes in Chromatin Fraction due to MMS Treatment

To further investigate differential profiling of chromatin-associated proteins, the response to MMS-induced changes in budding yeast was examined. A well-studied genotoxic agent, MMS alkylates DNA and results in activation of the DNA damage checkpoint, initially with detection of DNA damage, followed by a signaling cascade which results in the phosphorylation of protein targets involved in cell cycle control, DNA replication and repair (Harrison and Haber, 2006; Koundrioukoff *et al*., 2004). Comparison of chromatin fractions from MMS treated and control samples should indicate proteins that are differentially regulated and/or have a greater degree of chromatin association in response to MMS.

Four independent replicates of cultures were made for untreated samples and samples treated with 0.03% MMS, and chromatin enrichment was conducted as before. Differential protein abundance in the chromatin fraction was compared between MMS treated and control samples using DIGE (Figure 5.3). Additionally, whole-cell extracts and chromatin fractions were compared to calculate protein enrichment factors in the presence of MMS. The statistical power of detecting changes in abundance was also estimated, and at a statistical power of 0.8 ($\beta = 0.2$) with $\alpha = 0.05$, the four DIGE gels can theoretically be used to identify a change of 1.43 fold in spot abundance with a success rate of 80%. The normalized standard deviation of protein spots present on all gels was 0.216 for untreated samples and 0.220 for the MMS treated samples. Differential factor (DF) values for MMS treatment were determined through quantification using the DeCyder™ v.6.0 software as described in Experimental Procedures, with DF calculated from the ratio of the protein in the MMS treated sample vs. the control sample. Here, DF

includes contributions from both expression and changes in localization; for example, if DF increases but the EF ratios for the MMS+ treated and control samples are similar, the change is largely due to expression. It is also possible that DF to be positive and the EF ratio to decrease, indicating an increased protein expression and increased amount in the chromatin fraction, but a larger increase in non-chromatin associated protein. A total of 1763 spots were matched across the four replicates in the differential MMS experiment, of which 455 showed significant changes (increased or decreased) at $p < 0.05$ with FDR correction. Comparing the calculated EF values from chromatin enrichment for these 455 spots, 217 were both differentially regulated and enriched in chromatin fractions.

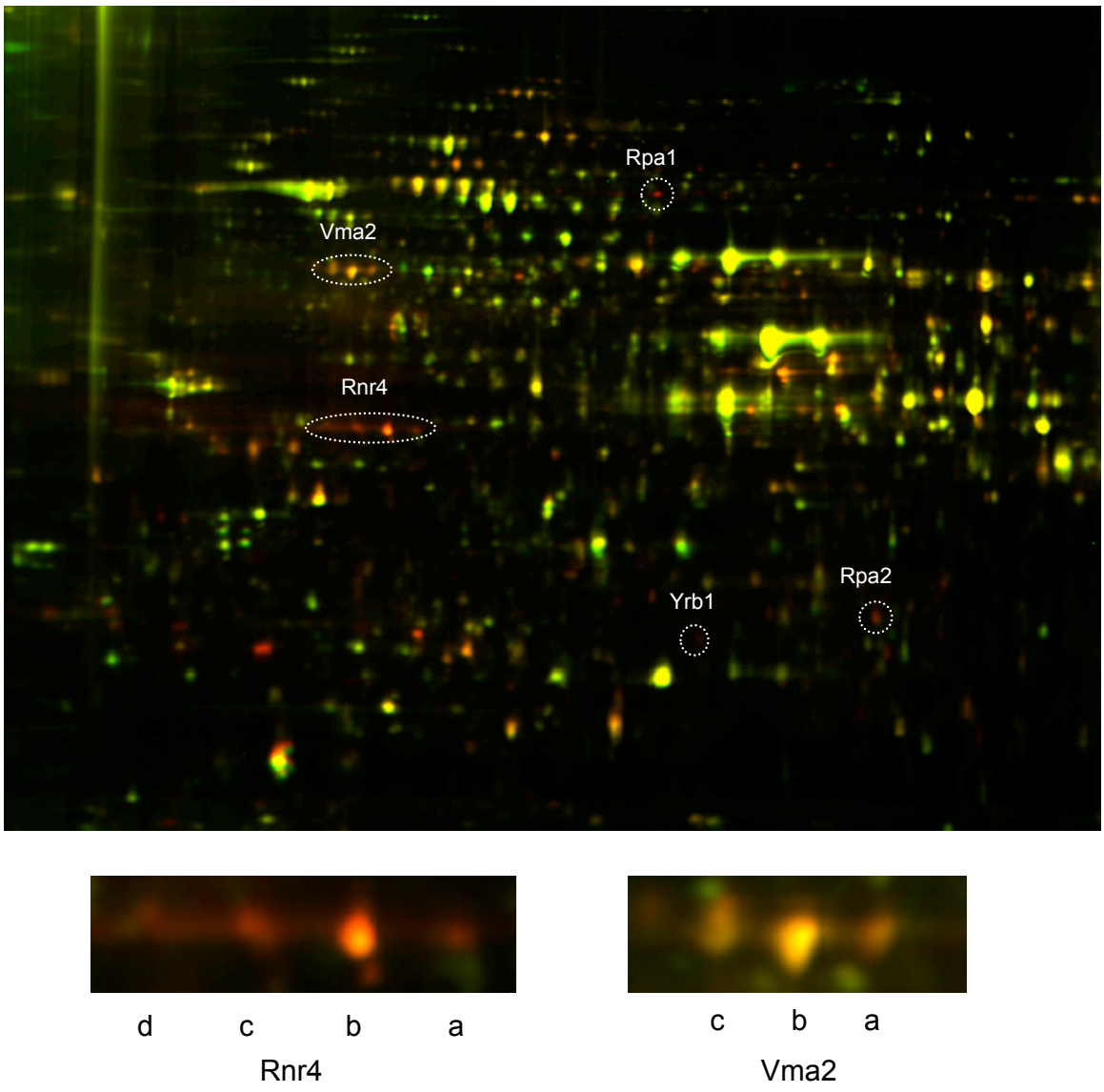

Figure 4.3. DIGE gel image comparing MMS treated and control chromatin fractions. A gel image from one of four replicates is shown for MMS-treated (red, Cy5) and untreated (green, Cy3) chromatin fractions. The Cy2 channel used for internal control is not shown. Five representative proteins (Rnr4, Rpa1, Rpa2, Vma2, Yrb1) are indicated along with an expansion of the region showing multiple identified isoforms for Rnr4 and Vma2.

4.2.3 Identification of MMS-Responsive Proteins

Protein spots from the MMS DIGE experiment were prioritized for identification according to the degree of chromatin enrichment (EF) and changes in observed abundance ('differential factor', DF). Spots that showed both positive EF and DF values (among the 217 described above) were of particular interest, as they indicated both chromatin-association and induction by MMS treatment, respectively. A preparative Coomassie-stained gel was made using chromatin fractions of the MMS treated samples (Figure 4.4), and protein spots were excised for identification by mass spectrometry. Identifications were made for 23 DF+ proteins and 12 DF- proteins (Table 5.2, Appendix B, Table B2). A subgroup of identified proteins corresponds to known checkpoint-regulated proteins, including Rnr4, Rpa1, and Rpa2. Rpa1 and Rpa2 are subunits of the hetero-trimeric replication factor A complex, which plays an integral role in DNA replication and checkpoint responses (Harrison and Haber, 2006; Longhese *et al*., 1996; Santocanale *et al*, 1995; Umezu *et al*., 1998). Among the spots with negative enrichment factors, Rnr4 isoforms exhibited some of the largest responses to MMS treatment as reflected by DF values (Table 5.2). The RNR complex controls the nucleotide pool for DNA synthesis and is a downstream target of the Rad53 checkpoint kinase (Huang and Elledge, 1997; Yao *et al*., 2003).

Along with the previously well-characterized proteins above, several additional DNA damage-associated proteins were identified as differentially expressed on MMS treatment including Bmh1, Pst2, Vma2, and Vma4 (see Table 5.2). Bmh1 is a 14-3-3 protein family member, which has been shown to directly modulate Rad53 activity (Usui and Petrini, 2003). Pst2, a predicted oxidative response protein, has also been implicated

in DNA damage responses (Umezu *et al*., 1998). Vacuolar-type H+ ATPase subunits Vma2 and Vma4 have been shown to play a role in DNA damage responses following treatment with MMS and cisplatin (Liao *et al*., 2006). In addition, several other proteins were identified that have not been well characterized in terms of their potential role following DNA damage, including Acf2, Arp3, Hsp31, Lsp1, Ste4, Ycp4, and Yrb1. Several proteins with low chromatin association (low EF values) and showing a differential response to MMS treatment were also identified (Table 4.2, Appendix B, Table B2). While these proteins are not chromatin associated per se, some (e.g. metabolic enzymes Ald6 and Pdc1) are consistent with a stress response in which yeast cells have a lowered metabolic activity and concomitant reduced growth competency. This observation is consistent with the model of suppressed protein synthesis upon DNA damage checkpoint execution or cellular stress (Hinnebusch and Natarajan, 2002). It is also possible that for some of these factors the effect of MMS may not have been due to DNA damage, since this alkylating agent can also act directly on proteins (Norman *et al*., 1986; Shin *et al*., 1996). A number of key DNA damage response factors including the kinases Mec1, Tel1, Rad53 and Chk1, and members of the 9-1-1 complex (Rad17, Mec3, Ddc1) (reviewed in Harrison and Haber, 2006) were not among the proteins that were identified in this screen. However, this is not surprising as only a subset of proteins that were chromatin- and/or MMS-enriched in the samples were characterized.

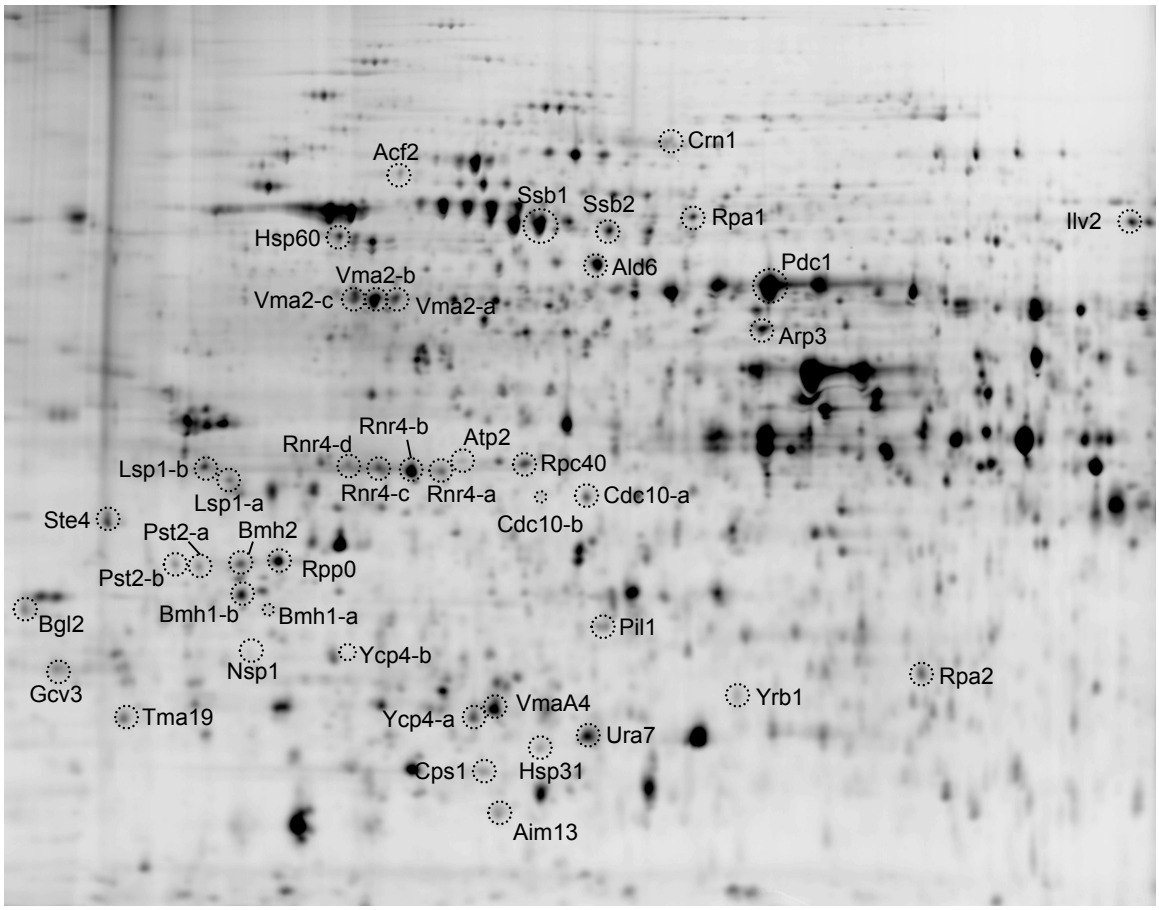

Figure 4.4. 2D-protein spot map showing differentially expressed proteins identified in the MMS treated yeast chromatin fraction. Proteins with statistically significant changes abundance on MMS treatment were identified by mass spectrometry and are marked with corresponding protein names. Protein identification data are summarized in the Appendix, Table B2.

Table 4.2. Statistical data for MMS-induced differentially expressed proteins in chromatin fraction. Multiple protein isoforms are indicated with a, b, c and d in parentheses. DF, differential factor, is fold change in abundance in the chromatin fraction on MMS treatment, where +DF indicates an increase and -DF a decrease. EF is the chromatin enrichment factor relative to the whole cell extract in either treated (MMS+) or control (MMS-) samples. See Appendix B, Table B2 for MS/MS identification data.

Protein name	DF	p-value (DF)	EF (+MMS)	p-value (EF, +MMS)	EF (-MMS)	p-value (EF, -MMS)
Acf2	1.48	0.02	1.57	0.011	-1.3	0.048
Aim13	1.7	0.0053	3.3	0.034	2.27	0.00097
Arp3	1.35	0.024	N/A	N/A	1.52	0.063
Atp2	1.52	0.0093	1.5	0.093	5.74	0.000041
Bmh1 (a)	1.92	0.0014	3.57	0.0039	-1.03	0.07
Cdc10 (a)	1.61	0.0034	7.28	0.0099	6.33	0.000015
Cdc10 (b)	1.38	0.044	1.5	0.18	2.43	0.0015
Cps1	1.61	0.01	2.16	0.0036	-2.57	0.00018
Crn1	1.78	0.0034	3.85	0.0024	2.36	0.0012
Gcv3	1.75	0.019	1.07	0.52	-1.9	0.00087
Ilv2	2.15	0.013	1.5	0.39	-1.15	0.086
Lsp1 (a)	1.51	0.0023	3.17	0.0011	1.79	0.022
Lsp1 (b)	1.84	0.0046	3.69	0.00072	-1.71	0.0078
Nsp1	1.58	0.005	3.07	0.014	1.65	0.017
Pil1	2.05	0.0013	9.6	0.0068	2.65	0.036
Pst2 (a)	1.5	0.0023	3.99	0.0074	1.55	0.0019
Pst2 (b)	3.83	0.0013	4.5	0.0074	-1.02	0.14
Rpa1	3.58	0.0007	4.16	0.01	-1.33	N/A
Rpa2	1.47	0.036	2.5	0.015	-1.12	0.089
Ste4	1.61	0.023	2.32	0.000092	-1	0.16
Vma2 (a)	1.92	0.0052	1.59	0.0063	-1.34	0.00019
Vma2 (b)	1.48	0.018	1.64	0.0041	-1.58	0.00018
Vma2 (c)	1.53	0.0097	1.65	0.021	1.1	0.05
Vma4	1.85	0.01	1.58	0.0048	-1.08	0.07
Ycp4 (a)	2.01	0.0007	5.4	0.00073	1.76	0.0005
Ycp4 (b)	1.69	0.037	5.31	0.00063	1.18	0.13
Yrb1	2.05	0.025	5.07	0.0011	1.77	0.004
Hsp31	1.63	0.0063	-1.64	0.0051	-1.84	0.000062
Rnr4 (a)	1.91	0.0014	-1.24	0.25	-1.47	0.013
Rnr4 (b)	3.9	0.000057	-2.08	0.012	-3.11	0.00011
Rnr4 (c)	3.89	0.000057	-1.17	0.27	-2.23	0.00025
Rnr4 (d)	2.41	0.0023	-1.06	0.74	1.3	0.015
Ald6	-1.84	0.00056	-2.21	0.021	-1.81	0.00014
Bgl2	-1.85	0.00068	-1.54	0.17	7.02	0.000022
Bmh1 (b)	-1.43	0.002	-1.53	0.0071	-1.07	0.059
Bmh2	-1.9	0.002	-2.08	0.021	-1.06	0.069
Hsp60	-1.72	0.00017	-1.56	0.091	1.31	0.0079
Pdc1	-1.69	0.00022	-2.27	0.013	-2.64	0.000099
Rpc40	-1.53	0.0016	2.31	0.013	3.98	0.000015
Rpp0	-1.7	0.00056	-2.15	0.028	-1.61	0.00037
Ssb1	-1.62	0.0084	-1.41	0.12	-1.27	0.00027
Ssb2	-1.83	0.0092	2.01	0.018	1.45	0.009
Tma19	-1.93	0.0027	-3	0.036	-1.02	0.14
Ura7	-1.85	0.0027	6.01	0.059	3.73	0.000022

4.2.4 Changes in Chromatin Association and Localization Due to MMS Treatment

The MMS DIGE experiment provided a direct measure of changes in protein abundance within the chromatin enriched fraction. This can represent a change in expression of the protein of interest, a change in the degree of chromatin association (including direct binding to DNA, interaction with DNA binding proteins, or simple inclusion in the chromatin pellet), or some combination of these factors. Here, the calculated EF ratios for MMS treated and control samples can be compared and changes in EF values can provide an estimate of changes in the degree of chromatin association (i.e. localization). The EF ratios for the control (MMS-) and treated (MMS+) samples are compared in Figure 4.5. The majority of proteins increased their degree of chromatin association in response to MMS treatment. Interestingly, different forms of the same protein often exhibited different changes in expression and chromatin association, including Rnr4, Vma2, Pst2, Lsp1, Ycp4, Cdc10 and Bmh1 (Table 4.2, Appendix B, Table B2). For example, four isoforms of Rnr4 were detected, all of which increased in chromatin abundance in response to MMS treatment (Figure 4.3). Rnr4 was previously reported to undergo increased translocation to the cytoplasm under genotoxic stress (Yao *et al*., 2003). Consistent with this, the isoform with the highest chromatin association, Rnr4-d, showed a decrease in the proportion of Rnr4-d associated with chromatin on MMS treatment as reflected by the decrease in enrichment factor from +1.30 to -1.06. However, the total amount of all forms of Rnr4 binding chromatin increased, as all forms had positive DF values. The most abundant isoform, Rnr4-b (Figure 4.3), had minimal association with chromatin with or without MMS treatment (Table 4.2). The observed values of DF and

EF indicate a complex response, with some isoforms increasing and others decreasing their relative degree of chromatin association (EF), with the total amount of cellular Rnr4 apparently increasing on MMS exposure.

All Vma2 isoforms demonstrated greater chromatin association (EF) as a consequence of MMS treatment, but isoforms Vma2-a and b, showed a more dramatic increase than Vma2-c. Comparing the DF and EF values in Table 4.2, the change in chromatin abundance can be largely attributed to an increase in chromatin association for Vma2 as opposed to increased cellular protein levels. Similarly, Rpa1 demonstrated a pronounced increase in chromatin association on MMS exposure, suggesting that the observed increase in chromatin abundance (DF) can be largely attributed to a change in cellular localization (Table 4.2). Conversely, Cdc10-b exhibited a small net increase in abundance in the chromatin fraction on MMS treatment (DF +1.38) but a decrease in EF from +2.43 to +1.50. This is consistent with an increase in cellular expression of Cdc10-b, but a smaller proportion of Cdc10-b associating with chromatin.

It has previously been observed that genes that are induced by DNA damaging agents are not those that are identified as protecting cells against DNA damage (Birrell *et al*., 2002). However, as proteins can respond more rapidly than genes through post-translational modifications or changes in localization, there may be a closer relationship between increased chromatin association and DNA-protective proteins. In contrast to gene expression data (Birrell *et al*., 2002), almost half of the proteins identified (10 of 22) were previously identified as responding to genotoxic agents in high-throughput screening studies. Specifically, *acf2*, *aim13*, *gcv3*, and *ycp4* knockout strains were identified as having significant fitness defects ($p < 0.05$) on MMS exposure,

with *aim13*, *bmh1*,*cdc10*, *cps1*, *gcv3*, *pil1*, *pst2*, *rnr4* knockout strains having fitness defects on exposure to hydroxyurea (Hillenmeyer *et al*., 2008).

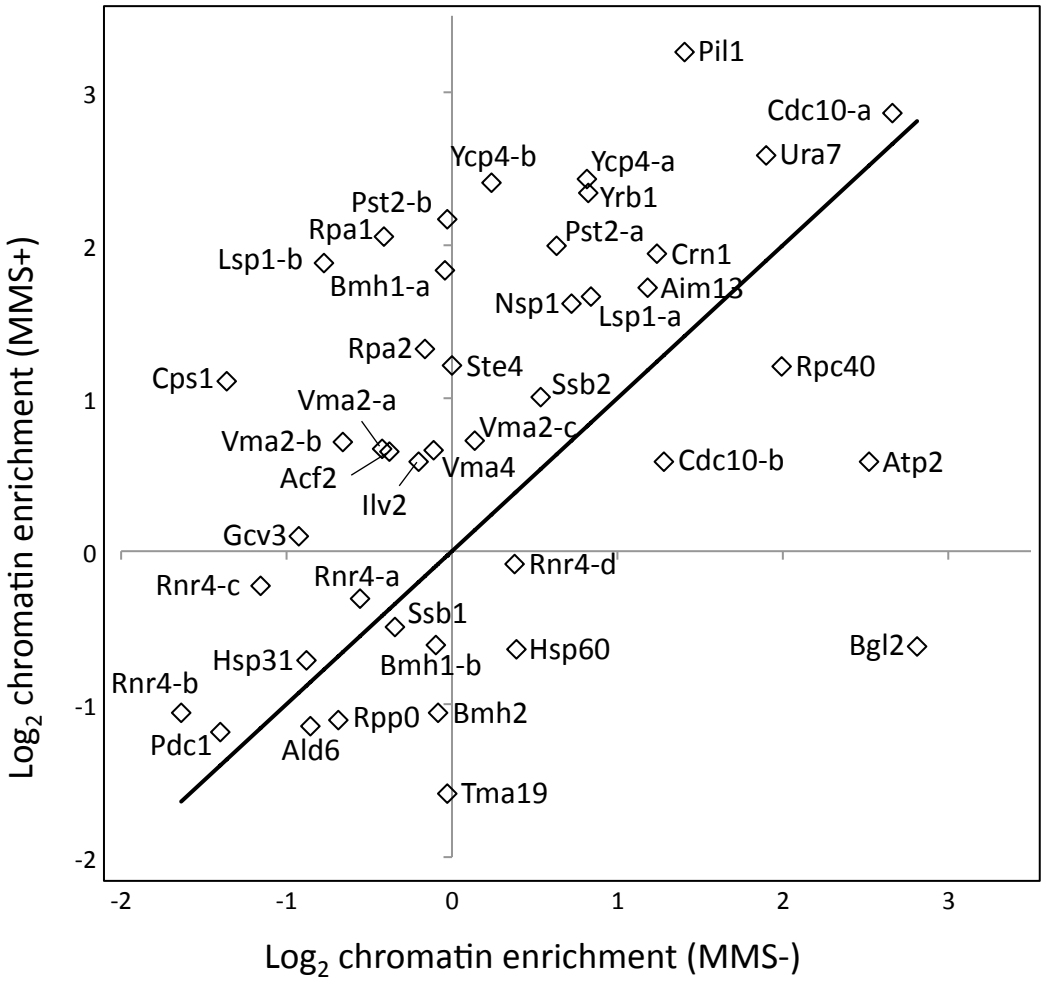

Figure 4.5. Chromatin Enrichment Factors (EF) in the presence and absence of MMS. Enrichment factors were calculated from the ratio of protein abundance in the chromatin fraction versus whole cell extract. A general increase in chromatin association is seen with MMS treatment, along with changes specific protein to given protein isoforms including Rnr4, Vma2, Pst2, Cdc10, Ycp4, Bmh1 and Lsp1.

4.2.5 Evaluation of Sensitivity to Genotoxic Agents for Mutant Yeast Strains

To further investigate MMS induced proteins identified via the DIGE analysis, yeast strains with mutations corresponding to the genes encoding several of these proteins were evaluated in growth assays in the presence of the genotoxic agents MMS or HU (Hanway *et al*., 2002; Varrin *et al*., 2005) Haploid cells either containing gene knockouts (*pst2*, *bmh1*, *hsp31*, *acf2*, *ste4*, *rnr4*) or, in the case of essential genes, lowered mRNA expression due to reduced mRNA stability, (DAmP strains, Open Biosystems) (*rpa1*, *rpa2*, *yrb1*, *arp3*) were employed. An isogenic wild-type strain was used as a negative control and a *rad53-11* strain (Santocanale and Diffley, 1998) with a mutant allele in the checkpoint kinase Rad53 as a positive control for sensitivity to genotoxic agents.

The primary interest was in proteins increasing in chromatin abundance, however haploid yeast knockout strains corresponding to a number of proteins decreasing in abundance were also investigated (Figure 4.6). None of these strains showed either enhanced or reduced susceptibility to MMS or HU relative to the isogenic wild-type strain. Among the strains corresponding to proteins with increased chromatin abundance, *acf2*, *arp3*, *hsp31*, and *ycp4* mutants did not show apparent changes in sensitivity relative to the wild-type strain (Figure 4.7). Interestingly, *pst2*, *ste4*, and *lsp1* mutants actually exhibited increased resistance to MMS, indicating a link to the DNA damage response, possibly through interrelated pathways such as MAP kinase signaling, eisosome trafficking and oxidative stress response. *rpa1*, *rpa2* and *rnr4* mutants have previously been shown to be sensitive to MMS or HU, in agreement with their DNA damage checkpoint regulation (Huang and Elledge, 1997; Santocanale *et al*.,

1995; Umezu *et al*., 1998; Yao *et al*., 2003). Here however, no significant response was seen for *rpa1*or *rpa2* DAmP strains to MMS treatment and *rpa1* to HU treatment. Subsequent western blot analysis of Rpa1 levels revealed that it was not reduced in the *rpa1* DAmP strain relative to the isogenic wild-type (Figure 4.8), accounting for the lack of sensitivity observed. Given that the *rpa2* DAmP strain was sensitive to HU, its Rpa2 level presumably was reduced compared to wild-type, however it may not have been sufficiently diminished to render cells more vulnerable to the effects of MMS. Also shown in Figure 4.8 is the decrease in protein abundance of Arp3 relative to the isogenic wild-type in the *Arp3* DAmP strain validating its use in evaluating sensitivity to genotoxic stress. The *rnr4* knockout strain similarly did not show increased genotoxic sensitivity. It is possible that other *RNR* genes may compensate for *rnr4* deletion (Gasch *et al*., 2001), and the RNR4 isoform is not required for cell viability. Most interestingly, the *yrb1* DAmP cells showed pronounced sensitivity to MMS (at more than 0.02%) and HU (at more than 25 mM).

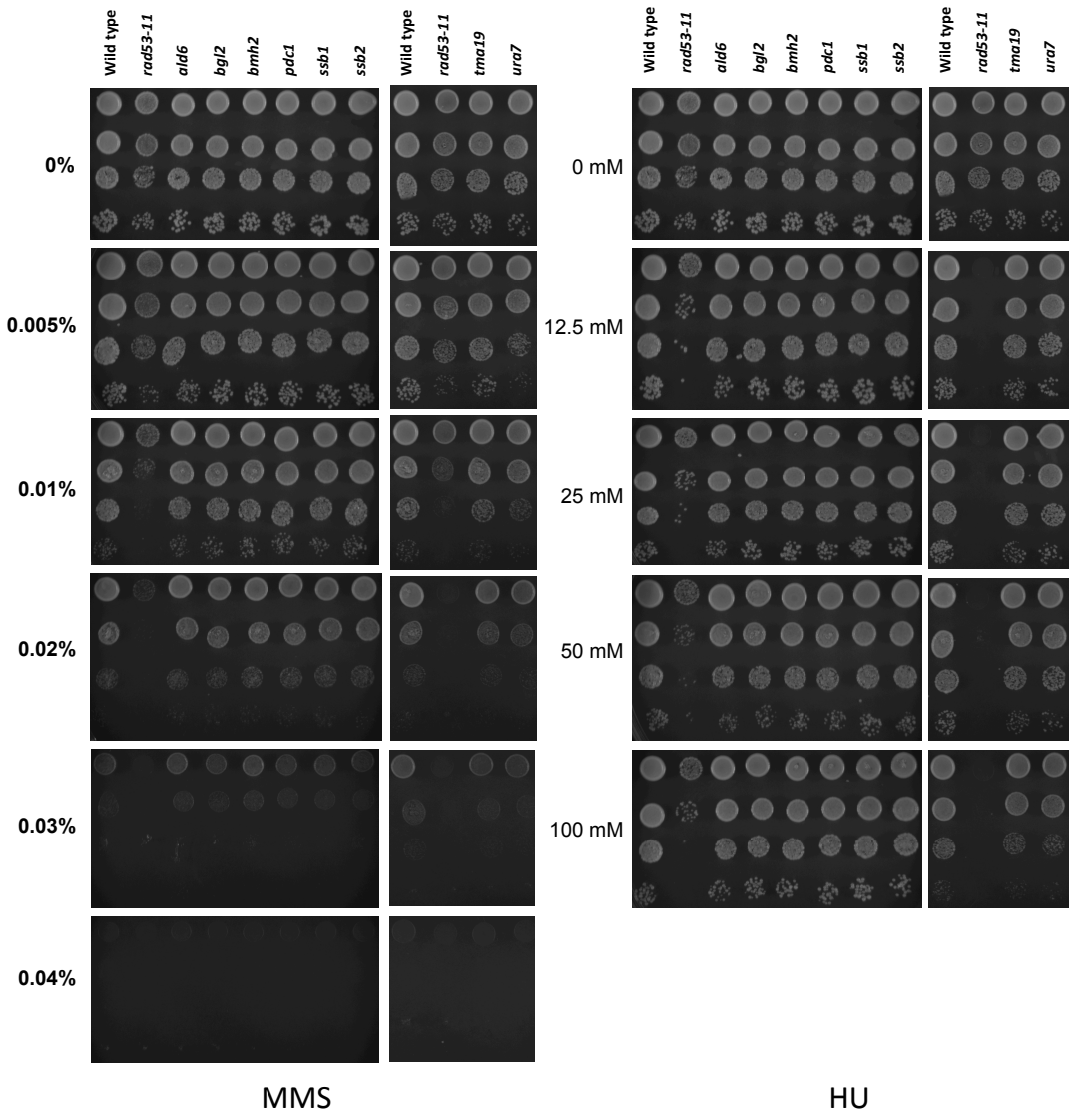

Figure 4.6. Spotting growth assay for genotoxic sensitivity corresponding to proteins decreasing in abundance on chromatin following MMS treatment. Haploid yeast knockout strains corresponding to proteins that showed a reduction in chromatin association following MMS exposure were obtained from Open Biosystems. The assay was performed on YPD plates containing indicated concentrations of MMS or HU. Cells were 10-fold serially diluted and incubated at 30°C for 2 days. An isogenic wild-type strain BY4741 was used as a negative control and *rad53-11* mutant strain as a positive control.

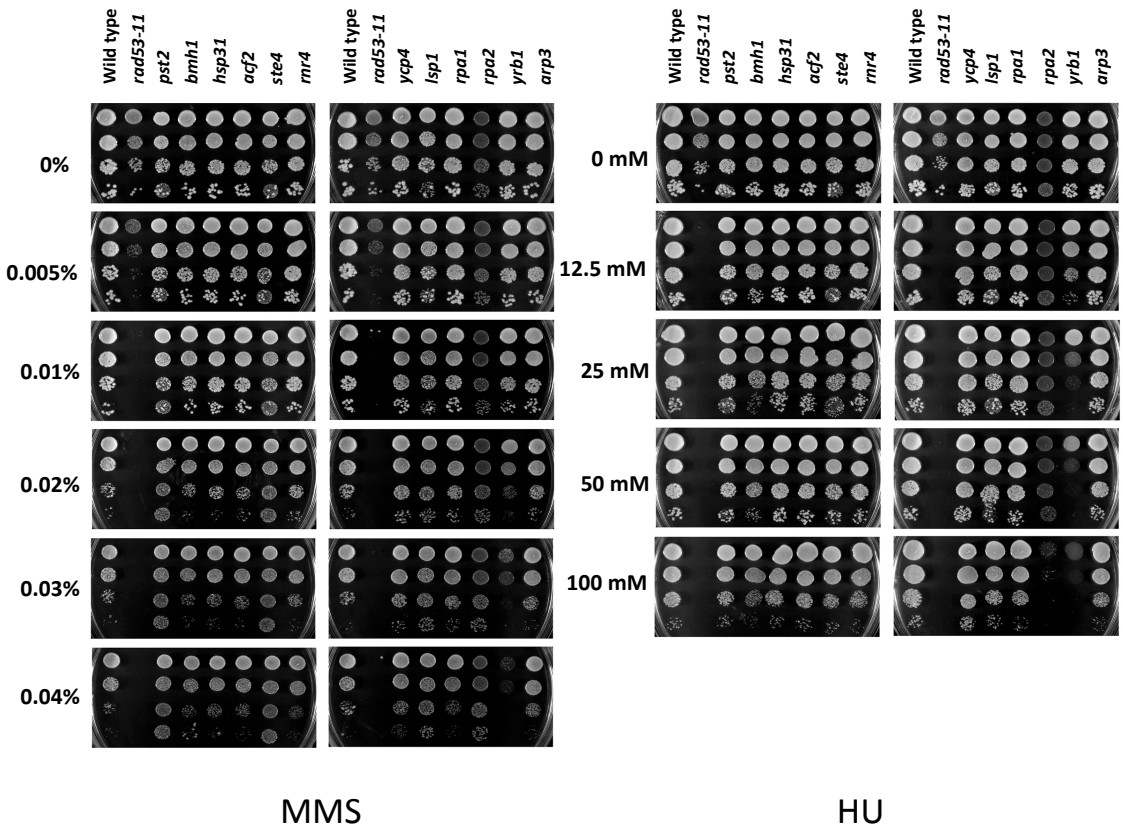

Figure 4.7. Spotting growth assay for genotoxic sensitivity corresponding to proteins increasing in abundance on chromatin following MMS treatment. The yeast cells were either knockout (*ycp4, lsp1, pst2, bmh1, hsp31, acf2, ste4*, and *rnr4*) or DAmP strains (*rpa1, rpa2, yrb1* and *arp3*). Wild-type, *rad53-11*, ald6, bgl2, bmh2, pdc1, ssb1, ssb2, tma19 and ura7 strains were analyzed as described in Figure 4.6.

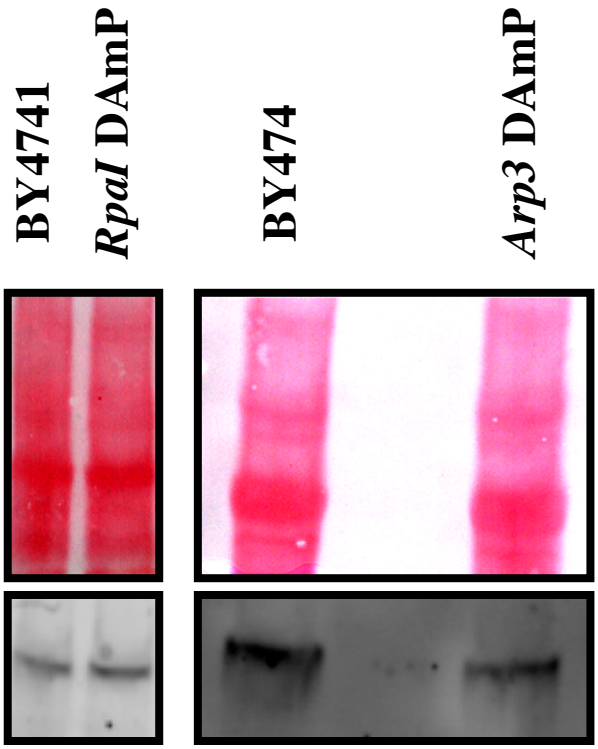

Figure 4.8. Western blot analysis of *RpaI* DAmP and *Arp3* DAmP strains. Whole cell extracts prepared from asynchronous cultures of these strains were used to evaluate whether protein abundance was in fact reduced compared to the isogenic wild-type (BY4741). *Arp3* DAmP showed a significant decrease in the levels of the Arp3 protein compared to the wild-type, whereas levels of RpaI in the corresponding DAmP strain were comparable to the wild-type.

4.3 Discussion

The differential proteomics technique of DIGE was combined with a chromatin fractionation and enrichment strategy. This was and applied to investigate the response to genotoxic agents in budding yeast cells. The approach facilitated the selective screening of important chromatin-associated proteins that can otherwise be difficult to observe by typical proteomics approaches, and was successful in identifying functionally relevant target proteins. Moreover, the method was effective for the differential analysis of yeast cells following chemical treatment, as demonstrated by the MMS exposure experiment. While the fractionation method used was effective at enrichment of chromatin binding factors, a number of the observed proteins were likely mitochondrial, suggesting that more specific fractionation methods could be applied. One possible approach would be to first isolate nuclei prior to chromatin enrichment. Overall, the described method was successful in permitting the differential analysis of chromatin binding proteins using a gel-based proteomics technique, largely overcoming the technical limitations for analyzing lower-abundance chromatin proteins.

While the methodology was effective at identifying known and potentially novel proteins involved in DNA damage response, the technique does not provide comprehensive coverage. Future refinements to the methodology may be able to increase the number of factors identified in similar studies. The gel methods could be expanded to increase the pH range over which proteins can be separated effectively, more sensitive mass spectrometers may be used to increase the success rate of protein identification, a greater degree of replication and experimental precision may be utilized to detect proteins undergoing small changes in abundance and/or localization.

Characterization of differentially expressed proteins based on DF analysis was extended using an analysis of the chromatin enrichment factors (EF), providing a quantitative estimate of protein localization not typically available within proteomics studies. The method was also informative in addressing changes in protein localization, as demonstrated in the change of enrichment factor depending on treatment. Chromatin fractionation was able to consistently reveal a large population of chromatin-associated proteins using a relatively straightforward sampling procedure, in which intact complexes are maintained, as indicated by the co-detection of functionally related chromatin proteins (i.e. Tables 4.1 and 4.2). A technical strength of DIGE itself, compared to MS-based methods, is that it is able to distinguish differences in response to compounds such as MMS for different protein isoforms or post-translational variants, as revealed in the Rnr4 isoforms in this study. In contrast, quantitative MS-based methods largely rely on digested peptides (Ong and Mann, 2005), making it more challenging to distinguish variable forms, as the peptides on which the change is located need to be correctly identified, quantified, and compared with peptides representing other forms of the protein.

With respect to the budding yeast DNA damage response, this study was in broad agreement with previous high-throughput studies on this response, using a variety of approaches such as microarray analysis (Gasch *et al*., 2001), phenotyping of deletion strains (Begley *et al*., 2002) and quantitative phosphoproteomics (Smolka *et al*., 2007). The microarray study showed the over-expression of the RNR complex (which is composed of four subunits Rnr1, Rnr2, Rnr3 and Rnr4) as the most significantly changed along with other key proteins such as Din7, Dun1, Rad54 and Rad51. The

phosphoproteome study screened the possible phosphorylation-mediated targets of Mec1/Tel1 and Rad53 kinases (Smolka *et al*., 2007), and identified proteins involved in DNA replication, cytokinesis, transcription, mitosis, RNA export, stress response, transcription, and nuclear transport. Compared to the above studies, the approach used here focused on a subset of the budding yeast proteome that is highly associated with chromatin. In addition to the confirmation of known checkpoint-regulated factors (e.g. Rpa1, Rpa2, Rnr4), several new proteins related to DNA damage response pathways have been identified. One such factor is the Ran-GTPase binding protein Yrb1, a component of the nuclear import-export system (Künzler *et al*., 2001) in which the ternary complex of Gsp1, Yrb1 and Rna1 controls the GTP/GDP balance across the nuclear membrane. It is proposed here that Yrb1 protein may represent a link between the nuclear transport system and DNA damage responses, as implied by a recent model for G_1/S cell cycle arrest during checkpoint execution (Ghavidel *et al*., 2007). It will now be of interest to determine which proteins dependent on Yrb1-mediated nucleocytoplasmic trafficking act downstream of this factor in affording protection to genotoxic agents.

In conclusion, a simple fractionation and DIGE-based approach for chromatin proteomics is presented, which can be broadly applied to investigate biological responses to chemical stress and other factors. This method was successfully applied to investigate changes that occur following exposure to the genotoxic agent MMS, confirming that it is effective in identifying novel proteins involved in cellular processes, such as the response to DNA damage.

Chapter 5: General Conclusions and Future Directions

5.1 A Mathematical Model of Replication Initiation is Robust and Predictive

The kinetic model of DNA replication initiation presented in this thesis aims to depict the dynamic processes that underlie its function. Modeling of the cell cycle has been undertaken by several groups, benefitting from the different scales and approaches considered. Overall, the goal of such an endeavor is to establish a falsifiable model of how the cell cycle is regulated from genetic regulation to modules of protein-based circuits. Successive experimental studies in a given scientific area build on accepted theories from which further questions arise. Similarly, a collaborative process of amalgamating new models is important. Very basic models of cell cycle oscillation have characterized this emergent behaviour and larger models of the entire cell cycle have refined this characterization. Also important is the diversity of perspectives from which to model the cell cycle, be it at the level of transition between replication species or focused on the temporal profiles of duplicating chromosomes through S phase. A crucial improvement in increasing the understanding of the cell cycle through modeling is being able to apply quantitative values to its description. The combination and contrasting of different models highlights areas that need to be investigated more thoroughly. In addition, as is the case with the model presented here, this process fills in major details towards a comprehensive and highly resolved understanding of the cell cycle.

For the purposes of the present model, emphasis is on the mechanistic assembly of protein complexes in G_1 phase, which subsequently give rise to replication forks throughout S phase. The proteins considered are the key players in this scheme and through quantitative analysis of their *in vivo* levels, the system kinetics derived by

parameter fitting permit predictions about system behavior, again on a quantitative scale. Distinctions between the model presented here and other cell cycle and even DNA replication models have been pointed out in detail in chapter 3. Briefly, parameter fitting is constrained only by the levels of replication proteins observed in live cells, and not by any optimization that seeks to restrict values according to idealized assumptions regarding the temporal nature origin firing or otherwise. The behaviour of this system is thus a direct output of the levels of replication proteins themselves. Apart from being consistent with experimental perturbations to replication proteins, the model has exposed sensitivities in the network that provide fodder for future experimental exploration. For example, the potential catalytic role of Cdt1 in loading multiple MCM complexes before being excluded from the nucleus is an interesting phenomenon to explore *in vivo*.

The regulation of Dbf4 and Cdc6 by the cell, both in terms of properly timed expression and degradation have been captured by the model. This feature is interesting in light of the overexpression of their human homologs in cancerous tissues. The model was extremely sensitive to fluctuations in levels of these two limiting factors, a facet demonstrated by their individual *in vivo* knockdowns. This underscores the important cellular function of preventing their degradation by the proteasome (Cdc6) or APC (Dbf4) during the time they exert their critical functions and by limiting their expression so that over-replication does not occur. This is mediated by the tight regulation of discrete cellular events by cyclins (specifically Clb5), another overarching theme in cell cycle studies.

Another interesting property of the system is the catalytic role of Cdt1 in loading Mcm2-7 at origins. The model suggests a very high value for the kinetics of this reaction.

Recent studies have elucidated the mechanism by which Cdt1 interacts with Orc6 to recruit helicase rings to pre-RCs (Chen *et al*., 2007; Takara and Bell, 2011). It remains to be established if and how Cdt1 molecules are recycled during G_1 and whether they recruit new Mcm2-7 complexes to pre-RCs after initial dissociation from this complex. The model supports this possibility given Cdt1-origin association is extremely transient, consistent with the literature (Randell *et al*., 2006). Contrary to Cdc6 and Dbf4, the model suggests that cells are refractory to depletion in Cdt1 levels well below the endogenous level, again supporting this observation. Investigating the mechanism by which Cdt1 is extruded from pre-RCs and the fate of such molecules until their nuclear export occurs a crucial next step in better characterizing helicase loading. Experiments using fluorescently-tagged Cdt1 and/or specific origins might allow the observation of distinct pools of Cdt1 being redistributed to different origins in late G_1, in keeping with a dynamic loading model.

While the model faithfully represents the DNA replication network, further refinements would help in understanding different aspects of initiation, which would then be integrated into the existing model. Although the requirement for an active CMG helicase at replication forks is effectively recapitulated by the modeling of Cdc45 and Mcm2, the quantitative evaluation of proteins such as Sld2, Sld3, Dpb11 and components of GINS might give a more accurate estimate of the rate of pre-IC (RC6 in the model) assembly. A methodological detail in fitting the model involved distinguishing between DNA-bound and unbound protein. Because the assembly of replication complexes occurs on the DNA this was important in accurately describing the system. Although proteins such as Cdt1, Cdc6 and Dbf4 exert their function at origins, there is the possibility that

they bind to non-origin sequences. For this reason estimates of non-specific binding were incorporated. Determining the precise levels of non-specific binding using techniques such as ChIP-seq for proteins used in the model would be beneficial in further resolving protein level quantitation.

The temporal separation of G_1 and S phase in the model is not explicitly coded. The overlap in the time during which pre-RCs can be formed and the commencement of fork firing is largely dependent upon the time profile of G_1-associated factors (e.g., Cdc6) incorporated into replication complexes. Because DNA-bound Cdc45 and Cdc6 overlap, it is possible that in order to fit the data, the network behaves in such a way that RC complexes containing Cdc6 can still be established after the first fork fires. Such complexes never evolve into fired forks due to the inhibitory CDK effects and end up as residual, "unused" pre-RCs. One source of inherent technical variability is the coherence of synchronized timecourse experiments such that in a given trial, a particular culture may enter S phase earlier. While we hold each timepoint sample to correspond to a specific point in the cell cycle, this is likely not to be completely accurate. The minor differences in timing do not seem to affect the system behavior, considering the theoretically consistent transition of the RCs. Modifying the timing of Cdc6, however such that its levels in the pellet fraction reach zero prior to the rise in Dbf4 would provide an interesting comparison with the current model behaviour. This could be performed by shifting its corresponding timepoints earlier, which can be justified by the delay in expression following an α-factor block. Just like the inclusion of factors such as GINS subunits in the model, it would provide a greater resolution of the events at the G_1/S transition.

Although the model presented in this thesis provides a unique perspective in that it uses the protein components of replication to derive an output of replication fork concentration, it matches the observations from models that examine the spatio-temporal pattern of origin firing (de Moura *et al.*, 2010; Spiesser *et al.*, 2009, Yang *et al.*, 2010). How are origin efficiency and the temporal firing program captured by the mean field approach of the replication model (individual origins are not modeled, but their overall output, i.e. [FORK] is)? For an understanding of this phenomenon, it is useful to observe the results of overexpression and protein knock-down within the model. One would expect that reducing a factor's overall abundance and on the DNA in the network would result in fewer origins fired (and vice versa). It turns out, however that each factor contributes differently in terms of being limiting or having the capacity to drive additional origin firing. As noted, Cdt1 seems to act catalytically within the network, loading Mcm2-7 complexes at a very high rate. This is a key finding of the model as the cellular abundance of Cdt1 is close to that of Cdc45, which seems to act stoichiometrically. An increase in Cdt1 abundance and activity ten-fold does not appreciably increase the number of origins fired, whereas in the case of Dbf4 and Cdc45, an analogous increase increases the number of potential origins that actually fire (Table 3.3).

Examining the temporal profile of the various reaction rates reveals that among the 332 potential origins "supplied" by the system, only a subset of them (~305) fire. A parameter that is tightly constrained is that which specifies the rate of RC4 breakup (v_{22}). Increasing its value causes an increase in the cycling of the system from RC1 through RC4, ultimately leading to less origins being fired. This plays into the notion of a

dynamic loading mechanism, wherein MCMs can be unloaded from the DNA requiring the continued presence of pre-RC components to reload them until DDK and CDK activity (represented by Dbf4 and Cdc45 association) produces a functional replication fork. Decreasing RC4 breakup increases forward flux through the system leading to increased origin firing. Any deviation from the value of v_{22} will either result in less origins firing (futile RC1→RC4 cycling) or an increase in firing, but at the risk of re-replication (a representation of a potential source of cancer) if other rates are kept constant. Referring back to the question of how the model reproduces the temporal firing pattern observed in other models, the efficiency of a hypothetical origin in the model is represented by the cumulative concentration of all the factors required for replication fork firing. During early replication complex cycling, an origin will have a high efficiency if it is provided with MCMs, Cdc45 and Dbf4. Crucially, MCMs are present earlier than Cdc45 and Dbf4 and represent the factor that would impart intrinsic efficiency to an origin/replication complex in transition. As origins begin to fire and the proportion of unfired origins (RC1→RC6) decreases relative to the amount of Dbf4 and Cdc45 ("limiting activators"), the probability of origin firing does indeed increase over the course of S phase. This is consistent with the proposed mechanism for a hybrid deterministic/stochastic pattern of origin firing described by de Moura *et al.* (2010) and Yang *et al.* (2010).

Ultimately the model is a useful tool in predicting behaviour of the network of DNA replication. These findings can be used to probe the mammalian system. Such a model can be employed to identify potential targets for cell cycle control (e.g. Dbf4 and Cdc45 are better targets than Cdt1 for deregulation), and is crucial in optimizing

individualized therapies for cancer and other human diseases as discussed in sections 3.3 and 5.3.

5.2 Exploring New Techniques for Isolating Novel Cell Cycle Proteins and Functions

The isolation of sub-cellular complexes or even organelles has provided researchers with the ability to enrich for proteins of interest. This is important for studying functional relationships within the context of localized modules. Fractionation techniques such as immunoprecipitation, gradient sedimentation, and electrophoresis assist in identifying proteins of low abundance or of localized concentration (Bauer and Kuster, 2003; Dreger, 2003; Pasquali *et al*., 1999). Typically, the protein landscape of enriched samples is then examined using multi-dimensional separation of proteins, and subsequent identification of peptides. The most widely implemented scheme involves 2D-PAGE followed by mass spectrometry (Sutton *et al*., 1995; Cohen *et al*., 2002; Watt *et al*., 2003 and reviewed in Huber *et al*., 2003). In some cases, complexes obtained by affinity purification can be directly analyzed by mass spectrometry (reviewed in Pache and Aloy, 2008).
Attempts to isolate sub-complexes in yeast has yielded great success as in the case of mitochondrial proteins (Prokisch *et al*., 2004; Reinders *et al*., 2006; Sickmann *et al*., 2003), membrane proteins, the proteome of the Golgi apparatus and related structures, as well as cytoplasmic and nuclear proteins (reviewed in Gavin *et al*., 2002). In each of these cases, it is important to verify the purity of the sample collected, usually through identifying characteristic markers via Western blotting.

2D-PAGE has been widely employed to separate proteins in order to facilitate their identification via downstream techniques. In chapter 4, a unique combination of fractionation and 2D-DIGE provides a useful technique to isolate proteins that have a differential association with chromatin in response to the DNA damaging agent, MMS. Several novel proteins were identified as having a differential chromatin association profile in response to DNA damage. Of these, Yrb1 was of particular interest as a strain expressing unstable transcripts of it showed acute genotoxic sensitivity to both MMS and HU.

Yrb1 (yeast ran-binding-protein-1) has been identified as a Ran GTPase that plays a role in neucleocytoplasmic trafficking. Mutations to this protein inhibit its function in facilitating nuclear import and export of proteins such as those involved in the yeast mating response as well as RNA nuclear export (Kunzler *et al*., 2001). In response to environmental changes, such as a mating signal or DNA damage, the transcription profile of the appropriate response genes is changed. The localization of proteins or transcripts involved in such a response changes with the need for export to the cytoplasm for translation and nuclear import to exert a transcriptional function. Given the results presented in chapter 4, Yrb1 is a strong candidate for mediating these changes. An intriguing DNA damage response mechanism involving relaying the signal of genomic catastrophe has been identified by Ghavidel *et al*. (2007). In this study, they demonstrate the role of unspliced tRNAs in inducing a G_1 checkpoint arrest through their localization pattern. Unspliced intron-containing tRNA is normally extruded from the nucleus via the export factor Los1 for processing. In the event of DNA damage, a Rad53-dependent cytoplasmic localization of Los1 occurs, preventing it from mediating the nuclear export

of the unspliced premature tRNA species. As a result, the nuclear accumulation of these tRNAs induces the transcription of GCN4, a ubiquitous transcription factor (Hinnebusch and Natarajan, 2002). GCN4 upregulates the expression of DNA damage repair genes (Natarajan, Meyer, Jackson 2001), while inhibiting CLN2 transcription (Ghavidel *et al*., 2007) resulting in a G_1 arrest.

The accumulation of unspliced tRNAs in response to MMS-induced DNA damage thus provides a mechanism to relay the message that transcription of genes involved in proliferation should cease while those implicated in DNA repair should be upregulated. The genotoxic sensitivity observed in Yrb1-depleted cells, shown in chapter 4 presents a promising area of interest, linking this protein to a role in the DNA damage response. It is possible that its function in nuclear trafficking extends to a parallel pathway with Los1 or an independent role in regulating the levels of tRNA export. Ultimately this is likely to affect the downstream target of these pathways, GCN4. Future studies investigating the interaction between Yrb1 and GCN4 transcriptional activation or the nuclear export of Gcn4 mRNA could shed light on the results observed in this thesis.

The protein coverage for DNA damage repair factors was not all-inclusive, not having isolated proteins such as Mec1, Tel1 and Rad53. This is perhaps a result of not identifying all potential gel spots or reflective of their limited differential chromatin association in response to MMS relative to other factors. One limitation in analysis of sensitivity to genotoxic stress was the poor knockdown of protein levels for at least one commercially-derived strain, *Rpa1* DAmP. It is possible that more proteins that were identified as having notable chromatin enrichment profiles when exposed to MMS do in fact impart sensitivity or even resistance. Their analysis in the genotoxic sensitivity assay

is potentially marred by the inefficient reduction of protein levels in the corresponding DAmP strain. The use of knockout strains or well-characterized mutants would be more suitable for further investigations.

Other peptide-labeling techniques for identifying differential protein expression amongst treatment samples have been developed such as isotope-coded affinity tagging (ICAT, Gygi *et al*., 1999) and isobaric tags for relative and absolute quantitation (iTRAQ, Ross *et al*., 2004). These are claimed to provide better protein coverage within samples compared to DIGE and have a greater variety of tagging dyes, allowing analysis of multiple treatments simultaneously. Future analysis of chromatin fractions by these methods may yield better results or cover a different spectrum of the protein landscape. It is noteworthy that in the study presented in chapter 4, different isoforms of several factors (e.g. Rnr4) bound differentially to chromatin after MMS treatment. These specific behaviours for protein isoforms are of great interest to understanding their biological functions and their visualization is optimal via DIGE-based analysis as ICAT and iTRAQ procedures cleave reactive groups, such as phosphates. This validates the methods used here as valuable in uncovering novel functions and identities of chromatin-binding proteins.

5.3 Future Prospects and a Link between DNA Replication and DNA Damage

All biological models strive to both accurately describe a biological process, system or mechanism as well as to uncover non-intuitive insights that may help in predicting network behaviour and suggesting potential experiments. These are both useful for

circumventing the resource intensive approach of step-by-step hypothesis driven "wet-lab" research. A general scheme for biological modeling is to first build a robust and predictive model, make testable predictions and incorporate new data into further iterations. The model of DNA replication initiation presented in this thesis provides a primer for exploring a process that is integral to cell survival and regulated proliferation. While there are many replication factors that were not included in the network framework, the model contains its essential components and faithfully describes how a group of factors interact at various points in the cell cycle to produce the replication forks required to complete duplication of the genome.

Moving forward, additions to the model would potentially involve inclusion of factors that increase the resolution of steps that for the purpose of reducing model complexity, are currently treated as lumped. Modeling the association of GINS (one or more of its component subunits) with the DNA would be an obvious step. This would aid in the distinction between Cdc45 that associates with origins and that which is included in an active CMG complex. Another area that could be explored is the modulation of the total number of potential origins (RC_{Total}) to investigate how having more or less sites of potential pre-RC formation would affect the rates with which proteins interact with one another. This would be well served by including a clear distinction between G_1 and S phase as the model at present (due to the overlap of Cdc6 and Cdc45) provides the potential for pre-RCs to form after the first firing event. Because inhibitory CDK mechanisms have been included in the model, this prevents the firing of such theoretical 'S phase pre-RCs', such that they do not actually contribute to fork formation. It is possible, however that they might fire if they are formed earlier in the cell cycle, before

CDK inhibition plays a role, increasing the overall number of origins. Questions regarding origin usage and efficiency would benefit from this analysis. Due to the methods used to scale the data, the amount of MCM present in the pellet was kept at a conservative amount such that the maximum concentration of MCM Pellet never exceeded the amount of potential origins. Doubling the amount of MCM on the chromatin (and subtracting appropriately from the soluble fraction) would provide excess MCM and insights into how extra MCMs regulate origin firing, particularly the events concerning the breakup of RC4 and the concept of dynamic loading.

A great deal of proteins were identified in Chapter 4 as having a differential affinity for chromatin in response to the DNA-damaging agent MMS. Interesting patterns of regulation even among isoforms of a given protein provide interesting avenues of future research regarding their specific roles in the DNA damage response pathway. While these experiments are at first glance isolated from the DNA replication model, the latter would benefit from exploring the roles of proteins that act in both pathways – DNA replication and checkpoint response. Mec1 and Dbp11 are factors that are intimately linked with both processes. The former acts as a regulator of nucleotide pools upon S phase entry to ensure a normal rate of S phase progression. It is also implicated in the priming of MCM subunit residues for subsequent phosphorylation by DDK (Sheu and Stillman, 2010). These represent its role in a normal, unperturbed cell cycle. Mec1 is also a key checkpoint kinase in the DNA damage and DNA replication checkpoint responses, as described in Chapter 1. Dpb11 mediates the interaction between Sld2 and Sld3, leading to the eventual formation of a stable CMG complex (modeled through the action of Cdc45 in this thesis). Notably, Mec1 is activated by Dpb11 during the checkpoint

response and so these proteins play critical roles in both DNA replication and DNA damage response. Expanding the network of the model to include these factors as well as other relevant checkpoint proteins would permit the dynamic investigation of DNA replication in a cell cycle perturbed by DNA damage-induced arrest. As was the case with highlighting emergent properties of the replication system in the current model, the proposed model would shed light on the non-obvious behaviours of and interactions between all factors included.

5.4 Perspectives on Cancer

5.4.1 Cancer and the Cell Cycle

As modern medicine forges ahead, the scope of targeted and personalized treatment has the multi-faceted disease of cancer in its sights. Decades of work have resulted in great advances in both treatment and prevention. Nevertheless, even more promising technologies are emerging, with the advent of targeted drug delivery systems and personalized treatments. In light of these promising avenues of research and treatment, it is useful to consider some of the fundamental processes that lead to the deregulation of the cell cycle.

A major goal of combating existing cancer is the ability to target cancerous tissues without collaterally harming healthy host cells. Many therapeutics are designed without considering the varying molecular basis of cell cycle deregulation, providing a largely unexplored approach to developing more targeted cures. While a great number of anti-cancer drugs target replication machinery components such as topoisomerase or elements

of the mitotic spindle, the efficacy varies from patient to patient due to the specific molecular etiology.

The DNA damage repair mechanisms that are tasked with ensuring the fidelity of the genome are ripe targets for disrupting the cell cycle on the path to genomic instability and consequent tumorigenesis (Fishel *et al*., 1993; Hanawalt and Sarasin, 1986). Chromosomal damage, improper segregation and an array of genomic aberrations have been implicated in cancer and related ailments such as Werner's syndrome and ataxia telangiectasia (Jeggo *et al*., 1991; Vogelstein *et al*., 1989). It has been shown that many environmental agents that have wide exposure interfere with the G_1/S checkpoint. These render cells susceptible to further genomic instability incurred by known genotoxic agents (Afshari and Barrett, 1993). As reviewed previously in this thesis, these are outcomes normally prevented by cell cycle checkpoints, their disruption therefore having been the subject of investigation for their potential roles in carcinogenesis (Lau and Jiang, 2006; O'Connor and Kohn, 1992; reviewed in Hartwell and Kastan, 1994).

Errors in the control of mitosis have also been implicated in cancerous pathologies. Organization of the spindle is deregulated in murine pancreatic tissue expressing the SV40 large T antigen. This results in chromosomal instability due to improperly segregated chromosomes (Levine *et al*., 1991). The c-*mos* proto-oncogene controlling meiosis is abnormally expressed in tumor cells, an effect caused by polyploidy (Singh and Arlinghaus, 1992). BRCA2-deficient tumors are derived via chromosomal instability implicating the gene in DNA damage repair processes (Venkitaraman, 2002). A role for BRCA2 in regulating mitotic functions has also been documented, leading to spontaneous

cancer development in mice with a defective copy of the gene (Choi *et al*., 2012; Rowley *et al*., 2011).

A correlation between age and susceptibility to cancer has long been established and postulated as existing due to the breakdown through mutation of the mechanisms that ensure proper cellular propagation (reviewed in Nowell, 1976 and Hartwell and Kastan, 1994). Cellular aging itself has been postulated to occur as a result of continued cycles of cell division. Thus the number of cell cycles determines the age of a cell as opposed to chronological time (Hayflick and Moorhead, 1961; Shay and Wright, 2000). A major contributor of this is the decrease in the activity of the enzyme telomerase as cells age. This enzyme aids in the replication of the 3' end of the lagging strand at the end of chromosomes. Thus, as cells age and lose telomerase function, they eventually reach a critical size at which point the cell undergoes an irreversible arrest. Termed "cellular senescence", it is suggested to be a natural method for preventing cancer as the arrest generally occurs before the chromosomes accumulate enough mutations to render them cancerous (Olovnikov, 1973; Shay *et al*., 2001). Consistent with this, the loss of telomeric sequences in *S. cerevisiae* was found to cause senescence and cell death (Lundblad and Szostak, 1989). In contrast, the maintenance of high levels of telomerase has been found in cancerous cells leading to the hypothesis that they are made immortal due to the lack of a senescence arrest. Because this represents a frequent step in oncogenesis, the targeting of telomerase is a potent approach for combating cancer (Holt and Shay, 1999; Shay, 1995; Shay and Wright, 1996; Wright and Shay 2001;).

5.4.2 DNA Replication and Cancer

An intermediate stage between natural cell proliferation and a neoplastic state is termed dysplasia (De Vita *et al*., 1993). Despite unique morphological and molecular differences in such cells, methods for detecting the symptoms of such changes have suffered from a paucity of detectable markers. Existing ones often have functionally redundant roles thus limiting the detection of cancer arising as a result of varying cellular defects. Widely-used biomarkers for cancer include PCNA and Ki-67, however they have demonstrated low efficacy in detecting brain tumors, meningiomas and tumors of the cervix (reviewed in Duncker and Semple, 2004). As one would expect, proliferating cells are those that undergo a replicative cycle and thus for most tumors, viable biomarkers are those that act in the initiation of DNA replication (Korkolopoulou *et al*., 2002 and 2005; Murphy *et al*., 2005). Proteins considered in the model described in this thesis are, therefore good candidates as cancer biomarkers. Orc6, as an example has been shown in two independent studies to be overexpressed in colorectal cancer tumors (Gavin *et al*., 2008; Xi *et al*. 2008).

Cdc6 levels were shown to be elevated in samples of cervical carcinoma (linked to human papilloma virus, HPV infection) compared to normal tissue (Williams *et al*., 1998). This contrast was significantly greater for Cdc6 than for the aforementioned Ki-67 and PCNA, a proof of principle for the use of replication proteins in detecting cancer cells. Robbles *et al*. (2002) demonstrated aberrant expression of Cdc6 in malignant prostate cancer. Staining of neuroepithelial samples with α-Cdc6 antibody showed a correlation between tumorous cells in the brain and detectable Cdc6 levels.

Subunits of the Mcm2-7 complex have also been shown to be effective predictors of neoplasia. The staining of tumorigenic tissue samples with α-Mcm7 (Hiraiwa *et al*., 1997), α-Mcm5 (Williams *et al*., 1998) and α-Mcm2 (Todorov *et al*., 1998) showed vast increases in their levels compared to normal tissues, again outperforming Ki67 and PCNA. Freeman *et al*. (1999) showed that the degree of staining with α-Mcm2 and α-Mcm5 indicated the severity of dysplasia, demonstrating a quantitative function for these proteins in preventative diagnostics. Mcm2 has been shown to be of similar use in diagnosing a variety of cancers such as those found in dendritic tissue, lung tissue, renal cells, esopageal squamous cells and meningiomas. The same is true for Mcm5 with respect to bladder and ureter-derived malignancies (Ishimi *et al*., 2003; reviewed in Duncker and Semple, 2004).

As discussed previously, the Dbf4-Cdc7 kinase complex is an essential activator of DNA replication and both components have been evaluated as cancer biomarkers. Overexpression of Dbf4, which is limiting (Tanaka *et al*., 2011) and Cdc7 has been linked to cancer. In yeast, overexpression of DDK increases the rate of mutation in cells exposed to a genotoxic agent (Sclafani *et al*., 1988). Thus, acting as a mutagenic catalyst, it was proposed to increase the probability of malignancy at high levels (Sclafani and Jackson, 1994). The human CDC7 protein is overexpressed in certain tumor cell lines as well as in lung and breast cancer tissues (Bonte *et al*., 2008; Hess *et al*., 1998). Similar results have been found for the human homologue of Dbf4, ASK in cancer cell lines as well as tumor samples (discussed in Sclafani *et al*., 2000).

5.4.3 Modeling of Cancer

As discussed in Chapter 3, mathematical models have the potential to uncover the fundamental mechanisms that cellular machines employ. Additionally, unknown aspects of the network are often highlighted and new thoroughfares for investigation are created. Following an explosion of genomic, proteomic and metabolomic data and novel analysis techniques in the past few decades, researchers must now reverse-engineer the processes that underlie cellular function (Hollywood *et al.* 2006; Jares, 2006). Processing the vast amount of information is made easier by the use of ODE-based models, such as the one presented in this dissertation. Because there are fundamental differences in the various types of cancer, specialized treatments must be developed with personalized treatments. Predictive models change the landscape of cancer therapy as they provide a tool with which to study the responses of the cell with minimal experimental cost. A large number of ODE-based mathematical models have thus been developed to study the causes of malignancy and resistance to therapeutics. This includes models of the basic cellular processes in normal cells as well as modeling of cancerous cells (e.g. Charlebois *et al.*, 2011; Cox *et al.*, 1980; Heng *et al.*, 2006; Spencer *et al.*, 2004; Stringer *et al.*, 2005; Itani *et al.*, 2010; reviewed in Materi and Wishart, 2007). Importantly they enable the prediction of global changes to the cell, particularly the side effects of a given treatment on a molecular level. With the increasing number of models and their careful integration, the manner in which science and medicine approach the treatment and prevention of cancer is being revolutionized.

References

1. Aebersold, R. & Mann, M. Mass spectrometry-based proteomics. *Nature* 422, 198-207 (2003).

2. Afshari, C. A. & Barrett, J. C. Cell cycle controls: potential targets for chemical carcinogens? *Environ. Health Perspect.* 101 Suppl 5, 9-14 (1993).

3. Alarcon, T. & Tindall, M. J. Modelling cell growth and its modulation of the G1/S transition. *Bull. Math. Biol.* 69, 197-214 (2007).

4. Alberghina, L., Rossi, R. L., Querin, L., Wanke, V. & Vanoni, M. A cell sizer network involving Cln3 and Far1 controls entrance into S phase in the mitotic cycle of budding yeast. *J. Cell Biol.* 167, 433-443 (2004).

5. Alcasabas, A. A. *et al.* Mrc1 transduces signals of DNA replication stress to activate Rad53. *Nat. Cell Biol.* 3, 958-965 (2001).

6. Alzate, O. in *Neuroproteomics* (CRC, 2009).

7. Amon, A. The spindle checkpoint. *Curr. Opin. Genet. Dev.* 9, 69-75 (1999).

8. Andersen, J. S. & Mann, M. Organellar proteomics: turning inventories into insights. *EMBO Rep.* 7, 874-879 (2006).

9. Aparicio, O., Geisberg, J. V. & Struhl, K. Chromatin immunoprecipitation for determining the association of proteins with specific genomic sequences in vivo. *Curr. Protoc. Cell. Biol.* Chapter 17, Unit 17.7 (2004).

10. Aparicio, O. M., Weinstein, D. M. & Bell, S. P. Components and dynamics of DNA replication complexes in S. cerevisiae: redistribution of MCM proteins and Cdc45p during S phase. *Cell* 91, 59-69 (1997).

11. Arias, E. E. & Walter, J. C. Strength in numbers: preventing rereplication via multiple mechanisms in eukaryotic cells. *Genes Dev.* 21, 497-518 (2007).

12. Azzam, R. *et al.* Phosphorylation by cyclin B-Cdk underlies release of mitotic exit activator Cdc14 from the nucleolus. *Science* 305, 516-519 (2004).

13. Barberis, M. & Klipp, E. Insights into the network controlling the G1/S transition in budding yeast. *Genome Inform.* 18, 85-99 (2007).

14. Barberis, M., Klipp, E., Vanoni, M. & Alberghina, L. Cell size at S phase initiation: an emergent property of the G1/S network. *PLoS Comput. Biol.* 3, e64 (2007).

15. Barik, D., Baumann, W. T., Paul, M. R., Novak, B. & Tyson, J. J. A model of yeast cell-cycle regulation based on multisite phosphorylation. *Mol. Syst. Biol.* 6, 405 (2010).

16. Bauer, A. & Kuster, B. Affinity purification–mass spectrometry. *European Journal of Biochemistry* 270, 570-578 (2003).

17. Beck, C. & Von Meyenburg, H. K. Enzyme pattern and aerobic growth of Saccharomyces cerevisiae under various degrees of glucose limitation. *J. Bacteriol.* 96, 479 (1968).

18. Begley, T. J., Rosenbach, A. S., Ideker, T. & Samson, L. D. Damage recovery pathways in Saccharomyces cerevisiae revealed by genomic phenotyping and interactome mapping. *Mol. Cancer. Res.* 1, 103-112 (2002).

19. Bell, S. P. & Dutta, A. DNA replication in eukaryotic cells. *Annu. Rev. Biochem.* 71, 333-374 (2002).

20. Bell, S. P. & Stillman, B. ATP-dependent recognition of eukaryotic origins of DNA replication by a multiprotein complex. *Nature* 357, 128-134 (1992).

21. Bellí, G., Garí, E., Piedrafita, L., Aldea, M. & Herrero, E. An activator/repressor dual system allows tight tetracycline-regulated gene expression in budding yeast. *Nucleic Acids Res.* 26, 942-947 (1998).

22. Berens, T. J. & Toczyski, D. P. Co-localization of Mec1 and Mrc1 is sufficient for Rad53 phosphorylation in vivo. *Mol. Biol. Cell* (2012).

23. Bernstein, B. E. & Schreiber, S. L. Global approaches to chromatin. *Chem. Biol.* 9, 1167-1173 (2002).

24. Bicknell, L. S. *et al.* Mutations in the pre-replication complex cause Meier-Gorlin syndrome. *Nat. Genet.* 43, 356-359 (2011).

25. Birrell, G. W. *et al.* Transcriptional response of Saccharomyces cerevisiae to DNA-damaging agents does not identify the genes that protect against these agents. *Proc. Natl. Acad. Sci. U. S. A.* 99, 8778-8783 (2002).

26. Blow, J. J., Ge, X. Q. & Jackson, D. A. How dormant origins promote complete genome replication. *Trends Biochem. Sci.* 36, 405-414 (2011).

27. Boeke, J. D., Garfinkel, D. J., Styles, C. A. & Fink, G. R. Ty elements transpose through an RNA intermediate. *Cell* 40, 491-500 (1985).

28. Bonte, D. *et al.* Cdc7-Dbf4 kinase overexpression in multiple cancers and tumor cell lines is correlated with p53 inactivation. *Neoplasia* 10, 920-931 (2008).

29. Borde, V. & Cobb, J. Double functions for the Mre11 complex during DNA double-strand break repair and replication. *Int. J. Biochem. Cell Biol.* 41, 1249-1253 (2009).

30. Bousset, K. & Diffley, J. F. The Cdc7 protein kinase is required for origin firing during S phase. *Genes Dev.* 12, 480-490 (1998).

31. Bowers, J. L., Randell, J. C., Chen, S. & Bell, S. P. ATP hydrolysis by ORC catalyzes reiterative Mcm2-7 assembly at a defined origin of replication. *Mol. Cell* 16, 967-978 (2004).

32. Branzei, D. & Foiani, M. The checkpoint response to replication stress. *DNA Repair (Amst)* 8, 1038-1046 (2009).

33. Bray, D. Protein molecules as computational elements in living cells. *Nature* 376, 307-312 (1995).

34. Breeden, L. L. Alpha-factor synchronization of budding yeast. *Methods Enzymol.* 283, 332-341 (1997).

35. Brown, P. O. & Botstein, D. Exploring the new world of the genome with DNA microarrays. *Nat. Genet.* 21, 33-37 (1999).

36. Bruck, I. & Kaplan, D. L. Origin Single-stranded DNA Releases Sld3 Protein from the Mcm2-7 Complex, Allowing the GINS Tetramer to Bind the Mcm2-7 Complex. *J. Biol. Chem.* 286, 18602-18613 (2011).

37. Bruck, I. & Kaplan, D. L. GINS and Sld3 compete with one another for Mcm2-7 and Cdc45 binding. *J. Biol. Chem.* 286, 14157-14167 (2011).

38. Brummer, A., Salazar, C., Zinzalla, V., Alberghina, L. & Hofer, T. Mathematical modelling of DNA replication reveals a trade-off between coherence of origin activation and robustness against rereplication. *PLoS Comput. Biol.* 6, e1000783 (2010).

39. Bueno, A. & Russell, P. Dual functions of CDC6: a yeast protein required for DNA replication also inhibits nuclear division. *EMBO J.* 11, 2167 (1992).

40. Burton, J. L. & Solomon, M. J. D box and KEN box motifs in budding yeast Hsl1p are required for APC-mediated degradation and direct binding to Cdc20p and Cdh1p. *Genes Dev.* 15, 2381-2395 (2001).

41. Calzada, A., Sacristan, M., Sanchez, E. & Bueno, A. Cdc6 cooperates with Sic1 and Hct1 to inactivate mitotic cyclin-dependent kinases. *Nature* 412, 355-358 (2001).

42. Candiano, G. *et al.* Blue silver: A very sensitive colloidal Coomassie G-250 staining for proteome analysis. *Electrophoresis* 25, 1327-1333 (2004).

43. Cann, K. L. & Hicks, G. G. Regulation of the cellular DNA double-strand break response. *Biochem. Cell Biol.* 85, 663-674 (2007).

44. Cao, J., Qi, X. & Zhao, H. Modeling gene regulation networks using ordinary differential equations. *Methods Mol. Biol.* 802, 185-197 (2012).

45. Caudron, F. & Barral, Y. Septins and the lateral compartmentalization of eukaryotic membranes. *Dev. Cell.* 16, 493-506 (2009).

46. Cereghino, J. L. & Cregg, J. M. Heterologous protein expression in the methylotrophic yeast Pichia pastoris. *FEMS Microbiol. Rev.* 24, 45-66 (2000).

47. Chabes, A. & Thelander, L. DNA building blocks at the foundation of better survival. *Cell. Cycle* 2, 171-173 (2003).

48. Chang, F. & Peter, M. Yeasts make their mark. *Nat. Cell Biol.* 5, 294-299 (2003).

49. Charlebois, D. A., Intosalmi, J., Fraser, D. & Kærn, M. An Algorithm for the Stochastic Simulation of Gene Expression and Heterogeneous Population Dynamics. *Arxiv preprint arXiv:1110.6469* (2011).

50. Charlebois, D. A., Abdennur, N. & Kaern, M. Gene expression noise facilitates adaptation and drug resistance independently of mutation. *Phys. Rev. Lett.* 107, 218101 (2011).

51. Chassagnole, C. *et al*. Using a mammalian cell cycle simulation to interpret differential kinase inhibition in anti-tumour pharmaceutical development. *BioSystems* 83, 91-97 (2006).

52. Chen, K. C., Wang, T. Y., Tseng, H. H., Huang, C. Y. F. & Kao, C. Y. A stochastic differential equation model for quantifying transcriptional regulatory network in Saccharomyces cerevisiae. *Bioinformatics* 21, 2883-2890 (2005).

53. Chen, K. C. *et al*. Integrative analysis of cell cycle control in budding yeast. *Mol. Biol. Cell* 15, 3841-3862 (2004).

54. Chen, K. C. *et al*. Kinetic analysis of a molecular model of the budding yeast cell cycle. *Mol. Biol. Cell* 11, 369-391 (2000).

55. Chen, S. & Bell, S. P. CDK prevents Mcm2-7 helicase loading by inhibiting Cdt1 interaction with Orc6. *Genes Dev.* 25, 363-372 (2011).

56. Chen, S., de Vries, M. A. & Bell, S. P. Orc6 is required for dynamic recruitment of Cdt1 during repeated Mcm2-7 loading. *Genes Dev.* 21, 2897-2907 (2007).

57. Cheng, Z., McConkey, B. J. & Glick, B. R. Proteomic studies of plant-bacterial interactions. *Soil Biol. Biochem.* 42, 1673-1684 (2010).

58. Cheng, L., Collyer, T. & Hardy, C. F. Cell cycle regulation of DNA replication initiator factor Dbf4p. *Mol. Cell. Biol.* 19, 4270-4278 (1999).

59. Cho, W. H., Lee, Y. J., Kong, S. I., Hurwitz, J. & Lee, J. K. CDC7 kinase phosphorylates serine residues adjacent to acidic amino acids in the minichromosome maintenance 2 protein. *Proceedings of the National Academy of Sciences* 103, 11521 (2006).

60. Cho, R. J. *et al.* A genome-wide transcriptional analysis of the mitotic cell cycle. *Mol. Cell* 2, 65-73 (1998).

61. Choi, E. *et al.* BRCA2 Fine-Tunes the Spindle Assembly Checkpoint through Reinforcement of BubR1 Acetylation. *Dev. Cell.* 22, 295-308 (2012).

62. Chu, G. Double strand break repair. *J. Biol. Chem.* 272, 24097 (1997).

63. Chu, D. S. *et al.* Sperm chromatin proteomics identifies evolutionarily conserved fertility factors. *Nature* 443, 101-105 (2006).

64. Ciejek, E. & Thorner, J. Recovery of S. cerevisiae a cells from G1 arrest by [alpha] factor pheromone requires endopeptidase action. *Cell* 18, 623-635 (1979).

65. Ciosk, R. *et al.* An ESP1/PDS1 complex regulates loss of sister chromatid cohesion at the metaphase to anaphase transition in yeast. *Cell* 93, 1067-1076 (1998).

66. Cobb, J. A. *et al.* Replisome instability, fork collapse, and gross chromosomal rearrangements arise synergistically from Mec1 kinase and RecQ helicase mutations. *Genes Dev.* 19, 3055-3069 (2005).

67. Cosma, M. P., Panizza, S. & Nasmyth, K. Cdk1 triggers association of RNA polymerase to cell cycle promoters only after recruitment of the mediator by SBF. *Mol. Cell* 7, 1213-1220 (2001).

68. Cox, E. B., Woodbury, M. A. & Myers, L. E. A new model for tumor growth analysis based on a postulated inhibitory substance. *Computers and Biomedical Research* 13, 437-445 (1980).

69. Craven, R. J., Greenwell, P. W., Dominska, M. & Petes, T. D. Regulation of genome stability by TEL1 and MEC1, yeast homologs of the mammalian ATM and ATR genes. *Genetics* 161, 493-507 (2002).

70. Cregg, J. M. *et al.* Expression in the yeast Pichia pastoris. *Methods Enzymol.* 463, 169-189 (2009).

71. Cross, F. R. Two redundant oscillatory mechanisms in the yeast cell cycle. *Dev. Cell*. 4, 741-752 (2003).

72. Da-Silva, L. F. & Duncker, B. P. ORC function in late G1: maintaining the license for DNA replication. *Cell. Cycle* 6, 128-130 (2007).

73. Davey, M. J., Indiani, C. & O'Donnell, M. Reconstitution of the Mcm2-7p heterohexamer, subunit arrangement, and ATP site architecture. *J. Biol. Chem*. 278, 4491-4499 (2003).

74. de Bruin, R. A., McDonald, W. H., Kalashnikova, T. I., Yates, J.,3rd & Wittenberg, C. Cln3 activates G1-specific transcription via phosphorylation of the SBF bound repressor Whi5. *Cell* 117, 887-898 (2004).

75. De Jong, H. Modeling and simulation of genetic regulatory systems: a literature review. *Journal of computational biology* 9, 67-103 (2002).

76. de Moura, A. P., Retkute, R., Hawkins, M. & Nieduszynski, C. A. Mathematical modelling of whole chromosome replication. *Nucleic Acids Res*. 38, 5623-5633 (2010).

77. De Piccoli, G. *et al*. Replisome Stability at Defective DNA Replication Forks Is Independent of S Phase Checkpoint Kinases. *Mol. Cell* (2012).

78. DeRisi, J. L., Iyer, V. R. & Brown, P. O. Exploring the metabolic and genetic control of gene expression on a genomic scale. *Science* 278, 680 (1997).

79. Deshpande, A. M. & Newlon, C. S. DNA replication fork pause sites dependent on transcription. *Science* 272, 1030-1033 (1996).

80. Detweiler, C. S. & Li, J. J. Cdc6p establishes and maintains a state of replication competence during G1 phase. *J. Cell. Sci*. 110 (Pt 6), 753-763 (1997).

81. Devault, A., Gueydon, E. & Schwob, E. Interplay between S-cyclin-dependent kinase and Dbf4-dependent kinase in controlling DNA replication through phosphorylation of yeast Mcm4 N-terminal domain. *Mol. Biol. Cell* 19, 2267-2277 (2008).

82. Dickerson, R. E. The DNA helix and how it is read. *Sci. Am*. 249, 94-98 (1983).

83. Diller, J. D. & Raghuraman, M. K. Eukaryotic replication origins: control in space and time. *Trends Biochem. Sci*. 19, 320-325 (1994).

84. Dimitrova, D. S. & Gilbert, D. M. The spatial position and replication timing of chromosomal domains are both established in early G1 phase. *Mol. Cell* 4, 983-993 (1999).

85. Dirick, L., Bohm, T. & Nasmyth, K. Roles and regulation of Cln-Cdc28 kinases at the start of the cell cycle of Saccharomyces cerevisiae. *EMBO J*. 14, 4803-4813 (1995).

86. Dirick, L. & Nasmyth, K. Positive feedback in the activation of G1 cyclins in yeast. *Nature* 351, 754-757 (1991).

87. Donaldson, A. D., Fangman, W. L. & Brewer, B. J. Cdc7 is required throughout the yeast S phasetoactivatereplication origins. *Genes Dev*. 12, 491-501 (1998).

88. Donovan, S., Harwood, J., Drury, L. S. & Diffley, J. F. Cdc6p-dependent loading of Mcm proteins onto pre-replicative chromatin in budding yeast. *Proc. Natl. Acad. Sci. U. S. A*. 94, 5611-5616 (1997).

89. Dowell, S. J., Romanowski, P. & Diffley, J. F. Interaction of Dbf4, the Cdc7 protein kinase regulatory subunit, with yeast replication origins in vivo. *Science* 265, 1243-1246 (1994).

90. Downey, M. *et al*. A genome-wide screen identifies the evolutionarily conserved KEOPS complex as a telomere regulator. *Cell* 124, 1155-1168 (2006).

91. Dreger, M. Proteome analysis at the level of subcellular structures. *Eur. J. Biochem*. 270, 589-599 (2003).

92. Drury, L. S., Perkins, G. & Diffley, J. F. The cyclin-dependent kinase Cdc28p regulates distinct modes of Cdc6p proteolysis during the budding yeast cell cycle. *Curr. Biol*. 10, 231-240 (2000).

93. Drury, L. S., Perkins, G. & Diffley, J. F. The Cdc4/34/53 pathway targets Cdc6p for proteolysis in budding yeast. *EMBO J*. 16, 5966-5976 (1997).

94. Duncan, R. & McConkey, E. How many proteins are there in a typical mammalian cell? *Clin. Chem*. 28, 749 (1982).

95. Duncker, B. P., Shimada, K., Tsai-Pflugfelder, M., Pasero, P. & Gasser, S. M. An N-terminal domain of Dbf4p mediates interaction with both origin recognition complex (ORC) and Rad53p and can deregulate late origin firing. *Proc. Natl. Acad. Sci. U. S. A*. 99, 16087-16092 (2002).

96. Dutta, A. & Bell, S. P. Initiation of DNA replication in eukaryotic cells. *Annu. Rev. Cell Dev. Biol*. 13, 293-332 (1997).

97. Edwards, M. C. *et al*. MCM2–7 Complexes Bind Chromatin in a Distributed Pattern Surrounding the Origin Recognition Complex inXenopus Egg Extracts. *J. Biol. Chem*. 277, 33049-33057 (2002).

98. Einhauer, A. & Jungbauer, A. The FLAG (TM) peptide, a versatile fusion tag for the purification of recombinant proteins. *J. Biochem. Biophys. Methods* 49, 455-465 (2001).

99. El-Bayoumy, K. *et al*. The effect of selenium enrichment on baker's yeast proteome. *J. Proteomics* 75, 1018-1030 (2012).

100. Elledge, S. J. Cell cycle checkpoints: preventing an identity crisis. *Science* 274, 1664-1672 (1996).

101. Elledge, S. J., Zhou, Z., Allen, J. B. & Navas, T. A. DNA damage and cell cycle regulation of ribonucleotide reductase. *Bioessays* 15, 333-339 (1993).

102. Elowitz, M. B. & Leibler, S. A synthetic oscillatory network of transcriptional regulators. *Nature* 403, 335-338 (2000).

103. Elsasser, S., Chi, Y., Yang, P. & Campbell, J. L. Phosphorylation controls timing of Cdc6p destruction: A biochemical analysis. *Mol. Biol. Cell* 10, 3263-3277 (1999).

104. Emery, A. & Nenarokomov, A. V. Optimal experiment design. *Measurement Science and Technology* 9, 864 (1998).

105. Evrin, C. *et al*. A double-hexameric MCM2-7 complex is loaded onto origin DNA during licensing of eukaryotic DNA replication. *Proc. Natl. Acad. Sci. U. S. A.* 106, 20240-20245 (2009).

106. Eytan, E., Moshe, Y., Braunstein, I. & Hershko, A. Roles of the anaphase-promoting complex/cyclosome and of its activator Cdc20 in functional substrate binding. *Proc. Natl. Acad. Sci. U. S. A.* 103, 2081-2086 (2006).

107. Falcon, A. A., Rios, N. & Aris, J. P. 2-Micron Circle Plasmids do Not Reduce Yeast Life Span. *FEMS Microbiol. Lett.* 250, 245-251 (2005).

108. Fantes, P. & Nurse, P. Control of cell size at division in fission yeast by a growth-modulated size control over nuclear division. *Exp. Cell Res.* 107, 377-386 (1977).

109. Feng, W. *et al*. Genomic mapping of single-stranded DNA in hydroxyurea-challenged yeasts identifies origins of replication. *Nat. Cell Biol.* 8, 148-155 (2006).

110. Ferreira, M. F., Santocanale, C., Drury, L. S. & Diffley, J. F. Dbf4p, an essential S phase-promoting factor, is targeted for degradation by the anaphase-promoting complex. *Mol. Cell. Biol.* 20, 242-248 (2000).

111. Field, J. *et al*. Purification of a RAS-responsive adenylyl cyclase complex from Saccharomyces cerevisiae by use of an epitope addition method. *Mol. Cell. Biol.* 8, 2159 (1988).

112. Fishel, R. *et al*. The human mutator gene homolog MSH2 and its association with hereditary nonpolyposis colon cancer. *Cell* 75, 1027-1038 (1993).

113. Fitch, I. *et al*. Characterization of four B-type cyclin genes of the budding yeast Saccharomyces cerevisiae. *Mol. Biol. Cell* 3, 805-818 (1992).

114. Forner, F., Foster, L. J., Campanaro, S., Valle, G. & Mann, M. Quantitative proteomic comparison of rat mitochondria from muscle, heart, and liver. *Mol. Cell. Proteomics* 5, 608-619 (2006).

115. Forsburg, S. L. The MCM helicase: linking checkpoints to the replication fork. *Biochem. Soc. Trans*. 36, 114-119 (2008).

116. Forsburg, S. L. Eukaryotic MCM proteins: beyond replication initiation. *Microbiol. Mol. Biol. Rev*. 68, 109-131 (2004).

117. Francis, L. I., Randell, J. C., Takara, T. J., Uchima, L. & Bell, S. P. Incorporation into the prereplicative complex activates the Mcm2-7 helicase for Cdc7-Dbf4 phosphorylation. *Genes Dev*. 23, 643-654 (2009).

118. Francis, M. R. & Fertig, E. J. Quantifying the dynamics of coupled networks of switches and oscillators. *PLoS One* 7, e29497 (2012).

119. Franke, J., Reimann, B., Hartmann, E., Köhler, M. & Wiedmann, B. Evidence for a nuclear passage of nascent polypeptide-associated complex subunits in yeast. *J. Cell. Sci*. 114, 2641-2648 (2001).

120. Freeman, A. *et al*. Minichromosome maintenance proteins as biological markers of dysplasia and malignancy. *Clin. Cancer Res*. 5, 2121-2132 (1999).

121. Freifelder, D. Bud position in Saccharomyces cerevisiae. *J. Bacteriol*. 80, 567 (1960).

122. Friedel, A. M., Pike, B. L. & Gasser, S. M. ATR/Mec1: coordinating fork stability and repair. *Curr. Opin. Cell Biol*. 21, 237-244 (2009).

123. Friedman, K. L. *et al*. Multiple determinants controlling activation of yeast replication origins late in S phase. *Genes Dev*. 10, 1595-1607 (1996).

124. Fu, Y. V. *et al*. Selective bypass of a lagging strand roadblock by the eukaryotic replicative DNA helicase. *Cell* 146, 931-941 (2011).

125. Fu, X., Ng, C., Feng, D. & Liang, C. Cdc48p is required for the cell cycle commitment point at Start via degradation of the G1-CDK inhibitor Far1p. *J. Cell Biol*. 163, 21-26 (2003).

126. Furuya, K., Poitelea, M., Guo, L., Caspari, T. & Carr, A. M. Chk1 activation requires Rad9 S/TQ-site phosphorylation to promote association with C-terminal BRCT domains of Rad4TOPBP1. *Genes Dev*. 18, 1154-1164 (2004).

127. Futcher, A. Analysis of the cell cycle in S. cerevisiae. (1993).

128. Futcher, B. Cell cycle synchronization. *Methods Cell Sci*. 21, 79-86 (1999).

129. Gadkar, K. G., Gunawan, R. & Doyle, F. J.,3rd. Iterative approach to model identification of biological networks. *BMC Bioinformatics* 6, 155 (2005).

130. Gambus, A. *et al*. GINS maintains association of Cdc45 with MCM in replisome progression complexes at eukaryotic DNA replication forks. *Nat. Cell Biol*. 8, 358-366 (2006).

131. Gardner, R., Putnam, C. W. & Weinert, T. RAD53, DUN1 and PDS1 define two parallel G2/M checkpoint pathways in budding yeast. *EMBO J*. 18, 3173-3185 (1999).

132. Garg, P. & Burgers, P. M. DNA polymerases that propagate the eukaryotic DNA replication fork. *Crit. Rev. Biochem. Mol. Biol*. 40, 115-128 (2005).

133. Gasch, A. P. *et al*. Genomic expression responses to DNA-damaging agents and the regulatory role of the yeast ATR homolog Mec1p. *Mol. Biol. Cell* 12, 2987-3003 (2001).

134. Gavin, A. C. *et al*. Functional organization of the yeast proteome by systematic analysis of protein complexes. *Nature* 415, 141-147 (2002).

135. Gavin, E. J., Song, B., Wang, Y., Xi, Y. & Ju, J. Reduction of Orc6 expression sensitizes human colon cancer cells to 5-fluorouracil and cisplatin. *PLoS One* 3, e4054 (2008).

136. Ge, X. Q., Jackson, D. A. & Blow, J. J. Dormant origins licensed by excess Mcm2–7 are required for human cells to survive replicative stress. *Genes Dev*. 21, 3331 (2007).

137. Gerard, C. & Goldbeter, A. From simple to complex patterns of oscillatory behavior in a model for the mammalian cell cycle containing multiple oscillatory circuits. *Chaos* 20, 045109 (2010).

138. Ghaemmaghami, S. *et al*. Global analysis of protein expression in yeast. *Nature* 425, 737-741 (2003).

139. Ghavidel, A. *et al*. Impaired tRNA nuclear export links DNA damage and cell-cycle checkpoint. *Cell* 131, 915-926 (2007).

140. Giaever, G. *et al*. Functional profiling of the Saccharomyces cerevisiae genome. *Nature* 418, 387-391 (2002).

141. Giannattasio, M., Lazzaro, F., Plevani, P. & Muzi-Falconi, M. The DNA damage checkpoint response requires histone H2B ubiquitination by Rad6-Bre1 and H3 methylation by Dot1. *J. Biol. Chem.* 280, 9879-9886 (2005).

142. Gibson, D. G., Bell, S. P. & Aparicio, O. M. Cell cycle execution point analysis of ORC function and characterization of the checkpoint response to ORC inactivation in Saccharomyces cerevisiae. *Genes Cells* 11, 557-573 (2006).

143. Gietz, R. D. & Woods, R. A. Transformation of yeast by lithium acetate/single-stranded carrier DNA/polyethylene glycol method. *Methods Enzymol.* 350, 87-96 (2002).

144. Gilbert, C. S., Green, C. M. & Lowndes, N. F. Budding yeast Rad9 is an ATP-dependent Rad53 activating machine. *Mol. Cell* 8, 129-136 (2001).

145. Glotzer, M. The molecular requirements for cytokinesis. *Science* 307, 1735-1739 (2005).

146. Glotzer, M., Murray, A. W. & Kirschner, M. W. Cyclin is degraded by the ubiquitin pathway. *Nature* 349, 132-138 (1991).

147. Goffeau, A. *et al.* Life with 6000 genes. *Science* 274, 546, 563-7 (1996).

148. Goldar, A., Marsolier-Kergoat, M. C. & Hyrien, O. Universal temporal profile of replication origin activation in eukaryotes. *PLoS One* 4, e5899 (2009).

149. Goldbeter, A., Berridge, M. & Cambridge University Press. in *Biochemical oscillations and cellular rhythms: the molecular bases of periodic and chaotic behaviour* (Cambridge university press New York:, 1996).

150. Goldbeter, A. A minimal cascade model for the mitotic oscillator involving cyclin and cdc2 kinase. *Proc. Natl. Acad. Sci. U. S. A.* 88, 9107-9111 (1991).

151. Gonzalez, M. A., Tachibana, K. E., Laskey, R. A. & Coleman, N. Control of DNA replication and its potential clinical exploitation. *Nat. Rev. Cancer.* 5, 135-141 (2005).

152. Granvogl, B., Ploscher, M. & Eichacker, L. A. Sample preparation by in-gel digestion for mass spectrometry-based proteomics. *Anal. Bioanal Chem.* 389, 991-1002 (2007).

153. Green, B. M. & Li, J. J. Loss of rereplication control in Saccharomyces cerevisiae results in extensive DNA damage. *Mol. Biol. Cell* 16, 421-432 (2005).

154. Green, B. M., Morreale, R. J., Ozaydin, B., Derisi, J. L. & Li, J. J. Genome-wide mapping of DNA synthesis in Saccharomyces cerevisiae reveals that mechanisms preventing reinitiation of DNA replication are not redundant. *Mol. Biol. Cell* 17, 2401-2414 (2006).

155. Guthrie, C. & Fink, G. R. in *Guide to yeast genetics and molecular and cell biology* (Academic Pr, 2002).

156. Gygi, S. P. *et al*. Quantitative analysis of complex protein mixtures using isotope-coded affinity tags. *Nat. Biotechnol*. 17, 994-999 (1999).

157. Haase, S. B. & Lew, D. J. Flow cytometric analysis of DNA content in budding yeast. *Meth. Enzymol*. 283, 322-332 (1997).

158. Hadwiger, J. A., Wittenberg, C., Richardson, H. E., de Barros Lopes, M. & Reed, S. I. A family of cyclin homologs that control the G1 phase in yeast. *Proc. Natl. Acad. Sci. U. S. A*. 86, 6255-6259 (1989).

159. Hakem, R. DNA-damage repair; the good, the bad, and the ugly. *EMBO J*. 27, 589-605 (2008).

160. Hanawalt, P. C. & Sarasin, A. Cancer-prone hereditary diseases with DNA processing abnormalities. *Trends in genetics* 2, 124-129 (1986).

161. Hanway, D. *et al*. Previously uncharacterized genes in the UV- and MMS-induced DNA damage response in yeast. *Proc. Natl. Acad. Sci. U. S. A*. 99, 10605-10610 (2002).

162. Hardy, C. F., Dryga, O., Seematter, S., Pahl, P. M. & Sclafani, R. A. mcm5/cdc46-bob1 bypasses the requirement for the S phase activator Cdc7p. *Proc. Natl. Acad. Sci. U. S. A*. 94, 3151-3155 (1997).

163. Harrison, J. C. & Haber, J. E. Surviving the breakup: the DNA damage checkpoint. *Annu. Rev. Genet*. 40, 209-235 (2006).

164. Hartwell, L. H., Hopfield, J. J., Leibler, S. & Murray, A. W. From molecular to modular cell biology. *Nature* 402 (1999).

165. Hartwell, L. H., Culotti, J., Pringle, J. R. & Reid, B. J. Genetic control of the cell division cycle in yeast. *Science* 183, 46-51 (1974).

166. Hartwell, L. H., Culotti, J. & Reid, B. Genetic control of the cell-division cycle in yeast. I. Detection of mutants. *Proc. Natl. Acad. Sci. U. S. A*. 66, 352-359 (1970).

167. Hartwell, L. H. & Kastan, M. B. Cell cycle control and cancer. *Science* 266, 1821-1828 (1994).

168. Hartwell, L. H. & Weinert, T. A. Checkpoints: controls that ensure the order of cell cycle events. *Science* 246, 629-634 (1989).

169. HAYFLICK, L. & MOORHEAD, P. S. The serial cultivation of human diploid cell strains. *Exp. Cell Res*. 25, 585-621 (1961).

170. Heath, I. B. Variant mitoses in lower eukaryotes: indicators of the evolution of mitosis. *Int. Rev. Cytol.* 64, 1-80 (1980).

171. Heller, R. C. *et al.* Eukaryotic origin-dependent DNA replication in vitro reveals sequential action of DDK and S-CDK kinases. *Cell* 146, 80-91 (2011).

172. Henchoz, S. *et al.* Phosphorylation- and ubiquitin-dependent degradation of the cyclin-dependent kinase inhibitor Far1p in budding yeast. *Genes Dev.* 11, 3046-3060 (1997).

173. Hendrickson, C., Meyn, M. A.,3rd, Morabito, L. & Holloway, S. L. The KEN box regulates Clb2 proteolysis in G1 and at the metaphase-to-anaphase transition. *Curr. Biol.* 11, 1781-1787 (2001).

174. Heng, H. H. Q. *et al.* Stochastic cancer progression driven by non–clonal chromosome aberrations. *J. Cell. Physiol.* 208, 461-472 (2006).

175. Herskowitz, I. Life cycle of the budding yeast Saccharomyces cerevisiae. *Microbiol. Rev.* 52, 536-553 (1988).

176. Hess, G. F. *et al.* A human homolog of the yeast CDC7 gene is overexpressed in some tumors and transformed cell lines. *Gene* 211, 133-140 (1998).

177. Hillenmeyer, M. E. *et al.* The chemical genomic portrait of yeast: uncovering a phenotype for all genes. *Science* 320, 362 (2008).

178. Hinnebusch, A. G. & Natarajan, K. Gcn4p, a master regulator of gene expression, is controlled at multiple levels by diverse signals of starvation and stress. *Eukaryot. Cell.* 1, 22-32 (2002).

179. Hollywood, K., Brison, D. R. & Goodacre, R. Metabolomics: current technologies and future trends. *Proteomics* 6, 4716-4723 (2006).

180. Holt, S. E. & Shay, J. W. Role of telomerase in cellular proliferation and cancer. *J. Cell. Physiol.* 180, 10-18 (1999).

181. Honey, S. & Futcher, B. Roles of the CDK phosphorylation sites of yeast Cdc6 in chromatin binding and rereplication. *Mol. Biol. Cell* 18, 1324-1336 (2007).

182. Hopp, T. P. *et al.* A short polypeptide marker sequence useful for recombinant protein identification and purification. *Biotechnology* 6, 6 (1988).

183. Hopwood, B. & Dalton, S. Cdc45p assembles into a complex with Cdc46p/Mcm5p, is required for minichromosome maintenance, and is essential for chromosomal DNA replication. *Proc. Natl. Acad. Sci. U. S. A.* 93, 12309-12314 (1996).

184. Hu, Y., Wang, G., Chen, G. Y., Fu, X. & Yao, S. Q. Proteome analysis of Saccharomyces cerevisiae under metal stress by two-dimensional differential gel electrophoresis. *Electrophoresis* 24, 1458-1470 (2003).

185. Huang, M., Zhou, Z. & Elledge, S. J. The DNA replication and damage checkpoint pathways induce transcription by inhibition of the Crt1 repressor. *Cell* 94, 595-605 (1998).

186. Huang, M. & Elledge, S. J. Identification of RNR4, encoding a second essential small subunit of ribonucleotide reductase in Saccharomyces cerevisiae. *Mol. Cell. Biol.* 17, 6105-6113 (1997).

187. Huh, W. K. *et al*. Global analysis of protein localization in budding yeast. *Nature* 425, 686-691 (2003).

188. Huyen, Y. *et al*. Methylated lysine 79 of histone H3 targets 53BP1 to DNA double-strand breaks. *Nature* 432, 406-411 (2004).

189. Hwang, L. H. *et al*. Budding yeast Cdc20: a target of the spindle checkpoint. *Science* 279, 1041-1044 (1998).

190. Hyrien, O., Marheineke, K. & Goldar, A. Paradoxes of eukaryotic DNA replication: MCM proteins and the random completion problem. *Bioessays* 25, 116-125 (2003).

191. Hyver, C. & Le Guyader, H. MPF and cyclin: modelling of the cell cycle minimum oscillator. *BioSystems* 24, 85-90 (1990).

192. Ideker, T. *et al*. Integrated genomic and proteomic analyses of a systematically perturbed metabolic network. *Science* 292, 929-934 (2001).

193. Ilves, I., Petojevic, T., Pesavento, J. J. & Botchan, M. R. Activation of the MCM2-7 helicase by association with Cdc45 and GINS proteins. *Mol. Cell* 37, 247-258 (2010).

194. Ingalls, B. P., Duncker, B. P., Kim, D. R. & McConkey, B. J. Systems level modeling of the cell cycle using budding yeast. *Cancer. Inform.* 3, 357-370 (2007).

195. Ingber, L. *Adaptive simulated annealing (ASA): Lessons learned* (Control and Cybernetics, Citeseer, 1996).

196. Irniger, S. & Nasmyth, K. The anaphase-promoting complex is required in G1 arrested yeast cells to inhibit B-type cyclin accumulation and to prevent uncontrolled entry into S-phase. *J. Cell. Sci.* 110 (Pt 13), 1523-1531 (1997).

197. Irniger, S., Piatti, S., Michaelis, C. & Nasmyth, K. Genes involved in sister chromatid separation are needed for B-type cyclin proteolysis in budding yeast. *Cell* 81, 269-278 (1995).

198. Ishimi, Y. *et al*. Enhanced expression of Mcm proteins in cancer cells derived from uterine cervix. *Eur. J. Biochem*. 270, 1089-1101 (2003).

199. Ismail, I. H., Nyström, S., Nygren, J. & Hammarsten, O. Activation of ataxia telangiectasia mutated by DNA strand break-inducing agents correlates closely with the number of DNA double strand breaks. *J. Biol. Chem*. 280, 4649 (2005).

200. Itani, S. *et al*. Cancer Modeling and Control.

201. Ito, T. *et al*. A comprehensive two-hybrid analysis to explore the yeast protein interactome. *Proceedings of the National Academy of Sciences* 98, 4569 (2001).

202. Jacobs, C. W., Adams, A. E., Szaniszlo, P. J. & Pringle, J. R. Functions of microtubules in the Saccharomyces cerevisiae cell cycle. *J. Cell Biol*. 107, 1409-1426 (1988).

203. Jares, P. & Campo, E. Genomic platforms for cancer research: potential diagnostic and prognostic applications in clinical oncology. *Clin. Transl. Oncol*. 8, 161-172 (2006).

204. Jaspersen, S. L., Charles, J. F. & Morgan, D. O. Inhibitory phosphorylation of the APC regulator Hct1 is controlled by the kinase Cdc28 and the phosphatase Cdc14. *Curr. Biol*. 9, 227-236 (1999).

205. Jeggo, P., Tesmer, J. & Chen, D. Genetic analysis of ionising radiation sensitive mutants of cultured mammalian cell lines. *Mutat. Res. /DNA Repair* 254, 125-133 (1991).

206. Jelier, R., Semple, J. I., Garcia-Verdugo, R. & Lehner, B. Predicting phenotypic variation in yeast from individual genome sequences. *Nat. Genet*. 43, 1270-1274 (2011).

207. Jiang, Y. H., Bressler, J. & Beaudet, A. L. Epigenetics and human disease. *Annu. Rev. Genomics Hum. Genet*. 5, 479-510 (2004).

208. Johnston, L. H. & Johnson, A. L. Elutriation of budding yeast. *Meth. Enzymol*. 283, 342-350 (1997).

209. Johnston, G. C., Ehrhardt, C. W., Lorincz, A. & Carter, B. L. Regulation of cell size in the yeast Saccharomyces cerevisiae. *J. Bacteriol*. 137, 1-5 (1979).

210. Jones, D. R., Prasad, A. A., Chan, P. K. & Duncker, B. P. The Dbf4 motif C zinc finger promotes DNA replication and mediates resistance to genotoxic stress. *Cell. Cycle* 9, 2018-2026 (2010).

211. Jourdain, S., Acker, J., Ducrot, C., Sentenac, A. & Lefebvre, O. The tau95 subunit of yeast TFIIIC influences upstream and downstream functions of TFIIIC.DNA complexes. *J. Biol. Chem*. 278, 10450-10457 (2003).

212. Kamimura, Y., Masumoto, H., Sugino, A. & Araki, H. Sld2, which interacts with Dpb11 in Saccharomyces cerevisiae, is required for chromosomal DNA replication. *Mol. Cell. Biol.* 18, 6102-6109 (1998).

213. Kamimura, Y., Tak, Y. S., Sugino, A. & Araki, H. Sld3, which interacts with Cdc45 (Sld4), functions for chromosomal DNA replication in Saccharomyces cerevisiae. *EMBO J.* 20, 2097-2107 (2001).

214. Kanemaki, M. & Labib, K. Distinct roles for Sld3 and GINS during establishment and progression of eukaryotic DNA replication forks. *EMBO J.* 25, 1753-1763 (2006).

215. Karp, N. A., McCormick, P. S., Russell, M. R. & Lilley, K. S. Experimental and statistical considerations to avoid false conclusions in proteomics studies using differential in-gel electrophoresis. *Mol. Cell. Proteomics* 6, 1354-1364 (2007).

216. Katou, Y. *et al.* S-phase checkpoint proteins Tof1 and Mrc1 form a stable replication-pausing complex. *Nature* 424, 1078-1083 (2003).

217. Kauffman, S. & Wille, J. J. The mitotic oscillator in Physarum polycephalum. *J. Theor. Biol.* 55, 47-93 (1975).

218. Khoudoli, G. A. *et al.* Temporal profiling of the chromatin proteome reveals system-wide responses to replication inhibition. *Curr. Biol.* 18, 838-843 (2008).

219. Kihara, M. *et al.* Characterization of the yeast Cdc7p/Dbf4p complex purified from insect cells. Its protein kinase activity is regulated by Rad53p. *J. Biol. Chem.* 275, 35051-35062 (2000).

220. Kilmartin, J. V. & Adams, A. E. Structural rearrangements of tubulin and actin during the cell cycle of the yeast Saccharomyces. *J. Cell Biol.* 98, 922-933 (1984).

221. Kim, D. R., Gidvani, R. D., Ingalls, B. P., Duncker, B. P. & McConkey, B. J. Differential chromatin proteomics of the MMS-induced DNA damage response in yeast. *Proteome Sci.* 9, 62 (2011).

222. Kitano, H. Computational systems biology. *Nature* 420, 206-210 (2002).

223. Klipp, E., Nordlander, B., Kruger, R., Gennemark, P. & Hohmann, S. Integrative model of the response of yeast to osmotic shock. *Nat. Biotechnol.* 23, 975-982 (2005).

224. Klis, F. M., Boorsma, A. & De Groot, P. W. Cell wall construction in Saccharomyces cerevisiae. *Yeast* 23, 185-202 (2006).

225. Knop, M. *et al.* Epitope tagging of yeast genes using a PCR-based strategy: more tags and improved practical routines. *Yeast* 15, 963-972 (1999).

226. Koc, A., Wheeler, L. J., Mathews, C. K. & Merrill, G. F. Hydroxyurea arrests DNA replication by a mechanism that preserves basal dNTP pools. *J. Biol. Chem.* 279, 223-230 (2004).

227. Koch, C. & Nasmyth, K. Cell cycle regulated transcription in yeast. *Curr. Opin. Cell Biol.* 6, 451-459 (1994).

228. Kolodner, R. D., Putnam, C. D. & Myung, K. Maintenance of genome stability in Saccharomyces cerevisiae. *Science* 297, 552-557 (2002).

229. Korkolopoulou, P. *et al*. Minichromosome maintenance proteins 2 and 5 expression in muscle-invasive urothelial cancer: a multivariate survival study including proliferation markers and cell cycle regulators. *Hum. Pathol.* 36, 899-907 (2005).

230. Korkolopoulou, P. *et al*. The combined evaluation of p27Kip1 and Ki-67 expression provides independent information on overall survival of ovarian carcinoma patients. *Gynecol. Oncol.* 85, 404-414 (2002).

231. Kormanec, J., Schaaff-Gerstenschlager, I., Zimmermann, F. K., Perecko, D. & Kuntzel, H. Nuclear migration in Saccharomyces cerevisiae is controlled by the highly repetitive 313 kDa NUM1 protein. *Mol. Gen. Genet.* 230, 277-287 (1991).

232. Koundrioukoff, S., Polo, S. & Almouzni, G. Interplay between chromatin and cell cycle checkpoints in the context of ATR/ATM-dependent checkpoints. *DNA Repair (Amst)* 3, 969-978 (2004).

233. Kovacech, B., Nasmyth, K. & Schuster, T. EGT2 gene transcription is induced predominantly by Swi5 in early G1. *Mol. Cell. Biol.* 16, 3264-3274 (1996).

234. Kuenzi, M. T. & Fiechter, A. Changes in carbohydrate composition and trehalase-activity during the budding cycle of Saccharomyces cerevisiae. *Arch. Mikrobiol.* 64, 396-407 (1969).

235. Kunkel, T. A. DNA replication fidelity. *J. Biol. Chem.* 279, 16895-16898 (2004).

236. Kunzler, M., Trueheart, J., Sette, C., Hurt, E. & Thorner, J. Mutations in the YRB1 gene encoding yeast ran-binding-protein-1 that impair nucleocytoplasmic transport and suppress yeast mating defects. *Genetics* 157, 1089-1105 (2001).

237. Kuroda, K., Kato, M., Mima, J. & Ueda, M. Systems for the detection and analysis of protein-protein interactions. *Appl. Microbiol. Biotechnol.* 71, 127-136 (2006).

238. Kurtzman, C. & Piškur, J. Taxonomy and phylogenetic diversity among the yeasts. *Comparative Genomics*, 29-46 (2006).

239. Labib, K. Building a double hexamer of DNA helicase at eukaryotic replication origins. *EMBO J*. 30, 4853-4855 (2011).

240. Labib, K. How do Cdc7 and cyclin-dependent kinases trigger the initiation of chromosome replication in eukaryotic cells? *Genes Dev*. 24, 1208-1219 (2010).

241. Labib, K. & Diffley, J. F. Is the MCM2-7 complex the eukaryotic DNA replication fork helicase? *Curr. Opin. Genet. Dev*. 11, 64-70 (2001).

242. Labib, K., Diffley, J. F. & Kearsey, S. E. G1-phase and B-type cyclins exclude the DNA-replication factor Mcm4 from the nucleus. *Nat. Cell Biol*. 1, 415-422 (1999).

243. Labib, K. & Gambus, A. A key role for the GINS complex at DNA replication forks. *Trends Cell Biol*. 17, 271-278 (2007).

244. Lalo, D., Carles, C., Sentenac, A. & Thuriaux, P. Interactions between three common subunits of yeast RNA polymerases I and III. *Proc. Natl. Acad. Sci. U. S. A*. 90, 5524-5528 (1993).

245. Lau, E. & Jiang, W. Perspective Is There A Pre-RC Checkpoint That Cancer Cells Lack? *Cell cycle* 5, 1602-1606 (2006).

246. Lau, E. & Jiang, W. Is there a pre-RC checkpoint that cancer cells lack? *Cell. Cycle* 5, 1602-1606 (2006).

247. Lee, D. G. & Bell, S. P. Architecture of the yeast origin recognition complex bound to origins of DNA replication. *Mol. Cell. Biol*. 17, 7159 (1997).

248. Lei, M., Kawasaki, Y. & Tye, B. K. Physical interactions among Mcm proteins and effects of Mcm dosage on DNA replication in Saccharomyces cerevisiae. *Mol. Cell. Biol*. 16, 5081-5090 (1996).

249. Lei, M. *et al*. Mcm2 is a target of regulation by Cdc7-Dbf4 during the initiation of DNA synthesis. *Genes Dev*. 11, 3365-3374 (1997).

250. Levine, D. S., Sanchez, C. A., Rabinovitch, P. S. & Reid, B. J. Formation of the tetraploid intermediate is associated with the development of cells with more than four centrioles in the elastase-simian virus 40 tumor antigen transgenic mouse model of pancreatic cancer. *Proc. Natl. Acad. Sci. U. S. A*.88, 6427-6431 (1991).

251. Lew, D. J. & Kornbluth, S. Regulatory roles of cyclin dependent kinase phosphorylation in cell cycle control. *Curr. Opin. Cell Biol*. 8, 795-804 (1996).

252. Li, X. *et al*. Large-scale phosphorylation analysis of α-factor-arrested Saccharomyces cerevisiae. *Journal of proteome research* 6, 1190-1197 (2007).

253. Li, F., Long, T., Lu, Y., Ouyang, Q. & Tang, C. The yeast cell-cycle network is robustly designed. *Proc. Natl. Acad. Sci. U. S. A.* 101, 4781-4786 (2004).

254. Li, J. J. & Herskowitz, I. Isolation of ORC6, a component of the yeast origin recognition complex by a one-hybrid system. *Science* 262, 1870-1874 (1993).

255. Li, M. A. & Bradley, A. Crafting rat genomes with zinc fingers. *Nat. Biotechnol.* 29, 39-41 (2011).

256. Liang, C. & Stillman, B. Persistent initiation of DNA replication and chromatin-bound MCM proteins during the cell cycle in cdc6 mutants. *Genes Dev.* 11, 3375-3386 (1997).

257. Liao, C., Hu, B., Arno, M. J. & Panaretou, B. Genomic screening in vivo reveals the role played by vacuolar H+ ATPase and cytosolic acidification in sensitivity to DNA-damaging agents such as cisplatin. *Mol. Pharmacol.* 71, 416-425 (2007).

258. Liku, M. E., Nguyen, V. Q., Rosales, A. W., Irie, K. & Li, J. J. CDK phosphorylation of a novel NLS-NES module distributed between two subunits of the Mcm2-7 complex prevents chromosomal rereplication. *Mol. Biol. Cell* 16, 5026-5039 (2005).

259. Lindegren, C. C. & Lindegren, G. Unusual Gene-Controlled Combinations of Carbohydrate Fermentations in Yeast Hybrids. *Proc. Natl. Acad. Sci. U. S. A.* 35, 23-27 (1949).

260. Longhese, M. P., Neecke, H., Paciotti, V., Lucchini, G. & Plevani, P. The 70 kDa subunit of replication protein A is required for the G1/S and intra-S DNA damage checkpoints in budding yeast. *Nucleic Acids Res.* 24, 3533 (1996).

261. Longhese, M. P., Foiani, M., Muzi-Falconi, M., Lucchini, G. & Plevani, P. DNA damage checkpoint in budding yeast. *EMBO J.* 17, 5525-5528 (1998).

262. Longtine, M. S. *et al.* Additional modules for versatile and economical PCR-based gene deletion and modification in Saccharomyces cerevisiae. *Yeast* 14, 953-961 (1998).

263. Loog, M. & Morgan, D. O. Cyclin specificity in the phosphorylation of cyclin-dependent kinase substrates. *Nature* 434, 104-108 (2005).

264. Lopes, M. *et al.* The DNA replication checkpoint response stabilizes stalled replication forks. *Nature* 412, 557-561 (2001).

265. Lundblad, V. & Szostak, J. W. A mutant with a defect in telomere elongation leads to senescence in yeast. *Cell* 57, 633-643 (1989).

266. Lundin, C. *et al*. Methyl methanesulfonate (MMS) produces heat-labile DNA damage but no detectable in vivo DNA double-strand breaks. *Nucleic Acids Res*. 33, 3799-3811 (2005).

267. Ma, B., Zhang, K. & Liang, C. An effective algorithm for peptide de novo sequencing from MS/MS spectra. *Journal of Computer and System Sciences* 70, 418-430 (2005).

268. MacKay, V. L. *et al*. The Saccharomyces cerevisiae BAR1 gene encodes an exported protein with homology to pepsin. *Proc. Natl. Acad. Sci. U. S. A*. 85, 55-59 (1988).

269. Majka, J., Niedziela-Majka, A. & Burgers, P. M. The checkpoint clamp activates Mec1 kinase during initiation of the DNA damage checkpoint. *Mol. Cell* 24, 891-901 (2006).

270. Mantiero, D., Mackenzie, A., Donaldson, A. & Zegerman, P. Limiting replication initiation factors execute the temporal programme of origin firing in budding yeast. *EMBO J*. 30, 4805-4814 (2011).

271. Marc, P., Devaux, F. & Jacq, C. yMGV: a database for visualization and data mining of published genome-wide yeast expression data. *Nucleic Acids Res*. 29, E63-3 (2001).

272. Masai, H. *et al*. Human Cdc7-related kinase complex. *J. Biol. Chem*. 275, 29042-29052 (2000).

273. Masai, H. & Arai, K. Cdc7 kinase complex: a key regulator in the initiation of DNA replication. *J. Cell. Physiol*. 190, 287-296 (2002).

274. Masai, H. *et al*. Phosphorylation of MCM4 by Cdc7 kinase facilitates its interaction with Cdc45 on the chromatin. *J. Biol. Chem*. 281, 39249-39261 (2006).

275. Masumoto, H., Sugino, A. & Araki, H. Dpb11 controls the association between DNA polymerases alpha and epsilon and the autonomously replicating sequence region of budding yeast. *Mol. Cell. Biol*. 20, 2809-2817 (2000).

276. Materi, W. & Wishart, D. S. Computational systems biology in drug discovery and development: methods and applications. *Drug Discov. Today* 12, 295-303 (2007).

277. McCune, H. J. *et al*. The temporal program of chromosome replication: genomewide replication in clb5{Delta} Saccharomyces cerevisiae. *Genetics* 180, 1833-1847 (2008).

278. Mechali, M. Eukaryotic DNA replication origins: many choices for appropriate answers. *Nat. Rev. Mol. Cell Biol*. 11, 728-738 (2010).

279. Mendez, J. & Stillman, B. Chromatin association of human origin recognition complex, cdc6, and minichromosome maintenance proteins during the cell cycle: assembly of prereplication complexes in late mitosis. *Mol. Cell. Biol.* 20, 8602-8612 (2000).

280. Mercer, T. R. *et al.* Targeted RNA sequencing reveals the deep complexity of the human transcriptome. *Nat. Biotechnol.* 30, 99-104 (2011).

281. Mitchison, J. M. in *The biology of the cell cycle* (Cambridge University Press, 1971).

282. Molloy, M. P., Brzezinski, E. E., Hang, J., McDowell, M. T. & VanBogelen, R. A. Overcoming technical variation and biological variation in quantitative proteomics. *Proteomics* 3, 1912-1919 (2003).

283. Montagnoli, A. *et al.* Identification of Mcm2 phosphorylation sites by S-phase-regulating kinases. *J. Biol. Chem.* 281, 10281-10290 (2006).

284. Mordes, D. A., Nam, E. A. & Cortez, D. Dpb11 activates the Mec1-Ddc2 complex. *Proc. Natl. Acad. Sci. U. S. A.* 105, 18730-18734 (2008).

285. Morrow, D. M., Tagle, D. A., Shiloh, Y., Collins, F. S. & Hieter, P. < i> TEL1</i>, an S. cerevisiae homolog of the human gene mutated in ataxia telangiectasia, is functionally related to the yeast checkpoint gene< i> MEC1</i>. *Cell* 82, 831-840 (1995).

286. Mortimer, R. K. & Johnston, J. R. Genealogy of principal strains of the yeast genetic stock center. *Genetics* 113, 35 (1986).

287. MORTIMER, R. K. Radiobiological and genetic studies on a polyploid series (haploid to hexaploid) of Saccharomyces cerevisiae. *Radiat. Res.* 9, 312-326 (1958).

288. Mouse Genome Sequencing Consortium *et al.* Initial sequencing and comparative analysis of the mouse genome. *Nature* 420, 520-562 (2002).

289. Munro, S. & Pelham, H. R. Use of peptide tagging to detect proteins expressed from cloned genes: deletion mapping functional domains of Drosophila hsp 70. *EMBO J.* 3, 3087-3093 (1984).

290. Muramatsu, S., Hirai, K., Tak, Y. S., Kamimura, Y. & Araki, H. CDK-dependent complex formation between replication proteins Dpb11, Sld2, Pol (epsilon}, and GINS in budding yeast. *Genes Dev.* 24, 602-612 (2010).

291. Murphy, N. *et al.* p16INK4A, CDC6, and MCM5: predictive biomarkers in cervical preinvasive neoplasia and cervical cancer. *J. Clin. Pathol.* 58, 525 (2005).

292. Murray, J. A., Scarpa, M., Rossi, N. & Cesareni, G. Antagonistic controls regulate copy number of the yeast 2 mu plasmid. *EMBO J*. 6, 4205-4212 (1987).

293. Myung, K., Datta, A. & Kolodner, R. D. Suppression of spontaneous chromosomal rearrangements by S phase checkpoint functions in Saccharomyces cerevisiae. *Cell* 104, 397-408 (2001).

294. Nakamura, T. M., Du, L. L., Redon, C. & Russell, P. Histone H2A phosphorylation controls Crb2 recruitment at DNA breaks, maintains checkpoint arrest, and influences DNA repair in fission yeast. *Mol. Cell. Biol*. 24, 6215 (2004).

295. Nasmyth, K., Adolf, G., Lydall, D. & Seddon, A. The identification of a second cell cycle control on the HO promoter in yeast: cell cycle regulation of SWI5 nuclear entry. *Cell* 62, 631-647 (1990).

296. Nasmyth, K. At the heart of the budding yeast cell cycle. *Trends Genet*. 12, 405-412 (1996).

297. Nasmyth, K. Evolution of the cell cycle. *Philos. Trans. R. Soc. Lond. B. Biol. Sci*. 349, 271-281 (1995).

298. Nasmyth, K. Control of the yeast cell cycle by the Cdc28 protein kinase. *Curr. Opin. Cell Biol*. 5, 166-179 (1993).

299. Nasmyth, K. & Haering, C. H. The structure and function of SMC and kleisin complexes. *Annu. Rev. Biochem*. 74, 595-648 (2005).

300. Nasmyth, K. & Nurse, P. Cell division cycle mutants altered in DNA replication and mitosis in the fission yeast Schizosaccharomyces pombe. *Mol. Gen. Genet*. 182, 119-124 (1981).

301. Natarajan, K. *et al*. Transcriptional profiling shows that Gcn4p is a master regulator of gene expression during amino acid starvation in yeast. *Mol. Cell. Biol*. 21, 4347-4368 (2001).

302. Navadgi-Patil, V. M. & Burgers, P. M. The unstructured C-terminal tail of the 9-1-1 clamp subunit Ddc1 activates Mec1/ATR via two distinct mechanisms. *Mol. Cell* 36, 743-753 (2009).

303. Navadgi-Patil, V. M. & Burgers, P. M. Yeast DNA replication protein Dpb11 activates the Mec1/ATR checkpoint kinase. *J. Biol. Chem*. 283, 35853-35859 (2008).

304. Navadgi-Patil, V. M., Kumar, S. & Burgers, P. M. The unstructured C-terminal tail of yeast Dpb11 (human TopBP1) protein is dispensable for DNA replication and the S phase checkpoint but required for the G2/M checkpoint. *J. Biol. Chem*. 286, 40999-41007 (2011).

305. Nelder, J. A. & Mead, R. A simplex method for function minimization. *The computer journal* 7, 308-313 (1965).

306. Nelson, L. D., Musso, M. & Van Dyke, M. W. The yeast STM1 gene encodes a purine motif triple helical DNA-binding protein. *J. Biol. Chem.* 275, 5573-5581 (2000).

307. Neuwald, A. F., Aravind, L., Spouge, J. L. & Koonin, E. V. AAA+: A class of chaperone-like ATPases associated with the assembly, operation, and disassembly of protein complexes. *Genome Res.* 9, 27-43 (1999).

308. Nguyen, V. Q., Co, C., Irie, K. & Li, J. J. Clb/Cdc28 kinases promote nuclear export of the replication initiator proteins Mcm2-7. *Curr. Biol.* 10, 195-205 (2000).

309. Nguyen, V. Q., Co, C. & Li, J. J. Cyclin-dependent kinases prevent DNA re-replication through multiple mechanisms. *Nature* 411, 1068-1073 (2001).

310. Nick McElhinny, S. A., Kissling, G. E. & Kunkel, T. A. Differential correction of lagging-strand replication errors made by DNA polymerases {alpha} and {delta}. *Proc. Natl. Acad. Sci. U. S. A.* 107, 21070-21075 (2010).

311. Nickoloff, J. A. & Hoekstra, M. F. in *DNA Damage and Repair: DNA repair in higher eukaryotes* (Humana Pr Inc, 1998).

312. Nieduszynski, C. A., Knox, Y. & Donaldson, A. D. Genome-wide identification of replication origins in yeast by comparative genomics. *Genes Dev.* 20, 1874-1879 (2006).

313. Nishitani, H., Lygerou, Z., Nishimoto, T. & Nurse, P. The Cdt1 protein is required to license DNA for replication in fission yeast. *Nature* 404, 625-628 (2000).

314. Njagi, G. & Kilbey, B. cdc7-1 a temperature sensitive cell-cycle mutant which interferes with induced mutagenesis in Saccharomyces cerevisiae. *Molecular and General Genetics MGG* 186, 478-481 (1982).

315. Norel, R. & Agur, Z. A model for the adjustment of the mitotic clock by cyclin and MPF levels. *Science* 251, 1076-1078 (1991).

316. Norman, J. O., Joe, C. O. & Busbee, D. L. Inhibition of DNA polymerase activity by methyl methanesulfonate. *Mutat. Res.* 165, 71-79 (1986).

317. Nougarede, R., Della Seta, F., Zarzov, P. & Schwob, E. Hierarchy of S-phase-promoting factors: yeast Dbf4-Cdc7 kinase requires prior S-phase cyclin-dependent kinase activation. *Mol. Cell. Biol.* 20, 3795-3806 (2000).

318. Novak, B. & Tyson, J. J. A model for restriction point control of the mammalian cell cycle. *J. Theor. Biol.* 230, 563-579 (2004).

319. Nowell, P. C. The clonal evolution of tumor cell populations. *Science* 194, 23-28 (1976).

320. Nurse, P. Cell cycle control genes in yeast. *Trends in genetics* 1, 51-55 (1985).

321. Nurse, P., Thuriaux, P. & Nasmyth, K. Genetic control of the cell division cycle in the fission yeast Schizosaccharomyces pombe. *Mol. Gen. Genet.* 146, 167-178 (1976).

322. Nyberg, K. A., Michelson, R. J., Putnam, C. W. & Weinert, T. A. Toward maintaining the genome: DNA damage and replication checkpoints. *Annu. Rev. Genet.* 36, 617-656 (2002).

323. O'Connor, P. &Kohn, K. *A fundamental role for cell cycle regulation in the chemosensitivity of cancer cells?* (Seminars in cancer biology Ser. 3, 1992).

324. Oehlen, L. J., McKinney, J. D. & Cross, F. R. Ste12 and Mcm1 regulate cell cycle-dependent transcription of FAR1. *Mol. Cell. Biol.* 16, 2830-2837 (1996).

325. Olovnikov, A. M. A theory of marginotomy. The incomplete copying of template margin in enzymic synthesis of polynucleotides and biological significance of the phenomenon. *J. Theor. Biol.* 41, 181-190 (1973).

326. Ong, S. E. & Mann, M. Mass spectrometry-based proteomics turns quantitative. *Nat. Chem. Biol.* 1, 252-262 (2005).

327. Orton, R. J. *et al.* Computational modelling of the receptor-tyrosine-kinase-activated MAPK pathway. *Biochem. J.* 392, 249-261 (2005).

328. Osborn, A. J. & Elledge, S. J. Mrc1 is a replication fork component whose phosphorylation in response to DNA replication stress activates Rad53. *Genes Dev.* 17, 1755-1767 (2003).

329. Oshiro, G., Owens, J. C., Shellman, Y., Sclafani, R. A. & Li, J. J. Cell cycle control of Cdc7p kinase activity through regulation of Dbf4p stability. *Mol. Cell. Biol.* 19, 4888-4896 (1999).

330. Owens, J. C., Detweiler, C. S. & Li, J. J. CDC45 is required in conjunction with CDC7/DBF4 to trigger the initiation of DNA replication. *Proc. Natl. Acad. Sci. U. S. A.* 94, 12521-12526 (1997).

331. Pache, R. A. & Aloy, P. Incorporating high-throughput proteomics experiments into structural biology pipelines: identification of the low-hanging fruits. *Proteomics* 8, 1959-1964 (2008).

332. Palumbo, P., Mavelli, G., Farina, L. & Alberghina, L. Networks and circuits in cell regulation. *Biochem. Biophys. Res. Commun.* 396, 881-886 (2010).

333. Parsons, A. B. *et al*. Exploring the mode-of-action of bioactive compounds by chemical-genetic profiling in yeast. *Cell* 126, 611-625 (2006).

334. Pasero, P., Duncker, B. P., Schwob, E. & Gasser, S. M. A role for the Cdc7 kinase regulatory subunit Dbf4p in the formation of initiation-competent origins of replication. *Genes Dev*. 13, 2159-2176 (1999).

335. Pasero, P., Shimada, K. & Duncker, B. P. Multiple roles of replication forks in S phase checkpoints: sensors, effectors and targets. *Cell. Cycle* 2, 568-572 (2003).

336. Pasquali, C., Fialka, I. & Huber, L. A. Subcellular fractionation, electromigration analysis and mapping of organelles. *J. Chromatogr. B Biomed. Sci. Appl*. 722, 89-102 (1999).

337. Pasteur, L. in *Mémoire sur la fermentation alcoolique* (Mallet-Bachelier, 1860).

338. Patel, P. K. *et al*. The Hsk1 (Cdc7) replication kinase regulates origin efficiency. *Mol. Biol. Cell* 19, 5550-5558 (2008).

339. Paulovich, A. G. & Hartwell, L. H. A checkpoint regulates the rate of progression through S phase in S. cerevisiae in response to DNA damage. *Cell* 82, 841-847 (1995).

340. Perrot, M. *et al*. Two-dimensional gel protein database of Saccharomyces cerevisiae (update 1999). *Electrophoresis* 20, 2280-2298 (1999).

341. Pessoa-Brandao, L. & Sclafani, R. A. CDC7/DBF4 functions in the translesion synthesis branch of the RAD6 epistasis group in Saccharomyces cerevisiae. *Genetics* 167, 1597-1610 (2004).

342. Pfander, B. & Diffley, J. F. Dpb11 coordinates Mec1 kinase activation with cell cycle-regulated Rad9 recruitment. *EMBO J*. 30, 4897-4907 (2011).

343. Pfleger, C. M. & Kirschner, M. W. The KEN box: an APC recognition signal distinct from the D box targeted by Cdh1. *Genes Dev*. 14, 655-665 (2000).

344. Poddar, A., Stukenberg, P. T. & Burke, D. J. Two complexes of spindle checkpoint proteins containing Cdc20 and Mad2 assemble during mitosis independently of the kinetochore in Saccharomyces cerevisiae. *Eukaryot. Cell*. 4, 867-878 (2005).

345. Pollard, K. J. & Peterson, C. L. Chromatin remodeling: a marriage between two families? *Bioessays* 20, 771-780 (1998).

346. Prokisch, H. *et al*. Integrative analysis of the mitochondrial proteome in yeast. *PLoS biology* 2, e160 (2004).

347. Puddu, F., Piergiovanni, G., Plevani, P. & Muzi-Falconi, M. Sensing of Replication Stress and Mec1 Activation Act through Two Independent Pathways Involving the 9-1-1 Complex and DNA Polymerase ε. *PLoS genetics* 7, e1002022 (2011).

348. Puddu, F. *et al*. Phosphorylation of the budding yeast 9-1-1 complex is required for Dpb11 function in the full activation of the UV-induced DNA damage checkpoint. *Mol. Cell. Biol*. 28, 4782-4793 (2008).

349. Qu, Z., Weiss, J. N. & MacLellan, W. R. Regulation of the mammalian cell cycle: a model of the G1-to-S transition. *Am. J. Physiol. Cell. Physiol*. 284, C349-64 (2003).

350. Raghuraman, M. K., Brewer, B. J. & Fangman, W. L. Cell cycle-dependent establishment of a late replication program. *Science* 276, 806-809 (1997).

351. Raghuraman, M. K. *et al*. Replication dynamics of the yeast genome. *Science* 294, 115-121 (2001).

352. Rahal, R. & Amon, A. Mitotic CDKs control the metaphase-anaphase transition and trigger spindle elongation. *Genes Dev*. 22, 1534-1548 (2008).

353. Randell, J. C., Bowers, J. L., Rodriguez, H. K. & Bell, S. P. Sequential ATP hydrolysis by Cdc6 and ORC directs loading of the Mcm2-7 helicase. *Mol. Cell* 21, 29-39 (2006).

354. Randell, J. C. *et al*. Mec1 is one of multiple kinases that prime the Mcm2-7 helicase for phosphorylation by Cdc7. *Mol. Cell* 40, 353-363 (2010).

355. Rao, H. & Stillman, B. The origin recognition complex interacts with a bipartite DNA binding site within yeast replicators. *Proc. Natl. Acad. Sci. U. S. A*. 92, 2224-2228 (1995).

356. Rattner, J. B., Saunders, C., Davie, J. R. & Hamkalo, B. A. Ultrastructural organization of yeast chromatin. *J. Cell Biol*. 93, 217-222 (1982).

357. Ravasz, E., Somera, A. L., Mongru, D. A., Oltvai, Z. N. & Barabasi, A. L. Hierarchical organization of modularity in metabolic networks. *Science* 297, 1551-1555 (2002).

358. Reinders, J., Zahedi, R. P., Pfanner, N., Meisinger, C. & Sickmann, A. Toward the complete yeast mitochondrial proteome: multidimensional separation techniques for mitochondrial proteomics. *J. Proteome Res*. 5, 1543-1554 (2006).

359. Remus, D. *et al*. Concerted loading of Mcm2-7 double hexamers around DNA during DNA replication origin licensing. *Cell* 139, 719-730 (2009).

360. Retkute, R., Nieduszynski, C. A. & de Moura, A. Dynamics of DNA replication in yeast. *Phys. Rev. Lett.* 107, 068103 (2011).

361. Richardson, H., Lew, D. J., Henze, M., Sugimoto, K. & Reed, S. I. Cyclin-B homologs in Saccharomyces cerevisiae function in S phase and in G2. *Genes Dev.* 6, 2021 (1992).

362. Robles, L. D. *et al.* Down-regulation of Cdc6, a cell cycle regulatory gene, in prostate cancer. *J. Biol. Chem.* 277, 25431 (2002).

363. Rock, J. M. & Amon, A. Cdc15 integrates Tem1 GTPase-mediated spatial signals with Polo kinase-mediated temporal cues to activate mitotic exit. *Genes Dev.* 25, 1943-1954 (2011).

364. Rodriguez, B. A. & Huang, T. H. Tilling the chromatin landscape: emerging methods for the discovery and profiling of protein-DNA interactions. *Biochem. Cell Biol.* 83, 525-534 (2005).

365. Ross, P. L. *et al.* Multiplexed protein quantitation in Saccharomyces cerevisiae using amine-reactive isobaric tagging reagents. *Mol. Cell. Proteomics* 3, 1154-1169 (2004).

366. Rouse, J. & Jackson, S. P. Lcd1p recruits Mec1p to DNA lesions in vitro and in vivo. *Mol. Cell* 9, 857-869 (2002).

367. Rowles, A., Tada, S. & Blow, J. J. Changes in association of the Xenopus origin recognition complex with chromatin on licensing of replication origins. *J. Cell. Sci.* 112 (Pt 12), 2011-2018 (1999).

368. Rowley, A., Cocker, J. H., Harwood, J. & Diffley, J. F. Initiation complex assembly at budding yeast replication origins begins with the recognition of a bipartite sequence by limiting amounts of the initiator, ORC. *EMBO J.* 14, 2631-2641 (1995).

369. Rowley, M. *et al.* Inactivation of Brca2 promotes Trp53-associated but inhibits KrasG12D-dependent pancreatic cancer development in mice. *Gastroenterology* 140, 1303-1313.e1-3 (2011).

370. Ryu, S., Lin, S. C., Ugel, N., Antoniotti, M. & Mishra, B. Mathematical modeling of the formation of apoptosome in intrinsic pathway of apoptosis. *Syst. Synth. Biol.* 2, 49-66 (2008).

371. Saha, A., Wittmeyer, J. & Cairns, B. R. Chromatin remodelling: the industrial revolution of DNA around histones. *Nat. Rev. Mol. Cell Biol.* 7, 437-447 (2006).

372. Sanchez, Y. *et al.* Regulation of RAD53 by the ATM-like kinases MEC1 and TEL1 in yeast cell cycle checkpoint pathways. *Science* 271, 357 (1996).

373. Santocanale, C. & Diffley, J. F. A Mec1- and Rad53-dependent checkpoint controls late-firing origins of DNA replication. *Nature* 395, 615-618 (1998).

374. Santocanale, C., Neecke, H., Longhese, M. P., Lucchini, G. & Plevani, P. Mutations in the gene encoding the 34 kDa subunit of yeast replication protein A cause defective S phase progression. *J. Mol. Biol.* 254, 595-607 (1995).

375. Santocanale, C., Sharma, K. & Diffley, J. F. Activation of dormant origins of DNA replication in budding yeast. *Genes Dev.* 13, 2360-2364 (1999).

376. Sauro, H. M. & Kholodenko, B. N. Quantitative analysis of signaling networks. *Prog. Biophys. Mol. Biol.* 86, 5-43 (2004).

377. Scaife, C. *et al.* 2-D DIGE analysis of the budding yeast pH 6-11 proteome in meiosis. *Proteomics* 10, 4401-4414 (2010).

378. Scheuermann, R. H. & Echols, H. A separate editing exonuclease for DNA replication: the epsilon subunit of Escherichia coli DNA polymerase III holoenzyme. *Proceedings of the National Academy of Sciences* 81, 7747 (1984).

379. Schreiber, A. *et al.* Structural basis for the subunit assembly of the anaphase-promoting complex. *Nature* 470, 227-232 (2011).

380. Schwab, M., Lutum, A. S. & Seufert, W. Yeast Hct1 is a regulator of Clb2 cyclin proteolysis. *Cell* 90, 683-693 (1997).

381. Schwab, M., Neutzner, M., Mocker, D. & Seufert, W. Yeast Hct1 recognizes the mitotic cyclin Clb2 and other substrates of the ubiquitin ligase APC. *EMBO J.* 20, 5165-5175 (2001).

382. Schwann, T. & Schleiden, M. Microscopic investigations on the accordance in the structure and growth of plants and animals. *Berlin (English translation by Henry Smith, the Sydenham Society, 1847)* (1839).

383. Schwartz, M. F. *et al.* Rad9 phosphorylation sites couple Rad53 to the Saccharomyces cerevisiae DNA damage checkpoint. *Mol. Cell* 9, 1055-1065 (2002).

384. Schwob, E., Bohm, T., Mendenhall, M. D. & Nasmyth, K. The B-type cyclin kinase inhibitor p40SIC1 controls the G1 to S transition in S. cerevisiae. *Cell* 79, 233-244 (1994).

385. Schwob, E. & Nasmyth, K. CLB5 and CLB6, a new pair of B cyclins involved in DNA replication in Saccharomyces cerevisiae. *Genes Dev.* 7, 1160-1175 (1993).

386. Sclafani, R. A. Cdc7p-Dbf4p becomes famous in the cell cycle. *J. Cell. Sci.* 113 (Pt 12), 2111-2117 (2000).

387. Sclafani, R. A. & Holzen, T. M. Cell cycle regulation of DNA replication. *Annu. Rev. Genet.* 41, 237-280 (2007).

388. Sclafani, R. A. & Jackson, A. L. Cdc7 protein kinase for DNA metabolism comes of age. *Mol. Microbiol.* 11, 805-810 (1994).

389. Sclafani, R. A., Patterson, M., Rosamond, J. & Fangman, W. L. Differential regulation of the yeast CDC7 gene during mitosis and meiosis. *Mol. Cell. Biol.* 8, 293-300 (1988).

390. Segal, M. & Bloom, K. Control of spindle polarity and orientation in Saccharomyces cerevisiae. *Trends Cell Biol.* 11, 160-166 (2001).

391. Semple, J. W. *et al.* An essential role for Orc6 in DNA replication through maintenance of pre-replicative complexes. *EMBO J.* 25, 5150-5158 (2006).

392. Semple, J. W. & Duncker, B. P. ORC-associated replication factors as biomarkers for cancer. *Biotechnol. Adv.* 22, 621-631 (2004).

393. Shay, J. W. Aging and cancer: are telomeres and telomerase the connection? *Mol. Med. Today* 1, 378-384 (1995).

394. Shay, J. W. & Wright, W. E. Hayflick, his limit, and cellular ageing. *Nat. Rev. Mol. Cell Biol.* 1, 72-76 (2000).

395. Shay, J. W. & Wright, W. E. Telomerase activity in human cancer. *Curr. Opin. Oncol.* 8, 66-71 (1996).

396. Shay, J. W., Zou, Y., Hiyama, E. & Wright, W. E. Telomerase and cancer. *Hum. Mol. Genet.* 10, 677-685 (2001).

397. Sheff, M. A. & Thorn, K. S. Optimized cassettes for fluorescent protein tagging in Saccharomyces cerevisiae. *Yeast* 21, 661-670 (2004).

398. Sherman, F. Getting started with yeast. *Meth. Enzymol.* 194, 21 (1991).

399. Sherwin, T. & Gull, K. Visualization of detyrosination along single microtubules reveals novel mechanisms of assembly during cytoskeletal duplication in trypanosomes. *Cell* 57, 211-221 (1989).

400. Sheu, Y. J. & Stillman, B. The Dbf4-Cdc7 kinase promotes S phase by alleviating an inhibitory activity in Mcm4. *Nature* 463, 113-117 (2010).

401. Sheu, Y. J. & Stillman, B. Cdc7-Dbf4 phosphorylates MCM proteins via a docking site-mediated mechanism to promote S phase progression. *Mol. Cell* 24, 101-113 (2006).

402. Shin, I., Kam, Y., Ha, K. S., Kang, K. W. & Joe, C. O. Inhibition of the phosphorylation of a myristoylated alanine-rich C kinase substrate by methyl methanesulfonate in cultured NIH 3T3 cells. *Mutation Research/Fundamental and Molecular Mechanisms of Mutagenesis* 351, 163-171 (1996).

403. Shirahige, K. *et al*. Regulation of DNA-replication origins during cell-cycle progression. *Nature* 395, 618-621 (1998).

404. Shirayama, M., Toth, A., Galova, M. & Nasmyth, K. APC(Cdc20) promotes exit from mitosis by destroying the anaphase inhibitor Pds1 and cyclin Clb5. *Nature* 402, 203-207 (1999).

405. Shirayama, M., Zachariae, W., Ciosk, R. & Nasmyth, K. The Polo-like kinase Cdc5p and the WD-repeat protein Cdc20p/fizzy are regulators and substrates of the anaphase promoting complex in Saccharomyces cerevisiae. *EMBO J*. 17, 1336-1349 (1998).

406. Shou, W. *et al*. Exit from mitosis is triggered by Tem1-dependent release of the protein phosphatase Cdc14 from nucleolar RENT complex. *Cell* 97, 233-244 (1999).

407. Singh, B. & Arlinghaus, R. B. The mos proto–oncogene product: Its role in oocyte maturation, metaphase arrest, and neoplastic transformation. *Mol. Carcinog*. 6, 182-189 (1992).

408. Slavikova, E. & Vadkertiova, R. The diversity of yeasts in the agricultural soil. *J. Basic Microbiol*. 43, 430-436 (2003).

409. Smolka, M. B., Albuquerque, C. P., Chen, S. H. & Zhou, H. Proteome-wide identification of in vivo targets of DNA damage checkpoint kinases. *Proc. Natl. Acad. Sci. U. S. A*. 104, 10364-10369 (2007).

410. Sopko, R. *et al*. Mapping pathways and phenotypes by systematic gene overexpression. *Mol. Cell* 21, 319-330 (2006).

411. Speck, C., Chen, Z., Li, H. & Stillman, B. ATPase-dependent cooperative binding of ORC and Cdc6 to origin DNA. *Nat. Struct. Mol. Biol*. 12, 965-971 (2005).

412. Speck, C. & Stillman, B. Cdc6 ATPase activity regulates ORC x Cdc6 stability and the selection of specific DNA sequences as origins of DNA replication. *J. Biol. Chem*. 282, 11705-11714 (2007).

413. Spellman, P. T. *et al*. Comprehensive identification of cell cycle-regulated genes of the yeast Saccharomyces cerevisiae by microarray hybridization. *Mol. Biol. Cell* 9, 3273-3297 (1998).

414. Spencer, S. L., Berryman, M. J., Garcia, J. A. & Abbott, D. An ordinary differential equation model for the multistep transformation to cancer. *J. Theor. Biol.* 231, 515-524 (2004).

415. Spiesser, T. W., Klipp, E. & Barberis, M. A model for the spatiotemporal organization of DNA replication in Saccharomyces cerevisiae. *Mol. Genet. Genomics* 282, 25-35 (2009).

416. Srividhya, J. & Gopinathan, M. A simple time delay model for eukaryotic cell cycle. *J. Theor. Biol.* 241, 617-627 (2006).

417. Stillman, B. Origin recognition and the chromosome cycle. *FEBS Lett.* 579, 877-884 (2005).

418. Stringer, J. R. *et al.* Modeling variation in tumors in vivo. *Proc. Natl. Acad. Sci. U. S. A.* 102, 2408 (2005).

419. Sugimoto, M., Kikuchi, S. & Tomita, M. Reverse engineering of biochemical equations from time-course data by means of genetic programming. *BioSystems* 80, 155-164 (2005).

420. Surana, U. *et al.* Destruction of the CDC28/CLB mitotic kinase is not required for the metaphase to anaphase transition in budding yeast. *EMBO J.* 12, 1969-1978 (1993).

421. Surana, U. *et al.* The role of CDC28 and cyclins during mitosis in the budding yeast S. cerevisiae. *Cell* 65, 145-161 (1991).

422. Sutton, C. W. *et al.* Identification of myocardial proteins from two-dimensional gels by peptide mass fingerprinting. *Electrophoresis* 16, 308-316 (1995).

423. Swat, M., Kel, A. & Herzel, H. Bifurcation analysis of the regulatory modules of the mammalian G1/S transition. *Bioinformatics* 20, 1506-1511 (2004).

424. Sweeney, F. D. *et al.* < i> Saccharomyces cerevisiae</i> Rad9 Acts as a Mec1 Adaptor to Allow Rad53 Activation. *Current biology* 15, 1364-1375 (2005).

425. Szent-Gyorgyi, C. & Isenberg, I. The organization of oligonucleosomes in yeast. *Nucleic Acids Res.* 11, 3717-3736 (1983).

426. Szyjka, S. J. *et al.* Rad53 regulates replication fork restart after DNA damage in Saccharomyces cerevisiae. *Genes Dev.* 22, 1906-1920 (2008).

427. Tak, Y. S., Tanaka, Y., Endo, S., Kamimura, Y. & Araki, H. A CDK-catalysed regulatory phosphorylation for formation of the DNA replication complex Sld2–Dpb11. *EMBO J.* 25, 1987-1996 (2006).

428. Takara, T. J. & Bell, S. P. Multiple Cdt1 molecules act at each origin to load replication-competent Mcm2-7 helicases. *EMBO J*. 30, 4885-4896 (2011).

429. Takayama, Y. *et al*. GINS, a novel multiprotein complex required for chromosomal DNA replication in budding yeast. *Genes Dev*. 17, 1153-1165 (2003).

430. Tanaka, S. *et al*. CDK-dependent phosphorylation of Sld2 and Sld3 initiates DNA replication in budding yeast. *Nature* 445, 328-332 (2006).

431. Tanaka, T. *et al*. Sld7, an Sld3-associated protein required for efficient chromosomal DNA replication in budding yeast. *EMBO J*. 30, 2019-2030 (2011).

432. Tanaka, S. & Diffley, J. F. Interdependent nuclear accumulation of budding yeast Cdt1 and Mcm2-7 during G1 phase. *Nat. Cell Biol*. 4, 198-207 (2002).

433. Tanaka, S., Nakato, R., Katou, Y., Shirahige, K. & Araki, H. Origin association of sld3, sld7, and cdc45 proteins is a key step for determination of origin-firing timing. *Curr. Biol*. 21, 2055-2063 (2011).

434. Tanaka, S. *et al*. CDK-dependent phosphorylation of Sld2 and Sld3 initiates DNA replication in budding yeast. *Nature* 445, 328-332 (2007).

435. Tanaka, T., Knapp, D. & Nasmyth, K. Loading of an Mcm protein onto DNA replication origins is regulated by Cdc6p and CDKs. *Cell* 90, 649-660 (1997).

436. Tang, W. *et al*. Proteomics studies of brassinosteroid signal transduction using prefractionation and two-dimensional DIGE. *Mol. Cell. Proteomics* 7, 728-738 (2008).

437. Tanny, R. E., MacAlpine, D. M., Blitzblau, H. G. & Bell, S. P. Genome-wide analysis of re-replication reveals inhibitory controls that target multiple stages of replication initiation. *Mol. Biol. Cell* 17, 2415-2423 (2006).

438. Team, R. R: A language and environment for statistical computing. *R Foundation for Statistical Computing Vienna Austria* (2010).

439. Tercero, J. A. & Diffley, J. F. Regulation of DNA replication fork progression through damaged DNA by the Mec1/Rad53 checkpoint. *Nature* 412, 553-557 (2001).

440. Tkacz, J. S. & MacKay, V. L. Sexual conjugation in yeast. Cell surface changes in response to the action of mating hormones. *J. Cell Biol*. 80, 326-333 (1979).

441. Todorov, I. T. *et al*. HsMCM2/BM28: a novel proliferation marker for human tumors and normal tissues. *Lab. Invest*. 78, 73-78 (1998).

442. Tong, A. H. *et al*. Systematic genetic analysis with ordered arrays of yeast deletion mutants. *Science* 294, 2364-2368 (2001).

443. Tonge, R. *et al*. Validation and development of fluorescence two-dimensional differential gel electrophoresis proteomics technology. *Proteomics* 1, 377-396 (2001).

444. Tourriere, H. & Pasero, P. Maintenance of fork integrity at damaged DNA and natural pause sites. *DNA Repair (Amst)* 6, 900-913 (2007).

445. Tsakraklides, V. & Bell, S. P. Dynamics of pre-replicative complex assembly. *J. Biol. Chem.* 285, 9437-9443 (2010).

446. Tye, B. K. & Sawyer, S. The hexameric eukaryotic MCM helicase: building symmetry from nonidentical parts. *J. Biol. Chem.* 275, 34833-34836 (2000).

447. Tyers, M. & Mann, M. From genomics to proteomics. *Nature* 422, 193-197 (2003).

448. Tyers, M., Tokiwa, G. & Futcher, B. Comparison of the Saccharomyces cerevisiae G1 cyclins: Cln3 may be an upstream activator of Cln1, Cln2 and other cyclins. *EMBO J.* 12, 1955-1968 (1993).

449. Tyson, J. J., Chen, K. & Novak, B. Network dynamics and cell physiology. *Nature Reviews Molecular Cell Biology* 2, 908-916 (2001).

450. Tyson, J. J., Novak, B., Odell, G. M., Chen, K. & Dennis Thron, C. Chemical kinetic theory: understanding cell-cycle regulation. *Trends Biochem. Sci.* 21, 89-96 (1996).

451. Tyson, J. J. Modeling the cell division cycle: cdc2 and cyclin interactions. *Proc. Natl. Acad. Sci. U. S. A.* 88, 7328-7332 (1991).

452. Tyson, J. J., Csikasz-Nagy, A. & Novak, B. The dynamics of cell cycle regulation. *Bioessays* 24, 1095-1109 (2002).

453. Uetz, P. Two-hybrid arrays. *Curr. Opin. Chem. Biol.* 6, 57-62 (2002).

454. Uetz, P. *et al*. A comprehensive analysis of protein-protein interactions in Saccharomyces cerevisiae. *Nature* 403, 623-627 (2000).

455. Uhlmann, F., Lottspeich, F. & Nasmyth, K. Sister-chromatid separation at anaphase onset is promoted by cleavage of the cohesin subunit Scc1. *Nature* 400, 37-42 (1999).

456. Uhlmann, F., Wernic, D., Poupart, M. A., Koonin, E. V. & Nasmyth, K. Cleavage of cohesin by the CD clan protease separin triggers anaphase in yeast. *Cell* 103, 375-386 (2000).

457. Umezu, K., Sugawara, N., Chen, C., Haber, J. E. & Kolodner, R. D. Genetic analysis of yeast RPA1 reveals its multiple functions in DNA metabolism. *Genetics* 148, 989-1005 (1998).

458. Unnikrishnan, A., Gafken, P. R. & Tsukiyama, T. Dynamic changes in histone acetylation regulate origins of DNA replication. *Nat. Struct. Mol. Biol.* 17, 430-437 (2010).

459. Usui, T., Foster, S. S. & Petrini, J. H. J. Maintenance of the DNA-damage checkpoint requires DNA-damage-induced mediator protein oligomerization. *Mol. Cell* 33, 147-159 (2009).

460. Usui, T. & Petrini, J. H. The Saccharomyces cerevisiae 14-3-3 proteins Bmh1 and Bmh2 directly influence the DNA damage-dependent functions of Rad53. *Proc. Natl. Acad. Sci. U. S. A.* 104, 2797-2802 (2007).

461. Valencia-Burton, M. *et al*. Different mating-type-regulated genes affect the DNA repair defects of Saccharomyces RAD51, RAD52 and RAD55 mutants. *Genetics* 174, 41-55 (2006).

462. Varrin, A. E., Prasad, A. A., Scholz, R. P., Ramer, M. D. & Duncker, B. P. A mutation in Dbf4 motif M impairs interactions with DNA replication factors and confers increased resistance to genotoxic agents. *Mol. Cell. Biol.* 25, 7494-7504 (2005).

463. Vas, A., Mok, W. & Leatherwood, J. Control of DNA rereplication via Cdc2 phosphorylation sites in the origin recognition complex. *Mol. Cell. Biol.* 21, 5767-5777 (2001).

464. Venkitaraman, A. R. Cancer susceptibility and the functions of BRCA1 and BRCA2. *Cell* 108, 171-182 (2002).

465. Visintin, R., Hwang, E. S. & Amon, A. Cfi1 prevents premature exit from mitosis by anchoring Cdc14 phosphatase in the nucleolus. *Nature* 398, 818-823 (1999).

466. Visintin, R. *et al*. The phosphatase Cdc14 triggers mitotic exit by reversal of Cdk-dependent phosphorylation. *Mol. Cell* 2, 709-718 (1998).

467. Visintin, R., Prinz, S. & Amon, A. CDC20 and CDH1: a family of substrate-specific activators of APC-dependent proteolysis. *Science* 278, 460-463 (1997).

468. Visintin, R., Stegmeier, F. & Amon, A. The role of the polo kinase Cdc5 in controlling Cdc14 localization. *Mol. Biol. Cell* 14, 4486-4498 (2003).

469. Vita Jr, V. D., Hellman, S., Rosenberg, S. & Markoe, A. M. Cancer: Principles and Practice of Oncology. *American Journal of Clinical Oncology* 9, 90 (1986).

470. Vogelauer, M., Rubbi, L., Lucas, I., Brewer, B. J. & Grunstein, M. Histone acetylation regulates the time of replication origin firing. *Mol. Cell* 10, 1223-1233 (2002).

471. Vogelstein, B. *et al*. Allelotype of colorectal carcinomas. *Science* 244, 207-211 (1989).

472. Wach, A., Brachat, A., Pohlmann, R. & Philippsen, P. New heterologous modules for classical or PCR-based gene disruptions in Saccharomyces cerevisiae. *Yeast* 10, 1793-1808 (1994).

473. Walker, G. M. in *Yeast physiology and biotechnology* (Wiley, 1998).

474. Walter, J. & Newport, J. Initiation of eukaryotic DNA replication: origin unwinding and sequential chromatin association of Cdc45, RPA, and DNA polymerase alpha. *Mol. Cell* 5, 617-627 (2000).

475. Wan, L. *et al*. Cdc28–Clb5 (CDK-S) and Cdc7–Dbf4 (DDK) collaborate to initiate meiotic recombination in yeast. *Genes Dev*. 22, 386 (2008).

476. Wan, L., Zhang, C., Shokat, K. M. & Hollingsworth, N. M. Chemical inactivation of Cdc7 kinase in budding yeast results in a reversible arrest that allows efficient cell synchronization prior to meiotic recombination. *Genetics* 174, 1767 (2006).

477. Wang, X. D., Qi, Y. X. & Jiang, Z. L. Reconstruction of transcriptional network from microarray data using combined mutual information and network-assisted regression. *Systems Biology, IET* 5, 95-102 (2011).

478. Watase, G., Takisawa, H. & Kanemaki, M. T. Mcm10 Plays a Role in Functioning of the Eukaryotic Replicative DNA Helicase, Cdc45-Mcm-GINS. *Curr. Biol*. (2012).

479. Weaver, R. F. Molecular Biology, WCB. (1999).

480. Weinert, T. A., Kiser, G. L. & Hartwell, L. H. Mitotic checkpoint genes in budding yeast and the dependence of mitosis on DNA replication and repair. *Genes Dev*. 8, 652-665 (1994).

481. Weinreich, M. & Stillman, B. Cdc7p-Dbf4p kinase binds to chromatin during S phase and is regulated by both the APC and the RAD53 checkpoint pathway. *EMBO J*. 18, 5334-5346 (1999).

482. Wells, W. A. Does size matter? *J. Cell Biol*. 158, 1156-1159 (2002).

483. Wildgruber, R., Reil, G., Drews, O., Parlar, H. & Görg, A. Web-based two-dimensional database of Saccharomyces cerevisiae proteins using immobilized pH gradients from pH 6 to pH 12 and matrix-assisted laser desorption/ionization-time of flight mass spectrometry. *Proteomics* 2, 727-732 (2002).

484. Williams, G. H. *et al*. Improved cervical smear assessment using antibodies against proteins that regulate DNA replication. *Proceedings of the National Academy of Sciences* 95, 14932 (1998).

485. WILLIAMSON, D. H. & SCOPES, A. W. The behaviour of nucleic acids in synchronously dividing cultures of Saccharomyces cerevisiae. *Exp. Cell Res.* 20, 338-349 (1960).

486. Wilmes, G. M. *et al*. Interaction of the S-phase cyclin Clb5 with an "RXL" docking sequence in the initiator protein Orc6 provides an origin-localized replication control switch. *Genes Dev.* 18, 981-991 (2004).

487. Winey, M. & O'Toole, E. T. The spindle cycle in budding yeast. *Nat. Cell Biol.* 3, E23-7 (2001).

488. Winzeler, E. A. *et al*. Functional characterization of the S. cerevisiae genome by gene deletion and parallel analysis. *Science* 285, 901 (1999).

489. Winzeler, E. A., Lee, B., McCusker, J. H. & Davis, R. W. Whole genome genetic-typing in yeast using high-density oligonucleotide arrays. *Parasitology* 118 Suppl, S73-80 (1999).

490. Wold, M. S. Replication protein A: a heterotrimeric, single-stranded DNA-binding protein required for eukaryotic DNA metabolism. *Annu. Rev. Biochem.* 66, 61-92 (1997).

491. Wright, W. E. & Shay, J. W. Cellular senescence as a tumor-protection mechanism: the essential role of counting. *Curr. Opin. Genet. Dev.* 11, 98-103 (2001).

492. Wu, J. R. & Gilbert, D. M. A distinct G1 step required to specify the Chinese hamster DHFR replication origin. *Science* 271, 1270-1272 (1996).

493. Wu, R., Wang, J. & Liang, C. Cdt1p, through its interaction with Mcm6p, is required for the formation, nuclear accumulation and chromatin loading of the MCM complex. *J. Cell. Sci.* 125, 209-219 (2012).

494. Wyrick, J. J. *et al*. Genome-wide distribution of ORC and MCM proteins in S. cerevisiae: high-resolution mapping of replication origins. *Science* 294, 2357-2360 (2001).

495. Wyrick, J. J. *et al*. Chromosomal landscape of nucleosome-dependent gene expression and silencing in yeast. *Nature* 402, 418-421 (1999).

496. XI, Y., FORMENTINI, A., NAKAJIMA, G., KORNMANN, M. & JU, J. Validation of biomarkers associated with 5-fluorouracil and thymidylate synthase in colorectal cancer. *Oncol. Rep.* 19, 257-262 (2008).

497. Yabuki, N., Terashima, H. & Kitada, K. Mapping of early firing origins on a replication profile of budding yeast. *Genes Cells* 7, 781-789 (2002).

498. Yan, H., Gibson, S. & Tye, B. K. Mcm2 and Mcm3, two proteins important for ARS activity, are related in structure and function. *Genes Dev*. 5, 944-957 (1991).

499. Yan, H., Merchant, A. M. & Tye, B. K. Cell cycle-regulated nuclear localization of MCM2 and MCM3, which are required for the initiation of DNA synthesis at chromosomal replication origins in yeast. *Genes Dev*. 7, 2149-2160 (1993).

500. Yang, L., Han, Z., Robb MacLellan, W., Weiss, J. N. & Qu, Z. Linking cell division to cell growth in a spatiotemporal model of the cell cycle. *J. Theor. Biol*. 241, 120-133 (2006).

501. Yang, S. C., Rhind, N. & Bechhoefer, J. Modeling genome-wide replication kinetics reveals a mechanism for regulation of replication timing. *Mol. Syst. Biol*. 6, 404 (2010).

502. Yao, R. *et al*. Subcellular localization of yeast ribonucleotide reductase regulated by the DNA replication and damage checkpoint pathways. *Proc. Natl. Acad. Sci. U. S. A*. 100, 6628-6633 (2003).

503. Yates, J. R.,3rd, Gilchrist, A., Howell, K. E. & Bergeron, J. J. Proteomics of organelles and large cellular structures. *Nat. Rev. Mol. Cell Biol*. 6, 702-714 (2005).

504. Yoo, Y., Wu, X. & Guan, J. L. A novel role of the actin-nucleating Arp2/3 complex in the regulation of RNA polymerase II-dependent transcription. *J. Biol. Chem*. 282, 7616-7623 (2007).

505. Young, M. R. & Tye, B. Mcm2 and Mcm3 are constitutive nuclear proteins that exhibit distinct isoforms and bind chromatin during specific cell cycle stages of Saccharomyces cerevisiae. *Mol. Biol. Cell* 8, 1587 (1997).

506. Yu, H. Regulation of APC-Cdc20 by the spindle checkpoint. *Curr. Opin. Cell Biol*. 14, 706-714 (2002).

507. Zachariae, W. & Nasmyth, K. Whose end is destruction: cell division and the anaphase-promoting complex. *Genes Dev*. 13, 2039-2058 (1999).

508. Zachariae, W., Schwab, M., Nasmyth, K. & Seufert, W. Control of cyclin ubiquitination by CDK-regulated binding of Hct1 to the anaphase promoting complex. *Science* 282, 1721-1724 (1998).

509. Zegerman, P. & Diffley, J. F. Checkpoint-dependent inhibition of DNA replication initiation by Sld3 and Dbf4 phosphorylation. *Nature* 467, 474-478 (2010).

510. Zegerman, P. & Diffley, J. F. Phosphorylation of Sld2 and Sld3 by cyclin-dependent kinases promotes DNA replication in budding yeast. *Nature* 445, 281-285 (2007).

511. Zou, L. & Elledge, S. J. Sensing DNA damage through ATRIP recognition of RPA-ssDNA complexes. *Science* 300, 1542 (2003).

512. Zou, L., Mitchell, J. & Stillman, B. CDC45, a novel yeast gene that functions with the origin recognition complex and Mcm proteins in initiation of DNA replication. *Mol. Cell. Biol.* 17, 553-563 (1997).

513. Zou, L. & Stillman, B. Assembly of a complex containing Cdc45p, replication protein A, and Mcm2p at replication origins controlled by S-phase cyclin-dependent kinases and Cdc7p-Dbf4p kinase. *Mol. Cell. Biol.* 20, 3086-3096 (2000).

Appendix A – Supplementary Information from Chapter 3

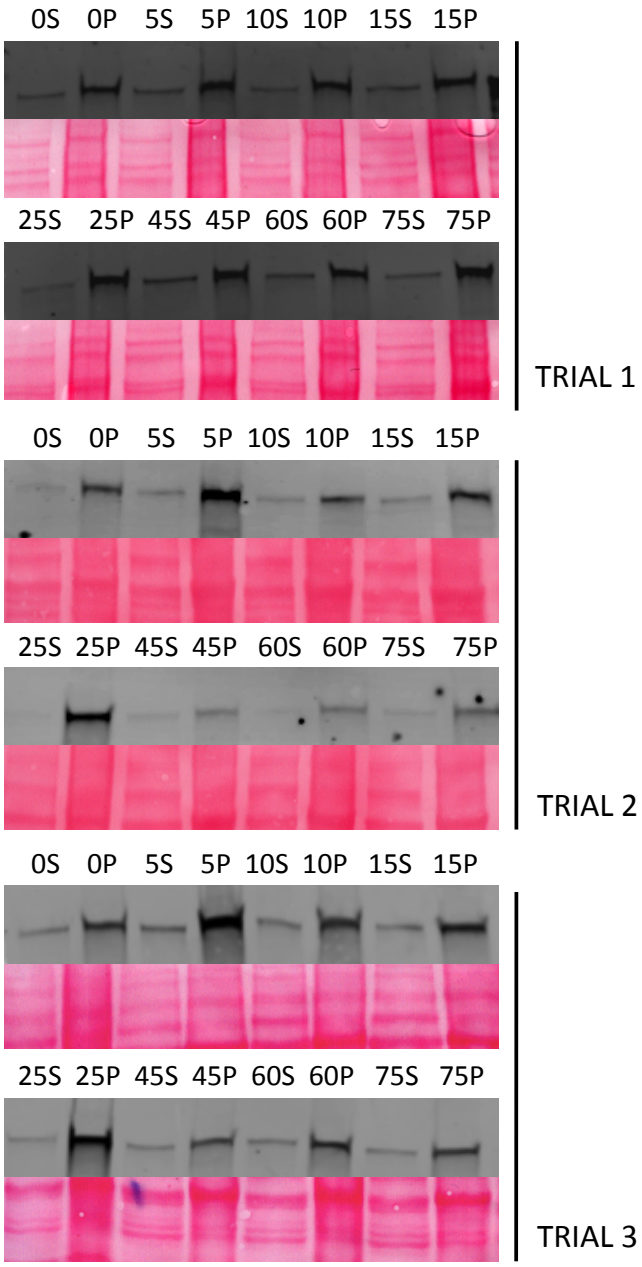

Figure A1. Western blotting of chromatin fractionation samples from three Cdc6-Myc timecourses. Mouse α-Myc (Sigma, 1:5000) and Alexa Fluor 488 goat α-mouse IgG (Invitrogen, 1:3000) antibodies were used to probe for Cdc6. Ponceau S staining is shown. Numbers correspond to timepoint at which samples were collected during the timecourse following release from α-factor block (T=0 corresponds to cells arrested in late G1, prior to release). The letter P denotes chromatin pellet samples, while supernatant samples are denoted by the letter S.

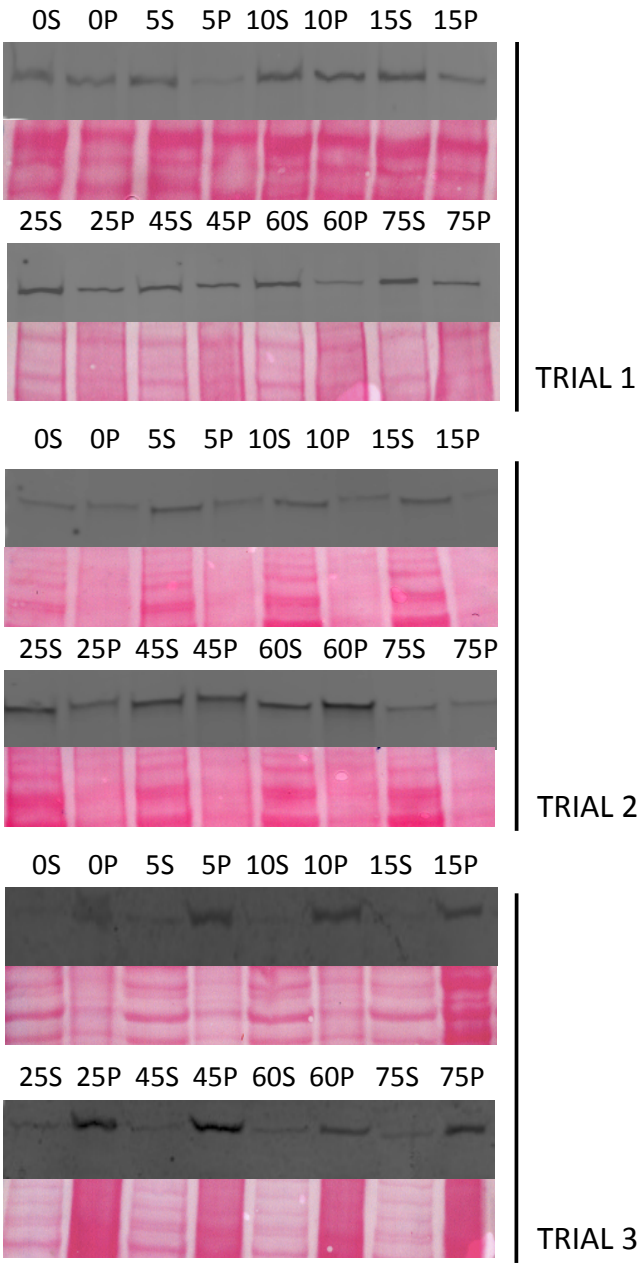

Figure A2. Western blotting of chromatin fractionation samples from three Cdc45-Myc timecourses. Mouse α-Myc (Sigma, 1:5000) and Alexa Fluor 488 goat α-mouse IgG (Invitrogen, 1:3000) antibodies were used to probe for Cdc45. Ponceau S staining is shown. Numbers correspond to timepoint at which samples were collected during the timecourse following release from α-factor block (T=0 corresponds to cells arrested in late G1, prior to release). The letter P denotes chromatin pellet samples, while supernatant samples are denoted by the letter S.

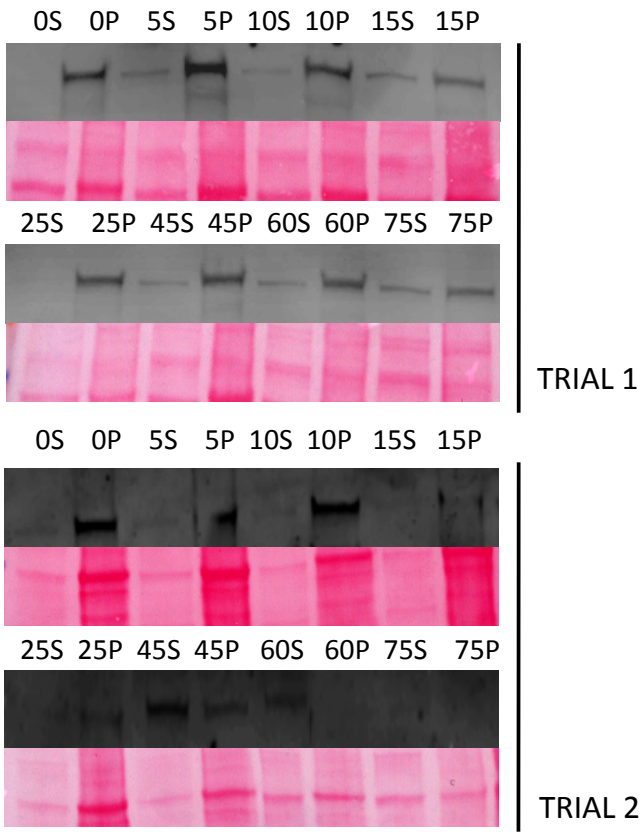

Figure A3. Western blotting of chromatin fractionation samples from two DY-26 (wild-type) timecourses. Mouse α-Myc (yN-19 goat polyclonal, Santa Cruz, 1:500) along with Alexa Fluor 488 donkey α-goat IgG (Invitrogen, 1:3000) antibodies were used to probe for Mcm2. Ponceau S staining is shown. Numbers correspond to timepoint at which samples were collected during the timecourse following release from α-factor block (T=0 corresponds to cells arrested in late G1, prior to release). The letter P denotes chromatin pellet samples, while supernatant samples are denoted by the letter S. Additional Mcm2 data from Pasero *et al*. (1999) was combined with this data set.

Table A1. Sample conversion of densitometry values obtained from chromatin fractionation western blots to molecules/cell numbers. This is shown for a single Cdc45-Myc timecourse.

Timepoint (min)	Densitometry reading (normalized*) Supernatant	Pellet	Sum	Weight (t)	Weighted value
0	19276469	823312	20099781	X 5	100498905.6
5	17568831	2556677	20125509	X 5	100627542.8
10	16406344	2807410	19213754	X 5	96068771.05
15	15247009	5756224	21003233	X 10	210032329.7
25	16778584	3828568	20607152	X 20	412143036.2
45	16956987	1884426	18841413	X 15	282621197.5
60	17420679	1513775	18934453	X 15	284016801.9
75	17048102	2015896	19063998	X 15	285959972.7

Weighted sum=	1771968558
AVG (/90)=	19688540

Mol/cell =	1730**
Scaling factor =	(mol/cell)/AVG
=	8.79 X 10^{-5}

* Values are normalized to intensity of Ponceau S staining as well as concentration ratios of supernatant to pellet

** Huh *et al.* (2003)

Multiply each timepoint by scaling factor to generate scaled data:

Timepoint	Supernatant	Pellet
0	1694	72
5	1544	225
10	1442	247
15	1340	506
25	1474	336
45	1490	166
60	1531	133
75	1498	177

Figure A4. Behaviour of mutant rescues simulated by the Chen *et al.* (2004) model remains unchanged in the combined model. Profiles of various species from the whole cell cycle model are shown as simulated by the combined model to illustrate the rescue of two mutants. These profiles are identical to those presented in Chen *et al.* (2004). (A) A triple-Cln mutant (*cln1Δcln2Δcln3Δ*) is rescued by the deletion of Sic1 (*cln1Δcln2Δcln3Δsic1Δ*). (B) Cells lacking Cdc20 and the S-phase cyclin, Clb5 are inviable (*Cdc20ΔClb5Δ*), but are rescued by deletion of Pds1 (*Cdc20ΔClb5ΔPds1Δ*).
Appendix B – Supplementary Information from Chapter 4

A

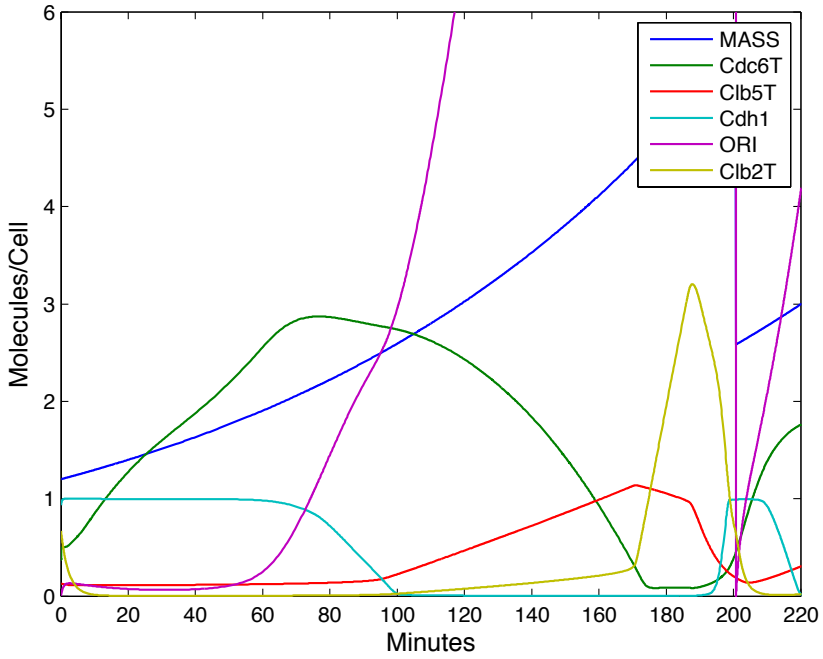
MASS
Cdc6T
Clb5T
Cdh1
ORI
Clb2T
Molecules/Cell
Minutes
0
1
2
3
4
5
6
0
20
40
60
80
100
120
140
160
180
200
220

B

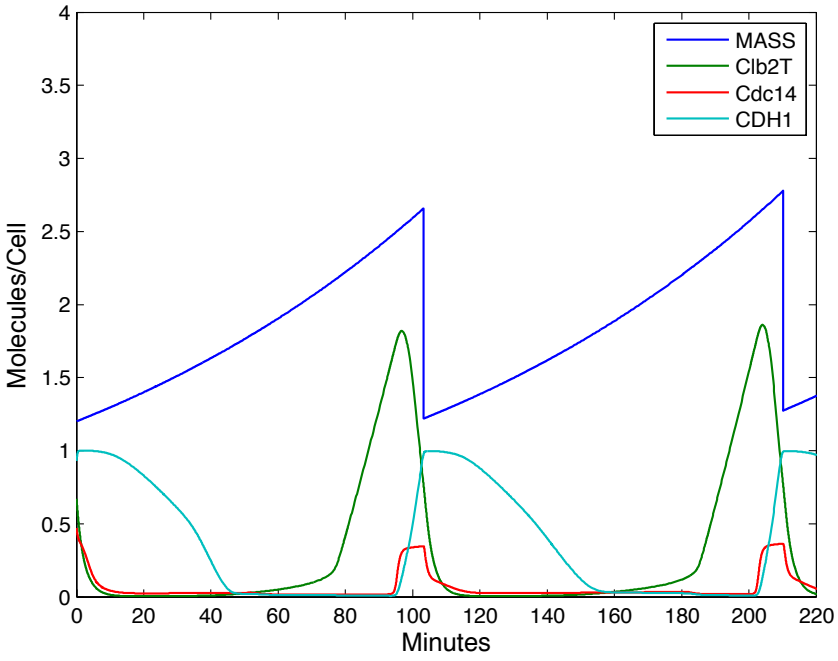
MASS
Clb2T
Cdc14
CDH1
Molecules/Cell
Minutes
0
0.5
1
1.5
2
2.5
3
3.5
4
0
20
40
60
80
100
120
140
160
180
200
220

Appendix B – Supplementary Information from Chapter 4

Table B1. Mass spectrometry data for proteins identified in chromatin-enriched sample.

Protein name	Systematic name[a]	Peaks score / sequence coverage (%) (Mascot score)[b]	Peptides matched	Mw (kDa)	EF	p-value[c]
Arp3	YJR065c	98.90 / 14.03	6	49.49	+1.74	0.0043
Arp4	YJL081c	99.97 / 31.49	17	54.78	+4.20	0.0010
Arp7	YPR034w	94.41 / 20.13	9	53.70	+2.53	0.0011
Arp9	YMR033w	46.06 / 5.35 (63)	2	53.02	+3.35	0.00035
Asc1	YMR116c	81.04 / 23.20	6	34.63	+2.88	0.0046
Atp2	YJR121w	99.99 / 38.36	15	54.74	+1.43	0.00025
Cdc10	YCR022c	97.10 / 17.38	5	40.00	+3.09	0.0045
Cgi121	YML036w	39.73 / 13.81 (73)	3	20.63	+3.37	0.00030
Crn1	YLR429w	97.65 / 8.29	5	72.49	+4.06	0.000025
Cys3	YAL012w	98.23 / 17.77	6	42.50	+1.65	0.00076
Egd2	YHR193c	54.70 / 15.50 (56)	2	18.68	+1.55	0.0016
End3	YNL084c	63.53 / 10.03 (109)	3	40.28	+10.4	0.00012
Gdi1	YER136w	96.87 / 22.20	9	51.16	+1.58	0.00019
Ilv2	YMR108w	93.25 / 9.17	5	74.87	+13.4	0.000031
Ilv5	YLR355c	96.35 / 25.37	7	44.30	+1.95	0.00050
Lat1	YNL071w	92.00 / 14.11	6	51.76	+2.42	0.00097
Lsp1	YPL004c	98.28 / 21.99	6	38.03	+5.54	0.00043
Pdb1	YBR221c	97.14 / 20.22	6	40.02	+3.93	0.000036
Pil1 (a)	YGR086c	87.21 / 31.27	8	38.31	+1.65	0.0029
Pil1 (b)	YGR086c	94.80 / 14.45	5	38.31	+2.31	0.00061
Pst2	YDR032c	74.95 / 12.12 (97)	2	20.93	+3.37	0.000062
Qcr2	YPR191w	98.72 / 26.90	8	40.44	+1.73	0.00036
Raf1	R0030w	98.33 / 32.04	6	21.26	+3.37	0.00030
Rpb3	YIL021w	90.73 / 20.44	5	35.26	+3.38	0.000022
Rpc40	YPR110c	97.49 / 26.27	8	37.65	+3.98	0.000015
Rpt1	YKL145w	84.18 / 19.06	9	51.93	+1.92	0.00091
Rvb2	YPL235w	29.20 / 9.10 (54)	5	51.56	+4.03	0.00055
Stm1	YLR150w	44.40 / 18.32 (220)	4	30.00	+2.21	0.000082
Swi3	YJL176c	96.50 / 14.20	4	63.11	+6.85	0.000065
Taf14	YPL129w	95.30 / 14.30	4	27.40	+4.32	0.000065
Tfc7	YOR110w	36.10 / 8.10 (78)	3	49.10	+3.89	0.000027
Tub2	YFL037w	70.61 / 6.64 (53)	2	50.58	+3.73	0.0010
Ume1	YPL139c	95.57 / 17.39	4	50.97	+2.22	0.00020
Ura7	YBL031c	67.53 / 3.45 (76)	2	64.65	+3.73	0.000022

[a] Saccharomyces Genome Database (SGD) identifier

[b] Protein identification score as described by Ma *et al.*, 2005. Score and sequence coverage are calculated using Peaks Studio version 2.4. If the Peaks search score was below the threshold of 80, additional confirmation was made using the Mascot MS/MS ion search with a confidence cutoff of $p<0.05$ (Mascot scores shown in parentheses).

[c] *p*-values of DIGE experiments are obtained with DeCyder FDR correction with four biological replicates.

Table B2. Mass spectrometric identification of MMS-induced differentially expressed proteins.

Protein name	Description	Systematic name[a]	MS/MS score /sequence coverage (%)[b]	Peptides matched	Mw (kDa)
Acf2	Cytoskeleton assembly factor	YLR144c	99.71 / 20.41	15	88.00
Aim13	Genome stability protein	YFR011c	85.27 / 27.06	5	18.83
Arp3	Actin-related protein 3	YJR065c	99.93 / 51.45	17	49.49
Atp2	ATPase beta chain	YJR121w	95.64 / 38.16	41	54.74
Bmh1 (a)	14-3-3 homolog	YER177w	99.64 / 70.41	30	30.05
Cdc10 (a)	Septin ring protein, cytokinesis	YCR002c	99.99 / 61.80	24	36.98
Cdc10 (b)	Septin ring protein, cytokinesis	YCR002c	97.12 / 17.39	6	36.98
Cps1	Gly-X carboxypeptidase	YJL172w	98.72 / 43.58	72	64.54
Crn1	Coronin	YLR429w	92.81 / 26.27	13	72.49
Gcv3	FUN40, glycine cleavage	YAL044c	94.10 / 47.46	13	19.55
Hsp31	Cysteine-type endopeptidase	YDR533c	99.78 / 66.24	16	25.64
Ilv2	Acetolactate synthase	YMR108w	99.99 / 39.88	32	74.87
Lsp1 (a)	Primary component of eisosome	YPL004c	99.31 / 25.81	8	38.03
Lsp1 (b)	Primary component of eisosome	YPL004c	77.31 / 17.3 (34)	6	38.03
Nsp1	Nucleoskeletal like protein	YJL041w	99.99 / 28.68	24	86.50
Pil1	Component of eisosome	YGR086c	94.80 / 14.45	5	38.31
Pst2 (a)	Flavodoxin-like protein	YDR032c	90.38 / 33.84	5	20.93
Pst2 (b)	Flavodoxin-like protein	YDR032c	94.19 / 52.02	6	20.93
Rpa1	Replication factor A 1	YAR007c	100.00 / 40.10	22	70.29
Rpa2	Replication factor A 2	YNL312w	82.44 / 37.0	6	29.90
Rnr4 (a)	Ribonucleotide reductase	YGR180c	99.02 / 43.77	11	39.98
Rnr4 (b)	Ribonucleotide reductase	YGR180c	99.83 / 33.33	19	39.98
Rnr4 (c)	Ribonucleotide reductase	YGR180c	81.68 / 22.03	9	39.98
Rnr4 (d)	Ribonucleotide reductase	YGR180c	97.64 / 31.59	12	39.98
Ste4	GTP binding protein	YOR212w	71.56 / 14.18 (113)	4	46.53
Vma2 (a)	Subunit 2 of V-ATPase	YBR127c	99.40 / 24.76	10	57.70
Vma2 (b)	Subunit 2 of V-ATPase	YBR127c	99.82 / 28.82	13	57.70
Vma2 (c)	Subunit 2 of V-ATPase	YBR127c	99.35 / 24.76	13	57.70
Vma4	Subunit 4 of V-ATPase	YOR332w	99.82 / 27.90	9	26.44
Ycp4 (a)	Flavodoxin-like protein	YCR004c	99.57 / 43.81	7	26.32
Ycp4 (b)	Flavodoxin-like protein	YCR004c	87.20 / 17.41(169)	3	26.32
Yrb1	Ran GTPase binding protein	YDR002w	52.21 / 26.37 (38)	6	22.92
Ald6	Aldehyde dehydrogenase	YPL061w	99.79 / 25.75	10	54.52
Bgl2	Glucan endo-1,3-beta-glucosidase	YGR282c	99.49 / 18.61	9	33.50
Bmh1 (b)	14-3-3 protein 1	YER177W	99.59 / 39.70	9	30.05
Bmh2	14-3-3 protein 2	YDR088w	97.78 / 25.64	6	31.13
Hsp60	Mitochondrial chaperone	YLR259c	99.90 / 26.22	12	60.69
Pdc1	Pyruvate decarboxylase	YLR044c	99.88 / 25.22	13	61.44
Rpp0	Acidic ribosomal protein P0	YLR340w	98.83 / 24.68	7	33.68
Rpc40	Component of RNA polymerase	YPR110c	98.10 / 19.70	6	37.65
Ssb1	DnaK-type molecular chaperone	YDL229w	99.86 / 21/21	9	66.54
Ssb2	DnaK-type molecular chaperone	YNL209w	99.74 / 26.10	13	66.54
Tma19	Histamine-releasing factor homolog	YKL056c	67.11 / 23.35 (69)	3	18.71
Ura7	CTP synthase	YBL039c	67.53 / 3.45 (76)	2	64.65

[a] Saccharomyces Genome Database (SGD) identifier

[b] Protein identification score as described by Ma *et al.*, 2005. Score and sequence coverage are calculated using Peaks Studio version 2.4. If the Peaks search score was below the threshold of 80, additional confirmation was made using the Mascot MS/MS ion search with a confidence cutoff of $p<0.05$ (Mascot scores shown in parentheses).

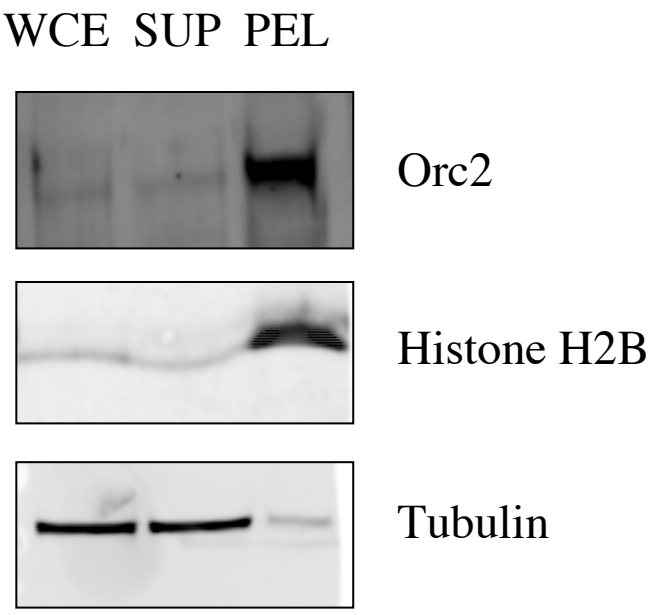

Figure B1. Western blot analysis of chromatin fractionation samples. Initial whole cell extract (WCE), as well as supernatant (SUP) and chromatin (PEL) fractions were subjected to SDS-PAGE and transferred to a nitrocellulose membrane. Detection was carried out with rabbit polyclonal α-Orc2 (1:1000 dilution, Duncker *et al*., 2002), mouse monoclonal α-TAT1 (1:500 dilution, Sherwin and Gull, 1989), and rabbit polyclonal α-histone H2B (1:1000 dilution, Cedarlane), using 1:3000 dilutions of either Alexa Fluor 647 goat α-rabbit IgG or Alexa Fluor 488 goat α-mouse IgG secondary antibodies. PEL fractions are concentrated tenfold relative to WCE and SUP. In each case, equal volumes of WCE and SUP fractions were loaded, with double (histone H2B, tubulin detection) or triple (Orc2 detection) the volume of the PEL fraction loaded. This resulted in approximately equal amounts of protein being analyzed for each sample.